DTU Library

Control of Indoor Airflows for Reduction of Human Exposure to Aerosol Contaminants

Bivolarova, Mariya Petrova

[Link back to DTU Orbit](#)

Control of Indoor Airflows for Reduction of Human Exposure to Aerosol Contaminants

Mariya Petrova Bivolarova

PhD Thesis

Department of Civil Engineering
2017

DTU Civil Engineering Report-376

Control of Indoor Airflows for Reduction of Human Exposure to Aerosol Contaminants

PhD Thesis

By

Mariya Petrova Bivolarova

International Centre for Indoor Environment and Energy

Department of Civil Engineering, Technical University of Denmark

DTU

Declaration

I hereby declare that this thesis was written by myself. I have not used any sources or materials other than those enclosed. The thesis has not been submitted further in this form or any other form, and has not been used to obtain any other equivalent qualifications at any other organization/institution.

<div style="text-align:center">

_____

Mariya Petrova Bivolarova

19 April 2017

2800 Kgs. Lyngby, Denmark

</div>

Acknowledgements

Many thanks to Maria Barova, Dusan Licina and Veronika Foldvary for their constant encouragement and friendship.

And most of all, to my wonderful parents, Toni and Petar Bivolarovi, who have guided and helped me from day one.

Thank you!

Table of Contents

List of figures

List of tables

List of abbreviations

ACF	Activated carbon fibre
ACH	Air exchange per hour
ACR	Air exchange rate
AHU	Air-handling unit
ASHRAE	American Society of Heating, Refrigerating and Air-Conditioning Engineers
BR	Building Regulations
CAV	Constant air volume
CBL	Convective Boundary Layer
CDC	Centre for Disease Control and Prevention
CFD	Computational Fluid Dynamic
DV	Displacement Ventilation
HEPA	High efficiency particulate air
HVAC	Heating Ventilation and Air-Conditioning
IAQ	Indoor Air Quality
i.e.	that is
ISO	International Organization for Standardization
MV	Mixing ventilation
MRSA	Methicillin-resistant Staphylococcus aureus
ppm	Parts per million
PV	Personalised ventilation
RMP	Round Moveable Panel
TVAD	Total volume air distribution
VAV	Variable air volume
VC	Ventilated seat cushion
VM	Ventilated mattress
RC	Radiant ceiling

Abstract

Air distribution in indoor environments is a critical factor of occupants' exposure to airborne contaminants. There is a wide range of gaseous and biological contaminants which deteriorate the indoor air quality and thus affect negatively occupants' health and performance. Increasing attention is being paid to analysing indoor airflow patterns and on understanding indoor pollution transmission to the breathing zone of occupants. However, studies rarely take into account the complex airflow interaction in the breathing zone, which may lead to inaccurate exposure prediction. Therefore, there is still a need for improved understanding of the air movement in the vicinity of the occupants. Tracer gas measurements are often used to study exposure to both indoor generated gases and airborne particles (aerosols). The tracer gas, however, cannot be used as a common substitute for aerosols of all sizes due to the different physical forces acting on them. Determining to what extent tracer gas can be used as substitute for aerosols when assessing occupants' exposure to indoor aerosols is needed and can be used for appropriate ventilation systems design. A properly developed ventilation method achieves the maximum efficiency with the minimum airflow rate, avoiding excessive installation and maintenance costs and more importantly, excessive energy use can be avoided. It is well-known that the most efficient method to prevent the risk of exposure is to control the contaminants directly or close to their source. A person, particularly his/her body, may be the primary source of unpleasant and even contagious contaminants in spaces. Dilution of the contaminated room air by supply of clean air, known as ventilation by dilution, is a recognised method for improving indoor air quality. The current method for ventilating an entire room based on total volume air distribution principles is often not efficient in providing high quality environment and satisfying every occupant. Hence, local exhaust ventilation applied in the vicinity of the occupants, i.e. close to the pollution source can offer a better solution.

The main objectives of the present thesis are: 1) to study the effect of typical airflows interactions around the human body (convective boundary layer, respiratory flow, and flow of local ventilation flow) on transport mechanisms of airborne contaminants and the resulting occupants' exposure; 2) to verify the use of tracer gas as a measure of exposure to indoor aerosols; 3) to develop and study local exhaust ventilation methods for exposure reduction to body-emitted contaminants in indoor environments.

The most important findings of the research performed in this thesis are summarized in the following:

In ventilated rooms with low air mixing, the interaction of the exhaled flow with the convective boundary layer (CBL) around a seated person increases the exposure to own body released pollution, especially when the pollution is generated close to the breathing zone. Breathing does not affect exposure to gaseous pollutants emitted from the lower part of the body. Local airflow from personalised ventilation directed against the face with mean air speed of 0.4 m/s can reduce

substantially the exposure regardless of the pollution source location. However, when the personalised airflow is combined with local source control, i.e. local exhaust of pollution, the exposure may increase depending on the airflow interaction at the breathing zone and the source location. Exposure assessment based on tracer gas concentration measurement can be incorrect if the measuring instrument has long response time and the complex airflow interaction in the breathing zone is not correctly simulated.

Results showed that in the breathing zone of a seated occupant, the tracer gas emerged as a reliable predictor for the exposure to aerosols with aerodynamic diameter 0.07, 0.7, and 3.5 μm in a room with mixing air distribution. An increase of the air change rate did not affect the comparable normalized concentration distribution of the tracer gas and the larger particles, namely 0.7μm and 3.5 μm. However, the ventilation rate was important for comparing the behaviour of the ultrafine particles (0.07 μm) and the tracer gas in the breathing zone. A moderate change of the room surface area did not influence the resemblance in the dispersion of the aerosols and the tracer gas. The results also showed that tracer gas can be used to indicate the exposure of a person lying in bed to 0.7 μm aerosols.

Furniture-integrated exhaust methods can be used as a pollution source control strategy in facilities where people are seated or bed-bound for considerable amounts of time. The current study examined ventilated mattress and ventilated seat cushion as local pollution exhaust methods. It was found that at reduced background ventilation rate, the use of the ventilated mattress and the ventilated seat cushion improved the air quality substantially when the pollution source was located near the exhaust openings. The pollution was removed from the room through the ventilated mattress or seat cushion's connection with the exhaust system before it was mixed with the room air. An alternate approach was to install a filter inside the mattress in order to clean the exhausted air of body effluents and recirculated it back into the room. This provides flexibility of bed location (the bed with own ventilation can be moved to ventilated or non-ventilated rooms) and avoids installation of additional ducting. This technique can also be applied in the case of the ventilated seat cushion. The ventilated mattress and seat cushion in conjunction with background ventilation at low supply flow rate are effective methods for reducing room pollution and exposure to the level that can be achieved with background ventilation alone at much higher supply flow rate. These findings suggest that the implementation of such user-centred ventilation methods can allow the ventilation rate requirements in buildings to be significantly reduced. The results also showed that the integrated exhaust methods provided body cooling to the parts in contact with their surface. The most affected body parts were the back, back side, pelvis, and thighs. It is expected that the local cooling will have a positive effect on thermal comfort in summer seasons and in regions with sub-tropical or tropical climate conditions. This positive effect must be verified with human subject experiments.

The results from the performed energy simulations showed that the use of the ventilated mattress and the ventilated seat cushion offers potential for energy savings. The ventilated mattress in conjunction with background ventilation at 3 air change per hour (ACH) can decrease the annual energy use by 24% to 52% for a double patient room located in a cold climate or hot and humid

climate in comparison with conventional mixing ventilation at 4 - 6 ACH. It was found that combining the ventilated seat cushion with mixing ventilation and a chilled ceiling in a call-centre with 14 employees, each using a ventilated seat cushion, reduced the annual energy use by 7 % compared to a system with only mixing ventilation.

Resumé

Fordelingen af luft i indendørs miljøer er en kritisk faktor for eksponering af luftbårne urenheder for bygnings brugere. Der er en lang række gasformer og biologisk forurenende stoffer, som forringer den indendørs luftkvalitet og dermed påvirker brugernes helbred og præstation negativt. Der er fortsat øget opmærksomhed omkring analyse af indendørs luftmønstre og forståelse af transmissionen af indendørs forurening til indåndingszonen af brugere. Undersøgelser tager dog sjældent hensyn til den komplekse interaktion af luftstrøm i indåndingszonen, som kan føre til unøjagtige forudsigelser af eksponeringen. Der er derfor stadig behov for en forbedret forståelse af luftbevægelserne nær brugerne. Målinger med tracer gas anvendes ofte til at studere eksponeringen af indendørs genererede gasser og luftbårne partikler (aerosoler). Tracer gas kan imidlertid dog ikke anvendes som en fælles erstatning for aerosoler af alle størrelser på grund af de forskellige fysiske kræfter, som påvirker dem. Ved vurderingen af brugernes eksponering af indendørs aerosoler, er der behov for at fastslå i hvilket omfang tracer gas kan anvendes som erstatning for aerosoler og kan således også anvendes til hensigtsmæssigt design af ventilationssystem. En veldesignet luftfordeling i rum opnår maksimal effektivitet med minimal luftstrøm. På denne måde kan høje installations- og vedligeholdelsesomkostninger og vigtigst af alt høje energiudgifter, undgås. Det er velkendt, at den mest effektive metode til at forebygge risikoen for eksponering, er kontrol af forureningerne direkte eller tæt på kilden. En person, især hans/hendes krop, kan være hovedkilden til ubehagelige og endda smitsomme forureninger i rum. Fortynding af den forurenede luft ved tilførsel af ren luft, kendt som fortyndingsventilation, er en anerkendt fremgangsmetode til at forbedre luftkvaliteten. Forøgelse af den tilførte luftmængde til at ventilere et helt rum, baseret på totalvolumen luftfordeling, er ofte ikke effektiv til at levere et højt kvalitets-miljø og tilfredsstille alle brugere. Derfor kan lokal udsugning anvendt i nærheden af brugerne, det vil sige tæt på forureningskilden, være en bedre løsning.

Hovedformålene med den foreliggende afhandling er: 1) at undersøge virkningen af typiske luftstrømmes interaktion omkring menneskekroppen (konvektionsgrænselaget, respirations strømmen og strømmen af lokal ventilation) på transportmekanismer af luftbårne forureninger og den resulterende eksponering for brugerne; 2) at verificere anvendelsen af tracer gas som et mål for eksponering af indendørs aerosoler; 3) at udvikle og studere lokale udsugningsventilationsmetoder til reduktion af eksponering af kropsbårne forurenende stoffer i indendørs miljøer.

De vigtigste resultater som er udført i denne afhandling, er sammenfattet i det følgende.

I ventilerede rum, med opblandingsventilation, interaktionen af udåndet luftstrøm med et konvektivt grænselag omkring en siddende person øger eksponeringen af egen frigivet forurening, specielt når forureningen er genereret ved indåndingszonen. Strømningen af udåndings luft påvirker ikke eksponering af forurenede luftarter fra den nedre del af kroppen. Lokal luftstrømning fra personlig ventilation rettet mod ansigtet med en gennemsnitlig lufthastighed på 0,4 m/s, kan reducere eksponeringen væsentligt uanset forureningskildens placering. Når den personlige luftstrøm kombineres med lokal udsugning af forureningen, kan eksponeringen imidlertid stige afhængigt af luftstrømmens interaktion ved indåndingszonen og kildens placering. Vurdering af eksponering

baseret på tracer gas målinger kan være forkert hvis måleinstrumentet har langsom responstid og hvis de komplekse luftstrømsinteraktioner i indåndingszonen ikke er korrekt simuleret.

Resultaterne viser at i indåndingszonen hos en siddende person, forudsiger tracer gas en pålidelig eksponering for aerosoler med en aerodynamisk diameter på 0,07, 0,7 og 3,5 μm i et rum med opblandingsventilation. En stigning i luftskiftet påvirkede ikke den sammenlignelige normaliserede koncentrationsfordeling af tracer gas og de større partikler, det vil sige 0,7 μm og 3,5 μm. Ventilationsraten var dog imidlertid vigtig for at sammenligne adfærden af de ultrafinepartikler (0,07 μm) og tracer gas i indåndingszonen. En moderat ændring af rummets overfladeareal havde ingen indflydelse på ligheden i spredningen af aerosolerne og tracer gassen. Resultaterne viser også, at tracer gas kan anvendes til at indikere eksponeringen af en person der ligger i en seng, til 0,7 μm aerosoler.

Integreret senge og stole udsugningsmetoder kan anvendes som en strategi til kontrol af forureningskilden i faciliteter hvor mennesker sidder eller er senge-bundet i en længere periode. Det akutelle studie undersøgte ventilerede madrasser og ventilerede sædehynder som en lokal udsugningsmetode. Der blev fundet, at ved en reduceret baggrunds ventilationsrate, vil brugen af en ventilerede madras og et ventilerede sædehynde forbedre luftkvaliteten væsentligt, når forureningskilden er lokaliseret nær udsugningsåbningerne. Forureningen fjernes ud af rummet gennem den ventilerede madras' eller ventilerede sædehyndes forbindelse med udsugningssystemet før luften er opblandet med rum luften. Det påvises at en effektiv metode er også at installere et filter inde i madrassen for at rense den forurenede udsugede luft og recirkulere luften tilbage til rummet. På denne måde er fleksibiliteten af sengens placering øget, (sengen med egen ventilation kan flyttes til ventilerede eller ikke-ventilerede rum), og dermed er installation af yderligere kanaler undgået. Denne teknik kan også anvendes på ventilerede sædehynder. Ventilationsmadrassen og ventilationssædehynden er effektive metoder til at reducere rum forurening og eksponering til samme niveau, som der kan opnås kun med rum baggrundsventilation med meget større luftmængde end der anvendes i dag. Disse resultater tyder på, at sådanne brugercentrerede ventilations metoder vil revolutionere ventilationsratekravene for bygninger til at blive reduceret i fremtiden. Resultaterne viser også, at begge integrerede udsugningsmetoder også giver afkøling til kropsdelene som er i kontakt med overfladen. De mest berørte kropsdele viste sig at være ryggen, bækken og lår. Det forventes at den lokale køling vil have en positiv effekt på den termiske komfort om sommeren og i regioner med subtropiske eller tropiske klimaforhold. Denne positive effekt skal verificeres med eksperimenter.

Resultater fra de udførte energisimuleringer viser, at brugen af ventilationsmadrassen og ventilationssædehynden har et potentiale for energibesparelser. Ventilationsmadrassen sammenholdt med baggrundventilation med et luftskifte på 3 gange i timen, vil mindske det årlige energiforbrug mellem 24% og 52% af et dobbelt patient værelse beliggende i et koldt klima eller varmt og fugtigt klima sammenlignet med konventionel opblandingsventilation med et luftskifte på 4 eller 6 gange i timen. Der blev fundet, at en kombination af ventilationssædehynden og opblandingsventilation og køle-loft i et call-centre med 14 medarbejdere, som hver bruger

sædehynden, reducerer the årlige energiforbrug med 7% sammenlignet med et system kun med opblandingsventilation.

1   Background

The quality of the air in buildings to which occupants are exposed influences their health, well-being and productivity. A main concern with respect to occupants' health is the concentration levels of contaminants in the indoor air.

Consequently, occupant exposure depends on the inhaled concentration of the contaminants which are present in the air directly surrounding the occupant's nose and mouth, generally termed the breathing zone. The contaminant concentrations in the breathing zone of a person will depend on the magnitude, direction, and interaction of the airflows in the vicinity of the person, as well as the source characteristics and location relative to the person. Thus an understanding of indoor airflow distribution and the effect on transport of airborne contaminants to the breathing zone is critical.

1.1   Human body as a pollution source

In indoor spaces, people are exposed to a wide range of gaseous and particulate contaminants which negatively impact their health, comfort and performance. Building materials, office equipment, occupants, etc. are some typical pollution sources. Great efforts to reduce indoor pollution sources, such as the development of low polluting materials, are currently underway. It is expected that in the future occupants themselves will remain the greatest indoor pollution source. The human body emits particulate contaminates (bio-aerosols) and gaseous contaminates (bio-effluents). Human respiration activities (exhalation, coughing, sneezing) generate bio-aerosols that may carry infectious viruses and bacteria (Douwes et al. 2003). Infectious bio-aerosols may cause airborne transmission of infection between occupants in spaces (Cao et al., 2015; Li et al. 2007; Morawska, 2006). Skin flakes generated due to human body movement and friction between the clothing and the skin also contain a wide variety of contagious pathogens which may become airborne (Davies and Noble, 1962; Noble et al., 1976; Spendlove et al., 1983). Bio-effluents are volatile and non-volatile organic compounds that may be detected by human olfactory system as odours. Oral cavity, armpits, groin, head and feet are the primary sites where bio-effluents are generated, mostly as a result of sweating and human waste (Dormont et al., 2013). Ozone reactions with skin oil produce sub-micron particles and volatile products which may cause headaches, eye and respiratory irritation and increased susceptibility to respiratory illness (Rai et al., 2013).

1.2   Air distribution methods for reduction of occupants exposure

Ventilation is recognised and widely used as a strategy for reducing occupants' exposure to indoor airborne contaminants. Its efficiency depends on the air distribution in occupied spaces. There are two major groups of air distribution methods: total volume air distribution and localized air distribution. In occupied buildings, the total volume air distribution is widely applied for maintaining indoor air quality and thermal environment at acceptable level. In practice, total volume air distribution methods are often inefficient for the following reasons: clean and cool air is supplied far from occupants and is mixed with room air by the time it reaches occupants; the air

distribution pattern often enhances the transport of pollution generated outside of the occupied zone into the occupied zone; large volumes of air are used to ventilate and condition the entire space, including unoccupied zones, leading to excessive energy consumption (Melikov 2011, 2016).

Localized air distribution methods, known as personalised ventilation (PV), are a better solution because the clean air is introduced directly to the breathing zone of an occupant. When properly implemented, these methods can provide 100% clean air for breathing (Bolashikov et al., 2003; Melikov, 2004). Other advantages include the possibility for each occupant to control the airflow as preferred and potential for energy savings (Schiavon and Melikov, 2009; Sekhar et al., 2005). Some of the disadvantages are increased initial costs and spread of pollution in the surroundings when the pollution source is introduced to the supplied personalised air, e.g. body released pollution (Cermak et al., 2006; Melikov et al., 2003).

A more efficient method for exposure reduction is to capture the pollutants at their source before they are mixed with the surrounding air and transported to the occupants' breathing zone. As discussed previously, the human body is a major pollution source; thus, furniture-integrated local exhaust ventilation is applicable in situations where occupants are in constant position, e.g. bed-bound while recovering in health-care facilities or seat-bound while in an aircraft, etc. Such methods may be designed to be user-interactive in order to offer individual control over the microenvironment. This will make it possible to achieve an optimal indoor environment for each occupant. The implementation of source control has potential for huge energy savings due to reduced need for ventilation, which is one of the most energy consumption processes in buildings.

1.3 Airflow interaction in the microenvironment around occupants

Air movement due to airflow interaction in the vicinity of the human body is a major contributor to the transport of air pollutants to the breathing zone of occupants (Bolashikov et al. 2010; Brohus and Nielsen 1995, 1996; Melikov, 2015; Zhu et al. 2005; Rim and Novoselac 2009; Licina et al. 2015a, 2015b; Salmanzadeh et al., 2012). The primary airflows in the microenvironment around a person are the exhalation flow from the respiration and the upward buoyant airflow generated by the human convective boundary layer (CBL). In a calm and uniform indoor environment, the convective boundary layer flow has the ability to transport gaseous and particle contaminants generated by the human body and its surroundings to the breathing zone (Licina et al. 2015a, 2015b). In air-conditioned buildings, it is recommended that the air movement in the occupied zone is limited to less than 0.2 m/s to prevent draft risk (ISO 7730, 2005). In such situations, the buoyancy-driven convective flow will interact mostly with the exhalation flow and this interaction will be the prevailing factor for determining the personal exposure. The exhaled flows from the mouth and nose present a different case, to be discussed in Chapter 2. The interaction of the CBL with these exhaled flows may have considerable effects on the inhaled air quality, depending on the location of the pollution source. The impact of the interacting airflows in the breathing zone on the inhalation of body bio-effluents has been studied little. Clarification of this phenomenon could be used to develop or improve existing methods, including localized air distribution, to reduce the personal exposure. However, a more complex airflow interaction will be encountered if localized

air distribution such as PV or local exhaust ventilation is used to control spread of the airborne contaminants. Therefore, it is also important to determine whether the application of such methods would have a great impact on the characteristics of the inhaled air.

1.4   Methods for personal exposure assessment

The use of thermal manikins in full-scale experimental studies allows for recreation of actual thermo-fluid conditions and close-to-reality scenarios. In experimental studies, measuring the contaminant concentrations in the breathing zone of a thermal breathing manikin (resembling an average person) has become the most direct method for personal exposure assessment, as some otherwise hazardous techniques cannot be used with people (Melikov, 2004). Some of these techniques include gas or particle tracer methods as well as smoke visualizations. The results of such studies contribute to the validation of computational fluid dynamics models as well as aid the design and optimization of indoor environments to prevent possible health risks. In most previous experimental investigations of personal exposure, the breathing cycle of the manikin is excluded or simplified to only inhalation, only exhalation, or inhalation and exhalation without the pause that typically exists after each inhalation (Melikov and Kaczmarczyk, 2007). There is a knowledge gap about the importance of the complete human breathing process and its effect on the accuracy of the measurements (to be discussed in Chapter 2 of the current thesis). In addition, human breathing is a highly transient flow and thus may create fast concentration fluctuations in the breathing zone. If the sampling frequency of the used instrument is not high enough to measure the fluctuations of the simulated pollution concentration, this may impose high uncertainty in the estimated exposure. Additionally, most studies in the field have focused on continuous concentration measurements in the breathing zone comprising the entire breathing cycle and disregarded inhalation only, which is important for the exposure. The importance of the dynamic characteristics of instruments for tracer gas concentration measurement in exposure assessments is argued in Chapter 2.

Another key aspect of performing experimental studies for exposure evaluation is the simulation of pollutants. Tracer gas measurements are often used to study exposure to indoor generated gaseous and aerosol contaminants. It is well known that tracer gas cannot represent large aerosols since it cannot mimic the gravitational, inertial and drag forces that act on them (Yan et al., 2009). Studies have used tracer gas as a surrogate for aerosols with aerodynamic diameter less than 5 μm to evaluate their spread and removal in ventilated rooms (Bolashikov et. al., 2012; Nielsen, 2009; Qian et. al., 2006). Because of their small settling velocity, these airborne particles remain suspended in the air for long time and thus follow the airflow currents very well (Tang et al., 2011). Few studies have been carried out to investigate the link between the distribution in ventilated spaces of tracer gas and aerosols with diameter of up to 5 μm. Evidence shows good agreement between the behaviour of tracer gas and aerosols. However, most studies have focused on only one specific room layout without changing parameters such as room ventilation rate, room surface area, and particle size. In some studies, the presence of occupants has been excluded or the occupancy simulations have been realized by heated cylinders for simplicity. As already emphasized, the existence of a person in a space will modify the airflow field in his/her surrounding area and therefore the contaminant field which determines actual personal exposure. Thus there remains a

lack of knowledge regarding whether tracer gas can be used to accurately identify exposure to different-sized aerosol particles.

1.5 Research Objectives

There are three primary research objectives of this thesis:

• To investigate the effect of typical airflows interactions around the human body on the transport mechanisms of airborne contaminants and the resulting exposure of occupants;

• To verify the use of tracer gas as a measure of exposure to indoor aerosols;

• To develop engineering techniques for exposure reduction to airborne contaminants in indoor environments.

1.6 Thesis outline

The thesis consists of experimental and numerical parts. The results are organized by theme in Chapters 2, 3 and 4. Each of the objectives above is addressed in these chapters. Each chapter is divided into Introduction, Method, Results and Discussion, and Conclusions. Most of the results from the research work have already been published in scientific papers. The specific topics already published in papers are presented in short form with references to the relevant publications.

After this introductory chapter, the thesis is structured as follows:

In Chapter 2, personal exposure to bio-effluents released from the human body under different airflow interaction scenarios in the breathing zone is investigated. The results show the influence of parameters such as breathing mode and source location on the exposure assessment. The impact of transverse airflow directed to the inhalation zone of the occupant and applied local source control on the exposure is also presented. The importance of the dynamic characteristics of instruments for tracer gas concentration measurement is studied. Recommendations for performing accurate measurements are outlined. Part of Chapter 2 is based on Paper I.

Chapter 3 compares the normalized concentration of tracer gas and different-sized aerosol particles measured in a room ventilated with overhead mixing air distribution. The effect of important factors such as air change rate, surface area of the room, and the CBL around a seated person (heated thermal manikin) on the measured aerosols and tracer gas concentrations is compared. The chapter is based on Paper II.

Chapter 4 comprises extensive research on development of localized exhaust methods for reduction of exposure to indoor air pollutants and identification of their performance. The research presented in this chapter focuses on use of local exhaust ventilation for pollution source control applied to two microenvironments: bed microenvironment and microenvironment around seated occupants. Use of local air cleaning combined with localized exhaust ventilation methods is studied. The possibility of

energy savings as a result of the implementation of such methods is also shown. The impact of the localized ventilation on the thermal comfort of occupants, measures for its improvement, and the related energy needs are studied. Some of the obtained results are published in Papers III-VII.

Chapter 5 summarizes the key findings of the research.

A list of publications that are part of the PhD study but not included in the thesis is provided in Appendix A. Finally, Appendix B consists of the published, accepted, and submitted papers which are part of the thesis (Paper I-VII).

1.7 List of papers

The thesis is based on the following appended papers (provided in Appendix B):

PAPER I

Bivolarova M., Kierat W., Zavrl E., Popiolek Z., Melikov A., (submitted). Effect of airflow interaction in the breathing zone on exposure to body released bio-effluents. Submitted to Building and Environment, March 2017.

PAPER II

Bivolarova, M., Ondràček J., Melikov A., Ždímal V, (accepted). A comparison between tracer gas and aerosol particles distribution indoors: the impact of ventilation rate, interaction of airflows, and presence of objects. Accepted for publication in Indoor Air on 02 April 2017.

PAPER III

Bivolarova, M., Melikov, A. K., Kokora, M., & Bolashikov, Z. D., 2015. Performance Assessments of a Ventilated Mattress for Pollution Control of The Bed Microenvironment in Health Care Facilities. In Proceedings of Healthy Buildings 2015, ISIAQ International Conference, Eindhoven, the Netherlands, May 18-20, paper ID 633.

PAPER IV

Bivolarova, M., Melikov, A. K., Kokora, M., & Bolashikov, Z. D., 2014. Local Cooling of The Human Body Using Ventilated Mattress in Hospitals. In Proceedings of ROOMVENT 2014, 13th SCANVAC International Conference on Air Distribution in Rooms, October 19-22, 2014, Sao Paolo, Brazil, p. 279-286.

PAPER V

Bivolarova, M., Mizutani, C., Melikov, A.K., Bolashikov, Z. D., Sakoi, T. and Kajiwara, K., 2014. Efficiency of Deodorant Materials for Ammonia Reduction in Indoor Air. In Proceedings of Indoor Air 2014, 13th International Conference on Indoor Air Quality and Climate, Hong Kong, July 7-12, 2014 , p. 573-580 p.8.

PAPER VI

Bivolarova, M., Melikov, A.K., Mizutani, C., Kajiwara, K., and Bolashikov, Z. D., 2016. Bed-integrated local exhaust ventilation system combined with local air cleaning for improved IAQ in hospital patient rooms. Build & Environ. 2016; 100:10-18.

PAPER VII

Bivolarova, M., Rezgals, L., Melikov, A. K., Bolashikov, Z. D., 2016. Seat-integrated localized ventilation for exposure reduction to air pollutants in indoor environments. In Proceedings of 9th International Conference on Indoor Air Quality Ventilation & Energy Conservation In Buildings, Oct., 2016 Seoul, Korea. Paper ID 1258.

2 Characterization of airflows interactions important for the transport of airborne contaminants and occupant exposure

2.1 Introduction

In this chapter, the first main objective of the study is addressed. The chapter presents results from the exposure assessment to body-generated bio-effluents due to the interaction of airflows in the breathing zone. A method of tracer gas concentration measurements and analyses of the collected data for accurate assessment of occupant exposure is suggested.

2.1.1 Airflow interaction in the microenvironment around the human body

Convective heat loss dissipated from the human body induces a buoyancy-driven flow of adjacent air. This upward convective flow forms a convective boundary layer (CBL) around the human body that transforms into a thermal plume above the head (Licina et al. 2014a; Melikov, 2015; Zukowska et al., 2012). The CBL is part of the so-called human body microenvironment and plays a major role in the heat and mass exchange between the human body and its environment and exposure of people to indoor pollution (Melikov 2015). The exchange depends on the characteristics of the microenvironment (body posture, movement and contact with surfaces, as well as external factors such as air movement, thermal radiation, etc.). For example, it has been found that at comfortable room air temperature (23°C), the velocity magnitude of the CBL in the breathing of a seated person in front of a table may range from 0.17 m/s to 0.124 m/s depending on clothing insulation, chair design, and the person's posture (Licina et al., 2014b). Human respiration flow also comprises part of the microenvironment. Breathing flow is transient and consists of inhalation, exhalation, and pause. The dynamics of the inhalation flow very close to the nose and to the mouth are similar (Haseltonm and Sperandio, 1988). However, the flow of exhalation through the nose and mouth is different. Large variations in the spread of exhaled flows exist between people (Gupta et al. 2010). The exhalation generates jets with relatively high velocities of 1–2 m/s (Haseltonm and Sperandio, 1988, Tang et al. 2013), which, depending on head position, can penetrate the CBL and result in a small amount of the exhaled air being re-inhaled (Hyldgård 1994, Melikov and Kaczmarczyk, 2007). The velocity of the exhaled jets decreases rapidly with the distance from the face. Two independent jets apart from each other and deflected downward from the horizontal axes are exhaled from the nostrils (Gupta et al. 2010, Tang et al. 2013, Hyldgård 1994). The jets do not collapse but diffuse in the surroundings. In a calm environment and at an upright head position, the jet exhaled almost horizontally from the mouth (with temperature of approximately 34°C and relative humidity close to 100%) moves upward at some distance from the face (Özcan et al. 2005, Nielsen et al. 2009).

The interaction between the CBL, the flow of exhalation, and the flow of ventilation is important for the exposure to pollution generated by the body and in the surroundings. The interaction of the exhalation flow from nose and the CBL increases the turbulence in the breathing zone (Marr et al. 2005, Özcan et al. 2005). Laverge et al. (2014) reported that in a room with background ventilation increased from 0.5 to 6 ACH, the influence of the CBL on the shape and volume of the inhalation

zone remained dominant. The buoyancy flow around the human body and the ventilation flow in spaces interact differently depending on whether they are assisting, opposing, or transferring each other (Melikov et al. 2003, Licina 2014a). Rim and Novoselac (2009) reported that simulating breathing activity of a seated thermal manikin can either increase or decrease the particle concentrations measured at the mouth and above the head, depending on the source location in the room. The study also showed that the respiratory flow of the manikin (inhalation and exhalation through nose) has noticeable impact on the airflow distribution in the breathing zone. Murakami (2004) studied the interaction of the CBL with the transient flow of respiration and its impact on the inhalation of pollution generated at lower room heights using computational fluid dynamics (CFD). Hyldgård (1994) reported on spread of pollution generated over the body in the surrounding as a result of interaction of the CBL, the flow exhaled from nose and invading ventilation flow.

Localized air distribution, such as personalised ventilation (PV), that supplies clean air directly to the breathing zone has been developed and studied (Bolashikov et al. 2003; Cermak et al. 2006; Cermak and Melikov 2007; Kaczmarczyk et al., 2004; Melikov et al., 2002, 2003, 2012, Melikov 2004, 2011, Niu et al. 2007). It has been documented that personalised flow against the face can penetrate the CBL and provide clean air for breathing when its target velocity is above 0.3-0.35 m/s (Bolashikov et al. 2003). Melikov et al. (2003) studied the interaction of the CBL, the flow exhaled from nose, and local airflow when supplied against the face and upward tangentially to the chest from the edge of a desk positioned in front of the body. The interaction was studied in the case of mixing and displacement room air distribution. The interaction of flows had great impact on the spread of pollution generated at the groin, armpits, and from exhalation, and therefore on the exposure of occupants to their own and others bio-effluents. Personalised flow can provide clean air for breathing but it also spreads body-generated pollution to the surrounding space and thus increases the exposure to other occupants. It is therefore more efficient to apply source control and remove human body-generated pollution by local suction before it is mixed with the surrounding air.

2.1.2 Contaminants from the human body and their transport in the human breathing zone

There is strong evidence that the human body is a significant contributor to particles (bio-aerosols) and gases (bio-effluents) in indoor air. The term "bio-aerosols" defines airborne biological particles including bacteria and bacteria-laden particles. Human body movement and friction between the clothing and the skin generate skin flakes that contain a wide variety of contagious pathogens such as Acinetobacter, Staphylococcus aureus or Clostridium etc. (Spendlove et al., 1983). High bacterial concentrations during occupancy were predominantly found on particles within the size range 3- to 5- µm (Qian et al., 2012). Such particles are small enough to pass through the fabric of most outfits and move in the convective boundary layer (Clark and Cox, 1974). Due to their low settling velocity, it is then likely that the particles will be transported upward to the breathing zone or enter the plume above the head and cause cross-contamination. 3- to 5-µm particles have high deposition efficiency in the human respiratory tract with substantial penetration to and deposition in the pulmonary region of the lung (Koullapis et al., 2016; Yeh et al., 1996). Studies have also shown that chemical reactions occur between ozone and skin oils present on the surface of human skin and

clothing, forming volatile products and sub-micron particles (Rai et al., 2013; Wisthaler and Weschler, 2010). It has been reported that some of these volatile products may cause respiratory irritation if inhaled (Jarvis et al., 2005). They also can cause eye irritation and headaches (Spengler and Wilson, 2003). Furthermore, recent studies provide evidence that body-emitted bio-effluents may significantly reduce occupants' health, comfort, and productivity (Tsushima et al., 2016; Zhang et al., 2016a, 2016b). Tsushima et al. (2016) reported that occupants' perceived air quality decreases more when the room air is polluted with body bio-effluents compared to air polluted with orally exhaled bio-effluents. Areas of the body such as axillae, feet, and groin are prone to odour production, i.e. bio-effluents (Wysocki and Preti 2004; Verhulst et al., 2010).

Previous research has documented (by means of full-scale measurements with thermal manikins or computational fluid dynamics) the importance of the CBL for its ability to transport pollutants to the inhalation zone of occupants (Bolashikov et al. 2010; Brohus and Nielsen 1995, 1996; Melikov, 2015; Zhu et al. 2005; Rim and Novoselac 2009; Rim et al., 2009; Licina et al. 2015a, 2015b; Salmanzadeh et al., 2012). Zhu et al. (2005) reported that a person at low activity level (inhalation of 10 times/min, and a volume of 0.6 L per inhalation) inhales air mostly from the front areas of the CBL, and little from the back and sides of the body. Pollutants entrained not only from the body but also from the surrounding air can be transported by the CBL to the inhalation zone of occupants (Licina et al., 2015a; Rim and Novoselac, 2009, Gao and Niu 2005; Brohus and Nielsen, 1996; Salmanzadeh et al., 2012). Yet, it has been shown that in a quiescent environment the concentration in the breathing zone of a sedentary occupant is the highest when gaseous contaminants are released from the person's body as opposed to pollution emitted farther away (Licina et al., 2015b). Rim et al. (2009) found out that the breathing zone of a standing person can have 1.2 to 2.5 times greater levels of products derived from ozone reactions with occupant surfaces, including human skin oils and clothing, compared to the rest of the room. The study concluded that the occupant thermal plume pulls air up and across the reactive occupant surface, and the occupant surface boundary layer therefore becomes depleted of ozone but enriched with reaction products. These previous studies indicate that direct contaminant emissions from the human body may cause high exposure. The importance of the separate and combined impact of the free convection flow and the flow of respiration on the exposure of bio-effluents released by an occupant's own body is also focused on in this part of the present study.

2.1.3   Measurement of exposure to gaseous contaminants

From the above discussion, it is clear that occupant exposure assessment is important. To identify the exposure to indoor pollution, physical experiments are performed in full-scale test rooms with breathing thermal manikins representing occupants. Tracer gas is used to simulate the contaminants. For example, tracer gas mixed with the exhaled air is used to simulate respiratory pollutants such as small droplets of viruses and bacteria that can follow a person's exhalation flow (Bolashikov et al., 2012; Nielsen, 2009; Popiolek et al., 2012; Qian et al., 2006). Tracer gas is released from different sites on the manikin's body to simulate body bio-effluents or in different locations around the room to simulate a particular pollution source. Measurements of the tracer gas concentration at the breathing zone (close to nose or mouth) of the manikin are performed in order to assess the

transport and the exposure to the generated pollution. Two important factors must be considered for accurate assessment of exposure: 1) the complex airflow interaction around the human body, especially at the breathing zone, and 2) the characteristics of the measuring instruments and the data analyses. The breathing thermal manikins of complex body shape and the size of an average person represent the CBL around the body as well as the human breathing cycle and mode with sufficient accuracy. Different ventilation flows can also be replicated in the full-scale rooms. Thus the airflow interaction around the human body and its impact on exposure can be approximated well and can be studied. However, the measurement of tracer gas concentration may be critical for the exposure assessment. Most often, the instruments used for concentration measurements are slow, with a response time that is much longer than the breathing cycle of a sedentary person (about 2.5 s inhalation, 2.5 s exhalation and 1 s pause). The measurements with tracer gases have been performed over relatively long time periods including both inhalation and exhalation phases. This may have an impact on the accuracy of the assessment because, in reality, the exposure depends only on the inhaled air contaminants, not on the exhaled air. This remains to be studied.

2.1.4 Specific objectives

There is a knowledge gap in the research on airflow interaction at the breathing zone and its effect on exposure to body released pollution. Few studies have considered the simulation of the transient respiration flow when estimating exposure to indoor pollutants using a thermal breathing manikin or CFD model of a person. Most of the studies focused on exposure to pollutants in the air exhaled by other occupants (i.e. the focus is cross-infection between room occupants) or pollution released somewhere in the room. The reported research on airflow interaction in the breathing zone and its effect on exposure of persons to their own bio-effluents is limited and incomplete. Local source control has been studied little. Bivolarova et al. (2016a, 2016b) showed that it is possible to locally exhaust human body pollution before it is mixed with the room air. Another problem is the method of measurement and data analyses. Most often, instruments with sampling frequency of several minutes are used to measure the concentration of the gas in the breathing zone under transient flow conditions that occur much faster. The results for the exposure are then analysed and presented using the average of the measured gas concentration for some period of time. Thus the dynamics of the airflows, especially in the breathing zone, which is complex and may create fast tracer gas concentration fluctuations, are disregarded. If the sampling frequency of the used instrument is not high enough to measure the fluctuations (variations) of the concentration, this may impose high uncertainty in the estimated exposure.

The first specific objective of this part of the study was to identify the importance of the dynamic characteristics of instruments for tracer gas concentration measurement and establish a method of data analysis for the accurate assessment of exposure. The second specific objective was to determine the impact of the breathing mode (inhalation mouth/exhalation nose/pause, inhalation nose/exhalation mouth/pause), the strength of the invading ventilation flow, the location of the pollution source, and the source control on the exposure of a person to his/her body-generated pollution. When a local exhaust of air is applied in the vicinity of the body, this will change the CBL and thus the entrainment of the pollutants to the breathing zone. Therefore, this study also

considers the application of localized exhaust ventilation. The results relating to the first objective are presented in the following in detail, while the results relating to the second objective are reported in detail in Paper I (Appendix B). In the following text, this paper is referred for details on the method.

2.2 Method

The same experimental facilities, measuring instruments and conditions were used to provide answer to the two specific objectives.

2.2.1 Experimental setup and facilities

Full-scale experiments with a seated thermal manikin were carried out in a climate chamber with controlled indoor air temperature and ventilation rate. The climate chamber had dimensions of 4.7 m x 6.0 m x 2.5 m (W x L x H). The chamber was ventilated by an upward piston air flow with air velocity of less than 0.05 m/s. Outdoor air was supplied from the entire floor area and exhausted through a square opening in the ceiling (see Figure 1). The chamber has been constructed to ensure a mean radiant temperature equal to the room air temperature and negligible radiant temperature asymmetry.

A breathing thermal manikin with realistic female body shape and size was used to simulate the dry heat loss of a seated occupant who performs light sedentary activity. The surface temperature of the manikin's body was controlled to be similar to the skin temperature of an average human under thermal comfort state when exposed to the same room conditions. The manikin was seated behind a desk on a computer chair (Figure 1). The distance between the manikin's abdomen and the edge of desk was 0.1 m during all measurements. The manikin and the desk were positioned in the centre of the chamber on a wooden plate (2 m x 1.21 m) in order to prevent disturbance of the CBL. The seated manikin had slightly backwards inclined body posture (10° from the vertical axis). The manikin was dressed in tight clothing, resulting in a total thermal insulation (together with the chair) of 0.55 clo (EN 7730, 2005). There was a short-haired wig on the manikin's head. The breathing function was simulated by artificial lungs. It was possible to adjust the breathing frequency, the pulmonary ventilation rate (L/min), and the temperature of the exhaled air.

In some experiments a seat-integrated local exhaust named "Ventilated seat cushion" also referred in the text as "ventilated cushion" (VC) was used to exhaust the contaminants emitted from the manikin's body. The VC was placed on top of the chair (see Figure 2). The surface of the VC in contact with the manikin's body had openings of diameter 6 mm used to suck air through the cushion. The openings were placed in eight horizontal channels to avoid blocking by the manikin's body. There were two openings per row and the distance between them was 0.135 m. The VC was connected to a local exhaust system which moved the exhausted air out of the chamber (Figure 1).

Personalised ventilation supplying clean air to the breathing zone of the thermal manikin via a round movable panel (RMP) was used in this study to generate external ventilation flow (Figure 2). The RMP was installed on the desk in front of the manikin and positioned so that the distance

between the outlet and the face of the manikin was 30 cm, which is one of the positions most preferred by users (Kaczmarczyk et al. 2002). The average air speed of the personalised flow, referred to hereafter as velocity of the personalised flow, was determined based on velocity field measured across the flow at a distance of 30 cm from the RMP without the presence of the manikin. Detailed descriptions of the manikin, the VC flow rate control system, and the experimental set-up are provided in Paper I.
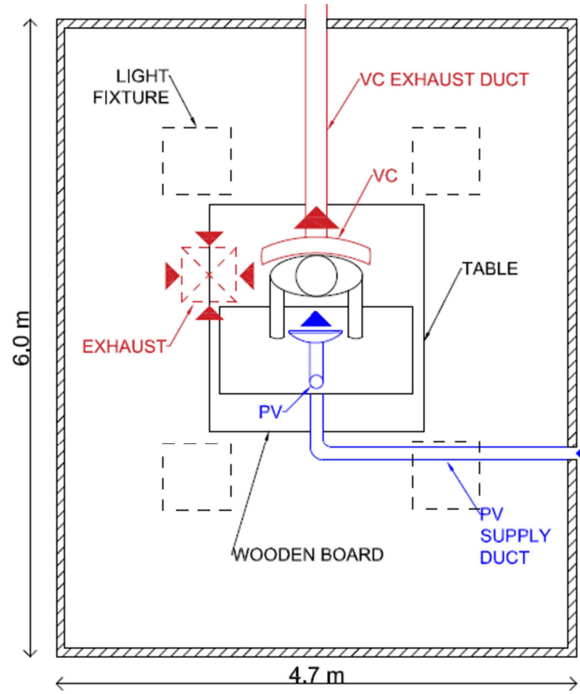
Figure 1: Experimental set-up in the climate chamber.
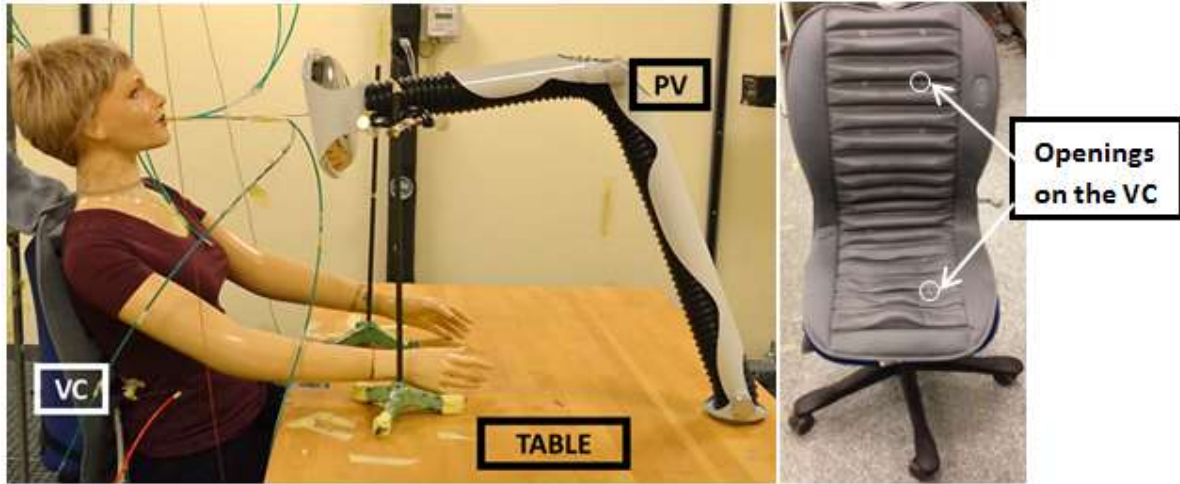
Figure 2: The thermal manikin seated on the chair with incorporated ventilated cushion in front of the table (left); the chair with the ventilated cushion (right).

2.2.2 Measuring procedure and instrumentation

Two tracer gases nitrous oxide (N_2O) and carbon dioxide (CO_2) were used to simulate bio-effluents contaminants emitted from the manikin's groin area and armpits respectively, below the clothing of the manikin. The tracer gases were constantly released with negligible initial momentum.

Two types of instruments were used to measure the concentration of CO_2 and N_2O – Innova gas monitors which use Photoacoustic Spectroscopy and specially developed instruments based on non-dispersive infrared absorption (NDIR) method. Two separate Innova 1312 gas monitors each coupled with an Innova 1303 gas sampler were used to measure the N_2O and CO_2 concentrations. The Innova gas monitors, called "slow" instruments, measured the tracer gases concentrations in four channels with a sampling rate of 0.025 Hz/per channel. The new nondispersive infrared detector, called a "fast" instrument, had a sampling rate of 4 Hz and time constant of 0.8 s. Frequency correction of the signals from the fast instruments was applied using Fourier transformation according to Kierat and Popiolek (2017).

Small plastic tubes (Ø 3 mm) were placed at the opening of the left nostril and the mouth of the manikin (between the centres of the lips, at 0.005 m distance) to collect tracer gas for analyses by the fast and the slow instruments (Figure 3). At each measurement location, a separate N_2O and CO_2 fast instrument sampled the gas concentration. The slow (the Innova gas monitors) instruments were sampling only at the mouth and not at the nose. The slow instruments were also used to measure the N_2O and CO_2 concentrations in the air supplied to the chamber, the PV supply air, and the exhaust air of the chamber. The Innova gas monitors and the fast meters were cross-calibrated before and after each experimental session.

Instantaneous air speed and temperature were measured at the mouth of the manikin. The air speed was measured with an omni-directional low velocity thermal anemometer and the air temperature was measured with a micro bead VECO thermistor.

Further information about all instruments, including their accuracy and resolution, is provided in Paper I.
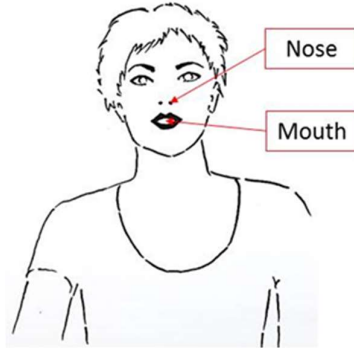
Figure 3: Tracer gas measuring points in the left nostril of the manikin and between the centres of its lips (at 0.005 m distance).

2.2.3 Experimental conditions

All measurements were conducted under steady state conditions. 100% clean outdoor air was supplied in the chamber without any recirculation. The air temperature in the chamber was controlled to be 23°C±0.2°C. The relative humidity was not controlled. It was measured during all experiments to be in the range of 30-40% (±5% relative error). The only heat sources in the chamber were the thermal manikin and four fluorescent light fixtures (6 W each) located on the ceiling (see Figure 1).

The simulated breathing process of the manikin corresponded to a person at light sedentary activity: breathing frequency was 10 times per min with a cycle of 2.5 s inhalation, 2.5 s exhalation, and 1 s pause and pulmonary ventilation equal to 6 l/min. This corresponds to a respiration flow rate of 14.4 l/min. The temperature of the exhaled air was set to 34°C. Experiments at two breathing modes, namely inhalation nose/exhalation mouth/pause and inhalation mouth/exhalation nose/pause, were studied. Experiments without breathing were performed for comparison.

The separate and combined effect of the personalised ventilation and the ventilated cushion exhaust airflow rate (1.5, 3 and 5 L/s) on the exposure was studied. The effect of the personalised ventilation flow was studied at two mean air velocities 0.2 m/s (3 L/min) and 0.4 m/s (6 L/min). The personalised air was supplied to the breathing zone at 23°C (isothermal condition). The studied experimental cases are listed in Table 1.

Table 1: Studied cases – combinations between breathing mode, use of VC and PV.

	No breathing			Inhalation nose/ Exhalation mouth				Inhalation mouth/ Exhalation nose	
VC [L/s]	OFF	1.5	5.0	OFF	1.5	3.0	5.0	OFF	1.5
PV [m/s]	OFF 0.2 0.4	OFF 0.2	OFF 0.2	OFF 0.2 0.4	OFF 0.2	OFF	OFF 0.2	OFF	OFF

2.2.4 Exposure assessment and data analyses

Continuous tracer gas measurements were performed simultaneously with the fast and the slow instruments. The data collected with the fast instruments were analysed in two different ways: 1) analyses based on samples collected during continuous measurement with and without breathing and 2) analyses based on samples measured only during the inhalation period in case of simulated breathing.

The results with the slow instrument were based on samples of continuous measurements in all cases, with and without breathing. The data obtained from the fast and slow instruments were used to calculate the 95th percentile, mean, and standard deviation (SD). The uncertainty of the tracer gas measurements was 20 ppm (95% confidence interval and coverage factor of 2). The excess concentration of CO_2 over the background level was used as criteria for exposure assessment to armpit-emitted pollutants.

An example of how the concentrations of the tracer gases were selected only for the inhalation period is shown in Figure 4. The signal in the figure represents instantaneous N_2O concentration measured at the nose and mouth when the manikin's breathing cycle was set to inhalation mouth/exhalation nose/pause. At first, signals measured at the mouth and nose were synchronized to each other using cross-correlation function. Next, the exhalation periods were identified on the measured signal as cyclically repeating fragments with very low concentration (about 0 ppm). In this way, a binary signal of the whole breathing process was obtained, making it possible to extract the inhalation periods (note in Figure 4 as "selected inhalation period"). The concentrations measured during 40 min steady state conditions were used in the analyses.
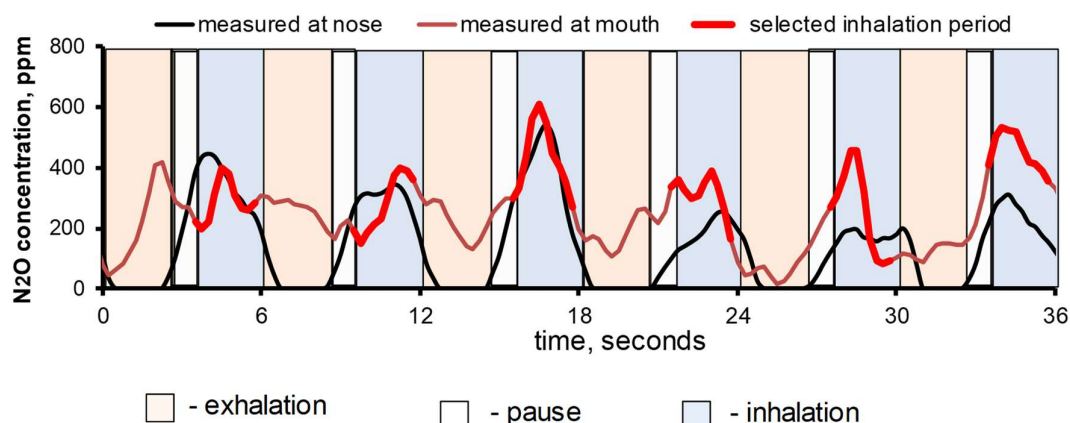
Figure 4: An example of the binary signal for the breathing mode inhalation mouth/exhalation nose/pause obtained from the measured instantaneous N_2O concentrations at the mouth and at the nose. The selected concentrations during the inhalation are marked with red.

2.3 Results and discussion

2.3.1 Measurements for exposure predictions to body-emitted bio-effluents

This section present the results from the tracer gas measurements carried out with the two types of instruments. The effects of different factors important for accurate prediction of exposure to body-emitted pollutants are discussed including: the dynamic characteristics of measuring instruments, source location relative to the breathing zone, measurement only during inhalation period, measuring period during transient breathing and effect of different airflow interaction taking place in the breathing zone.

The N_2O and CO_2 concentrations measured during 40 min steady state conditions were used in the analyses. The analyses of the results showed that in order to determine the mean, the SD and the 95th percentile of the tracer gas concentrations with standard uncertainty of less than 5%, a measuring interval of 30 min was sufficient for the fast instruments. In the case of the slow instruments the uncertainty of the estimated quantities (mean, SD and 95th percentile) for an interval of 40 min was found to be 10%. Note that these observations were made after reaching stable tracer gas concentrations.

The concentration measurements of N_2O and CO_2 presented in the next Figures 5 and 6 were carried out with the respiration mode inhalation nose/exhalation mouth/pause when the breathing was activated. Figure 5 shows the mean, the SD, and the 95th percentile of the N_2O (released from groin) and CO_2 (released from armpits) concentrations for different measuring periods. Results based on analyses of continuous measurements that include the whole breathing period (i.e. inhalation, exhalation, pause) and results based on the measurements with the fast instruments only during the inhalation period are compared. The mean N_2O concentration (Figure 5a) based on measurements with the fast instrument only during the inhalation periods was about 35% higher

compared to the measurements during the entire breathing period (inhalation/exhalation/pause) with both "fast" and "slow". This result indicates that the exposure to the bio-effluents from the groin was the highest in the moment of inhalation compared to the periods of exhalation and pause. In contrast, when the CO_2 was sampled with the fast instrument, no difference was observed in the mean, the SD and the 95th percentiles of the CO_2 concentration when they were estimated for the whole breathing cycle and only for the inhalation period (Figure 5b). The reason why there is no difference between 'inhalation' and 'whole breathing' may be because the exhalation jet from the mouth interacts with the manikin's convective boundary layer and causes mixing in the breathing zone of the pollution generated at the armpits (i.e. CO_2 tracer gas). The mixing effect is not diminished during the 1 second pause thus resulting in uniform CO_2 concentration during the whole breathing cycle. As seen, the mean, SD and 95th percentile of the N_2O and CO_2 concentrations obtained with the slow instrument were different than those obtained with the "fast" (Figure 5). The results suggest that underestimation (Figure 5a) or overestimation (Figure 5b) of exposure can be derived from measurements with slow instruments. Based on additional measurements (not shown) it was found that a measuring interval of more than 90 min (after steady state gas concentration was observed) with the slow instruments was needed to estimate the mean, the SD and the 95th percentile of the tracer gas concentrations with uncertainty of less than 5%. Therefore, it is recommended that the tracer gas concentration be measured at the breathing zone for an adequately long time for accurate determination of the needed quantities.

Figure 6 shows results obtained in a more complicated case of airflow interaction at the breathing zone, i.e. when personalised flow with mean velocity of 0.4 m/s from front was applied in addition to the free convection flow and the flow of exhalation. The results in Figure 6 are based on analyses of continuous measurements that include the whole breathing period and results based on measurements with the fast instruments only during the inhalation period. In Figure 6a, results from additional measurements conducted without breathing are shown. The comparison of the results shows large differences. In the case of pollution generated at the groin and simulated breathing, the concentration measured with the fast instrument was higher than that measured with the slow instrument (Figure 6a). No difference is observed in the N_2O concentration measured with the fast instrument only during the inhalation period and the N_2O measured for the whole breathing period when PV flow was supplied to the inhalation zone. This result can be attributed to the effect of the personalised flow, which was penetrating the convective boundary layer and demolishing the jet of exhalation from the mouth and thus creating a uniform flow. With no breathing simulation, the N_2O concentration measured with either the fast or the slow instruments show the same mean values. However, the 95th percentile estimate based on the measurements with the fast instrument is higher than that measured with the slow instrument. When the pollution was generated at the armpits, the concentration determined with the slow instrument was higher than that determined with the fast instrument. The results suggest that the slow instrument is unable to detect the complete range of the tracer gas fluctuations due to its low frequency response time. The mean, SD, and 95th percentile of the CO_2 concentration obtained for only the inhalation periods were slightly higher than the ones estimated for the whole breathing period (Figure 6b). It seems that the PV flow, which is opposing

to the exhalation flow, had an impact on the dispersion of the armpit-emitted pollutants in the breathing zone.

a)

b)
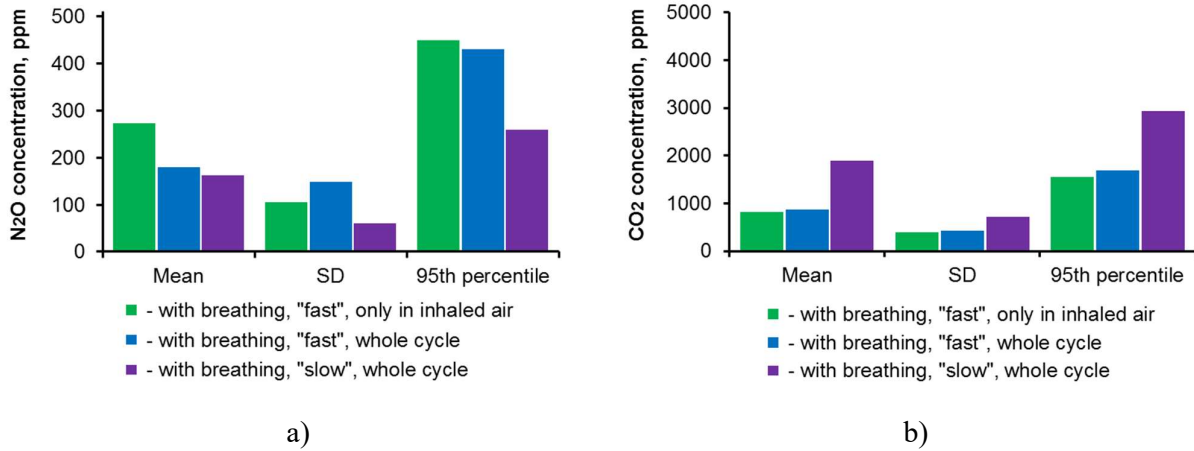
Figure 5: Concentration measurements with fast and slow instruments of tracer gas released at (a) the groin (N_2O) and (b) the armpits (excess CO_2) of a breathing thermal manikin.

a)

b)
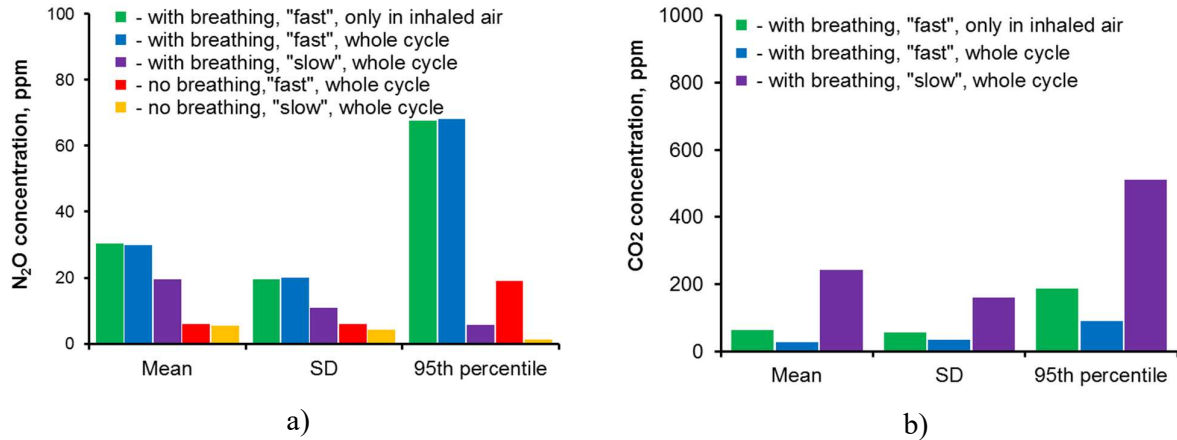
Figure 6: Concentration measurements with fast and slow instruments of tracer gas released at (a) the groin (N_2O) and (b) the armpits (excess CO_2) of a breathing thermal manikin in case with personalised flow directed against the face.

Tracer gas measurements are widely used to assess exposure to indoor pollution. Based on continuous measurements, the mean concentration is calculated and used for assessment of exposure. The results of this part of the current thesis confirm that careful consideration of the airflow interaction at the breathing zone, the dynamic characteristics of the tracer gas measuring instruments, and the measuring time are important for accurate tracer gas measurement. Depending on the airflow interaction at the breathing zone and the location of the tracer gas source, the concentration measured at the nose of the manikin can be much different when fast or slow instrument is used. The concentration can also be much different when it is measured only during

the inhalation period versus when it is measured continuously during the whole breathing cycle, resulting in different exposure assessment.

The results also show that the 95th percentile of the concentration has much higher values than the mean concentration. Often tracer gas measurements are used to predict the risk of airborne cross-infection. The question is: Which of these two quantities is more important for exposure assessment in general and in particular for prediction of the risk of airborne cross-infection? Although the answer of this question remains to be studied, it is recommended to use fast instruments for concentration measurement, especially in cases when complete mixing of pollution is not present in the air at the breathing zone. It is also recommended to perform exposure analysis on concentration measurements only during inhalation period. Note that in this section account only one breathing mode, namely inhalation nose/exhalation mouth/pause, was taken into account. In the section that follows, results obtained for the breathing mode inhalation mouth/exhalation nose/pause are also presented and compared with tracer gas (N_2O and CO_2) concentrations measured in case of no breathing.

2.3.2 Effect of airflow interaction in the breathing zone on the exposure to body bio-effluents

The following part is based on Paper I (Appendix B). Detailed information on the results, discussion and conclusions can be found in this appended paper.

2.3.2.1 Occupant exposure due to interaction of CBL and flows of exhalation

The air quality in the breathing zone of the manikin depending on the source location and the flow interaction between the CBL and exhalation flow from nose or mouth is illustrated in Figure 7 and Figure 8. Inhalation nose/exhalation mouth is abbreviated as InN/ExM and inhalation mouth/exhalation nose as InM/ExN. The results show no large effect of the breathing mode on the occupant's exposure when the pollution source is located at the groin area (Figure 7). From this figure, it can be observed that the N_2O concentration measured without breathing is similar to the concentration measured with breathing. The slightly higher concentration obtained in the case of exhalation through the mouth can be explained by the flow interaction at the breathing zone. The pollution generated at the groin is moved upward by the CBL in front of the manikin's body. The exhaled jet entrains air from the surroundings, including from the CBL, and thus "pulls" more pollution to the breathing zone. The interaction of the jet exhaled horizontally from the mouth with the CBL causes mixing, which calms down during the pause. The CBL re-establishes and moves the contamination to the zone of inhalation. In the case of exhalation from the nose, the two jets released from the nostrils are diverted 30°-50° downward towards the chest and do not collide but diffuse as two independent jets (Cermak et al., 2002). The jets are opposing to the CBL at the chest and interact mainly with its sides. The resulted mixing has less effect on the central zone of the CBL, calms down during the pause, and does not affect the transport of pollution from the groin. Thus it remains nearly the same as in the case without breathing. The standard deviation of the concentration fluctuations in the three cases is also almost the same, suggesting the same level of mixing. Graphic representation of the described airflow interactions and their effect on the transport of the groin-emitted bio-effluents to the inhalation zone is illustrated in Paper I.

In contrast, when the pollution is generated at the armpits, a much higher difference in the mean, SD, and 95th percentile of CO_2 concentrations during the two studied breathing modes is measured (Figure 8). The mean CO_2 concentration is 46% lower when the manikin is inhaling air through the nose compared to when it is inhaling from the mouth. The difference between the 95th percentile values is 52%. These results indicate that the personal exposure depends on the breathing mode and location on the body from which bio-effluents are released. The measurements at the mouth and nose of the manikin when the breathing function was turned off showed that the mean CO_2 concentration was slightly lower than the concentration measured at the nose (inhalation nose/exhalation mouth). As discussed previously, the jet emerging from the mouth interacts with the CBL and causes mixing which calms down during the pause period. In this case (as well as in the case without breathing), most of the pollution generated at the armpits is transported upward and little part is entrained by the flow from the mouth resulting only in a small increase of the exposure compare to the case without breathing. In the case of exhalation from the nose, the jets discharged from the nostrils interact with the CBL and intensify the mixing in the areas close to the source location (i.e. armpits). As a result, more CO_2 is mixed with the CBL, transported upward, and inhaled through the mouth. Therefore, as it can be seen the mean, SD, and 95th percentile of the CO_2 concentration are higher when air is inhaled through the mouth compare to the other two cases. This is an important observation since assessment of exposure to own body-released bio-effluents without breathing simulation may lead to incorrect exposure assessment depending on the location of the pollution source. Graphic representation of the described airflow interactions and their effect on the transport of the bio-effluents emitted from the armpits to the inhalation zone is also illustrated in Paper I.
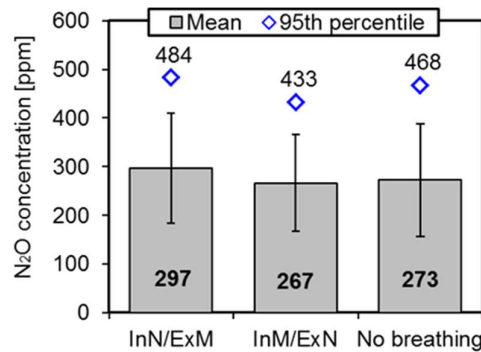
Figure 7: Mean and 95th percentile of N_2O concentration (pollution from the groin).
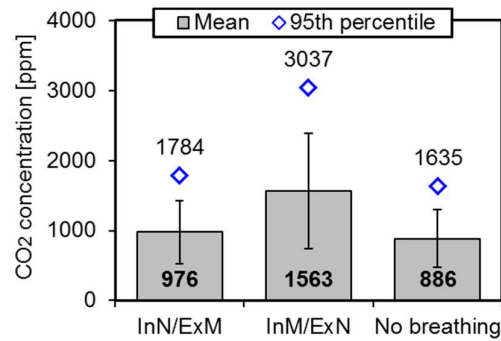
Figure 8: Mean and 95th percentile of excess CO_2 concentration (pollution from the armpits).

2.3.2.2 Effect of the local exhaust flow from the ventilated cushion on the occupant's exposure

The results of the experiment performed to study the importance of the VC at 1.5 L/s under the different breathing modes, namely inhalation nose/exhalation mouth and inhalation mouth/exhalation nose, as well as no breathing are shown in the appended Paper I for both N_2O and CO_2 tracer gas measurements. The results reveal that the use of the VC as local source control is very efficient for reducing the exposure to groin-emitted pollutants. This is an important result since Licina et al. (2015b) reported that the source of pollutants emitted at the lower body parts, such as the groin, spreads more across the room compared to the pollutants from the upper body parts. It can therefore be assumed that the application of the VC will be beneficial not only for the occupant who is using it but also for the other occupants in the room. However, the ventilated cushion operating at 1.5 L/s was less effective in reducing armpit-emitted pollutants. The reason was that the cushion was not in good contact with the manikin's body at the area of the armpits (see Figure 2 left) and thus the relatively strong CBL flow prevailed in transporting the released pollutants. Furthermore, it was found that the effect of the exhaled jet is important for the performance of the local source control. When the VC works at 1.5 L/s, it pools air and some pollution from the armpits but this does not have an effect on the inhaled pollution concentration. The reason for this is that the entrainment effect of the exhaled jet from the mouth is stronger than that from the nose; when the exhalation was from the nose, the increased mixing of the pollutants from the armpits overcame the performance of the VC in removing the pollution. As a result, the concentration increased in the inhaled air. It was also found that when breathing was not present the performance of the VC at 1.5 l/s was not disturbed and some of the pollutants from the armpits were removed by the VC. This result again argues the importance of breathing as related to the airflow interaction in the inhalation zone.

The importance of the source control was studied at higher exhaust airflow rates of 3 and 5 L/s. The experiments were performed only for the case of inhalation through the nose/exhalation through the mouth. The results are shown in Paper I. Some of the results can be also seen in Figures9 and 10 below. In general, the ventilated cushion was able to capture the emitted pollutants both at the groin and the armpits when the flow rate of the exhaust air was increased from 1.5 L/s to 3 and 5 L/s. However, our results show that the design needs improvement in order to be able to evacuate

pollution generated at the armpits more efficiently. It should be noted that body posture and movement play important role in the case of seated occupants.

2.3.2.3 Effect of the interaction of CBL, flow of exhalation and facially applied ventilation flow on the occupant's exposure

The results of the measurements of CO_2 concentration (pollution generated at the armpits) under more complex flow interaction including CBL, exhalation from the mouth, and personalised flow against the face are shown in Figures 9 and 10. The obtained mean, SD, and 95th percentile concentrations were normalized by the mean concentration obtained in the respective case with or without breathing simulation and without the use of VC and PV. The purpose of the normalization was to quantify the effects of the VC and PV on the exposure. Normalized concentration lower than "1" indicates that inhaled pollution concentration is reduced, i.e. reduced exposure. Results for the groin-emitted contaminants measured under the same conditions are shown and discussed in Paper I. Figure 9 shows results obtained with breathing function ON. Figure 10 shows results measured without breathing. The comparison of the normalized concentrations in Figures 9 and 10 shows that in case with and without breathing the use of PV at 0.2 m/s reduces slightly the exposure to CO_2. The effect of PV at 0.2 m/s was found to be more prominent for the N_2O (results shown in Paper I). In Figure 9, it can be seen that the use of the VC at 1.5 L/s does not work efficiently. As in the case without VC, the CBL moves part of the CO_2 upward to the face where it is inhaled. Therefore, no difference in the concentration of CO_2 in the inhaled air exists with or without VC in operation (Figure 9 – bars 1 and 3). Without breathing, the inhaled CO_2 concentration decreases because the entrainment effect of the exhaled jet is not present and more CO_2 is transported above the shoulders and the head by the CBL and less to the face (bar 1 in Figure 9 and bar 1 in Figure 10; bar 3 in Figure 9 and bar 3 in Figure 10). The minimal effect of the VC at 1.5 L/s is also observed when it is combined with the PV at 0.2 m/s. This is because the supplied clean personalised air is mixed with the polluted air of the CBL and dilution takes place (Figure 9 bar 4 and Figure 10 bar 4). A similar effect from the PV at 0.2 m/s was observed for the groin-emitted pollutants. However, the personalised flow at 0.2 m/s is not able to completely penetrate the CBL, which pushes the PV flow upward (visualization of the PV flow is shown in Paper I). The exposure is reduced due to the efficient local removal of CO_2 when the flow rate through the VC is increased (bars 3 and 5 in Figures 9 and 10). The CBL can produce a vertical air velocity up to 0.25 m/s (Homma and Yakiyama, 1988; Licina et al. 2015c), which is comparable to or higher than the maximum indoor velocity recommended in standards. Thus in rooms with little mixing (e.g. displacement ventilation) but also in rooms with mixing ventilation (e.g. diffuse ceiling), the flow velocity within the CBL will be stronger than the ventilation flow and will increase the exposure to own body bio-effluents. Removal of contaminants at the location where it is generated is the first step to be applied for exposure reduction.

The results in the figures also show that increasing the PV velocity to 0.4 m/s makes it possible to remove the CBL at the face and provide clean air to the breathing zone (Figure 9 bar 7 and Figure 10 bar 6). In the case of combined use of the VC at 5 L/s and the PV at 0.2 m/s, the interaction of the PV flow with the CBL generates mixing, resulting in an increase of CO_2 in the inhaled air

(entrainment of CO_2 by the exhaled jet may also help exposure to CO_2). This can be seen in Figure 9 bars 5 and 6. The results in Figures 9 and 10 show that with breathing the concentration of CO_2 in the inhaled air is higher compared to without breathing because the exhaled jet entrains CO_2, meaning that more CO_2 is mixed with the CBL and is transported to the nose (Figure 9 bar 3 and Figure 10 bar 3). Without breathing, more of the generated pollutants are moved upward above the shoulder and the head by the CBL on the side of the body. The impact of the entrainment of CO_2 by the exhaled jet and thus on the increase of exposure is present even when the VC runs at 5 L/s (Figure 9 bar 6). This is because the VC removes the CO_2 from the back side of the armpits, while the exhaled jet entrains the CO_2 present at the front of the armpits.

Higher absolute values of the 95th percentiles of the CO_2 concentration were observed in the cases with breathing and PV (at both velocities of 0.2 m/s and 0.4 m/s) compared to the corresponding cases without breathing (results shown in Paper I). Thus the effect of breathing on the transport of pollutants from the upper part of the body to the breathing zone can be recognized not only in a calm environment but also when flow opposing the flow of exhalation is generated. Rim and Novoselac (2009) also reported that breathing increases the exposure. However, they found that in case of stratified flow in the room after activation of the breathing, the concentrations of fine and course particles released at floor level, i.e. far from the breathing zone of a seated breathing thermal manikin, increase at the mouth. In the current study, it was found that breathing was not important for the exposure to pollution generated far from the zone influenced by the exhaled flows, e.g. groin. This result is in agreement with previous studies reporting that the breathing mode has no significant effect on the personal exposure to room polluted air, which was supplied by upward piston flow (Melikov and Kaczmarczyk, 2007). Brohus and Nielsen (1996) performed exposure measurements with a breathing thermal manikin in a room with displacement ventilation. They reported that there is no significant difference between breathing through the nose and breathing through the mouth in the case of a heated point source released in the room. The discrepancy between the results presented here and those of Rim and Novoselac (2009) could be due to the different source locations. A further study with more focus on different source characteristics is therefore suggested.
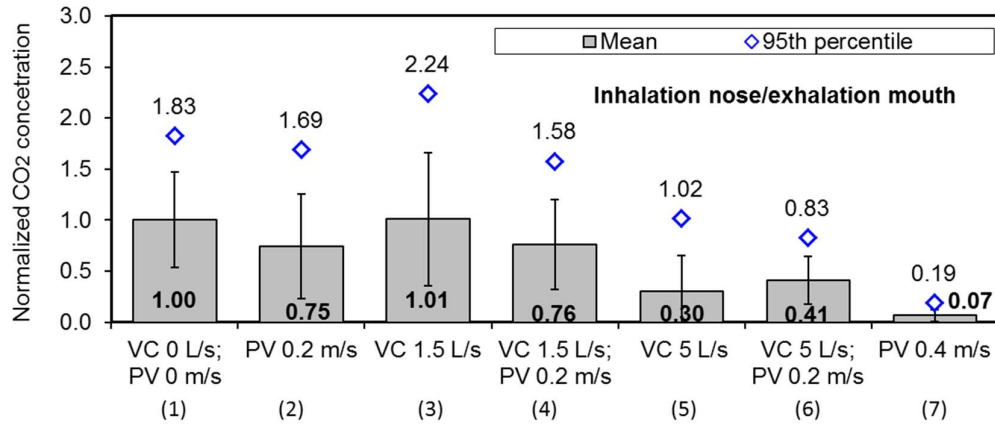
Figure 9: Normalized excess CO_2 concentration with breathing ON. Mean and 95th percentile are normalized by the mean concentration measured during VC 0 L/s, PV 0 m/s.
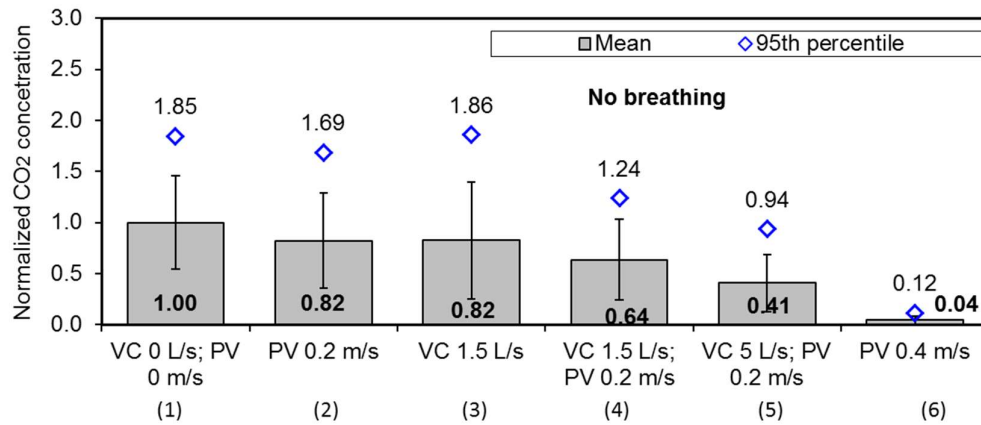
Figure 10: Normalized excess CO_2 concentration with breathing ON. Mean and 95th percentile are normalized by the mean concentration measured during VC 0 L/s, PV 0 m/s.

In this part of the study for the first time the exposure to body released bio-effluents as a result of complex interaction of flows and local source control is examined by proper tracer gas concentration measurements only during the inhalation period. The results were obtained at limited number of experimental conditions. Different body size and posture, head positioning, clothing design, breathing mode, cycle, respiration rate and other individual difference between people, as well as table positioning, chair design, room air and radiant temperature, direction and characteristics of the ventilation flow at the vicinity of the body, etc. will affect the airflow interaction at the breathing zone and thus the exposure. Therefore further studies are recommended.

2.4 Conclusions

This part of the study investigated the method of tracer gas concentration measurement, including measuring instruments with different response time and analyses of the collected data for correct assessment of exposure. The influence of the complex interaction of breathing flow, convective flow around the human body and ventilation flow directed against the face on the exposure to body bio-effluents was examined together with the effects of source location and control. The experimental results show the following:

- Exposure assessment based on tracer gas concentration measurement can be incorrect if the measuring instrument has long response time and the complex airflow interaction at the breathing zone is not correctly simulated;

- The 95th percentile of the concentration measured during inhalation is much higher than the mean concentration. This needs to be considered during exposure assessment and prediction of the risk of airborne cross infection;

- Due to the complex airflow interaction at the breathing zone the tracer gas concentration should be measured for sufficiently long time for accurate determination of the needed quantities;

- Exposure to body bio-effluents depends on the complex airflow interaction of the CBL, flow of exhalation (breathing mode), and locally applied ventilation flow on the breathing zone;

- The interaction of the exhaled flow with the CBL increases the exposure to own body released pollution especially when the site is close to the breathing zone;

- Breathing does not influence exposure to gaseous pollutants emitted from the lower part of the body.

3 Use of tracer gas measurements as reliable indicator for transport and exposure to aerosols indoors

3.1 Introduction

This chapter presents results of the relationship between the transport behaviour of gas and aerosols. The following part is based on paper II, where detailed information can be found.

3.1.1 Indoor Aerosol Particles and health effects

People are frequently exposed to different pollutants present in the air. Airborne particles (also known as aerosols) are a major exposure concern due to their effects on human health. They can penetrate the respiratory system and cause inflammatory effects (Koullapis et al., 2016; Long et al., 2001). Particles with biological origins, such as bacteria and fungi, can activate allergic alveolitis and allergic asthma symptoms among occupants (Burge, 1990). Bio-aerosols, including bacteria and viruses, present special health threat due to the risk of infection. For instance, droplets expelled by people during breathing, coughing or sneezing can carry pathogens (e.g. Mycobacterium tuberculosis) and cause the transmission of infectious diseases to other occupants (Bolashikov and Melikov, 2009; Li et al., 2007). Infection occurs when a receptive person inhales infectious droplet nuclei and the particles deposit in the lungs (Seitz et al., 1998). Therefore, it is vital to have a good understanding of the spread of aerosols in occupied spaces.

3.1.2 Behaviour of tracer gas and aerosol particles

Many studies have shown that the effect of airflow distribution on personal exposure to indoor air pollutants varies with regards to the air distribution method used (Bjørn and Nielsen, 2002; Bolashikov et. al.,2012; Cermak and Melikov, 2007; Li et. al., 2007; Nielsen et. al. , 2008; Olmedo et. al., 2012; Rim and Novoselac, 2009; Zhao et al., 2004). Full-scale experiments and computational fluid dynamics (CFD) predictions are among the most popular methods used today to help understand the air pollution distribution in ventilated rooms (Chen, 2009; Tang et. al. , 2011).

CFD provides highly time- and space-resolved simulations though there are uncertainties and errors associated with the CFD boundary conditions and numerical schemes (Sørensen and Nielsen, 2003; Wang et. al., 2012). Therefore, it is essential that the computational simulations be validated with data obtained from experimental measurements. Full-scale experiments are valuable because they include actual thermo-fluid conditions, which allow studies to be performed at close to real conditions. A number of experimental studies relied only on tracer gas measurements to investigate the dispersion of both gaseous and particle indoor-emanated contaminants. Tracer gases have been used in studies with different indoor-specific scenarios such as office space, aircraft cabin, hospital ward, etc. As already mentioned in the previous chapter, tracer gases such as SF_6, N_2O and CO_2 have been used to mimic the movement of infectious aerosol droplets emitted by air exhaled from a breathing thermal manikin in simulated hospital wards (Bolashikov et. al., 2012; Nielsen, 2009; Qian et. al., 2006). However, particles are larger and heavier than gas molecules and may not be accurately represented by tracer gas. There are several differences between the behaviour of tracer

gas and aerosol particles. The key difference is observed when they approach a surface; the tracer gas molecule reflects from the surface, whereas the aerosol particle attaches to the surface via an adhesive force. Moreover, the probability of particle deposition on a surface depends strongly on particle size. Ultrafine particles, up to diameters of a couple hundred nanometres, exhibit Brownian motion and deposit on all surfaces by diffusion; the smaller the particle the more intense the diffusional deposition is observed. Particles larger than several hundred nanometres in diameter exhibit non-negligible mass and inertia. They can be deposited either by gravitational settling at longer residence times on upward-facing surfaces or by inertial impaction at higher Stokes numbers on surfaces facing their original direction of motion. The larger the particles, the higher the observed deposition rates. Particles in the middle size range, e.g. between 200 nm to 1 μm, are only weakly influenced by the above-mentioned mechanisms and their deposition rates are negligible.

It has been implied that airborne particles (particularly exhaled droplet nuclei) smaller than 5 μm can be simulated with tracer gas, since they can be suspended in the air for long time due to their small settling velocity (Tang et al.,2011; Nielsen, 2009; Seitz et al., 1998). These studies suggested that the particles will follow the air stream. However, only a few studies have conducted direct comparisons of tracer gas and particle behaviour in ventilated rooms. Zhang et al. (2009) made a direct comparison of the distribution of SF_6 tracer gas and 0.7 μm particles in an air-conditioned full-scale airliner cabin mock-up. They measured the tracer gas and particles concentrations in eight locations at six different heights and found similar distribution of the two simulated pollutants in most part of the cabin (except one location close to the ceiling). The difference between gas and particles distribution has also been investigated in an actual first-class aircraft without simulated occupancy (Li et al., 2014). The concentration of SF_6 and the 3 μm aerosol particles matched with each other well in the measured sections when they were generated from the same location. A study by Noakes et al. (2009), simulating a hospital isolation room with mixing air distribution (10 ACH), showed agreement between the behaviour of N_2O tracer gas and 3 – 5 μm particles, both of which were released from a heated cylinder (resembling a patient in bed). Another related study by Beato-Arribas et al. (2015) concluded that CO_2 tracer gas and aerosolised *Bacilus subtilus bacteria* (< 2μm) are comparable in their distribution in a single isolation hospital mock-up ventilated at 12 ACH. One disadvantage of these studies is that the measurements of the pollutant concentrations at the breathing zone of a simulated person with realistic body geometry and skin temperature distribution were not performed. The complex human body shape and the buoyancy flows generated from the body are important for transport of pollution at the vicinity of the body, exposure, and air distribution in spaces (Melikov, 2004; Zukowska et. al., 2012).

As already shown in Chapter 2, the convective boundary layer (CBL) around the human body adds to the complexity of a room's airflows interactions and occupants' exposure to pollutants (Licina et. al., 2015a, 2015b; Melikov, 2015; Rim and Novoselac, 2009). Licina et al. (2015a, 2015b) studied the importance of the CBL around a sitting person and its impact on the transport of gaseous and particle pollutants towards the breathing zone. However, the exposure to particles and tracer gas was studied in different set-ups and thus cannot be directly compared. Rim and Novoselac (2009) investigated the concentration distribution of particulate and gaseous pollutants in the vicinity of a

human body at the same time. They considered the effects of the source position and the overall airflow patterns on the inhalation exposure to the airborne pollutants. These studies provide valuable information on the relationship between air distribution patterns in rooms and the transport of gaseous and aerosol particles. However, they did not provide information on how separate parameters, such as air change rate and increase of surface area by objects in rooms (furniture, etc.), may affect the deposition of particles and, therefore, the relationship between the distribution of gas and aerosol particles in the breathing zone of the occupant. Such information is especially important when studies aim to evaluate the personal exposure to airborne particles in ventilated spaces using only tracer gas.

3.2 Specific objectives

Conducting experiments with particles is generally much more challenging than experiments with tracer gases. Due to the particles' complex nature and highly variable sizes, it is not easy to find and select available measuring techniques (Morawska et. al., 2013). The advantages of using only tracer gas in exposure measurements are: an easy and inexpensive setup, possibility of sampling at many locations and relatively simple processing of the measured data. On the other hand, the gas cannot be used as a complex substitute for particles of all sizes due to the gravity, inertia, and drag force effects acting on them.

The specific objective of this part of the study was to verify the use of tracer gas as a relatively accurate means of identifying exposure to different well-defined indoor aerosol particle sizes. It was examined the relationship between gas and particles dispersion in a room with overhead mixing air distribution. An important aim was to identify the influence of factors, such as air change rate, the surface area inside the room, and the CBL around a sitting person (heated thermal manikin), on the distribution of monodispersed aerosol particles and tracer gas. Also investigated were the effects of the interaction between the CBL generated by a person lying in bed and local exhaust airflow on the dispersion of particles and tracer gas released close to a human body.

3.3 Method

3.3.1 Experimental set-up and design

To meet the above stated specific objectives experiments were performed in a test room of 2.6 m (height) x 4.7 m (length) x 1.66 m (width). The room was carefully sealed prior to the experiments in order to avoid undefined infiltration. The room was air conditioned via mixing total volume air distribution. Outdoor air was supplied to the room through a two-way square ceiling diffuser with solid faceplate (the directions in which the two air jets were discharged by the supply diffuser are shown in Figure 11. The air supply diffuser was mounted in the centre of the ceiling. Just before entering the test room the supplied outdoor air was filtered by a high-efficiency particulate (HEPA) filter, class H14, to ensure particle-free air. The air was exhausted through a ceiling-mounted circular diffuser (Ø 200 mm). The ventilation rate during the experiments was either 3.5 ACH or 7 ACH. A full description of the test room and the ventilation system control is provided in Paper II. Detailed descriptions of the supply and exhaust diffusers can be also found in this publication.

The air temperature inside the room was controlled and kept at 23.2°C ± 0.2°C during all experiments. The temperature around the room was kept at 23.2°C ± 0.2°C as well. The relative humidity inside the room was recorded with a HOBO data logger (Model ONSET U12-013) and was in the range of 30% - 38% ±2% throughout all experiments.

Five experimental scenarios were investigated in order to evaluate the effect of different parameters on the distribution of tracer gas and particles:

Empty room (Scenarios 1 and 2): Scenarios 1 and 2 were performed in an empty room (i.e. isothermal conditions) ventilated at 3.5 ACH and 7 ACH, respectively.

Furnished room with unheated manikin (Scenario 3): in this scenario a real-size unheated (isothermal conditions) dressed thermal manikin was seated (on a computer chair) behind a table in the room. The distance between the abdomen of the manikin and the table was 0.1 m. The ventilation rate in the room was 7 ACH.

Furnished room with heated manikin (Scenario 4): in this scenario the thermal manikin was switched on to represent realistic thermal conditions in an occupied indoor environment. The manikin was the only heat source in the room. The ventilation rate in the room was 7 ACH. The supply air temperature was set to 21.6 °C±0.2°C to keep the room 23°C.

In Scenarios 3 and 4, the manikin was heated but not breathing. It was dressed in a tight long-sleeve shirt, trousers, underwear, socks, and shoes (the total clothing insulation was 0.48 clo). The manikin was previously described in Chapter 2. The average total heat released from the manikin was 74.9 W ±0.24 W (in Scenario 4), simulating the dry heat loss from a human body in a thermally comfortable state.

Single-bed hospital room (Scenario 5): In this scenario a patient hospital room was simulated. The test room was furnished with a bed with the thermal manikin lying on top (Figure 12). A localized exhaust system, ventilated mattress (VM), was placed on top of the regular mattress. The VM had an exhaust opening that was positioned below the gluteal region of the manikin. The manikin was dressed in short-sleeve hospital pyjamas (thermal insulation of 0.60 Clo). The measured average total heat released from the manikin was 73.2 W ±0.13 W. The ACH in the room was 3.5 and the supply air temperature was 21.7°C in order to keep a room temperature of 23°C. The exhaust airflow rate of the ventilated mattress was adjusted to be 1.5 L/s. The exhausted air of the VM was taken out of the room through a separate exhaust system.

3.3.2 Tracer gas and particle generation

During the experiments for Scenarios 1-4, particles of one of the three well-defined sizes (0.07, 0.7, and 3.5 μm) and nitrous oxide (N_2O) tracer gas were generated simultaneously at a constant rate from one location in the room (Figure 11). The three particle sizes were selected to represent particles from the ultrafine, fine, and coarse size ranges, each of which were influenced by different deposition mechanisms. Previous studies (Boor et. al., 2015; Spilak et. al., 2014) have shown that

fine and coarse particles deposited on the surface of a mattress can be re-suspended by a person's movement in bed. In scenario 5 fine particles with 0.7 μm size were released to compare their behavior with that of the tracer gas and at the same time to study the efficiency of the local exhaust ventilation when capturing particles. The pollution source for Scenarios 1-4 was located 0.8 m behind the manikin at a height of 1 m above the floor (Figure 11). The pollution source for Scenario 5 was located close to the gluteal region of the manikin (Figure 12b). The flows of the tracer gas and the particles were mixed in a T-piece connected to a plastic ball (Ø 0.038 m) with a number of small openings equally distributed across its surface. This provided low initial velocity to the tracer gas and particles released into the room. Two different aerosol generators were used to produce monodisperse particles with aerodynamic diameters of 0.07, 0.7, and 3.5 μm. Detailed descriptions of the aerosol generators and the procedure used to release the particles and the tracer gas are given in Paper II (Appendix B).

3.3.3   Measuring points and instrumentation

The N_2O gas and particle concentrations were measured at three points in the room during all scenarios: at the exhaust air, at the centre of the room (1.7 m height), and either at the mouth of the manikin or, in the case of empty room, at a height of 1.12 m at the exact position of the manikin's mouth when it was installed. The sampling tubes for the particles and tracer gas at the mouth of the manikin were placed at the upper lip at a distance of <0.01 m.

The particle number size distributions and total number concentration were measured with several types of aerosol spectrometers: Scanning Mobility Particle Sizer – SMPS 3936L (consisting of an Electrostatic Classifier EC 3080, Differential Mobility Analyzer DMA 3081, and Condensation Particle Counter CPC 3775), Optical Particle Sizer OPS 3330, Aerodynamic Particle Sizer APS 3321, and Condensation Particle Counter CPC 3022 (all TSI Inc., USA). The tracer gas concentration was measured simultaneously at all locations using an Innova 1303 multi-channel sampler and an Innova 1312 gas monitor.

Measurements of the particles and the tracer gas concentrations were carried out continuously from the start of the particle injection and the tracer gas until a steady-state tracer gas concentration was observed. A sufficient number of repeated measurements was obtained in order for the variability of the results to be about 10%. After completion of each measurement, the concentration decay of aerosols and tracer gas was also measured in most cases.
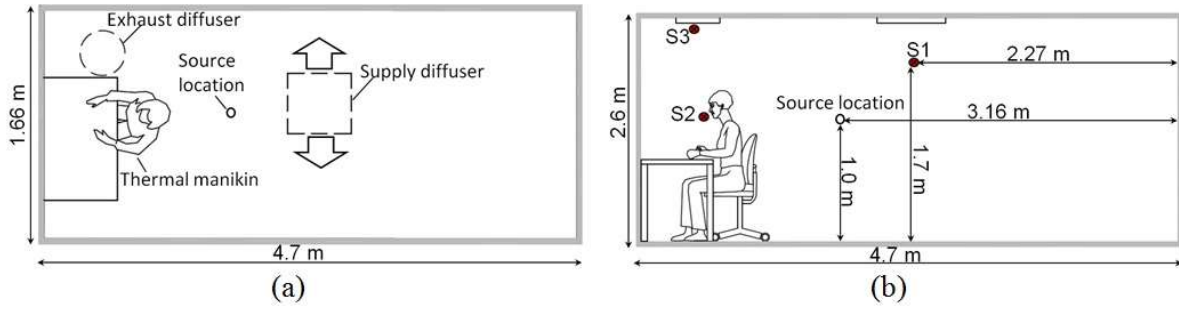
Figure 11: Top view (a) and side view (b) sketches of the room layout for scenarios 3 and 4. Tracer gas and particle air sampling points are designated with S1, S2, and S3.
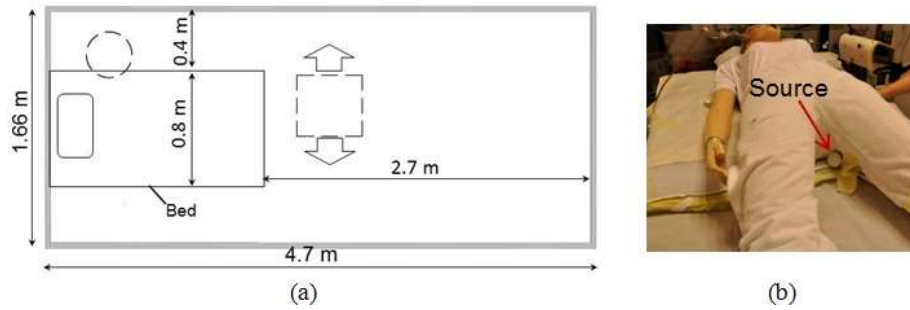
Figure 12: Experimental setup for scenario 5: (a) top view sketch of the room layout (b) pollution source close to the thermal manikin's gluteal region.

The data were analysed by estimating the average concentration of particles (#/cm³) and tracer gas (parts per million (ppm)) during the steady-state time period. The results were then normalized by the average concentration at the exhaust air. This type of normalization allowed comparison between all data sets across all the particles sizes. When the normalized concentration was less than "1" it meant that the concentration obtained at the measured location (breathing zone or centre of the room) was lower than the concentration at the exhaust (i.e. lower contaminant exposure). The variability (coefficient of variation (CV)) of the measurements of the particles and tracer gas is shown in the results as error bars on the column chart. The CV, calculated as the ratio of standard deviation to mean concentration obtained for each location, was less than 10% in most measurements and in the range of 11% - 19% for only a few measurements. All uncertainties estimated based on the measured particle concentrations were 10% of the mean value for all particle instruments. All uncertainties of the tracer gas concentration measurements were calculated to be 5% of the mean.

Further analyses were performed on the particles concentration decay measurements in scenarios 1-4 in order to estimate the overall loss rates of aerosol particles of different sizes. The overall particle loss rate was derived from a simplified mass balance equation:

$$C_i(t) = C_\infty + (C_0 - C_\infty) \cdot e^{-\lambda^* \cdot t}$$

(1)

where $C_{i(t)}$ represents concentration of aerosol particles of a given size indoors at time t, C_0 is the concentration of aerosol particles when the particle generation was stopped, C_∞ is the concentration of aerosol in a steady-state and λ^* is the overall particle loss rate. Details of how equation (1) was derived are provided in Paper II.

The measured concentrations ($C_{i,tn}$) during Scenario 5 were normalized to the tracer gas and particle concentrations measured at time $t_0 = 0$ s at the manikin's mouth and centre of the room ($C_{i,t0}$). The normalized concentrations ($C_{i,tn} / C_{i,t0}$) for each sampling location were calculated by the following equation:

$$C_{norm} = C_{i,tn} / C_{i,t0} \hspace{4cm} (2)$$

where $C_{i,tn}$ is the measured tracer gas or particle concentration at time t_n and $C_{i,t0}$ is the measured gas or particle concentration at time t_0.

3.4   Results and Discussion

3.4.1   Overall particle loss rate for scenarios 1-4

Figure 13 shows overall particle loss rates obtained using the fitting of the simplified solution of the mass balance model to the experimental data. Generally, it can be stated that in Scenarios 1-4, the fine particles (0.7 μm) reached the lowest values of overall particle loss rate, meaning that these particles should have had the most similar behaviour to the tracer gas. In other words, these particles were the least influenced by main deposition mechanisms (Brownian motion or gravitational settling). The results show that the increased surface (presence of manikin, table, and chair) mainly influenced ultrafine particles (0.07 μm) deposited on all surfaces as opposed to coarse particles, which deposited predominantly on upward facing surfaces. This agrees with the finding reported by Thatcher et al. (2002) that large particles are not strongly influenced by increases in vertical and downward facing surface area. On the contrary, submicron particles are more strongly affected, since they deposit effectively to surfaces of all orientations due to Brownian diffusion. By contrast, coarse particles deposit by gravitational settling and settle mostly on upward facing surfaces – represented only by the table and manikin's cross-sections. In Figure 13, it can also be observed that at the higher airflow rate the loss rate of the particles of all sizes increased. These results are consistent with other research, which found the same effect of increasing the room airflow rate on particle deposition (Thatcher et al., 2002; Mosley et al., 2001). In general, aerosol particle deposition indoors is important because it decreases the air particle concentration and thus the occupants' exposure. It is interesting to note that in this study the convective flow created a "protective" boundary layer around the heated manikin surface and decreased the overall particle loss rate for fine and coarse particles in the breathing zone of the manikin. Thus the interaction of the background flow and the CBL are important for the transport of and exposure to aerosols. The results also show that the further increase in the air change rate also enhanced the overall loss rate.
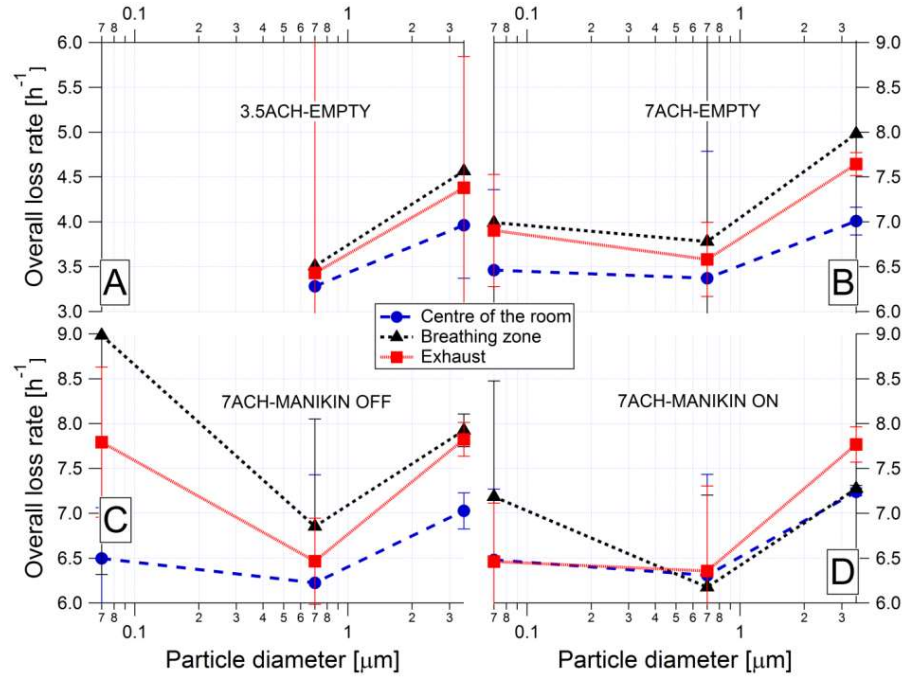
Figure 13: Aerosol particle overall loss rates calculated for different positions and particle sizes for different scenarios: A) 3.5 ACH in an empty room, B) 7 ACH in an empty room, C) 7 ACH, manikin heating OFF, D) 7 ACH, manikin heating ON. Points represent values determined by fitting the model equation. The error bars represent the values of root mean square error (RMSE), which corresponds to differences between model and the measured data. The connecting lines do not have any physical meaning and were added just to lead the readers' eye.

3.4.2 Effect of ventilation rate and interaction of airflows and objects

The results in Figure 14 show that there was a non-uniform concentration distribution in the room (when steady-state was reached) for the gas and particles at both 3.5 ACH and 7 ACH. Yet, the normalized concentration of the N_2O tracer gas, the fine particles, and the coarse particles followed similar distributions at the measured points during Scenarios 1-4. This indicates that airborne particles behave like tracer gas for air change rates exceeding 3.5 ACH. However, it can be seen that the transport behavior of ultrafine particles is influenced by the ventilation rate more than fine and coarse particles. Brownian diffusion is an important deposition mechanism for ultrafine particles (Nazaroff, 2004). The results suggest that at the lower ventilation rate the Brownian diffusion seems to be governing the airflow pattern in the room when compared to the higher ventilation rate. The Brownian motion moves the particles in all directions with the same probability unless there is another driving force directing the particles. Whenever the particle gets close to the surface, it must overcome the boundary layer. The deposition is thus also influenced by the thickness of the boundary layer. In the case of the Brownian diffusion, the wall acts as a particle sink, causing concentration gradient across the boundary layer and therefore resulting in diffusional flux of particles towards the wall. However, the magnitude of this effect needs to be verified by direct measurements on the walls. Nevertheless, it is possible to hypothesize that ultrafine particles

will not act as tracer gas in a room where the air change rate (ACR) is low (in our case 3.5 ACH or lower). In contrast, at 7 ACH and with an empty room, the distribution of 0.07 μm particles was similar to that of the other particles and gas, suggesting that the particles followed the airflow pattern in the room better than in the 3.5 ACH case. These results are in agreement with Rim and Novoselac's findings (2009), which showed that highly mixed airflow (4.5 ACH) in a room creates relatively uniform and comparable gas and particles concentration patterns in the vicinity of a breathing thermal manikin.

Figures 14B and 14C show that the increase in the contact surface area of room objects with room air by the addition of a table and seated unheated manikin did not change the similarity of the distribution pattern of the 0.07 μm, 0.7 μm, and 3.5 μm particles to that of the tracer gas. Despite these results, it should be noted that the additional surfaces were relatively small in comparison to the surface of the empty room. That is why no significant change was observed in the normalized concentration distribution.

The interaction between the CBL generated around the body of the heated manikin with the background room changed the air distribution in the room and resulted in a more homogeneous environment (Figure 14D). Nonetheless, it did not influence the similar transport pattern of the particles and the gas. On the contrary, it seems that when there is generated CBL around the manikin, the difference in the normalized concentration distributions between the 0.07 μm particles and the tracer gas at the breathing zone decreases. This finding suggests that tracer gas can be used as a measure of occupants' exposure even to ultrafine particles.
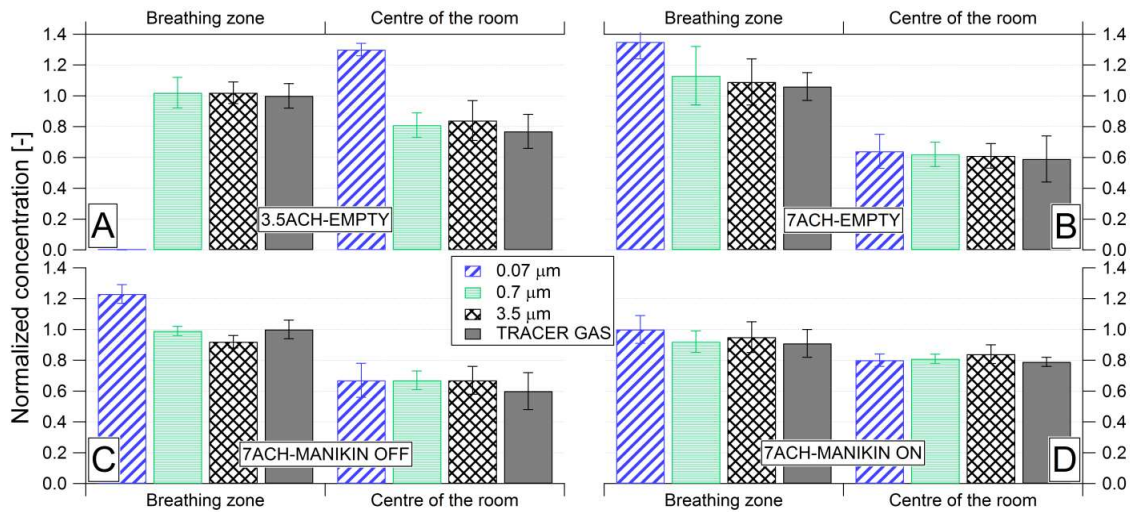
Figure 14: Comparison of normalized concentrations across N2O tracer gas and different-sized particles for the first four scenarios: A) 3.5 ACH in empty room, B) 7 ACH in empty room, C) 7 ACH, manikin heating OFF, and D) 7 ACH, manikin heating ON.

3.4.3 Results obtained in the case of single-bed hospital room

Figure 15 illustrates the variation of the normalized concentrations of the tracer gas and 0.7 μm particles measured at the mouth, centre of the room, and the exhaust as a function of time. The ventilated mattress (VM) worked from the start of the gas and particles generation, i.e. at time 0 s. The results show that the particles behave exactly the same as the tracer gas when a person is in a supine position and his/her CBL is disturbed by local exhaust airflow. To develop a full picture of the tracer gas and particle behaviour when released from a lying person, additional studies will be needed that include measurements of other particle sizes and do not include a local exhaust in the bed. However, the findings from this experiment are important for studies attempting to evaluate the efficiency of local exhaust ventilation methods for removing fine particles by using tracer gas instead. It has been found that a significant fraction of human-induced resuspension of particles from mattresses and bedding can be inhaled by a sleeping occupant (Boor et. al., 2015; Spilak et. al., 2014). The airflow interaction in the microenvironment of a person has a fundamental effect on his/her exposure to pollutants generated in the vicinity of the body (Melikov, 2015). Hence, in order to improve a person's inhaled air quality, it is suggested that the microenvironment close to the human body is locally controlled.
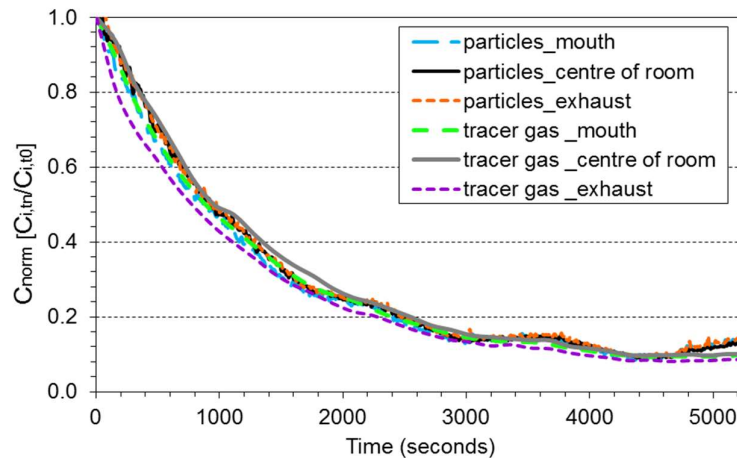
Figure 15: Comparison of the normalized 0.7 μm particle concentration with tracer gas normalized concentration based on release close to the manikin's body, and effect of local exhaust ventilation.

3.4.4 Implication and limitations of the results

The results presented in this chapter suggest that tracer gas can be used to assess the removal of particles (range: 0.07-3.5 μm) to validate the performance of mixing air distribution in certain room layouts. Comparison of tracer gas and particle normalized concentrations measured at the mouth of the heated manikin also suggest that tracer gas can be used to predict potential personal exposure to 0.07 μm, 0.7 μm, and 3.5 μm particles. There are many disease-causing microorganisms that have similar particle sizes to the ones used in this study. For instance, most contagious bacteria have sizes within the fine range of 0.2 – 1 μm. Furthermore, airborne droplet nuclei (evaporated droplets generated by human respiratory activities) range from 1-5 μm (Curseu et al., 2009).

Although these results support the use of tracer gas techniques to predict the distribution of aerosol particles they cannot be extrapolated to all particle sizes, especially for particles in the coarse-mode range larger than 3.5 μm. The study did not take into account also other air distribution patterns, such as displacement air distribution or other positions of the supply and exhaust diffusers. The study is also restricted to processes taking place only in rooms without recirculation. The location and type of the source and occupants' activity may also have different effects on particle and gas dispersion. The current source location may produce better particle and gas comparisons in contrast, for example, if the source was located close to a surface such as the floor, for which particle deposition losses before mixing would be more important. The lack of proper simulations of the occupant's breathing flow in this study might lead to some incorrect predictions, especially for coarse particles (as shown by Rim and Novoselac, 2009). This needs to be studied further. Based on the findings in Chapter 2, it can be speculated that the breathing will not change the results since contaminant source in the current investigation was further away from the breathing zone of the manikin.

It is advisable that future studies on the same topic that include more measuring points performed at different local air change rates. More research is needed to provide data on rooms with different furniture layout, source location, thermal plumes generated by various heated objects, and occupant movement.

3.5 Conclusions

This study focused on the comparison of the dispersion of tracer gas and airborne particles' concentrations in a full-scale test room. The effects of parameters such as particle size, air change rate, change in the room surface area, and CBL around an occupant body on the gas and the particles distribution were studied. The results show that:

- Particles in the fine size range (0.7 μm) are the least influenced by deposition mechanisms and thus should have the most similar behaviour to the tracer gas;

- The ultrafine particles and the N_2O tracer gas did not behave in the same way at 3.5 and 7 ACH in the empty room as well as in the furnished room without heat sources. Therefore, tracer gas might not be suitable method to study behaviour of ultrafine particles;

- The studied ventilation rates did not affect the similar transport pattern of the 3.5 μm and the 0.7 μm particles and the tracer gas;

- Increasing the room surface area did not influence the similarity of the 0.7 μm and 3.5 μm particle dispersal to that of the tracer gas;

- At the breathing zone of the seated heated manikin, N_2O gas emerged as a reliable predictor of the exposure to all tested different-sized particles. Furthermore, the results of this study suggest that tracer gas can be used to indicate the exposure of a person lying in bed to resuspended 0.7 μm particles close to his/her body.

4 Development of engineering techniques for reduction of aerosol exposure indoors

4.1 Introduction

The research presented in this chapter focuses on use of bed- and chair- integrated local exhaust ventilation for pollution source control applied in the vicinity of the human body. The use of local air cleaning combined with the developed advanced air distribution methods is studied. The possibility to save energy as a result of the implementation of such methods is also shown.

4.1.1 Total volume air distribution

At present, mechanical ventilation based on total volume air distribution is typically used to ventilate and condition indoor occupied spaces. The main total volume air distribution (TVAD) methods are mixing air distribution (or mixing ventilation) and displacement air distribution (or displacement ventilation). Mixing ventilation (MV) is used to dilute the indoor air pollutants and provide uniform contaminant concentrations across a room by mixing the clean supplied outdoor air with the polluted air. In reality, however, the supply air is rarely fully mixed with the room air. Studies have shown that when supplying two times more outdoor air in rooms with mixing ventilation, the direction of the airflow pattern may even enhance the transport of pollutants to the occupied zone (Bolashikov and Melikov, 2011; Bolashikov et al., 2012; Pantelic and Tham, 2013). The air flow pattern in rooms with DV is mainly governed by the convection flows from the heat sources, transporting air from the lower part of the room into the upper part (Mundt, 1995). Displacement ventilation (DV) is known to provide cleaner air for breathing especially when the contaminant source is also a heat source (Brohus and Nielsen 1996). However, high exposure can still exist in rooms with displacement air distribution. It is possible to have in the occupied zone stratified exhaled or coughed air of a standing or lying person due to the temperature gradient (Bjørn and Nielsen 2002; Nielsen et al., 2012; Melikov et al., 2012; Qian et al., 2006). Thus, Li et al. (2011) made a general conclusion that displacement ventilation should not be used in areas where there is a risk of cross-infection, such as in hospitals. It has also been shown that displacement air distribution can increase inhaled pollution concentrations when the pollution source is located close to the floor where the clean air is supplied (Rim and Novoselac, 2009). A field study in rooms with displacement ventilation found that approximately 50% of the occupants were dissatisfied with the perceived air quality (Melikov et al., 2005).

The total volume ventilation principles have several disadvantages (Melikov, 2011). Two important disadvantages of the total volume air distribution methods are: 1) the clean air is supplied out of the occupied zone, so upon reaching the occupants' breathing zone it is already mixed with the pollutants present in the room; 2) it does not account for individual preferences since occupants have limited control over the supplied airflow characteristics (temperature, velocity and direction). Based on the previous research, it is evident that the transport and removal of airborne contaminants in indoor environments is defined by the air distribution. However, it is challenging to control the overall airflow pattern in rooms, given that different environments have distinct air currents.

Temperature, velocity, and contaminant distributions in indoor spaces are determined by complex interactions of air jets from supply devices and buoyancy flows resulting from the temperature difference between the room air and the air in contact with a warm or a cold surface (e.g. thermal plumes from occupants, computers, lighting, cold/warm surfaces of windows, etc.) (Melikov, 2016). Another disadvantage of TVAD methods is that the energy use is significant since the entire air volume inside a room has to be conditioned. This implies that more air needs to be supplied and temperature of supply air may need to be higher or lower. This certainly requires a larger fan and larger diameter ducts in order to handle a large airflow and thus less flexibility in space use.

4.1.2 Advanced air distribution methods for pollution exposure reduction in indoor environments

As was discussed and also demonstrated in Chapter 2of this thesis, advanced air distribution such as personalized ventilation (PV) can decrease exposure to indoor air pollution (Bolashikov et al. 2003; Cermak et al., 2006; Cermak and Melikov,2007; Melikov et al., 2003; Melikov, 2004; Nielsen, 2009; Niu et al., 2007). Studies investigating human response to personalized ventilation (PV) have showed that Sick Building Syndrome symptoms (headache, dizziness, fatigue, etc.) decrease when PV is used in conjunction with TVAD compared to rooms with mixing ventilation alone (Kaczmarczyk et al., 2004, 2006). Yet, the PV system cannot prevent the spread of pollution in the surrounding air when the pollution source is exposed to the supplied personalized air (e.g. body released pollution), which may cause cross-contamination. Melikov et al. (2003) and Cermak et al. (2006) reported that the PV combined with displacement ventilation may increase exposure to pollutants released in the vicinity of the personalized flow, e.g., exhaled air and body bio-effluents. The results presented in Chapter 2 of this thesis also show that the PV at certain conditions may increase exposure to body-emitted pollutants. Hence, the first important strategy for improving occupants' inhaled air is to reduce the generated pollution to minimum and also to remove the pollution at the location of the source. Localized exhaust ventilation methods has been developed in the recent years and proven to be efficient methods for minimizing the spread of contaminants in the breathing zone of the occupants (Bolashikov et al. 2010,2015; Cao et al., 2015; Dygert and Dang, 2012; Melikov et al., 2011; Melikov, 2011; Melikov and Dzhartov, 2013; Yang et al., 2014). One limitation of these methods is that they mainly focused on controlling and preventing the airborne transmission of infectious diseases due to human expiratory activities, i.e. breathing and coughing, or reducing exposure to room pollution. Only the study by Dygert and Dang (2012) was focused on bio-effluents emitted from the armpits, and reported that seat-back integrated suction had potential to improve the indoor air quality (IAQ) in a high-density seating application.

The research reported in this thesis shows that it is possible to reduce spread of gaseous and aerosol contaminants released from or close to the human body by using a seat-integrated (as shown in Chapter 2) or bed-integrated (Chapter 3) local exhaust ventilation. This part of the study aims to determine key factors with regard to the performance of these two methods. It is shown that the performance of the two methods can be enhanced by combining them with local air cleaning. In this way the polluted air will be cleaned locally and discharged back into the room. Typical removal methods for gaseous contaminants work on the principles of physical adsorption and chemical

reaction. Activated carbon is one of the most widely used adsorbents. There have been a number of studies on the performance of activated carbon for controlling gaseous pollutants, when it is incorporated in air filters for HVAC systems or used in portable air cleaners (Bekö et al., 2009; Cal et al., 1997; Lee and Davidson, 1999; Sidheswaran et al., 2012). However little is known about its application as a localized filter for removing gaseous contaminants within the vicinity of the human body incorporated in air filters for HVAC systems or used in portable air cleaners (Bekö et al., 2009; Cal et al., 1997; Lee and Davidson, 1999; Sidheswaran et al., 2012). However little is known about its application as a localized filter for removing gaseous contaminants within the vicinity of the human body.

4.1.3   Energy-saving and thermal comfort using advanced air distribution methods

PV has shown to be able to improve the perceived air quality and occupant thermal comfort, especially at high room air temperatures (Kaczmarczyk et al., 2004, 2006; Melikov and Kaczmarczyk, 2012; Sekhar et al., 2005; Sun et al., 2013; Yang et al., 2010). This, in turn, can lead to energy savings. Previous research has compared the energy performance of personalized ventilation to conventional total volume ventilation. Studies have shown that an effective energy saving strategy is to expand the maximum allowed air temperature in office rooms while thermal comfort is still maintained by the PV's convective cooling (Schiavon et al.2010; Schiavon and Melikov, 2009; Sekhar et al., 2005). This energy saving strategy, however, can be recommended only in rooms where the occupants spend most of their time at their work place. Energy savings with PV can also be achieved by reducing the outdoor airflow rate due to the greater efficacy of the PV compared to TVAD (Faulkner et al. 1999). Schiavon and Melikov (2009) discovered that this strategy would lead to energy savings in hot and humid climates. However, it does not always suggest a reduction of the energy use in cold climates since the outdoor air has a free cooling effect which is favourable for spaces with high cooling demand. The previous studies provide valued information on the potential of PV to improve occupants' thermal comfort at reduced energy use. In Chapters 1 and 2, the potential of the studied local source control methods to improve inhaled air quality is demonstrated. However, their performance with regard to energy saving and thermal comfort is unknown and needs to be explored. It is expected that the local exhaust methods, namely the ventilated mattress and the ventilated cushion, will provide local body cooling. Studies have reported that ventilated office chairs or car seats may provide thermal comfort to occupants at elevated ambient temperatures (Kogawa et al., 2007; Watanabe et al., 2009; Wyon, 1989). As a result the background air temperature can be elevated above the limits recommended in the standards. This suggests that the methods have potential for energy savings, which ought to be studied.

4.2 Objectives

- To develop and study the performance of a bed-integrated local pollution exhaust method for exposure reduction to human body bio-effluents in general patients room in hospitals;

- To study the effect of bed-integrated local exhaust method combined with local air cleaning method on exposure reduction to body bio-effluents and improved IAQ in patients rooms;

- To develop and study the performance of a seat-integrated local pollution exhaust method for exposure reduction to body bio-effluents in an office working environment;

- To study the performance of the local exhaust methods with regard to thermal comfort;

- To identify the energy saving potential of the local exhaust ventilation methods.

4.3 Parametric study on the performance of bed-integrated local exhaust method for hospital patient room application

This part of the study examines the performance of bed-integrated local exhaust method named ventilated mattress, and the specific objective is to provide a set of data that answer the following questions:

- How efficient is this method in terms of occupant exposure to body bio-effluents when combined with background ventilation at reduced ventilation rate compared to background ventilation alone at high ventilation rates?

- What is the optimal location of the local exhaust opening of the ventilated mattress in order to decrease to a minimum level bio-effluents generated from different body parts?

- Can different lying positions and local exhaust opening sizes change the efficiency of the ventilated mattress in capturing and exhausting the bio-effluents released from the body?

- Can the ventilated mattress cool the body parts in contact with its surface and how pronounced is the cooling effect at various room air temperatures and body covering?

4.3.1 Experimental method

4.3.1.1 Hospital patient room

A mock-up of a double-bed hospital room for patient care (Figure 16) was built in an environmental chamber (length × width × height = 5.3 m × 4.7 m × 2.6 m). The distance between the beds was adjusted to be 1.06 m. On each bed of dimensions 0.9 m x 2.0 m x 0.8 m (W x L x H) there was a regular mattress with thickness of 0.06 m. The walls and the floor of the chamber were made of wooden chipboard and the ceiling of gypsum tiles. One of the walls was single glazed. Air temperature outside the chamber was controlled to be close to the temperature inside the chamber in order to reduce the heat transfer through the walls. The chamber was sealed prior to the experiments. Five ceiling-mounted light fixtures (6 W each) provided the background lighting.

4.3.1.2 Thermal manikin and heated dummies

One thermal manikin and two heated dummies were used as occupant simulators in the room. The thermal manikin was used to simulate a lying patient in bed. The thermal manikin was the same one described in Chapter 2 (more details are also provided in Paper III). The manikin consists of 23 body parts. Each body part was individually controlled to maintain surface temperature equal to the skin temperature of an average person in a state of thermal comfort at the exposed conditions. The heated dummy lying in the second bed was adjusted to generate heat with power of 80 W. A second heated dummy was used to simulate a doctor standing next to the manikin's bed at a 0.55 m distance from the bed. The total generated heat power of the "doctor" was 230 W corresponding to a standing person with low metabolic rate class 1(ISO, 2004a). The dummies consisted of three parts: legs, torso, and head. All parts were made from galvanized metal; the head and legs were

circular with diameters of 0.2 m and 0.12 m, respectively. The torso was a cuboid with dimensions 0.6 m × 0.35 m × 0.2 m (H × L × W). The total height of each dummy was 1.65 m. Six light bulbs were used to heat the dummy: one was installed in the head, one in the torso, and two in each leg. One small fan was placed in the torso to warm the dummy more homogeneously. During the experiments the dummy placed on the bed was always covered with a light quilt (thermal insulation 3.2 clo) whereas the manikin was covered up to the neck only in some of the experiments. The manikin was dressed in a short-sleeve hospital pyjama (thermal insulation 0.60 clo).

4.3.1.3   Air distribution methods

The ventilated mattress was placed on top of the regular mattress of the thermal manikin's bed (Figure 17). The ventilated mattress (VM) was used in some of the experiments to locally exhaust the simulated contaminants emitted from the manikin's body. Part of the surface of the VM was designed as an exhaust opening from which contaminants generated by the human body (e.g. bio-effluents) were discharged. The ventilated mattress had two local exhaust openings, each with the same dimensions: 0.8 m x 0.16 m (L x W). The position of the two exhaust openings was either in the area where the patient's feet were or in the gluteal region of the thermal manikin (see Figure 17). The exhaust openings of the VM were covered with textile mesh with a free area ratio of approximately 90%. There was a 0.25 m thick plastic mesh inside the ventilated mattress which provided support and allowed the exhaust air to move through the whole mattress. For the purpose of the experiments, the VM was connected to a separate exhaust system having an axial fan outside the chamber with a flexible duct (ø 80 mm). The exhaust flow rate of the VM was regulated by changing the frequency of the fan and by adjusting the damper installed in the duct connected to the VM. In order to adjust the desired airflow rate exhausted from the VM, two air flow sensors (MFS-C-080) were installed in the duct. The pressure difference at the MFS sensors was measured with a differential pressure micro-manometer FCO510 (accuracy of 0.01 Pa [$0.15 \times 10{-}5$ psi] ±0.25% of reading).

A series of experiments was conducted under mixing and displacement ventilation. In the case of mixing ventilation, the supply diffuser was a three-way discharge solid-face plate diffuser of square geometry. The diffuser was mounted in the ceiling (Figure 16). Air supply diffusers with different sizes were used to achieve similar air jet pattern at room ventilation rates of 1.5, 3, and 6 ACH. The free area of the MV diffusers was 0.011 m^2 at 1.5 ACH (27 L/s), 0.015 m^2 at 3 ACH (54 L/s), and 0.023 m^2 at 6 ACH (109 L/s). Three different sized semi-circular perforated supply diffusers were also used for the displacement ventilation under the different ventilation rates. The height and width of the DV diffusers used to supply 1.5 ACH (27 L/s), 3 ACH (55 L/s), and 6 ACH (109 L/s) were 0.71 m x 0.25 m, 0.71 m x 0.3 m, and 0.97 m x 0.33 m, respectively. The supply diffuser for the displacement was placed in the middle of the glazed wall of the chamber (Figure 16). The near zone of the three displacement diffusers, defined as the horizontal distance from the diffuser to the place in a room where the maximum velocity decreases to 0.2 m/s, was measured to be no longer than 0.4 m. In all cases the air was exhausted through two perforated square diffusers (with free area 0.047 m^2) located symmetrically on the ceiling above the patients' heads (Figure 16). The exhausted air was always equally balanced between the two air extract diffusers.

4.3.1.4 Measured parameters and measuring equipment

The manikin was referred to as a source patient since it was used as a source of bio-effluents. CO_2, Freon 134a and N_2O were used to simulate emissions of bio-effluents from the manikin's feet, pelvic area and armpits, respectively. The CO_2, Freon 134a and N_2O were released through porous sponges at constant emission of 2.3 L/min, 0.15 L/min and 0.2 L/min, respectively. The N_2O flow rate was equally distributed and the gas was dosed from both armpits of the manikin. The tracer gases were dosed above the clothing. The concentration of the three tracer gases was sampled by an Innova 1303 sampler and analysed using a second multi-gas monitor Innova 1312 connected to the Innova 1303 sampler. The Innova 1303 sampler had 6 channels. The sampling time of the Innova 1312 was 40 s/channel and 6 channels were measured in sequence, giving a period of 4 min between measurements in the same location. The Innova gas monitor was equipped with three optical filters for detecting each of the gases. The instrument was calibrated prior to the experiment and the measuring error of the instrument was ±5%.

The concentration of the three gases was measured simultaneously at six points:

1) The breathing zone (BZ) of the dummy (i.e. 1.50 m height above the floor) standing next to the manikin's bed, referred to as "doctor";

2) The mouth of the source patient (i.e. manikin);

3) The BZ of the exposed patients (i.e. the dummy in the bed);

4) The air supply diffuser;

5) The duct of the total exhaust room air;

6) In the centre of the room between the two beds and close to the source patient's feet at 1.7 m height from floor, referred to as "1.7 m centre".

The sampling tube used to sample the concentration of the tracer gases at the mouth of the thermal manikin was placed 0.005 m from the mouth.

Temperature measurements inside the test room were performed using calibrated thermistor sensors (uncertainty 0.3°C). The measured data were recorded via a multi-point data logger. The monitored locations were the following: at the total volume ventilation supply, exhaust diffuser above the exposed patient, and in the centre of the room at 1.1 m and 1.7 m above floor, and on the wall behind the doctor at 1.1 m above the floor. Those measurement locations were used to keep the conditions in the chamber steady during the experiments. A HOBO data logger was used to measure and record the relative humidity in the chamber with an uncertainty of 2.5%.

Four calibrated omni-directional low-velocity sensors were used to measure the velocity inside the test room and also to identify the near zone of the displacement diffusers. The measurement range of air velocity was 0.05–1.0 m/s; the accuracy was 0.02 m/s ±1% of the reading.
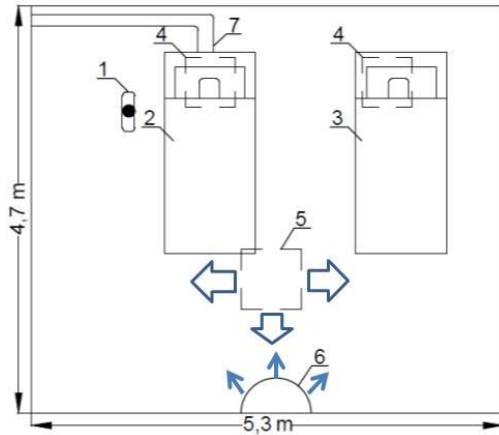
Figure 16: Top view sketch of the chamber layout (left): 1 – "doctor", 2 – "source patient", 3 – "exposed patient", 4 – room air exhaust diffusers, 5 - MV air supply diffuser, 6- DV air supply diffuser, 7- VM exhaust duct. (right) Interior of the chamber.
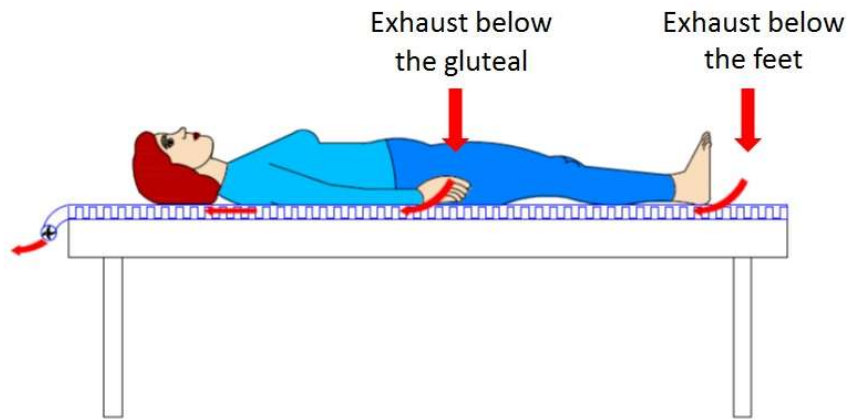
Figure 17: Ventilated mattress (VM) with two exhaust openings: below the gluteals and below the feet

4.3.1.5 Experimental conditions

The experiments were conducted at three background ventilation rates, namely 27, 55 and 109 L/s (1.5, 3, and 6 ACH), without the use of the ventilated mattress. During the experiments with the VM, the background ventilation rate in the room was kept at 1.5 ACH. 100% clean outdoor air was supplied in the room throughout all experiments. The air temperature inside the test chamber was controlled and kept at 23°C±0.3°C during all experiments. The temperature around the chamber was kept 23°C±0.3°C as well. The relative humidity in the chamber was not controlled; it was measured to be in the range of 25 – 40%. The room air temperature as well as the ventilation rate of 6 ACH were selected according to the ASHRAE Standard 170 (2013) design requirements for

recovery wards and general patient room in hospitals, which are 21-24°C and 4-6 ACH, respectively. The standard recommends the relative humidity to be within the range 30-60%.

There is still no accepted international European standard for health care facilities. In the current study the designed air change rate of 1.5 ACH was selected based on the ventilation requirements in the Danish technical report FprCEN/TR 16244 "Ventilation for Hospitals" (2011). The technical report recommends a minimum outdoor flow rate of 10 L/s per bed in patient bedrooms. An additional 7 L/s per m^2 (floor area) was provided, corresponding to the required ventilation rate for building emissions according to the EN 15251 (2007), category III, very low polluting building. The design 3 ACH was chosen to provide data for the tracer gases concentrations in the room when the ventilation rate is doubled.

The efficiency of the VM depends on factors such as body posture of the person, exhaust flow rate, location on the mattress and size of the exhaust opening relative to the source and use of summer quilt, i.e. body is covered or not. Therefore, the effect of all these parameters was studied.

The manikin was positioned in a way that corresponds to three different sleeping positions. In the supine position the manikin was positioned on its back on the centre line of the bed and the arms positioned on the side of the torso. In the second position, the manikin was again positioned on the centre line of the bed, but lying on its right side, facing the "doctor" (Figure 16). In this lateral position, the left arm was held alongside the torso, while the other was positioned away from the torso with a 30° forward angle at the elbow. In the third position, the manikin was again on the centre line of the bed and was turned on the chest. In this prone position, the arms were oriented along the torso and the face of the manikin was turned to the left facing the doctor. The prone and lateral positions were tested only with the ventilated mattress in operation under MV at 1.5 ACH. In all cases when the quilt was present the whole body of the manikin was covered up to its shoulders (only the neck and the head were uncovered by the quilt).

The experimental conditions and different configurations are listed in Table 2. In the table, for instance, the abbreviation "DV 1.5 ACH" stands for displacement ventilation under 1.5 ACH.

Table 2: Experimental conditions with regard to air quality in the room.

№	cover	Lying position of the manikin	Position of the VM exhaust opening	Surface area of the exhaust opening	VM flow rate	Background Ventilation
1	quilt	supine	feet	0.13 m^2	1.5 L/s	DV 1.5 ACH
2	quilt	supine	feet	0.13 m^2	1.5 L/s	
3	quilt	supine	gluteal	0.13 m^2	1.5 L/s	
4	quilt	supine	gluteal	0.13 m^2	1.5 L/s	
5	-	supine	feet	0.13 m^2	1.5 L/s	
6	-	supine	feet	0.13 m^2	1.5 L/s	
7	-	supine	gluteal	0.13 m^2	1.5 L/s	
8	-	supine	gluteal	0.13 m^2	1.5 L/s	
9	quilt	supine	-	-	-	DV 1.5 ACH
10	quilt	supine	-	-	-	DV 3 ACH
11	quilt	supine	-	-	-	DV 6 ACH
12	-	supine	-	-	-	DV 1.5 ACH
13	-	supine	-	-	-	DV 3 ACH
14	-	supine	-	-	-	DV 6 ACH
15	quilt	supine	feet	0.13 m^2	1.5 L/s	MV 1.5 ACH
16	quilt	supine	feet	0.13 m^2	1.5 L/s	
17	quilt	supine	gluteal	0.13 m^2	1.5 L/s	
18	quilt	supine	gluteal	0.13 m^2	1.5 L/s	
19	-	supine	feet	0.13 m^2	4.5 L/s	
20	-	supine	feet	0.13 m^2	4.5 L/s	
21	-	supine	gluteal	0.13 m^2	4.5 L/s	
22	-	supine	gluteal	0.13 m^2	4.5 L/s	
23	quilt	supine	-	-	-	MV 1.5 ACH
24	quilt	supine	-	-	-	MV 3 ACH
25	quilt	supine	-	-	-	MV 6 ACH
26	-	supine	-	-	-	MV 1.5 ACH
27	-	supine	-	-	-	MV 3 ACH
28	-	supine	-	-	-	MV 6 ACH
29	quilt	prone	feet	0.13 m^2	1.5 L/s	MV 1.5 ACH
30	quilt	prone	gluteal	0.13 m^2	1.5 L/s	
31	quilt	lateral	feet	0.13 m^2	1.5 L/s	
32	quilt	lateral	gluteal	0.13 m^2	1.5 L/s	
33	quilt	supine	feet	0.06 m^2	1.5 L/s	
34	quilt	supine	gluteal	0.06 m^2	1.5 L/s	

The ability of the ventilated mattress to cool the thermal manikin lying in the bed was examined at numerous combinations of the flow rate through the mattress (1.5, 3, 6 and 10 L/s), room air temperature (23, 26 and 29ºC) and body covering (body covered with sheet 0.32 clo), with light quilt (3.2 clo) and without body covering. All experimental conditions are listed in Table 3. During the experiments the background room ventilation was MV at 1.5 ACH. The exhaust part of the VM was located below the feet and had a surface area of 0.13 m^2.

Table 3: Experimental conditions with regard to thermal comfort.

№	Type of cover	Room air temperature	VM flow rate
1	quilt	23°C	-
2	sheet	23°C	-
3	no cover	23°C	-
4	quilt	23°C	1.5 L/s
5			3 L/s
6			6 L/s
7	sheet	23°C	1.5 L/s
8			3 L/s
9			6 L/s
10	no cover	23°C	1.5 L/s
11			3 L/s
12			6 L/s
13	sheet	26°C	1.5 L/s
14			3 L/s
15			6 L/s
16	no cover	26°C	1.5 L/s
17			3 L/s
18			6 L/s
19	sheet	26°C	-
20	no cover	26°C	-
21	sheet	29°C	1.5 L/s
22			3 L/s
23			6 L/s
24			10 L/s
25	no cover	29°C	1.5 L/s
26			3 L/s
27			6 L/s
28			10 l/s
29	sheet	29°C	-
30	no cover	29°C	-

4.3.1.6 Experimental procedure

At the start of the experiments, the desired background ventilation rate was set using the control of the ventilation system, the tracer gases dosing was started and the thermal manikin and the dummies were switched on. For the experiments with the ventilated mattress, the exhaust airflow rate from VM was adjusted prior to the experiment start. The background exhaust flow rate was decreased by the same amount of air that was exhausted by the VM in order to avoid under-pressure in the room. All measurements started after steady-state conditions were achieved, i.e. constant level of the three

tracer gases in the total volume exhaust and constant heat loss from the manikin. Twenty samples of the tracer gases were acquired for each measurement point. The heat loss, the surface temperature for each body segment, and the average surface temperature for the whole body of the manikin were recorded for seven minutes with a sampling rate of 10 seconds.

4.3.1.7 Criteria for assessment

The performance of the ventilated mattress combined with either mixing or displacement ventilation was evaluated with regard to the measured tracer gas concentrations at the mouth of the occupants as well as in the room and exhaust room air. The obtained 20 samples of the tracer gases were averaged and normalized according to the following equation:

Normalized concentration $= C_i/C_{i,Ref}$ (3)

where C_i is the averaged concentration determined at a certain measuring point, $C_{i,Ref}$ is the average concentration determined at the same measuring point during the reference condition of 1.5 ACH without using the VM. When the normalized concentration is less than "1" it means that the exposure to the simulated body bio-effluents was reduced due to the ventilated mattress. The reference condition was when only background ventilation, DV or MV, was in operation at 1.5 ACH. Thus the data of the normalized concentrations with DV and the data with MV have different $C_{i,Ref}$. The tracer gas results obtained during the conditions with mixing ventilation alone (at 1.5, 3 and 6 ACH) when the manikin was covered and when not covered were averaged. After steady state was reached, the presence of the cover did not change the concentration of the tracer gases in the measuring points when there was only MV. In the cases with DV, it was found that the measured concentration in some of the measuring points differ in the presence of the quilt compared to that without quilt. Thus for the conditions with DV there were two reference conditions used for the normalization of the averaged data – DV at 1.5 ACH with cover and without cover.

The excess concentration of CO_2 over the background level was used as criteria for exposure assessment to feet-emitted pollutants.

To assess the cooling provided by the ventilated mattress, heat loss from the segments and whole body of the thermal manikin as well as their surface temperatures were measured. The collected data were used to calculate the equivalent temperature, t_{eq}, for the segments and the whole body. The equivalent temperature is defined as "The uniform temperature of the imaginary enclosure with air velocity equal to zero in which a person will exchange the same dry heat by radiation and convection as in the actual non-uniform environment" (ISO, 2004b). The equivalent temperature for each segment and whole body of the manikin was calculated using the equation:

$$t_{eq,i} = t_{s,i} - \frac{P_i}{h_i}$$ (4)

Where,

$t_{eq,i}$ – equivalent temperature of the body segment, [°C]

$t_{s,i}$ – average skin surface temperature of the body segment, [°C]

P_i – average dry heat loss of the body segment, [W/m²]

h_i – heat transfer coefficient of the body segment (acquired from the calibration of the manikin performed prior to the experiments), [W/m²·K].

The segmental and whole body cooling effect of the ventilated mattress was assessed by the change in the equivalent temperature determined for the studied condition compared to the equivalent temperature, $t_{eq,i,ref}$, determined at a given reference condition. The calculations were performed in two ways as presented in equations (5) and (6):

$$\Delta t_{eq1} = t_{eq,i} - t_{eqi,ref1} \tag{5}$$

$$\Delta t_{eq2} = t_{eq},i - t_{eq,i,ref23} \tag{6}$$

Where $t_{eq,i}$ and $t_{eq,i,ref1}$ (°C) is the segmental or whole body equivalent temperature determined for the same room air temperature respectively with and without ventilated mattress in operation, $t_{eq,i,ref23}$ is the segmental or whole body equivalent temperature determined without ventilated mattress at 23°C. Δt_{eq1} is a measure for the cooling performance of the ventilated mattress and Δt_{eq2} may be used to assess the thermal comfort provided with the ventilated mattress at elevated temperature (26 °C) compared to comfortable temperature of 23°C without additional cooling of the body. Negative values of $\Delta teq1$ mean that the mattress increases the heat loss from the body, i.e. provides cooling. Negative values of Δt_{eq2} mean that people will report cooler thermal sensation compared to that at 23°C without mattress and positive values will mean warmer thermal sensation.

4.3.1.8 Uncertainty of the measurement

The measured data of the tracer gas concentration were analysed in accordance with ISO/IEC Guide for the expression of uncertainty (ISO, 2008). The absolute expanded uncertainty with 95% confidence interval and coverage factor of 2 was estimated based on the bias and resolution of the Innova instrument as well as the reproducibility (i.e. the estimated standard deviation) of the measured concentrations. The relative expanded uncertainties (the ratio of the expanded uncertainty to the average of the measurements) were within the range 7-18%. The uncertainty of the heat loss measurements from the manikin segments was 1%.

4.3.2 Results and Discussion

4.3.2.1 Performance of the ventilated mattress in terms of exposure reduction to bio-effluents generated from different body parts

The abbreviations used to code the studied cases presented in the next Figures 18 and 19 should be read as follows. For example, the abbreviation "VM (1.5 L/s)_F with cover (1.5 ACH)" should be understood as the ventilated mattress was exhausting 1.5 L/s with its exhaust opening below the feet, the manikin was covered by the quilt and the background room ventilation rate was 1.5 ACH.

"VM (1.5 L/s)_G" stands for the ventilated mattress exhausting 1.5 L/s air with its exhaust opening present below the gluteal of the manikin.

Figures 18 and 19 were obtained only for supine position of the manikin. The results from the tracer gas measurements under displacement air distribution are shown in Figure 18. The results indicate that when the manikin was covered with the quilt and the VM was operating only at 1.5 L/s, the concentration of all three tracer gases measured in all points was reduced completely or almost to 100%. The efficiency of the VM in evacuating the pollutants released from feet and groin was the same regardless of the location of the exhaust opening. In the case when the tracer gas (N_2O) was emitted from the armpits of the manikin, its normalized concentrations were slightly higher (Figure 18c) when the VM's exhaust opening was under the feet compared to when it was under the gluteal. This is due to the fact that the local exhaust at the feet was further away from the pollution source and the airflow rate of 1.5 L/s was not sufficient to completely remove the pollutants from the armpits. The results in Figure 18 show that the normalized concentration of the three tracer gases with DV alone at 3 or 6 ACH differed more during the conditions with the covered manikin than those without the cover. The normalized values at the measuring points also varied with the location of the pollution source. It should be noted that the DV alone at 6 ACH did not provide better air quality in the breathing zone of the source patient than that at 3 ACH (Figures 18a, 18b and 18c). For the condition of DV at 6 ACH and manikin with cover, the normalized concentrations of the tracer gases in the mouth of the manikin were even slightly higher compared to DV at 3 ACH with and without cover. These results suggest that the displacement air distribution in the room did not influence the microenvironment around the lying thermal manikin. This fact shows that supplying high amount of clean air is not effective in protecting bed-bound patients from their own contaminants. Interestingly, the observed normalized concentrations for the pollution source's feet and groin measured at 1.7 m above the floor in the centre of the room were almost the same under DV at 6 ACH and 3 ACH. This can be attributed to similar vertical concentration distribution at 3 ACH and 6 ACH in this particular point since its location was close to the supply diffuser where there were no heat sources to change the airflow pattern. The pollution source's location was also important. At the same measuring point but for the pollution source armpits (Figure 18c), under the condition of 6 ACH and manikin with cover the normalized concentration was much higher than that at 6 ACH without cover and 3 ACH with/without cover. More measurements of the vertical concentration of the pollutants from the armpits need to be carried out in various points in the room in order to explain this effect.

In general, the results in Figure 18 show that the presence of body cover affected the spread of simulated pollutants in the room, in some conditions with DV alone (3 or 6 ACH), it increased the exposure. These results are probably due to the flow resistance introduced by the quilt covering the source patient, changing the diffusion pattern of the tracer gases. The quilt modified the free convective boundary layer around the thermal manikin, causing the convective air currents to move not only upward but also along the two sides of the manikin. This effect was shown by Clark (1981). After the contaminants escaped from below the cover into the room, the DV gave rise to a vertical flow of the contaminants, resulting in a high concentration gradient in the measuring points.

This must be verified with additional measurements and smoke visualizations. It appears that different locations of the VM exhaust opening and the pollution source can result in completely different exposures and concentration levels in the room. In the cases without body cover, high exposure reduction with the VM can be achieved when the positioning of the local exhaust opening is close to the body part where the pollution is released (Figure 18a, condition 'VM (1.5 L/s)_F no cover' and Figure 18b, condition 'VM (1.5 L/s)_G no cover'). Substantial reduction of the pollution from the armpits was also observed in all measuring locations (except for the mouth of the source patient) when the VM was exhausting the air below the gluteal area (Figure 18c, condition 'VM (1.5 L/s)_G no cover'). Due to the source proximity to the breathing zone of the manikin, the VM sucking 1.5 L/s was not enough to evacuate most of the armpit-emitted pollutants. One limitation of the experiments under DV was that the efficiency of the VM was not studied at an exhaust flow rate higher than 1.5 L/s when the manikin was not covered. However, this was studied under the experiments with mixing ventilation as shown in Figure 19.

a)

b)
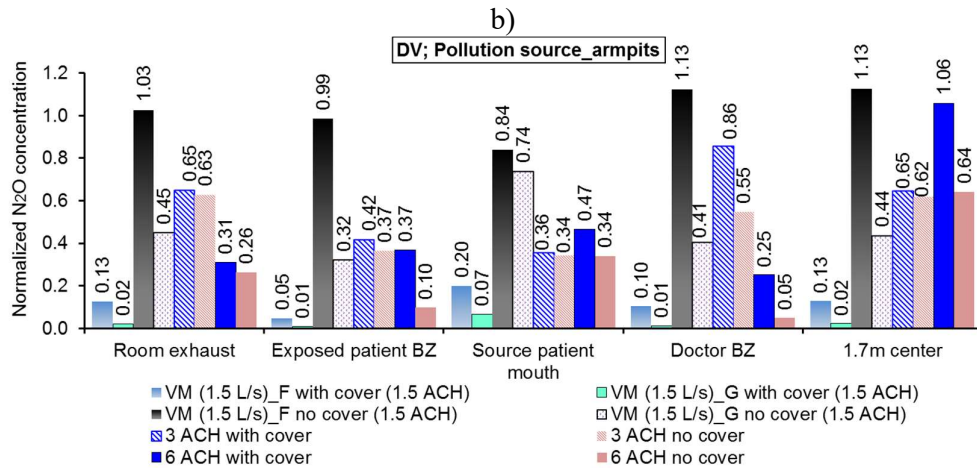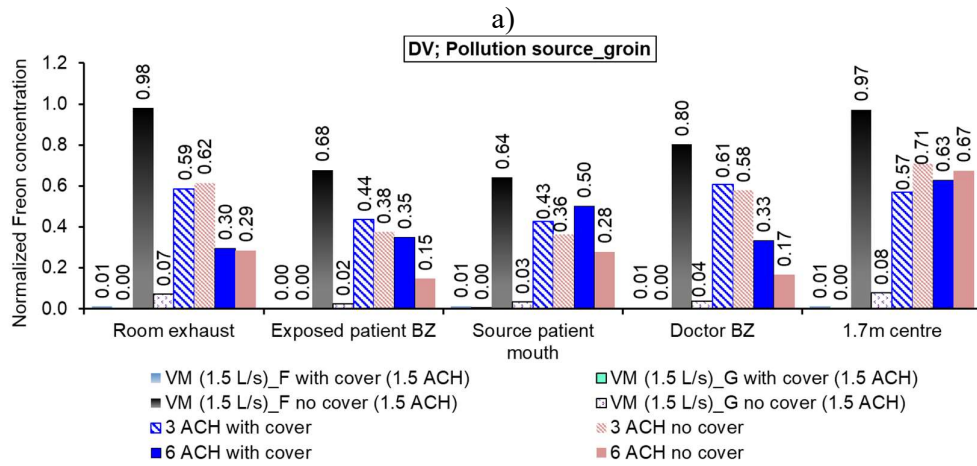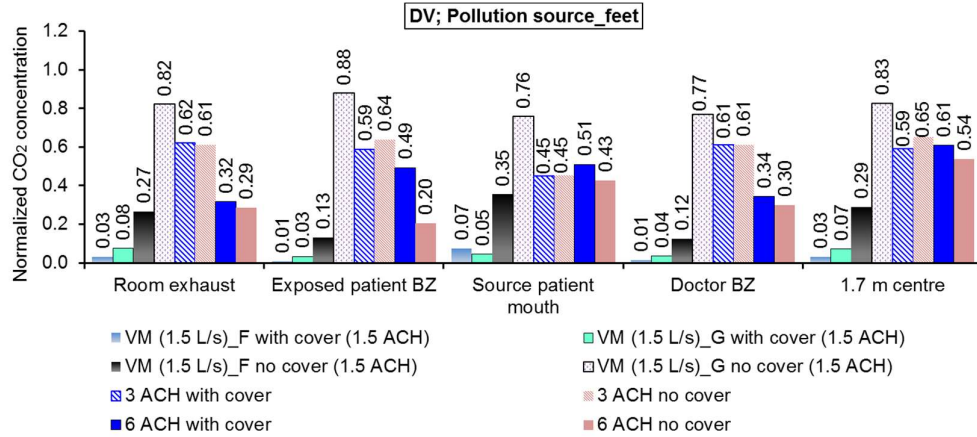
c)

Figure 18: Normalized concentration without and with the VM when the exhaust opening was either below the feet or below the gluteal, and when the manikin was covered with quilt or not. The results are presented for the conditions under displacement ventilation at 1.5, 3 and 6 ACH when: a) pollution source was patient's feet (CO_2), b) pollution source was patient's groin (Freon) and c) pollution source was patient's armpits (N_2O.)

The results obtained when the VM is operated with mixing background air distribution (MV) are shown in Figure 19. The results show that when the manikin is covered with a quilt the concentration of all three pollutants is fully reduced using the VM under 1.5 ACH. It was found 100 % efficiency of the ventilated mattress when the local exhaust opening was below the gluteal and pollution source were the manikin's armpits. Taken together these and the above results with DV, it can be concluded that high exposure reduction to bio-effluents emitted from the feet, groin and armpits can be achieved when the local exhaust is placed below the gluteal area of the person. However this is not the case when the patient is not using a cover, i.e. without the quilt acting as barrier for the pollution. In this case the VM reduces the exposure only to pollutants released near its exhaust opening. It should be noted that in the case of armpit-emitted pollutants and no cover the VM under 1.5 ACH still provided similar or better air quality compared to the conditions under 3 and 6 ACH when only MV was operating (Figure 19c, the condition 'VM (4.5 L/s)_G no cover' compared to the conditions '3 ACH' and '6 ACH'). The increase of the exhaust flow rate from 1.5 L/s to 4.5 L/s through the mattress was still not sufficient to fully capture the pollutants released further away from the VM's local exhaust (Figure 19a, condition 'VM (4.5 L/s)_G no cover'; Figure 19b, condition 'VM (4.5 L/s)_F no cover' and Figure 19c, condition 'VM (4.5 L/s)_G no cover'). The results in Figure 19b and 19c show that the normalized concentrations at the mouth of the source patient are almost the same under 3 ACH and 6 ACH. Surprisingly, the normalized concentration of the simulated bio-effluents from the groin is equal to 1.01 at 3ACH (Figure 19b) which indicates that the concentration did not decrease when the supply flow rate was increased 2 times (from 1.5 ACH to 3 ACH). The further increase of the supply flow rate (from 3 ACH to 6 ACH) reduced the concentration with only 5% compared to the reference case MV at 1.5 ACH. These results confirm the fact that when the source is located close to the breathing zone conventional methods such as ventilation by dilution are not effective and instead local exhaust should be used. The non-uniform concentration observed in the room also suggests caution in estimating inhalation exposure using mass balance models that assume well-mixed conditions.
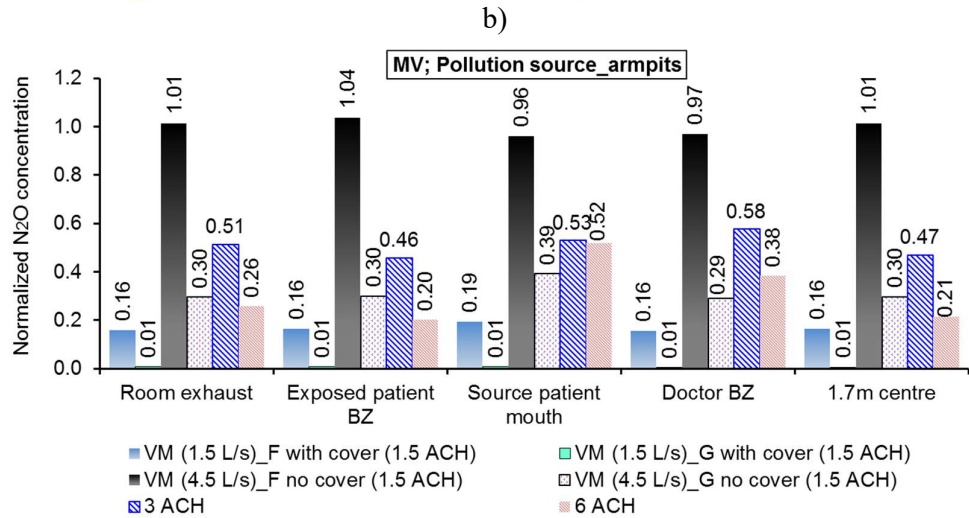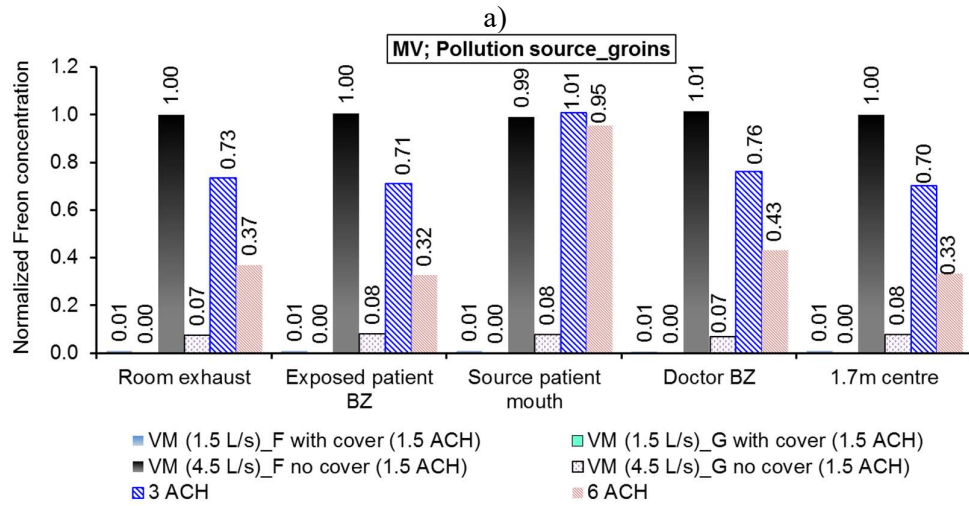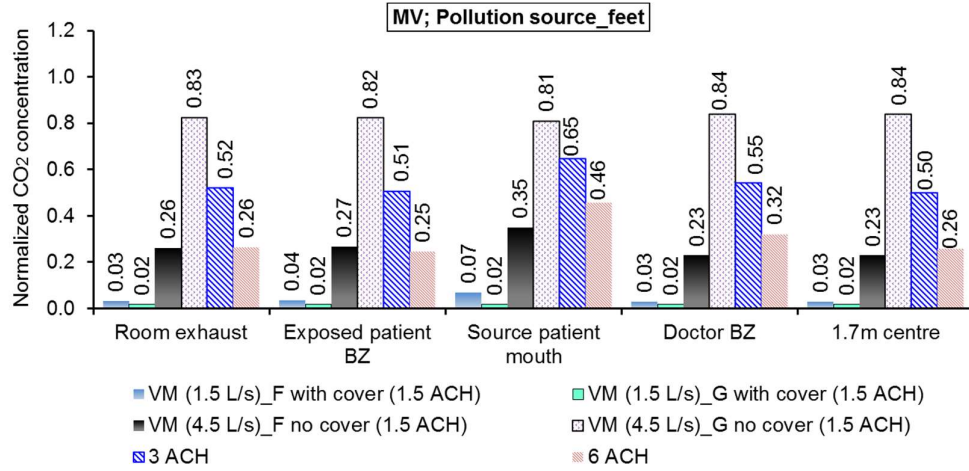
Figure 19: Normalized without and with the VM when the exhaust opening was either below the feet or below the gluteal, and when the manikin was covered with quilt or not. The results are presented for MV at 1.5, 3 and 6 ACH when: a) pollution source was patient's feet (CO_2), b) pollution source was patient's groin (Freon) and c) pollution source was patient's armpits (N_2O).

4.3.2.2 Performance of the ventilated mattress - Impact of body posture and size of the local exhaust opening

To better characterize the performance of the VM, its efficiency was studied under different lying positions of the manikin and sizes of the local exhaust opening below the gluteal. The manikin was covered with the quilt up to the shoulders during these experiments.

Two sizes of the local exhaust opening of the mattress were tested: 1) 0.8 m (length) x 0.16 m (width) equal to exhaust surface area (ESA) of 0.13 m^2 and 2) 0.4 m (length) x 0.16 m (width) equal to ESA of 0.06 m^2. Based on the results in Figure 18 and Figure 19 experiments with exhaust opening under the gluteal were performed to investigate the effect of body posture on the performance of the VM to remove body bio-effluents. Note that the results in Figure 18 and Figure 19 were obtained for VM's exhaust opening with ESA 0.13 m^2.

Figure 20 show the normalized concentration in the breathing zone of the occupants and in the room when the pollution was released at the feet of the source patient and the background ventilation was mixing air distribution under 1.5 ACH. It is clear that when the exhaust opening has larger surface area more pollutants are exhausted. The same effect was observed when the pollution was generated from the armpits. The results are shown in Paper III (Appendix B).
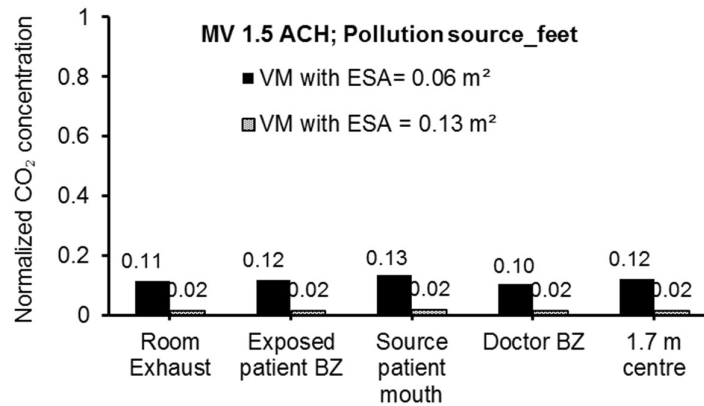
Figure 20: Comparison of the normalized concentration with two different sizes of the local exhaust opening of the VM located below the gluteal and for the pollution source patient's armpits. The air change rate was 1.5 ACH and the "source patient" was lying on its back.

The results for the impact of the manikin's body posture on the performance of the ventilated mattress in terms of groin-emitted pollutants are shown in Figure 21. As shown, the normalized concentration in all measuring points was zero regardless the lying position (Figure 21). The results for the pollution emitted from the feet and armpits are presented in Paper III. Generally, the results show that when the pollution was emitted from the feet the manikin's different lying positions did not have a big effect on the efficiency of the VM to remove the pollution out of the room. Depending on the lying position of the manikin the pollution distribution from the armpits was different. When the tracer gas was released from the armpits the normalized concentration in all six measuring locations was the highest (in the range 0.23-0.42) for the prone position (lying on its

stomach) indicating decreased IAQ. A possible explanation for this might be that large area of the exhaust opening of the mattress was blocked because of the different body curvature of the manikin in this position. In supine position the manikin's pelvis (area 0.055 m^2) and small area of the arms were the parts in contact with the opening. In prone position the front thighs (each with area of 0.083 m^2) together with the arms were only blocking the exhaust opening. The VM's performance can be improved by designing a larger than 0.13 m^2 exhaust opening along the mattress. A further study with more focus on different designs of the local exhaust opening is therefore suggested.
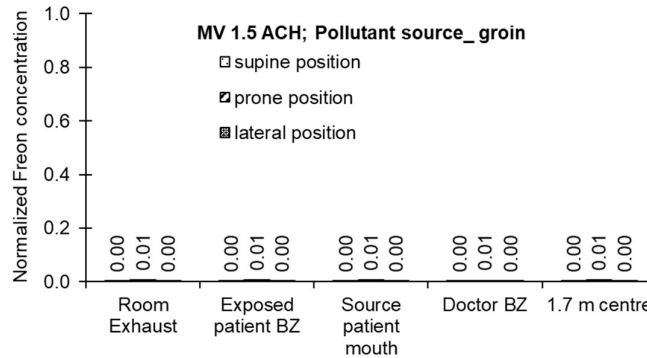
Figure 21: Comparison of the normalized concentration for the three different lying positions of the manikin and for the pollution sources patient's groin. The results were obtained at 1.5 ACH using the VM with ESA = 0.13 m^2

As shown, the bed-integrated local exhaust, namely the ventilated mattress, reduced the gaseous pollutants released from different parts of the body. As already discussed in the previous chapters, the feet, groin and armpits are usually the sites of the body prone to generate unpleasant odour. Therefore it is expected that this method will significantly improve the quality of the room air in facilities where people are bed-bound unable frequently to take baths. Mattresses and bedding are possible sources of gaseous pollutants such as volatile organic compounds (VOCs) and flame retardant chemicals (Boor et al., 2014; Kemmlein et al., 2003). These can be removed by use of VM. In the previous chapter the ability of the VM to remove fine particles released close to the manikin's body was shown. The VM has the potential to remove also skin flakes shed from the body which are considered one of the main carriers of *Methicillin-resistant Staphylococcus aureus* (MRSA). Nowadays, the risk of infections, especially the MRSA, is still a major patient threat in hospital environments (Beggs et al., 2015).

The application of the VM has a potential to increase flexibility in the use of hospital rooms. The HVAC system in all patients' rooms can be designed to maintain 3 ACH. In the rooms where higher ACH rate is required, the additional improvement of the IAQ can be achieved with the use of the local exhaust ventilation (VM) method coupling it with the exhaust system of the room background ventilation. However, it should be taken into account that a building with many beds installed will require also more powerful exhaust fans in the air handling unit as each VM connection to the total volume exhaust will introduce extra resistance to the system. Future studies could therefore focus on the pragmatic design of the VM, how to deal with clogging of ducts, etc. It may be considered to

apply the VM without connecting it to the main ventilation system by cleaning the air locally and recirculate it instead of exhausting. This approach will be presented in one of the following sections in this chapter.

4.3.2.3   Performance of the ventilated mattress in terms of thermal comfort

Figure 22 shows the change of the equivalent temperature, Δt_{eq1}, as a result of the use of the mattress. The results obtained at 23ºC and flow rate of 1.5, 3 and 6 L/s through the mattress were compared when the manikin's body was not covered and when it was covered with light quilt. As expected the results reveal that the body segments in contact with the ventilated mattress were cooled. The head region (crown, left and right face and the back of neck) were almost not affected by the cooling provided with the VM. Increase of the ventilation flow through the mattress increased the heat loss from most of the body segments. Back side (lower back) and the back (gluteus) were the most cooled body segments. Similar results were obtained also at 26 and 29ºC when the VM was in operation and the manikin was covered with a sheet (results shown in Paper IV, Appendix B). The use of body covering increased the cooling from the VM (cf. Figure 22a and 22b). The increase of the cooling effect was observed for the whole body and all body segments except the head region that was not covered. These results are most likely because when there was no body cover, the manikin was exposed to the thermal conditions created by the background mixing ventilation. At the comfortable range of room air temperature (i.e.21-24°C), the surfaces of the VM in contact with the body can be heated under individual control of user to provide comfort.
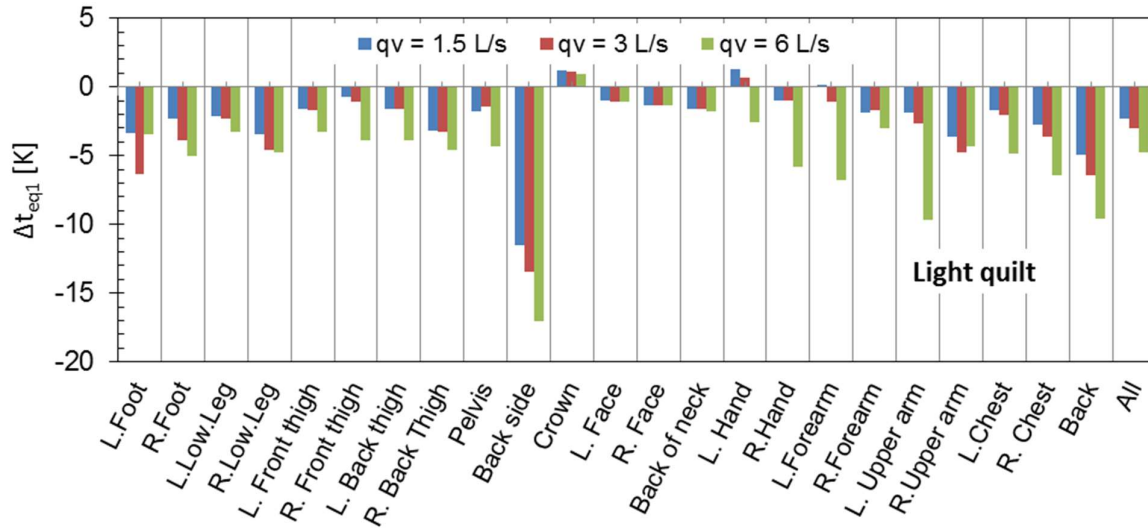
a)
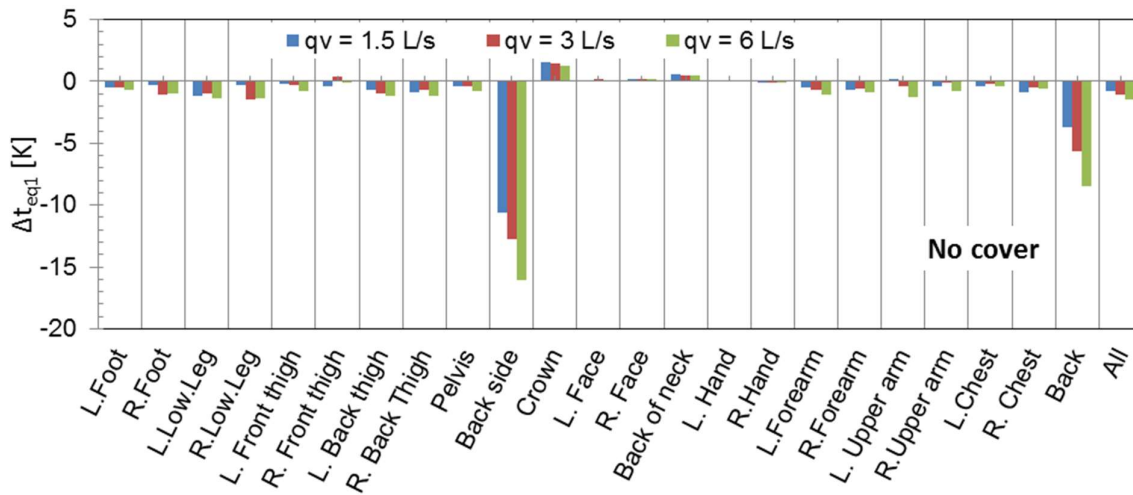
b)

Figure 22: Change in the equivalent temperature, Δ_{teq1}, for manikin's segments and whole body at different flow rates of the VM. Results when the body is covered with light quilt (a) and not covered (b) are shown. Room air temperature was 23°C.

The ability of the VM to improve person´s thermal comfort at elevated room temperature was studied at 26°C. For this purpose the change in the equivalent temperature Δ_{teq2} was used to assess the thermal comfort provided with the ventilated mattress at elevated temperature (26°C) compared to comfortable temperature of 23°C without additional cooling of the body. As mentioned, negative values of Δ_{teq2} mean that people will report cooler thermal sensation compared to that at 23°C without mattress and positive values will mean warmer thermal sensation. Some of the obtained results are shown in Figure 23. The results in the figure show that the increase of the room temperature will make the person lying in bed with the VM in operation to feel warmer than at 23°C. This thermal sensation will be felt for the body as a whole and for all body segments except

the back side and the back. The results suggest that at these two body parts, especially at the back side, a person in a bed with VM will feel locally cooler than at 23°C. The analyses of the results reveal also that at 26°C a person lying in a bed with VM will feel cooler when his/her body is covered with sheet compared to when the body is not covered (results shown in Paper IV).

The results suggest that the use of the VM at elevated room temperature will decrease the local thermal sensation at the back side and the back compared to the thermal sensation at 23°C. For the remaining body parts and for the whole body the thermal sensation will be warmer than at 23°C. The increase of the airflow rate through the VM and covering of the body with sheet will improve the thermal sensation when the mattress is in operation and will move it toward the thermal sensation reported at 23°C. However the large differences in local thermal sensation as a result of the non-uniform body cooling may cause discomfort. This needs to be studied in carefully designed human subject experiments. Another question related to the ventilated mattress practical application that could be asked is if the high exhaust flowrates of the VM may "glue" the cover and hospital pyjamas on the bed and result in blocking the openings and reduce performance. It should be noted that such effect was not observed during the measurements even at the highest tested VM's flow rate of 10 L/s.
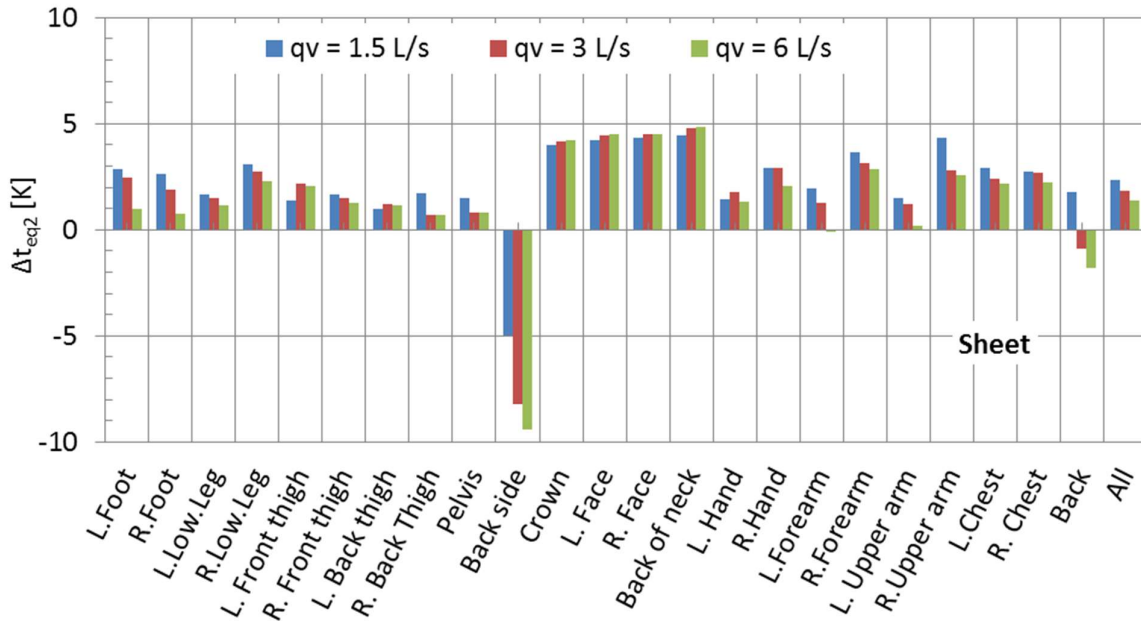
Figure 23: Change in the equivalent temperature, Δt_{eq2}, at room air temperature of 26°C compared to room air temperature of 23°C. VM was in operation. Results when the body is covered with sheet and not covered are shown.

4.3.3   Conclusions

The main goal of this part of the thesis was to determine if the ventilated mattress (VM) is able to reduce occupant's exposure to body bio-effluents in rooms with bed-bound persons as it is usually the situations in health care facilities' patient rooms. The exposure to bio-effluents generated from

the feet, groin and armpits of a lying in bed patient ("source patient") was studied in a full scale mock-up of a hospital room with a second patient lying in bed and a standing doctor. The cooling of the source patient's body caused by the VM was investigated as well. A number of conclusions can be drawn as the follows.

- Non-uniformities in the distribution of body bio-effluents may occur in patient rooms ventilated only with displacement ventilation depending on the location of the source and presence of body covering. DV alone at 6 ACH provided similar air quality in the breathing zone of the source patient as that at 3 ACH;

- The application of the VM helped to decrease the exposure and risk of cross-contamination to bio-effluents emitted from the source patient's body in the room;

- In rooms with either mixing or displacement ventilation at reduced background ventilation rate, from 6 ACH down to 1.5 ACH, the room air quality can be improved greatly when the emission of the body pollutants takes place near the VM's exhaust opening in cases with and without presence of body covering. This reduction of the background ventilation rate may lead to energy savings;

- With presence of body covering, the VM with airflow rate 1.5 L/s under the condition of 1.5 ACH (MV or DV) removed completely the body bio-effluents in the occupied zone compared to MV or DV at 3 ACH and 6 ACH;

- High exposure reduction to bio-effluents emitted from the feet, groin and armpits can be achieved when the VM's exhaust opening is placed below the gluteal area of the person. The size of the local exhaust opening and the lying position of the person on the mattress may affect the efficiency of the VM. It is recommended to use large local exhaust openings in the mattress to overcome this issue;

- The ventilated mattress provides cooling to the thermal manikin's body segments it was in contact with. The cooling increased with the increase of the airflow rate through the mattress and decreased with increase of the room temperature. The cooling increased when manikin's body was covered with sheet or light quilt. The back side and the back are the body segments that were cooled intensively since most of their surface area was in contact with the mattress. The surfaces of the VM in contact with these body segments can be heated under individual control of user to provide comfort.

4.4 Efficiency of air cleaning textiles for combined use with the VM

Ammonia is one of the compounds that contributes greatly to the offensive odour of human waste (feces and urine) (Nishida et al., 1981). Ammonia (NH_3) has an unpleasant odour therefore it can reduce indoor air quality and affect negatively occupants' health and perceived air quality. A questionnaire survey study shows that there is a problem with unpleasant odours in hospitals

(Itakura et al., 2007). The study found that 88.5% of the nurses sensed odours in hospitals, of whom 81.0% considered it a problem and 67.2% recognized a need for improvement.

The purpose of this part of the current study was to evaluate the potential of different textiles to remove ammonia. The specific aim of the study was to find out which deodorant textile will be the most efficient cleaning method so its application in bed-microenvironment can be studied in combination with the ventilated mattress.

The effect of air temperature and relative humidity on the air cleaning efficiency of three different textiles was investigated. These experiments were carried out to show potential applications of air cleaning materials. It was not an objective of this study to assess the composition or the specific cleaning properties of the deodorant textiles. This part of the study is based on the appended Paper V (Appendix B). Thus further details can be found in the paper.

4.4.1 Experimental method

4.4.1.1 Textile samples

Three types of textile materials were studied for their efficiency to absorb ammonia gas. The studied materials were activated carbon fibre (ACF) material that had been chemically treated with acid, cotton fabric treated with iron phthalocyanine and copper (Cu) (referred as ¨treated cotton fabric¨), and untreated cotton fabric. The untreated cotton fabric was used as a reference case. All studied materials are trade mark materials and therefore their composition and amount of chemicals used to impregnate them is not announced.

4.4.1.2 Experimental set-up and procedure

Samples of ACF, cotton with iron phthalocyanine with Cu and untreated cotton fabric were cut in square pieces, each with an area of 0.04 m^2, and comparatively evaluated for their ammonia gas removal capacity. A test rig was specially developed for this study. The test rig consisted of a small box attached to a heated plate (Figure 24) whose surface temperature was maintained 34°C (average skin temperature of the human body at rest). The heated plate had dimensions of 0.2 width x 0.2 length x 0.05 height m. The heated plate was isolated from the bottom and the sides with polystyrene to allow the heat to transfer only upwards through the textile sample that was placed so as to completely cover the top surface. The test rig was placed in a climate chamber with controlled air temperature and relative humidity. Air was supplied from the climate chamber to the test rig using a DC fan (0-24 V). During the experiments, the airflow supplied to the box was controlled at a low, constant flow rate of 0.46 L/s, corresponding to a velocity of 0.04 m/s at the cross-sectional area of the box, where a sample was placed horizontally on the top of the heated plate.

Cotton soaked in ammonium hydroxide (NH$_4$OH) solution was put on top of the heated plate, covering the whole surface area of the plate in order to generate ammonia gas. 200 mL of 0.03% NH$_4$OH solution was prepared prior each experiment to achieve approximately 20 ppm initial concentration of NH$_3$ in the air. The concentration of ammonia gas was measured downstream of the tested sample. A sample fixed on a stainless steel mesh was placed over the soaked cotton. The

purpose of the mesh was not to allow the tested material to be in a direct contact with the liquid NH₄OH solution. Ammonia concentration was sampled and analysed using Innova 1303 multi-channel sampler and a photoacoustic gas monitor Innova 1312 (±5% accuracy).
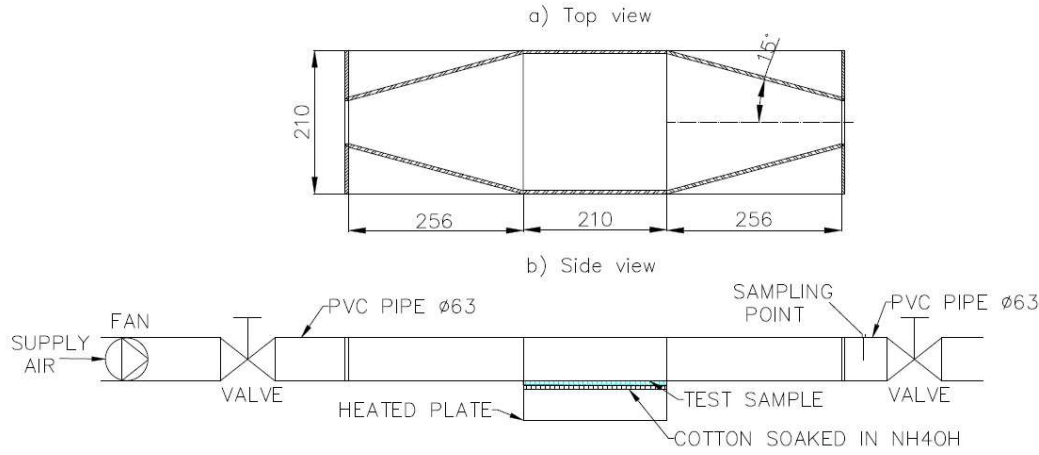
Figure 24: A schematic drawing of the experimental set-up.

4.4.1.3 Experimental conditions

Each sample of the three studied materials was exposed separately to ammonia gas for 1 hour. A series of experiments was conducted under four different conditions, i.e. at low and high levels of relative humidity (25% and 80%) at two air temperatures (20 and 28°C). Since ammonia concentration naturally decays with time during the evaporation process, control experiments with no sample in place, i.e. with only cotton soaked in aqueous NH₄OH on the plate, were carried out under the same 4 conditions as described above.

4.4.1.4 Data analysis

For each experiment, a freshly prepared ammonium hydroxide solution was used. The concentration decay of the ammonia gas for each condition was investigated. For this purpose, the measured data were normalized to the maximum value of ammonia concentration in each condition for each different sample. The normalized data were compared in order to identify the cleaning performance of the deodorant materials. The normalized concentrations (C_i/C_{max}) for each material were calculated by the following equation:

Normalized concentration = C_i/C_{max} (7)

where C_i is the measured value of ammonia concentration and C_{max} is the maximum of the measured concentrations for each experiment.

4.4.1.5 Results and discussion

Figure 25 shows the concentration variation of NH_3 as a function of time for all materials samples at air temperature and high relative humidity of 20°C and 80%, respectively. It can be seen that the

highest NH₃ concentration decrease was achieved when using the activated carbon fiber (ACF). The ACF reduced the ammonia gas almost to zero concentration at the end of the experiment. When comparing the other textiles with the control case without sample, no cleaning effect was found. There was thus no difference in the NH₃ concentration between the cotton fabric treated with iron phthalocyanine and copper and the untreated cotton fabric. The results for the other experimental conditions (shown in Paper V) demonstrate clearly that the temperature and relative humidity do not affect the deodorant efficiency of the ACF material. Only a slight decrease in the cleaning efficiency of the ACF was observed at the end of the exposure when the relative humidity was increased from 25% to 80%. A study by Lee and Davidson (1999) showed that the adsorption efficiency of different type of activated carbon fibers decreased when the relative humidity was increased from 20% to 50%. The mechanism for this effect of humidity was believed to be that micro-pores in the activated carbon were blocked by water molecules, leaving a reduced number of sites for the adsorption of gas molecules. In the present study, an effect of increase in RH level on the performance of the acid-treated ACF material was not observed. This could be explain with the fact that ammonia reacts with a number of acids, thus the air cleaning effect of the ACF occurs due to chemical adsorption (chemisorption). Normally, water vapour facilitates chemisorption, whereas it usually hinders physical adsorption (ASHRAE, 2011). This, however, means that lower than 25% RH level might decrease the ACF performance.

In the case of the cotton textile treated with iron phthalocyanine and copper the test results indicate poor performance compared to that of ACF. A recent study showed that this material had been able to reduce ammonia concentrations from 100 ppm to less than 20 ppm (Mizutani et al., 2013). However, these results were obtained in a static test in which the material was brought into equilibrium with the ammonia gas without applying any air movement, in contrast to the present study. The present results indicate that even though the air velocity in the test rig was very low, 0.04 m/s, the time taken for the ammonia molecules to pass through the material was too short for a reaction to occur.
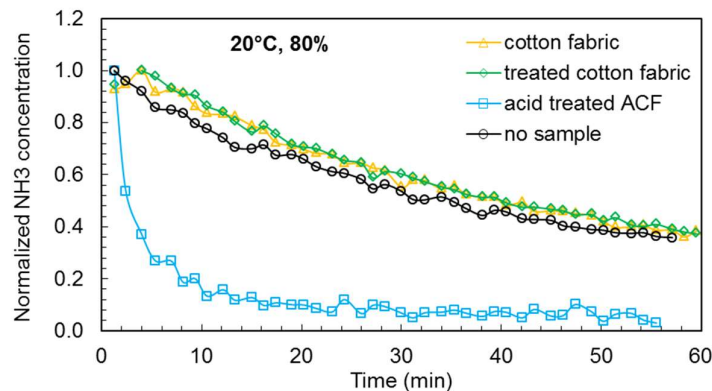
Figure 25: Normalized ammonia gas concentration for all material samples and without any sample measured at 20 °C temperature and 80% relative humidity. ACF stands for activated carbon fibre. Treated cotton fabric stands for cotton fabric treated with iron phthalocyanine and copper.

4.4.2   Conclusions

This part of study compared the removal of ammonia gas in the ambient air by acid treated activated carbon fibre (ACF) material and a cotton fabric that had been treated with iron phthalocyanine and copper (Cu) in small-scale experiments. The experimental results show the following:

- Activated carbon fibre (ACF) material that had been treated with acid efficiently removed ammonia gas at low and high air temperature and relative humidity under conditions simulating its emission from clothed skin at 34°C with an ambient air velocity of 0.04 m/s;

- An increase in relative humidity from 25% to 80% slightly decreased this removal efficiency;

- Cotton textile treated with iron phthalocyanine and Cu was not found to remove ammonia under the studied conditions.

4.5 Ventilated mattress combined with air cleaning material

The application of the VM combined with local air cleaning (in this case acid-treated ACF material was used) for improving the IAQ in patient rooms in health care facilities was examined. The performed experiments presented in this section set out to determine to what extent it will be possible to clean the exhausted by the VM polluted air and reduce exposure to body emitted ammonia gas in a general patient room using local air cleaning? This question is addressed in research Paper VI (Appendix B).

4.5.1 Experimental method

4.5.1.1 Experimental set-up and equipment

Experiments were carried out in a stainless-steel climate chamber furnished with a single-bed to simulate a hospital patient room. The dimensions of the chamber were as follows: length e 3.6 m, width - 2.5 m and height - 2.5 m. The climate chamber was air conditioned using upward flow of 100% outdoor air supplied from the entire floor. During the measurements, three fans were constantly operating to generate complete mixing in the chamber. The room air was exhausted through a circular opening located on the ceiling (Figure 26).The bed used in this experiments was already described in Section 4.3.1.1 of this chapter.

Two heated dummies were used to simulate a patient lying in the bed and a standing doctor next to the patient's bed. The standing dummy was positioned 0.2 m from the side of the bed near the head of the lying dummy, Figure 26. The total generated heat power was 62 W for the "patient" and 130 W for the "doctor". During the experiments, the legs and the torso of the lying dummy were fully covered with a bed sheet or in some cases with a piece of the ACF material used as a blanket.

The ventilated mattress (VM) was placed on top of the regular mattress of the bed. The exhaust opening of the VM was located under the area where the legs of the dummy were connected to the torso (i.e. corresponding to the gluteal region of a human body). The surface area of the local exhaust opening was 0.13 m^2. The VM was connected to a separate exhaust system. A small axial fan, placed inside the chamber, was connected with a straight duct (ø 0.08 m) to the VM. Through this separate system the ammonia gas was exhausted from the mattress and discharged out of the chamber. In one experiment, the exhausted air was discharged back into the chamber after it was locally cleaned by the ACF material installed within the mattress. During the experiments when the ventilated mattress was in operation its exhaust air flow rate was kept constant, equal to 1.5 L/s. The equipment and procedure used to control the VM flow rate was described in Section 4.3.1.3 and also more details are provided in Paper VI.
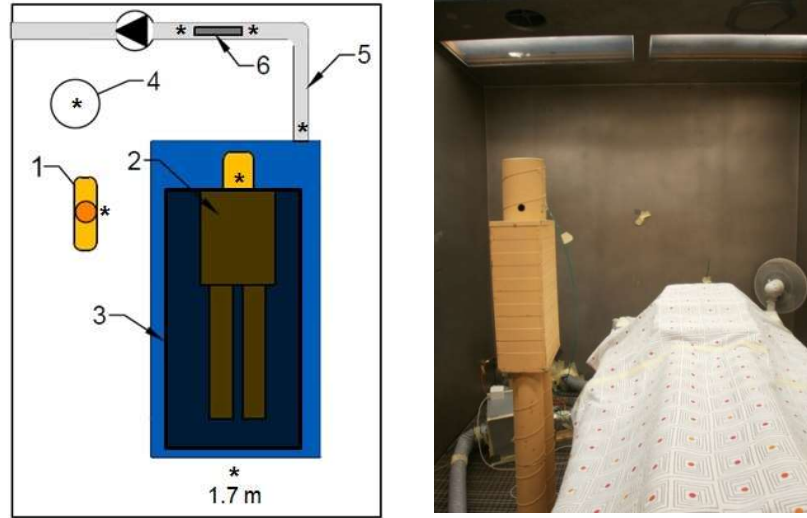
Figure 26: Experimental setup: (left) Floor plan of the chamber showing the position of the sampling gas tubes (*), where 1 - "doctor", 2 - "patient", 3 - a double bed sheet or ACF material used as a blanket, 4 - total exhaust opening, 5 - exhaust duct of the VM connected to a fan, 6 – 'duct ACF' position; (right) Interior of the chamber with the standing dummy next to the bed with the ventilated mattress and the lying dummy covered with a sheet.

The used activated carbon fibre (ACF) material was the one found in the previous experiments (Section 4.4) with high efficiency to reduce ammonia gas. Experiments with the ACF material were performed under three conditions: 1) installed as two single rectangular sheets inside the mattress below and above its mesh like a "sandwich" (Figure 27); 2) a rectangular piece of the ACF fabric was attached to a cylindrical frame which was installed across the exhaust duct of the mattress (referred as "duct ACF" in Figure 26) or 3) the ACF material was used as a patient's cover. The cleaning effect of the ACF used as a patient's body cover (blanket) was studied only to show potential applications of air cleaning materials. It was not an objective of this study to examine the properties of the ACF material.
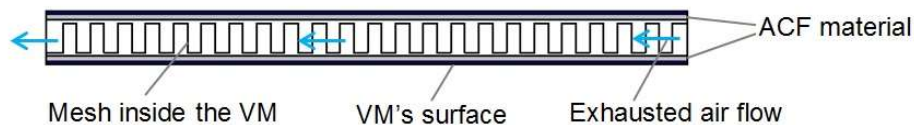
Figure 27: Diagrammatic representation of the "sandwich" ACF material installed inside the VM.

4.5.1.2 Measured parameters and measuring equipment

Ammonia gas was released from the lying dummy's "groin" area to simulate body generated bio-effluents. The ammonia gas was released from a perforated plastic ball at constant rate of 0.2 L/min. Information about the gas generation procedure is provided in Paper VI (Appendix B).

The ammonia gas was measured by two Innova 1303 Multipoint Samplers and its ammonia gas concentration was analysed using Innova 1312 gas monitor connected to the two Innova 1303 Samplers. Each of the Innova 1303 samplers had 6 channels. The sampling time of the Innova 1312 was 40 s/channel and 12 channels were measured in sequence, giving a period of 8 min between measurements in the same location. The Innova gas monitor was calibrated prior to the experiment and its lower detection limit for NH_3 gas was 0.1 ppm. The measuring error of the instrument was 5% of the actual value. The NH_3 concentration in the chamber was measured at the breathing zone (BZ) of both the "doctor" and the "patient", at the total exhaust opening, and at 1.7 m height 0.2 m from the patient's legs. The ammonia gas was sampled in the exhaust duct of the VM, downstream of the "sandwich" ACF, and downstream and upstream of the duct ACF material (Figure 26). The rest of the channels were placed in several positions outside the chamber as a control measure during the experiment to check if there were leakages from the chamber. No leakages were measured. No NH_3 was measured in the supply air as well.

A HOBO data logger was used to measure and record the relative humidity in the chamber with an uncertainty of 2.5%. The air temperature in the chamber was measured by an air temperature sensor with an uncertainty of 0.3°C as described by Simone et al. (2013).

4.5.1.3 Experimental conditions

The chamber was ventilated at 1.6 ACH during all the measurements. 1.6 ACH corresponded to 10 L/s, which is the minimum requirement of supply air flow rate per person or bed for patient rooms, as proposed in the FprCEN/TR 16244 (2011) technical report for hospital ventilation. The temperature inside the chamber was 29 ± 1°C. This temperature was in the range recommended in standards and guidelines for patient rooms (20-32°C). For instance, conditions of 32°C air temperature and 35% relative humidity has been found beneficial in treating certain types of arthritis (ASHRAE, 2003). An air temperature of 32°C is sometimes kept for burn patients and 30 °C in paediatric surgery (ASHRAE, 2003). Furthermore, a study on the performance of the method under high room air temperatures is important when considering perceived air quality which, decreases with increase of air temperature and humidity (Fang et al., 2004). The ASHRAE standard 170- 2013-Ventilation of health care facilities recommends a maximum of 60% RH in patient rooms (ASHRAE, 2013). However, in countries with hot and humid climate (e.g. Singapore, Malaysia, Japan, etc.) this recommendation might be difficult to fulfil. Yau and Chu (2009) reported that the air temperature in two Malaysian hospitals varied in the range of 20-32.2°C and the measured RH varied in the range of 44%-79%. Thus, considering the possible practical applications of the studied method, the relative humidity in the chamber was controlled and kept in some experiments at 25% (with ±5% relative error) and in some at 70% (with ±6% relative error). Note that the impact of buoyancy flows in the room was neglected by keeping the temperature high. But even if the room temperature was low the buoyancy flows would be diminished because mixing fans were used.

The experimental conditions comprised:

1 - Background ventilation only operating at 1.6 ACH (abbreviated '1.6 ACH');

2 - The VM was operating without using the ACF material ('1.6 ACH + VM');

3 - The VM operating and the ACF material was installed on the cylindrical frame placed inside the exhaust duct of the VM ('1.6 ACH + VM + duct ACF');

4 - The VM operating and having the ACF material installed as a "sandwich" ('1.6 ACH + VM + "sandwich" ACF');

5 - the VM operating with the ACF material installed as a "sandwich" and with recirculation of the air exhausted by the VM back into the chamber ('1.6 ACH + VM + "sandwich" ACF + recirculation');

6 - Using only the ACF material as a cover, i.e. the VM was turned off, ('1.6 ACH + ACF cover');

7 - The VM operating in conjunction with the ACF used as a cover ('1.6 ACH + VM + ACF cover').

4.5.1.4 Experimental procedure and exposure assessment

The total volume ventilation system and the two dummies were switched on all the time to keep the air temperature in the chamber stable. Prior to the experiments with the ventilated mattress in operation, the air flow rate through the mattress was adjusted to 1.5 L/s. The experiments were started after reaching steady state level of the desired room air temperature and relative humidity. When used, the ACF was set to the desired position prior to the experiment. Afterwards ammonia gas dosing was started.

When steady state, i.e. constant gas concentration at the sampling points was reached, 20 values of the NH_3 concentration for each measuring point were acquired. The data were then analysed by averaging the 20 values collected during one experimental condition.

The exposure reduction in the room due to the effectiveness of the VM and the ACF material was quantified as follows:

$$Exposure\ reduction = \frac{C_{i,Ref} - C_i}{C_{i,Ref}} \times 100\% \tag{8}$$

where C_i is the average concentration (ppm) of the contaminant acquired at a measuring point when the VM or ACF or both were used in the experiment and $C_{i,Ref}$ is the average concentration (ppm) acquired at the same measuring point during the reference condition '1.6 ACH' background ventilation only. The closer to 100% the better the performance of the studied method is.

4.5.1.5 Uncertainty of the measurements

The measured data of ammonia gas concentration were analysed in accordance with ISO/IEC Guide for the expression of uncertainty (ISO 2008). The uncertainties are given in the results as error bars on the column charts.

4.5.2   Results and Discussion

Figure 28 compares the exposure reduction due to the use only of the VM at 1.6 ACH and when the "sandwich" ACF was installed inside the VM. The results indicate that up to 71% of the body-emitted pollutants were removed by the ventilated mattress before they were mixed with the inhaled air (the condition '1.6 ACH + VM' in Figure 28). The same percentage of exposure reduction (up to73 %) was achieved when the sucked polluted air was locally cleaned inside the VM by the ACF material and recirculated back to the room (the condition '1.6 ACH + VM +"sandwich" ACF+ recirculation' in Figure 28). In every experiment equal amount of NH_3 gas was released from the patient's groin and also the VM exhaust flow rate was kept unchanged, therefore the amount of sucked contaminants in the mattress was the same during the two experiments. Thus, the results in Figure 28 suggest that the drawn polluted air was fully cleaned by the ACF material. Hence, about 30% of the polluted air was not captured by the local suction and it was therefore mixed with the background room air. Nevertheless, it is an important finding that the VM can be used to improve the IAQ even when it is not connected to a separate exhaust system. The analysis of the ammonia gas under the operation of the VM combined with the "sandwich" ACF at 70% RH demonstrated similar exposure reduction to that during the corresponding condition at 25% RH. These results suggest that the VM combined with the ACF material can be used also in countries with hot and humid climate.

The method of incorporating the ACF material inside the mattress to clean the drawn polluted air and then recirculate it back to the room will increase the flexibility of the patient's bed location, allowing the bed to be moved around. The recirculation mode of operation of the VM will avoid using additional ducting and making changes in already existing background room ventilation. Yet, the thesis does not engage with cost benefit analysis which is needed to evaluate investment costs if every bed shall have a fan.
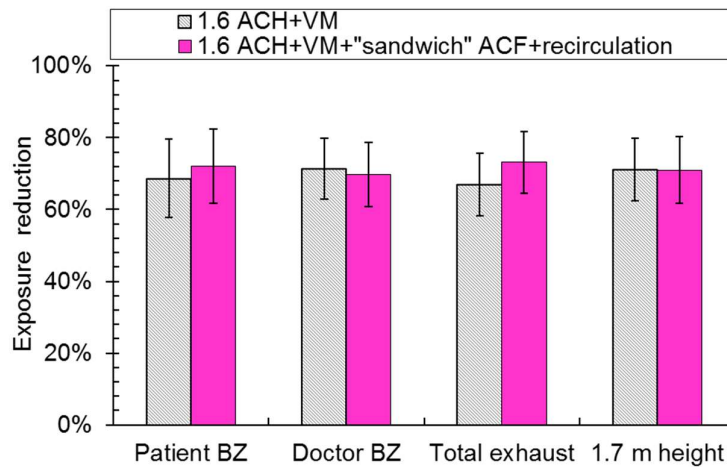
Figure 28: Comparison of the exposure reduction when only the VM was used and when the VM was combined with "sandwich" ACF material relative to the background mixing ventilation alone. Room air temperature was 29°C and relative humidity 25%.

Figure 29 shows the exposure reduction when the ACF material was used as a cover for the patient and when the VM and the ACF cover were used together. When only the ACF cover was used, the exposure reduction in all points, except at the patient's breathing zone (BZ), was more than 80%. Such method of local air cleaning will be much more efficient in practice than the widely used room air cleaners. However, there are limits of applying cleaning textiles as a cover. In reality, the patient will move and thus the body odours may escape before reacting with the material. Hospital clothing for the patients and bed linens made from different air cleaning textiles could be a solution since the velocities between the skin and the human body are low (<0.05 m/s). Therefore there will be more time for a reaction to occur. The most significant result in Figure 29 is that the exposure to ammonia gas was almost entirely reduced (up to 96% exposure reduction) when employing both the ventilated mattress and the ACF cover. It should be noted that during this case the ventilated mattress was extracting the pollutants out of the room through the separate exhaust system. Thus, the rest of the pollutants, which were not captured by the VM, were cleaned by the ACF cover. The high exposure reduction efficiency of the ACF fabric applied as a cover for the patient is a good illustration of the potential of using existing, new and forthcoming textile materials in combination with the VM.

Recently, a new non-woven fabric coated with nanoparticles that has antibacterial effect has been introduced on the market (NBC Meshtec, 2017). The new material can inactivate different bacteria including MRSA, *Klebsiella pneumonia, Bacillus coli*, etc. MRSA is a bacterium that can cause a variety of problems ranging from skin infections and sepsis to pneumonia to bloodstream infections (CDC, 2017). As already discussed, desquamated skin flakes from the body can be carriers of the pathogenic bacterium (Davies and Noble, 1969). Another study reported that some of the frequently contaminated objects in a hospital included also the bed linens and the patient's gown (Boyce et al., 1997). It has been shown that it is likely particles deposited on mattresses and blankets to re-suspend and reach the breathing zone of the lying person (Spilak et al., 2014). Beside the use of

integrated local exhaust ventilation, another source control method for cleansing the inhaled air in hospital patient rooms can be the use of textile materials with antibacterial and deodorizing properties in form of covers, bed linens, gowns, etc. Both textile threats can be interwoven in a threat and used to make new material combining the germicidal and deodorant effects.
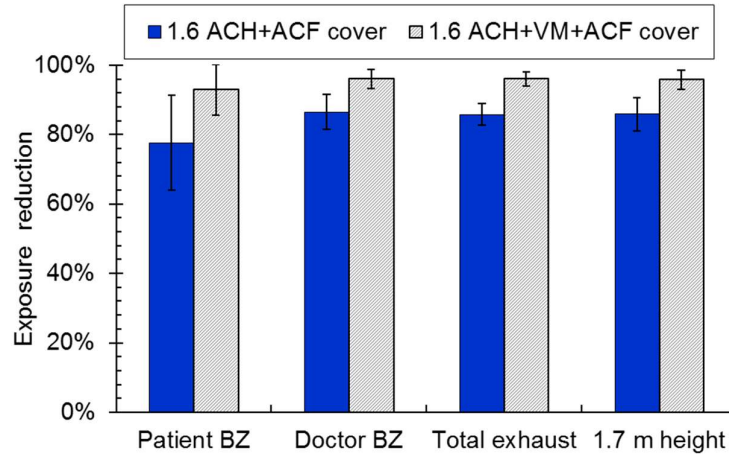
Figure 29: Exposure reduction using only the ACF cover and when the VM was combined with the ACF cover compared to the case of background mixing ventilation alone.

The application of the VM combined with air cleaning will increase the flexibility of the bed. The VM can be also combined with the patented personalized hospital bed ventilation for preventing airborne spread of infectious respiratory diseases (Melikov et al., 2016b). An optimal control of the air pollutants generated from both the body and the respiratory activities of patients can be provided using these two local ventilation methods.

4.5.3 Conclusions

In this part of the study, measurements in a full-scale mock-up of a hospital patient room were carried out to assess the performance of the VM combined with air cleaning. Ammonia gas was used to simulate a constant emission of airborne pollution from the groin of a lying in bed patient. Acid-treated ACF material, which is able to clean air from ammonia, was used for local cleaning method. The results of this investigation show the following:

- The results show that the ACF fabric applied as a patient's cover is an effective method of reducing exposure to ammonia gas by more than 80%;

- The combined use of the VM and ACF cover was the most efficient exposure reduction strategy, since more than 90% of the ammonia gas in the room air was removed;

- The ammonia exposure in the patient room was reduced by 70% when the drawn polluted with ammonia air was cleaned with the ACF material inside the VM and afterwards was discharged it back to the room.

It can be expected that energy saving in hospital patient room will be achieved with the application of the studied here method. The energy saving potential is explored later in this chapter.

4.6 Efficiency of seat-integrated local exhaust system

In Chapter 2 of this thesis, it was shown that the application of seat-integrated local exhaust ventilation, namely the ventilated cushion (VC), has a potential to reduce body-emitted bio-effluents. In this part of the study two sets of experiments were conducted to identify the performance of the VC with regard to indoor air quality and thermal comfort. The first set of experiments is based on the research Paper VII (Appendix B). The aim was to evaluate the performance of the VC with regard to the influence of location of the pollution source, room air temperature and background ventilation rate on the pollutant removal efficiency of the VC. The second sets of experiments aim to study the cooling of the human body when it is in contact with the ventilated cushion in a quiescent indoor environment.

4.6.1 Experimental method - Set 1

4.6.1.1 Experimental set-up and facilities

The first set of experiments was performed in a room furnished to simulate a single office room. The dimensions of the room were 5.9 m x 6 m x 3.2 m (W x L x H). The room had two single-pane windows each with dimensions 1.2 m x 1.7 m (W x H). A typical office working environment was simulated by a thermal manikin seated on a computer chair in front of a desk with a laptop on it (Figure 30). Mixing air distribution was used to supply 100% outdoor air to the room through a square diffuser mounted in the middle of the ceiling. Air supply diffusers with different sizes were used to achieve similar air jet pattern at different ventilation rates. The diffuser which was used to provide room ventilation rate of 1 ACH (31.8 L/s) and 1.5 ACH (45.4 L/s) had free area of 0.011 m^2; a diffuser with free area of 0.019 m^2 was used at 3 ACH (94.4 L/s) and at 6 ACH (188.8 L/s).The diffusers were supplying the outdoor air in three ways (position 7 in Figure 30). A rectangular exhaust grill (970 mm x 170 mm) mounted on the wall close to the ceiling was used to exhaust the air from the room (position 8 in Figure 30).

A non-breathing thermal manikin was used as a sitting occupant. The manikin's body consisted of 17 independently heated and controlled body parts. The used in the experiments manikin had the same size and body shape as the thermal manikin described in the Chapter 2 of the thesis. The control of the manikin was the same as well. The manikin was sitting on the ventilated cushion which was placed on a computer chair. The design and control of the ventilated cushion was described in Chapter 2. More details can be found also in Paper VII.
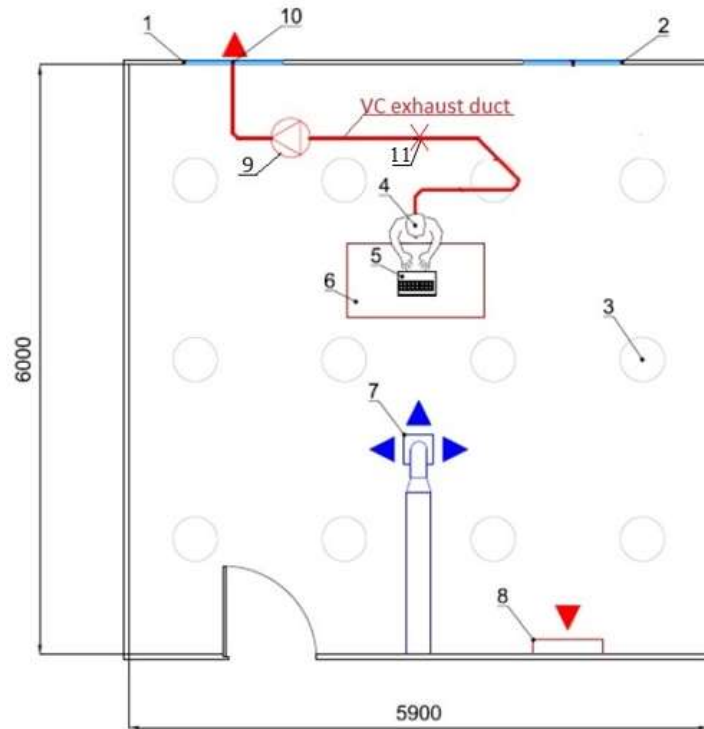
Figure 30: Room layout in the single office ventilated with mixing air distribution: 1; 2 – windows, 3 – lights (12 in total), 4 – occupant, 5 – laptop PC, 6 – table, 7 – supply, 8 – total exhaust, 9 – fan, 10 – air exhaust, 11 – air flow sensor MFS-C-0080.

4.6.1.2 Measured parameters and measuring equipment

Tracer gases, namely carbon dioxide (CO_2) and nitrous oxide (N_2O), were used to simulate bio-effluents emitted by the manikin's armpits and groin region respectively. The emission rate of CO_2 and N_2O were adjusted to be 0.4 L/min and 0.1 L/min respectively. The tracer gases were released through porous sponges that were attached to the polluting body parts below the clothing of the manikin. The air mixed with the tracer gases was sampled and its gas concentration was analysed under steady-state conditions using two Innova 1303 multi-channel samplers and two gas monitors Innova 1312. The instruments were calibrated prior to the experiments in the ranges $5 \div 3500$ ppm and $0.5 \div 350$ ppm for CO_2 and N_2O respectively. The concentration of each tracer gas was measured at six points: 0.005 m from the mouth of the manikin (referred as breathing zone), 0.5 m above the head, at the supply, exhaust air from the room, at 1.1 m height on the left side of the table (40 cm away), and in the centre of the room at 1.7 m height.

The air temperature and air velocities were measured around the manikin. The used measuring instruments were described in Chapter 4.3.1.4.The air temperature and velocity were measured at five heights – 0.1 m, 0.6 m, 1.1 m, 1.7 m and 1.9 m above the floor. The measurements were performed at the sides and behind the manikin. The distance from the manikin was kept 40 cm.

4.6.1.3   Experimental conditions

During the measurements the air temperature in the room was kept 26°C (summer condition) and 20°C (winter condition). The manikin was seated behind a table with a laptop. The posture of the manikin was kept to be slightly inclined (10° from the axis) with back supported by the backrest of the chair, arms put on the table towards the laptop and gap between the table and the manikin's abdominal equal to 10 cm. The laptop was consistently operated at the maximum performance (by using the software HeavyLoad). The generated heat load was 60 W. The room lighting was provided by 12 ceiling mounted light fixtures, 32 W each, spread over the entire ceiling.

Full-scale experiments were conducted at four background ventilation rates -1, 1.5, 3 and 6 ACH. The office room was assumed to be located in a low-polluting building. According to the European Standard EN 15251 (2007) the ventilation rate required for diluting emissions (pollutants) from the building components (building and furnishing, and HVAC system) is 0.7 L/s per m^2 floor area for IAQ category II and 1 L/s per m^2 floor area for IAQ category I. The required ventilation rate for diluting emissions (bio-effluents) from people is 7 L/s per person for IAQ category II and 10 L/s per person for IAQ category I. The total required ventilation rate for each category is the sum of these two calculated ventilation rates. The required total ventilation rate for the simulated single office in this study (35.4 m^2 floor area and 1 occupant in the room) was calculated to be 31.8 L/s (1 ACH) for category II and 45.4 L/s (1.5 ACH) for category I. The ventilated cushion was operated only with the background ventilation of category II. Additionally, two more cases at high background ventilation rates were performed at room air temperature 26°C - 94.4 L/s (3 ACH) and 188.8 L/s (6 ACH). All experimental conditions are listed in Table 4. In order to avoid the infiltration from outside and surroundings, during the experiments the room was kept at a slight overpressure. In all cases the exhaust in the room was kept 3 L/s lower than the total exhaust from the room. In addition, the total volume exhaust airflow rate was decreased by the same amount of air that was exhausted by the VC.

During the winter experimental conditions the manikin was dressed in panties, singlet, light-weight long sleeve blouse, thick sweater, normal trousers, thick long socks and thin soled shoes. This outfit resulted in Clo value of 0.99. During the summertime experimental conditions the manikin was dressed in panties, short sleeve shirt, normal trousers, normal socks and thin soled shoes with the overall Clo value of 0.47. The manikin was set to operate in a "comfort mode" which corresponded to a heat production of an average person in a state of thermal comfort under the used clothing thermal insulation and thermal environmental conditions in the room.

Table 4: Conditions for the experiments in the office room mock-up.

Case No.	Room temperature	Clothing level	Ventilated cushion	Background ventilation
1	20 °C	1 Clo	OFF	1 ACH (Reference case)
2	20 °C	1 Clo	1.5 L/s	1 ACH
3	20 °C	1 Clo	3 L/s	1 ACH
4	20 °C	1 Clo	5 L/s	1 ACH
5	20 °C	1 Clo	OFF	1.5 ACH
6	26 °C	0.5 Clo	OFF	6 ACH
7	26°C	0.5 Clo	OFF	3 ACH
8	26°C	0.5 Clo	OFF	1.5 ACH
9	26°C	0.5 Clo	OFF	1 ACH (Reference case)
10	26°C	0.5 Clo	1.5 L/s	1 ACH
11	26 °C	0.5 Clo	3 L/s	1 ACH
12	26 °C	0.5 Clo	5 L/s	1 ACH

4.6.1.4 Experimental procedure and data analysis

Prior to the measurements the necessary background ventilation rate, air temperature and VC exhaust flow rate was adjusted. The tracer gas dosing was started and kept constant. The temperature in the room was continuously monitored by a temperature sensor connected to a HOBO data logger located at the centre of the room at 1.2 m height. The manikin and the laptop were switched on. At each sampling point, 40 values of the tracer gas concentration were collected after reaching steady state.

The air temperature and air velocities measurements around the manikin were performed only at 1 ACH and 1.5 ACH and took place after the experiments with the tracer gas were conducted.

In order to assess the efficiency of the VC in removing body bio-effluents, the measured concentrations were averaged and normalized by the average concentration at the same sampling location during the reference condition when the VC was not operating at 1 ACH background ventilation rate. The excess CO_2 concentration over the background level was used as criteria for exposure assessment to armpit-emitted pollutants.

The measured data of the tracer gas concentration were analysed in accordance with ISO/IEC Guide for the expression of uncertainty (ISO 2008). The relative expanded uncertainties of the tracer gas measurements were within the range 7-20% with the highest uncertainty at the mouth of the manikin and above its head.

4.6.2   Experimental method – Set 2

4.6.2.1   Experimental set-up and facilities

The cooling effect of the VC was studied in a still indoor environment by conducting experiments in the air distribution room described in Chapter 2. The room set-up was also the same (see Figure 31). However, in this case the table was not equipped with personalized ventilation. The manikin was seated on the VC during the whole experiment.

Figure 31: Room layout in the quiescent environment with the manikin dressed in summer clothing.

4.6.2.2   Experimental conditions

For the purpose of the thermal comfort measurements in the quiescent environment, the VC performance was studied at four different room air temperatures – 20, 23, 26 and 29°C ± 0.2°C. The same outfits described in Set 1were used in these experiments. At 20 and 23°C the thermal clothing insulation of the manikin was 1 Clo, at 26 and 29°C – 0.5 Clo. A table was positioned in front of the manikin at a distance of 10 cm from the manikin's abdomen. The only heat sources in the room were the manikin and four ceiling light fixtures (6 W each). The exhaust flowrates of the VC were kept the same as for the measurements conducted in the office mock-up (1.5, 3 and 5 L/s). All experimental conditions are listed in Table 5.

Table 5: Conditions of the thermal comfort measurements

	Case No.	Room temperature	Clothing level	Ventilated cushion
Reference case	1	20°C	1 Clo	OFF
	2	20°C	1 Clo	1.5 L/s
	3	20°C	1 Clo	3 L/s
	4	20°C	1 Clo	5 L/s
Reference case	5	23°C	1 Clo	OFF
	6	23°C	1 Clo	1.5 L/s
	7	23°C	1 Clo	3 L/s
	8	23°C	1 Clo	5 L/s
Reference case	9	26°C	0.5 Clo	OFF
	10	26°C	0.5 Clo	1.5 L/s
	11	26 °C	0.5 Clo	3 L/s
	12	26 °C	0.5 Clo	5 L/s
Reference case	13	29°C	0.5 Clo	OFF
	14	29°C	0.5 Clo	1.5 L/s
	15	29 °C	0.5 Clo	3 L/s
	16	29 °C	0.5 Clo	5 L/s

4.6.2.3 Experimental procedure and data analysis

The thermal comfort measurements were started after all the necessary conditions were met (room temperature, exhaust flow rate from the VC) and the manikin was in steady state. The heat loss, the surface temperature for each body segment, and the average surface temperature for the whole body of the manikin were recorded for 9 minutes with a sampling rate of 10 seconds. The assessment of the cooling provided by the ventilated cushion was based on the estimated equivalent temperature for each body segment of the manikin. The assessment method is described in detail in Section 4.3.1.7 of the current chapter. The calculations were made according to equation (9):

$$\Delta t_{eq} = t_{eq,i} - t_{eq,i,ref} \tag{9}$$

where

Δt_{eq} – cooling effect of the VC, [K]

$t_{eq,i}$ – equivalent temperature of the body segment (obtained at the studied condition), [°C]

$t_{eq,i\,ref}$ – equivalent temperature of the body segment (obtained at a given reference condition), [°C].

Negative values of Δt_{eq} mean that the VC increases the heat loss from the body, i.e. provides cooling.

The uncertainty of the heat loss measurements from the manikin segments was 1%.

4.6.3 Results and Discussion

4.6.3.1 Performance of the ventilated cushion in terms of exposure reduction to contaminants

Figures 32a and 32b present the normalized tracer gas concentrations of the simulated pollutants from groin and armpits which were obtained at room air temperature of 20°C. The results obtained with the VC at 1 ACH and only when there was background ventilation at 1 ACH and 1.5 ACH are compared. The normalized concentration for the reference case (background ventilation only) at 1 ACH is shown as a dashed line at the value of 1. The normalized concentrations were approximately equal in the measuring locations in the room during one condition. These results indicate that there was good mixing in the room. For the conditions when the VC was used, the normalized concentrations of the two pollution sources was in all measuring points lower than that at 1 ACH and 1.5 ACH background ventilation only. The concentrations of both pollutants in all measuring locations was reduced by about 30% by increasing the background ventilation rate with 13.6 L/s (from 1 ACH (31.8 L/s) to 1.5 ACH (45.4 L/s)) whereas exhausting 1.5 L/s through the VC at 1 ACH reduced the pollutants' concentrations by about 60%. It means that the VC combined with 1 ACH reduced the simulated bio-effluents with 30% more than supplying into the room 1.5 ACH. According to the Standard EN 15251 (2007) background ventilation rate of 45.4 L/s (1.5 ACH) corresponds to IAQ of category I for a single office in a low polluting building. It can therefore be assumed that the implementation of the VC would provide better air quality at lower ventilation rate per person. This may lead to energy savings. Figure 32 shows also that the pollution concentration decreased with the increase of the exhaust flowrate through the VC. When the VC was exhausting 5 L/s, the normalized concentrations of the contaminants in all measuring points was reduced almost to zero (Figure 32a and 32b). Therefore, it is expected that the VC, operating at 5 L/s, will improve the quality of inhaled air in terms of body-emitted gaseous pollutants since it will prevent their spread in the room. In Figure 32a the normalized concentration in the breathing zone of the occupant is slightly higher with MV at 1.5 ACH compared to the reference condition with MV at 1 ACH. These results are unexpected and can be attributed to the complex flow interaction in the breathing zone of the manikin. The results from the measured air velocities around the manikin at 20°C with 1 ACH and 1.5 ACH were within the same range of 0.063-0.073 m/s at 1.1 m height (i.e. the height of the manikin's mouth). The turbulence intensity levels at 1 ACH and 1.5 ACH were also in the same range of 38-59%.This suggests that the airflow distribution close to the breathing zone of the manikin at 1.5 ACH was similar to that at 1 ACH and thus resulted in similar N_2O concentration levels. However, this was not observed when the contaminants were released from the armpits (Figure 32b). Sophisticated air velocity measurements in the breathing zone and around the manikin needs be carried out to investigate this effect.

The results of the normalized concentrations at all measured locations for the pollution emitted from the armpits at room air temperature 26°C are shown in Figure 33. Results obtained at background ventilation of 1.5, 3 and 6 ACH with VC turned OFF and when the VC operated at 1.5, 3 and 5 L/s at background ventilation of 1 ACH are shown. The results in Figure 33 show that the normalized concentrations in all measured locations with VC at all three flow rates is much lower than 1. Worth

noting is that the outfit of the manikin during the experiments at 26°C was also changed (as this is what would happen in reality – lighter clothes at summer conditions and thicker clothes at winter conditions). It is well-documented that the velocity of the CBL flow around a seating person depends on the type of clothing and the temperature of the surrounding air (Licina et al. 2014b). In turn the change in the velocity field of the CBL influences the transport of the pollutants emitted from the body. The presented in this part of the study results indicate that the VC performs in the same way under summer and winter conditions. Yet, it should be noted that the practical application of the VC may be changed under other room conditions and occupant behavior. The current study does not consider different total volume air distribution, body postures, different outfits (e.g. wearing a skirt) and other pollution sources such as the clothing of the person. Human respiration as it was shown in Chapter 2 might change the results obtained for the contaminants from the armpits. Several issues, related to control and optimization of the VC as well as human response remain to be studied. Nevertheless, it can be expected that the VC will be efficient in preventing the spread of emitted from or close to the body pollutants including fine aerosols. It should be noted that a filter can be easily incorporated inside the VC, where the polluted air will be cleaned locally and discharged it back into the room (as it was shown in Section 4.5.2 of this chapter). The "plug and play" method can be applied, which will prevent the use of additional ducting. This will increase the flexibility of the chair and it will be possible the chair equipped with the VC to be moved without difficulty.

Figure 33 shows that the use of the VC with exhaust airflow rate 3 L/s and 5 L/s reduced the pollution concentration to the level of 3 ACH and 6 ACH alone, respectively. This was observed for the measuring points in the room and the room exhaust air. Higher exposure reduction was obtained at the mouth of the thermal manikin with the VC at only 1.5 L/s compared to mixing ventilation at 3 ACH and 6 ACH. Similar results were obtained when the pollution source was the groin (results are shown in Paper VII, Appendix B). These results demonstrate that the supply of high amount of outdoor air is not always effective to reduce occupants' exposure to their own contaminants where dilution has not occurred. Instead, it is effective to apply chair-integrated exhaust ventilation in indoor environments where the occupants are predominantly sitting in order to reduce exposure to bio-effluents from the body.
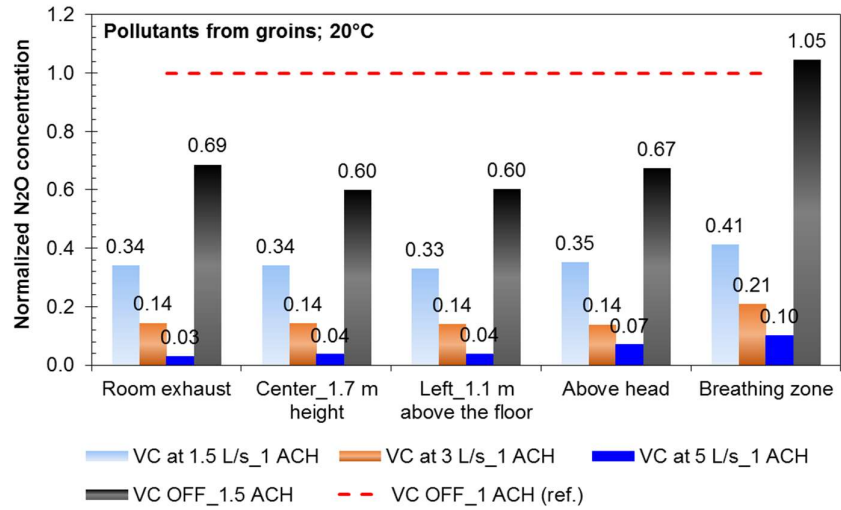
a)
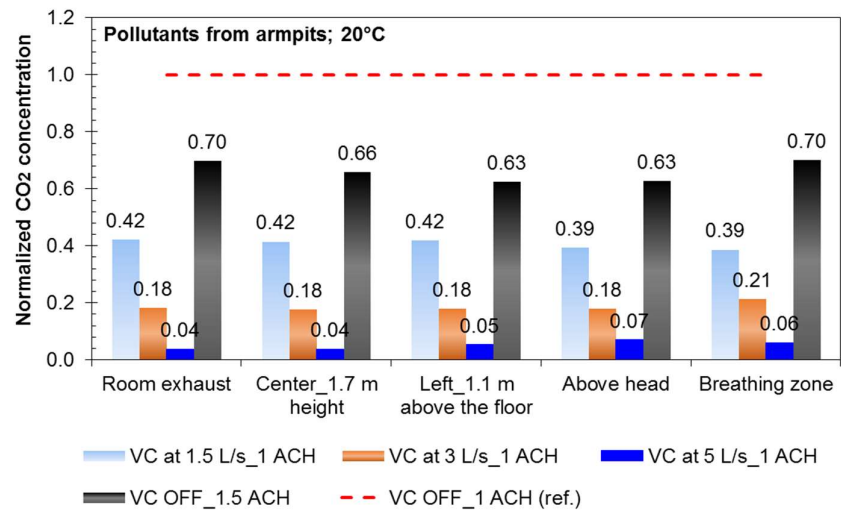
b)

Figure 32: Normalized concentration at the measuring points when the pollution source was emitted from a) the groin region and b) the armpits.
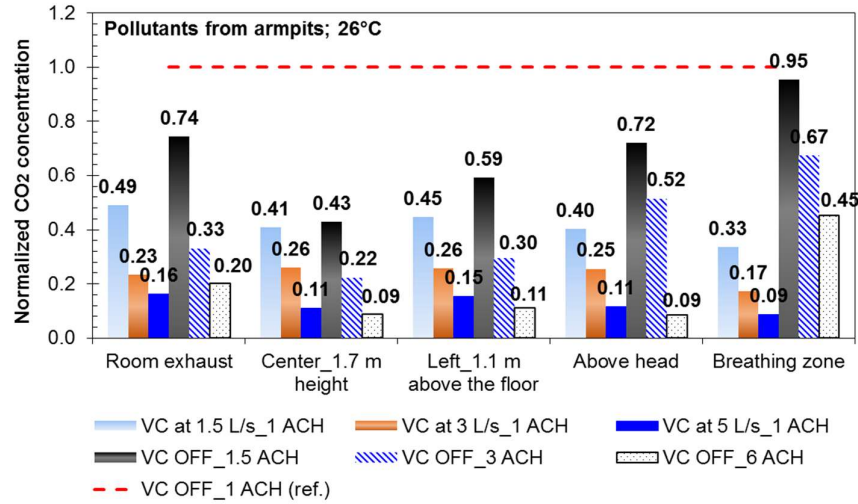
Figure 33: Normalized concentration at the measuring points when the pollution source was emitted from the armpits at room air temperature of 26°C.

4.6.3.2 Performance of the ventilated cushion in terms of thermal comfort

The thermal comfort experiments were performed in a quiescent and uniform environment which allowed assessing the VC cooling effect on the body that is caused only by the air movement through the cushion without any external factors. As it was expected, the results show that the body parts of the manikin in contact with the VC were cooled, namely left and right thigh, pelvis and back. In Figure 34 the VC cooling effect on these body segments including the whole body (denoted as "All" in Figure 34) at four different room air temperatures (20, 23, 26, and 29°C) is shown. The results in the figure show that the cooling effect increased with the increase of the airflow rate through the VC. As seen, the most cooled body segment was the back of the manikin. The pelvis was slightly less cooled and the thighs were the least cooled body segments in contact with the VC. It can also be seen that the right thigh was cooled more than the left one. It seems possible that these results are due to that the manikin was not seated on the VC symmetrically. The left thigh was turned aside from the exhaust openings of the VC and therefore it was less exposed to the cooling by the VC. The cooling effect for the whole body of the manikin was smaller compared to the back and pelvis. This is because the cooling effect for the whole body was averaged of the dry heat loss obtained for each body segment including the once which were not directly subjected to cooling; hence the magnitude of the whole body cooling was diminish. Cooling from the VC decreased with the increase of the room air temperature. Substantial effect of the local cooling provided by the VC was observed especially on the back even though the clothing insulation of the manikin was 50% less at 26 and 29°C compared to that at 20 and 23°C. The cooling was equivalent to a decline of the room air temperature by several degrees: 2.9, 6.2 and 8.6 K at 20°C, 2.3, 4.8 and 6.7 K at 23°C, 1.4, 3.5 and 5.3 K at 26°C and 1.2, 2.7 and 3.7 K at 29°C respectively at 1.5, 3 and 5 L/s ventilation through the VC. The large differences in local thermal sensation of the body parts as a result of the non-uniform body cooling may cause discomfort. However, a study based on 109 human subjects tests found out that the thermal sensation from the back and chest have dominant

influence on the overall sensation (Zhang et al., 2004). Thus in practice the VC may have strong impact on the whole body thermal sensation. Although this needs to be studied with human subject experiments it also implies that the VC can be used in warm climates and during seasons when the outdoor temperature is high. Such application of the VC has the potential to save energy in buildings in which cooling is provided by mechanical ventilation. In such situation the building can be controlled with extended temperature set-point for cooling while still maintaining occupants' thermal comfort. The large local cooling effect of the VC at the lower room temperatures may not be accepted by people. This negative effect can be avoided by local heating of the VC exhaust air. However this will increase the energy use. This issue needs to be studied.
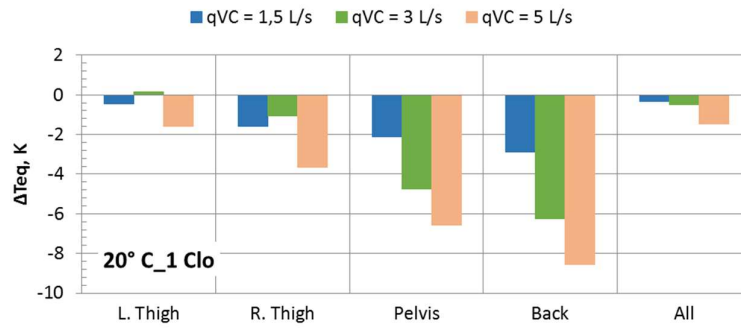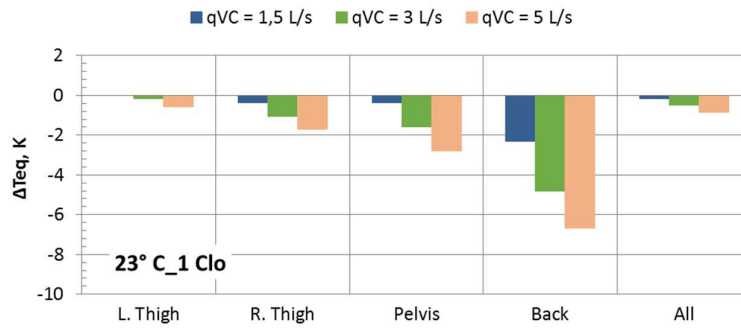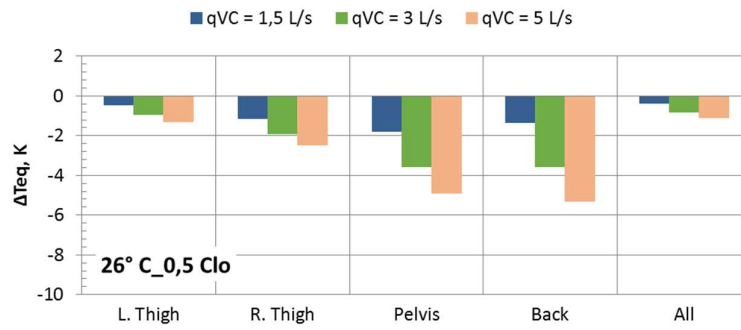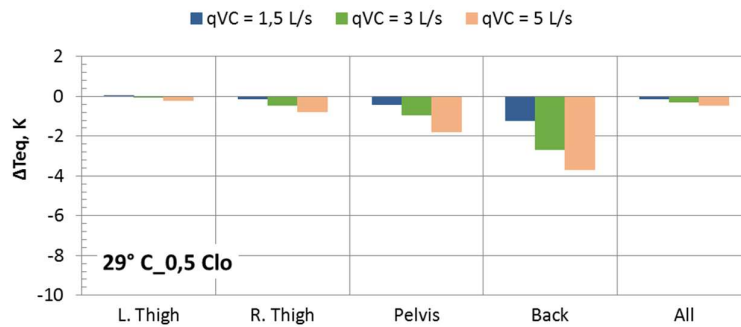
Figure 34: Cooling effect on the body parts in contact with the VC in a uniform environment at air temperature of 20, 23, 26, and 29°C.

4.6.4   Conclusions

This part of the thesis investigates the performance of the ventilated cushion with regard to indoor air quality and thermal comfort. The experimental results show the following:

- In rooms with mixing ventilation the use of the VC can reduce occupants' exposure to body bio-effluents;

- Exhausting 1.5 L/s of air through the VC in order to reduce the bio-effluents' concentrations in the room and combining it with total volume ventilation at 1 ACH proved to be 30% more efficient than total volume ventilation alone at 1.5 ACH;

- The use of the VC can reduce the pollution concentration in the room to the levels obtained at 3 ACH and 6 ACH;

- Exhausting air at 1.5 L/s through the VC reduced the concentration in the breathing zone by 67% which was 12% more efficient than not using the VC and supplying 6 times more cleaner air (188.8 L/s) into the room with the background ventilation;

- Exhausting air through the VC provides local cooling to the body parts in contact with the cushion in uniform environment. The higher the exhaust flowrate, the more cooling is provide;

- The cooling effect provided by the VC decreases with the increase of room air temperature. The most cooled body part is the back;

- The VC has a potential to provide thermal comfort in warm climates and during seasons when the outdoor temperature is high;

- Local heating of the VC's surface that is in contact with the body may be needed during winter conditions.

4.7 Energy-saving potential of the VM and VC

This part of the current study investigates the use of the ventilated mattress (VM) and the ventilated cushion (VM) with regards to their energy performance. Energy simulations were carried out to clarify the energy saving potential of the VM and VC combined with reduced background ventilation and radiant ceiling cooling/heating with respect to traditional total volume ventilation used today with the recommended by the existing guidelines and standards air volumes and supply air parameters.

4.7.1 Method

4.7.1.1 Simulation tool

The energy simulations were performed using the building energy performance simulation software IDA ICE 4.7 (EQUA Simulation, IDA Indoor Climate and Energy).

4.7.1.2 IDA ICE simulations models

Patient room: In order to analyse the energy saving potential of the VM, energy simulations were performed for a double-patient hospital room. The simulated double patient room volume was 72 m^2 (4 m x 6 m x 3 m, L x W x H), which complies with the minimum area requirements for multiple patients room (AIA Guideline, 2006). The patient room model had one external facade facing south and included a window with dimensions of 1.2 m x 2.27 m (W x L) and surface area of 2.72 m^2. The window had shading device composed of external blinds, which were automatically drawn when the incident light exceeded 100 W/m^2 on the inside of the glass. The remaining walls, ceiling and floor were considered as internal walls. The main thermal properties of the patient room envelop are listed in Table 6. The patient room was simulated in subtropical and cold climatic region considered to be located in the cities Singapore and Copenhagen, respectively.

Call-centre: A call-centre was considered a suitable environment to be studied, as call-centre operators usually perform seated work for longer periods of time. The number of operators on duty, room size and time of operation (time by the desk) were adopted by the study of Wargocki et al. (2004), who studied the IAQ and work-performance in a call-centre located in Denmark. The call-centre room was planned as an open-space office with a floor area of 154 m^2 and a volume of 447 m^3 (17.5 m x 8.8 m x 2.9 m, L x W x H). The simulation took place in Copenhagen. There were no internal partitions in both models. The construction enveloping the call-centre consisted of an external brick wall (U-value = 0.26 W/m^{2}K), roof (wooden construction with U-value = 0.10 W/m^{2}K), internal lightweight concrete wall (U-value = 0.54 W/m^{2}K) and internal floor (concrete slab with U-value = 2.9 W/m^{2}K). The roof and two of the walls were considered external. The external walls were facing east and west. On each external wall there were 7 windows (Figure 35). Each window had an area of 2.25 m^2 in total 31.5 m^2 and a window-to-floor surface ratio of 20%. The windows were composed of three layers of 4 mm panes with 2 layers of 12 mm air gap in between. The overall U-value was 1.1 W/m^{2}K, a g-value (solar heat gain coefficient) equal to 0.68, and a light transmittance equal to 0.74. All windows of the call-centre had integrated blinds

between the window panes. The blinds were drawn when the incident light exceeded 100 W/m^2 on the inside of the glass.

All internal walls of the two models, namely the patient room and the call-centre, were considered adiabatic, and the effect of thermal mass was taken into account. The selected building materials and U-values complied with the Danish Building Regulations (BR15, paragraph 7.6.1). The external constructions fulfilled the minimum amount of insulation (0.30 for external walls and 0.20 for roof constructions) according to building location and weather data.

The ASHRAE IWEC weather files for Copenhagen and Singapore (downloaded from the EQUA Climate Data Download Centre) were used as weather input data in the simulation models. The ambient CO_2 level was manually set to 400 ppm.

Table 6: Thermal properties of the patient room envelop.

Envelope	Layers	Thickness [m]	U-value [W/m^2K]
External wall	Render	0.01	0.537
	L/W concrete	0.25	
	Render	0.01	
Internal floor	Floor coating	0.005	2.385
	L/W concrete	0.002	
	Concrete	0.15	
Internal wall	Gypsum	0.026	0.37
	Air gap	0.032	
	Light insulation	0.03	
	Clay brick	0.200	
	Gypsum	0.01	
Window glazing: Pikington Suncool 70/40 (6C(74)-15Ar-4-15Ar-S(3)4)	g-value	0.4	1.1
	Solar transmittance	0.34	
	Visible transmittance	0.66	

Figure 35: 3D model of the call centre with external facade facing east.

4.7.1.3 Climatic systems

Patient room: Constant air volume (CAV) with steam humidifier and radiant ceiling panels were used to air-condition the patient room. The steam humidifier was needed to meet the relative humidity requirements for general patient rom in health care facilities, 30-60% (ASHRAE 170 2013). The ventilation and air-conditioning systems for the room were operating 24 hours/day through the whole simulated year.

Call-centre: The call-centre was air-conditioned with variable air volume (VAV) system, water radiator and in some cases chilled ceiling to remove excess heat. All HVAC systems for the call-centre were running one hour before the occupancy started and one hour after the occupancy ended resulting in the following schedules: Monday to Friday 6:00 to 24:00, Saturday 6:00 to 16:00, and Sunday 13:00 to 22:00.

In both simulation models, it was assumed a 70 % of the total ceiling area to be covered with radiant heating and cooling panels in order to avoid radiant asymmetry. The radiant ceilings were dimensioned to maintain the required thermal conditions in the models without causing water condensation on the panels. Condensation on the panels was avoided by limiting the supply water temperature to be above the indoor dew-point temperature. According to Babiak et al. (2013), the temperature of a cooling surface should not be reduced below 17 °C and for heating should not exceed 27°C. In Tables 7 and 8 are shown the input parameters of the radiant ceilings installed in the two models.

Table 7: Parameters for the radiant heating/cooling panels in the patient room.

Parameters	Cooling	Heating
Panel width [m]	0.6	0.6
Panel length [m]	4	4
Panel area [m^2]	2.4	2.4
Capacity per panel [W]	162	216
Number of panels [m]	7	7
Total capacity [W]	1133	1513
dT(room operative-mean water) [°C]	8	12.3
dT(outlet water-inlet water) [°C]	1.9	3.4

Table 8: Parameters for the radiant cooling panels in the call-centre.

Maximum indoor air temperature	26°C	28°C
Parameters	-	-
Panel width [m]	1	1
Panel length [m]	8	8
Panel area [m^2]	8	8
Capacity per panel [W]	641	525
Number of panels [m]	9	9
Total capacity [W]	4724	5767
dT(room operative-mean water) [°C]	7.9	9.2
dT(outlet water-inlet water) [°C]	6.3	7.6

4.7.1.4 Internal heat gains and occupancy

Patient room – the total internal heat gain in the patient room was about 451 W. The gain included heat production by two patients each with metabolic rate 0.8 met (0.46 W/m^2), which corresponded to a person being in reclined position (ISO 7730, 2005). Heat gain from medical equipment was considered to be 114 W per occupant, which corresponds to the average heat gain from a blood warmer (ASHRAE, 2003). The heat load from general lighting was 3 W/m^2. On each patient bed there was a ventilated mattress. The fan power of each ventilated mattress (VM) was set to consume 20 W (enough to provide exhaust airflow rate in the range of 1.5 - 5 L/s). In the simulations, it was assumed that the ventilated mattresses are operating at recirculation mode (i.e. the exhaust polluted air was cleaned by a filter inside the mattress and recirculated back into the room). Yearly energy simulations were carried out for occupancy schedule of 24 hour/day including weekends. Consequently, all equipment and systems were operating at the same schedule.

Call-centre - The room was occupied by 14 phone operators with activity level set to 1.2 met (70 W/m^2). The operators were present in the call centre from Monday to Friday, from 7:00 to 23:00 including no breaks. On Saturday the operators were present from 7:00 to 15:00 and on Sunday 14:00 to 22:00 including no breaks either of the days. It was assumed the all 14 operators were coming to the centre at the same time. No holidays were included in the simulations. The heat gain from general lighting was estimated to 5 W/m^2. The heat load from equipment (14 desk lamps, 6 wall monitors, and 28 personal monitors) was 1450 W in total. Both lighting and other equipment followed the schedule of the occupants. Outside these hours they were turned off. The software takes into account the production of both sensible and latent heat from the occupants.

4.7.1.5 Simulated conditions

This part of the study was performed to compare different strategies suggested in the literature to achieve energy-savings in buildings based on radiant and convective heating and cooling including utilization of personalized ventilation (Hoyt et al., 2009; Kazanci PhD thesis, 2016; Panu et al., 2016; Shiavon and Melikov, 2009). Consequently these strategies were applied in the case of the studied local source control methods, the VM and the VC and they follow as:

1) Reducing the outdoor airflow rate due to the higher ventilation effectiveness of VM and VC.

2) Expanding the upper room temperature limit for thermal comfort by taking advantage of the cooling provided by the VM or the VC and the radiant ceiling panels;

3) Reducing the outdoor airflow rate due to the higher ventilation effectiveness of VM and VC and providing ceiling-mounted radiant panels for local heating and cooling.

Patient room – The simulated conditions for the patient room were conducted to investigate three potential low-energy systems, namely the VM combined with mixing ventilation (MV), MV with radiant ceiling panels (abbreviated as RC) and VM combined with MV and RC. These systems were compared with the conventional MV alone. The annual energy use in the simulated cases when the MV was used alone was estimated at room ventilation rates of 4 and 6 ACH which are the

recommended minimum total ventilation rates for general patient rooms using a constant air volume mechanical system (ASHRAE standard 170, 2013). For the simulated cases with the VM combined with MV, the background airflow rate was reduced to the minimum amount required to maintain the desired operative temperature in the room but still the supplied flow rate fulfilled the requirements for general patient rooms, 10 L/s per occupant, according to the technical report FprCEN/TR 16244:2011. In the calculations it was also taken into account the standard ventilation rate for building emissions from low polluting building category I which was 1 $L/s/m^2$ according to the EN 15251 (2007). These standard criteria were used also for the estimation of the supplied background ventilation rate when the MV was combined with the radiant ceiling panels. For the condition when the VM was operating in conjunction with the MV and the RC it was assumed that the required airflow rate per patient, 10 L/s, can be reduced with 50% due to the efficiency of the VM. The temperature of the air supplied by the background ventilation was calculated based on the total heat load, supply air flow rate and upper room air temperature set-point of 24°C. In the calculations it was also taken into account the recommended temperature difference between the supply and room air not to be higher than 10°C to achieve proper mixing (Müller et al., 2013; Kazanci and Olesen, 2015). The supplied air temperature and airflow rate for the simulated cases are listed in Table 9. In the ASHRAE standard for health care facilities (ASHRAE Standard 170, 2013), the design temperature for patient rooms is recommended to be in the range of 21-24ºC for both cooling and heating seasons and relative humidity in the range from 30% to 60%. Therefore, during all simulations the operative temperature and the relative humidity (RH) in the room were controlled and equaled to 21-24°Cand approximately 50% RH, respectively.

Table 9: Supply air temperature and flow rate at the studied air-conditioning systems.

Location	System	Air flow rate	Supply air temperature
Copenhagen	MV	80 L/s (4 ACH)	18°C
		120 L/s (6 ACH)	19°C
	MV/VM	60 L/s (3 ACH)	16°C
	MV/RC	44 L/s (2.2 ACH)	17°C
	MV/RC/VM	34 L/s (1.7 ACH)	17°C
Singapore	MV	80 L/s (4 ACH)	17°C
		120 L/s (6 ACH)	19°C
	MV/VM	60 L/s (3 ACH)	15°C
	MV/RC	44 L/s (2.2 ACH)	17°C
	MV/RC/VM	34 L/s (1.7 ACH)	17°C

Call-centre - Energy simulations with the VC operated together with reduced background MV and radiant ceiling panels for cooling were performed and compared to MV alone at airflow rate based on the air quality requirements defined in the standard EN 15251 2007 for category II, very low polluting buildings. According to this category, the standard requires 7 L/s per occupant (q_{occ}). In the simulations, it was assumed that the 7 L/s could be decreased by 53%, 81% and 89% when the VC flow rate was 1.5, 3 and 5 L/s, respectively. This assumption was based on the exhaust efficiency of the VC to reduce bio-effluents from the body shown in the current study, Section 4.3.2.1. Hence, when exhausting 1.5, 3 and 5 L/s through the VC, the background airflow rate per

occupant was reduced to 3.2, 1.3 and 0.8 L/s, respectively. The ventilation rate for building emissions (q_b) was selected to be 0.35 L/s.m^2 which corresponds to the standard criteria of very low polluting buildings (EN 15251, 2007). Finally, the total airflow rate (q_{tot}) was calculated for each case as follows:

$$q_{tot} = A \cdot qb + q_{occ} \cdot n + q_{vc} \cdot n,$$ (10)

Where:

q_{tot} -   Total volume ventilation rate of the room [L/s],

A -   Room floor area [m^2],

q_b -   Ventilation rate for emissions from buildings [L/s]

q_{occ} -   Ventilation rate per person from the MV [L/s],

N -   Number of persons in the room,

q_{vc} Ventilation rate per person from the VC [L/s].

Since, VAV ventilation was used in the call centre, the estimated q_{tot} was the maximum possible supply ventilation rate. The VAV system adapted the airflow rate needed to keep the required CO_2 and operative temperature limits in the call centre. The supply air temperature was kept constant for all simulations and it was set to16°C. Two different operative temperature set-points were used, that were 20/26°C and 20/28°C. The design operative temperature range of 20-26°C complies with recommendations for thermal comfort conditions for category II in the EN 15251 (2007). The maximum allowed room temperature was expanded from 26°C to 28°C in order to study the importance of using the VC cooling effect for possible energy-savings. The maximum CO_2 level was set to 900 ppm (500 ppm above outdoors) which complies with category II in the EN 15251 (2007).The minimum airflow rate was set to 0.35 L/s.m^2 (corresponding to airflow rate due to pollution from the building). For the reference case MV alone, the VAV system's maximum supply airflow rate was calculated based on the total heat load in the call centre for supply air temperature of 16°C and room temperature of 24°C. The total heat load due to occupants, equipment and solar gain was calculated to be 4044 W. The maximum supply airflow rates for the simulated cases are listed in Table 10.

Table 10: Maximum supply airflow rates from the VAV system in the call centre for different VC exhaust flow rates and air-conditioning systems.

	System	Max total air flow rate
VC: 0 L/s	MV	421 L/s
VC: 0 L/s	MV/RC	152 L/s
VC: 1.5 L/s	MV/RC/VC	120 L/s
VC: 3 L/s	MV/RC/VC	114 L/s
VC: 5 L/s	MV/RC/VC	135 L/s

In both models infiltration due to wind driven flow was taken into account and it was equal to 0.5 ACH at a pressure difference of 50 Pa (BR15).

4.7.2 Results and Discussion

4.7.2.1 Energy-saving potential of the ventilated mattress in a double patient room

The annual energy use per square meter of the patient room (kWh/m^2 year) located in Copenhagen and Singapore for the simulated air-conditioning strategies are compared in Figure 36 and 37, respectively. The results in the figures show the total delivered energy which includes the energy used by the air handling units (AHUs), the energy supplied to the radiant panels and the energy used by pumps, equipment such as the ventilated mattress, lighting, etc. Coefficient of performance (COP) of 3.8 was selected for the delivered electric energy for cooling in the air handling unit and the water coils of the radiant panels. COP of 3.8 is a typical value used for cooling. It normally varies between 3.5 and 4 (Kosonen et al., 2013). A primary energy factor of 0.9 was chosen to calculate the primary energy used for heating by the coils in the air handling unit and the radiant panels.

The results obtained for the patient room situated in Copenhagen and Singapore (Figures 36 and 37) show that the annual energy use decreases with decreasing the background ventilation rate. Figures 36 and 37 show also that MV at airflow rate of 3 ACH in combination with the VM achieves energy saving compared to the minimum air flow rate, 4 ACH, recommended by the ASHRAE Standard 170 (2013). Compared to the MV alone at 4 ACH, the use of the VM combined with mixing ventilation at 3 ACH decreased the annual energy use by 24 % and 27 % for the climate of Copenhagen and Singapore, respectively. Compared to MV at 6 ACH, the reduction of the energy was 49% and 52% respectively for Copenhagen and Singapore. These results provide support for the hypothesis that substantial energy savings can be achieved by applying local source control in hospitals. Further energy savings were achieved when the background flow rate was reduced to 1.7 ACH and the VM was operating together with heating and cooling radiant ceiling panels. In the MV/RC/VM case the annual energy use was reduced by more than 60% compared to the mixing ventilation alone at 6 ACH for both simulated climates. Substantial energy savings can be also achieved without the VM at background ventilation of 2.2 ACH combined with radiant heating and cooling. Although the requirements for patients' thermal comfort will be provided, this energy saving strategy might cause problems with perceived air quality. It has been documented that ventilating patient rooms with only 2 ACH may cause stuffy air (Memarzadeh and Manning, 2000).

As seen in Figure 37, the annual energy use is generally higher for all simulated conditions when the patient room is located in Singapore compared to the cold climate of Copenhagen. These differences can be explained by the high energy demand to achieve the desired operative temperature and relative humidity in the room located in Singapore. Since, the average monthly dry bulb temperature in Singapore is 27.5°C and the relative humidity is about 84% (Licina and Sekhar, 2012). Substantial energy is needed for over-cooling the air to a lower temperature and for re-heating it afterwards in order to reduce the outdoor relative humidity from 84 % to 50% (RH recommended in hospital patient rooms).

It is expected that the local cooling of the VM will have positive effect on the thermal comfort in rooms suited in warm environments. Energy saving can be achieved by operating the background ventilation system at expanded upper set-point for the room temperature and providing local body cooling using the VM. In order to verify this, an additional simulation was conducted in the case of MV/RC/VM at 1.7 ACH for the climate of Singapore. It was found that when the upper set-point for the operative temperature in the room was set to 26°C, the total energy use was about 369 kWh/m^2 year which is almost 12% lower compared to the energy used to keep the room temperature at 24°C (Figure 37, combined MV/RC/VM system). However, as was already discussed previously in this chapter, the non-uniform body cooling may cause local thermal discomfort. Hence, local body heating may be required to counteract the undesired cooling. The use of local heating will increase the energy use. Further study and simulations on this issue are needed.

In Section 4.5.2 of this chapter it was shown that it is possible to improve the indoor air quality when the exhausted by the VM polluted air is cleaned inside the mattress and recirculated back into the room. This mode of operation of the VM was considered in the current simulations. A great advantage of this approach is that the "plug and play" principle can be applied, i.e. the bed with the ventilated mattress can be moved from room to room and only plugged in the electrical grid. In this case modification of the background exhaust system will not be needed as well as adding ducting and plugs for connecting the ventilated mattress.

The air-conditioning systems worked 24 hours and the patients occupied the beds for 24 hours. However in real life patients may spend several hours and/or out of bed and/or out of the room. The impact of room occupancy on the energy savings needs to be studied. In addition, the findings from this part of the study are to some extent limited as the annual energy use was estimated including only a patient room. This simplification may change the range of saved energy use due to application of the VM, if for instance an entire hospital floor with several patient rooms and multiple beds equipped with a VM was simulated. This needs to be further studied.
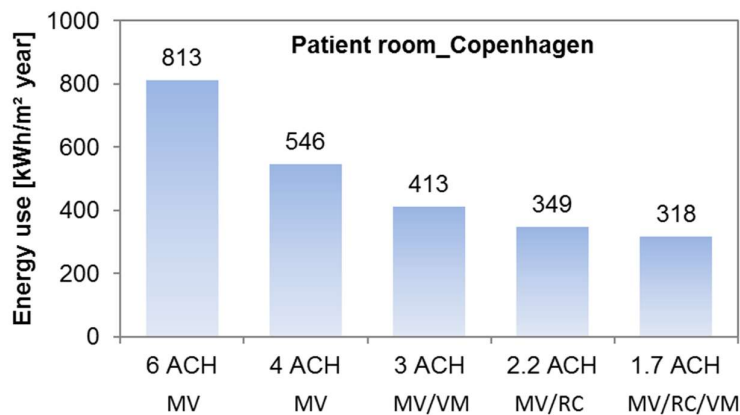
Figure 36: Annual energy use for the air-conditioning systems in a double patient room in Copenhagen.
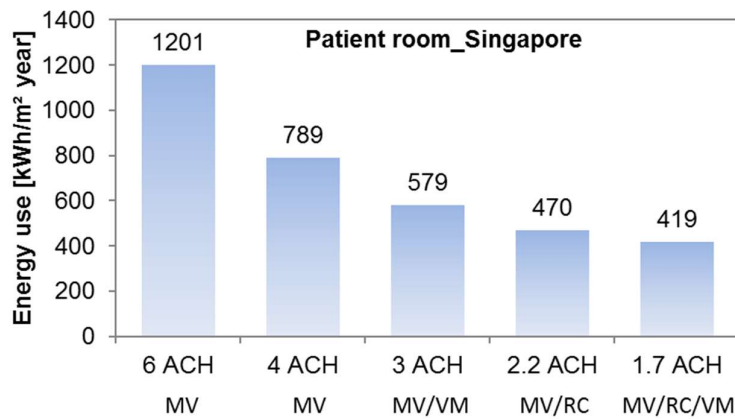
Figure 37: Annual energy use for the air-conditioning systems in a double patient room in Singapore.

4.7.2.2 Energy-saving potential of the ventilated cushion

The results of the annual energy use per square meter of all simulated conditions in the call centre are shown in Figure 38. To estimate the annual use of primary energy delivered to the call centre, several assumptions regarding the energy generation/transformation were made. District cooling with a COP value of 4 was used to supply cold water to the AHU cooling coil and the chilled ceiling. District heating with a primary energy factor equal to 0.6 was used to supply heat to the AHU heating coil and the radiators, and electricity with a primary energy factor equal to 1.8 was supplied to the electrical systems such as fans, circulation pumps and lighting. The selected COP and primary energy factor values complied with low energy class 2020 building according to the Danish Building Regulations 2015 (BR 15).

The results of the energy simulations presented in Figure 38 show that energy savings can be achieved when applying sustainable heat removal i.e. radiant ceiling panels for cooling (also known as chilled ceiling) combined with MV. In the MV/RC case and room operative temperature within 20/26°C, appliance of the chilled ceiling (without VC) decreased the energy use with 7% compared to the case with only MV. For this temperature set-points, 20/26°C, the results in Figure 38 show that applying the VC combined with reduced background ventilation (MV) and RC (i.e. case MV/RC/VC) did not lead to further energy savings compared to the case MV/RC. But neither the energy use increased in this case. Thus removal of human body bio-effluents by means of VC (i.e. increase of air quality) can be achieved without the need to increase the energy use. The VC operating at the three different airflow rates kept the energy use constant at 52 kWh/m^2 and at 50 kWh/m^2 for the temperature set-points 20/26°C and 20/28°C, respectively. These results indicate that the increased airflow rate from the VC, namely from 1.5 L/s to 3 L/s and 5 L/s, applied on the 14 workstations does not increase the energy use. This can be explained with the principle of the VAV control. This result may be explained by the fact that the airflow rate was VAV controlled. Therefore, the airflow rate was automatically reduced when the designed q$_{tot}$ (the maximum airflow rate) was not required to maintain the CO$_2$ and the temperature set-points. If the ventilation system

had been designed as a CAV system, the increase in the energy use would have been proportional to the increase of the supply flow rate as it was shown in the results from the patient room. A CAV system in general is more energy consuming compared to a VAV system, consequently the yearly energy use would be higher for all simulation cases. Further studies on energy saving potential may therefore comprise other control set-points of the HVAC systems for CO_2 in order to improve the demands for maximum airflow rates. As expected, when the set-points for the room operative temperature were expanded in the MV/RC/VC cases (20/28°C) the energy use was decreased with about 11% compared to MV alone and with 4% compared to the MV/RC operating at set-points 20/26°C. This was because extended upper temperature set-point was achieved at reduced background ventilation rate (q_{tot} reduced from 421 L/s in MV to 152 L/s in MV/RC and to the range 114-135 L/s in the conditions with MV/RC/VC). As already discussed in section 4.6.3.2 at elevated room temperature thermal comfort can be improved by the local cooling provided by the ventilated cushion.

The energy-saving potential of the ventilated cushion combined with background mixing ventilation at reduced ventilation rate and chilled ceiling was studied only for the case of mixing air distribution. The energy saving in the case of displacement background ventilation is to be studied. To estimate the amount of energy use for the call-centre, the background ventilation, the chilled ceiling and the VC were controlled by the same room-based set-points for CO_2 and temperature. In practice, the background ventilation and the chilled ceiling may be controlled by a room CO_2 and temperature sensor, but the VC airflow rate is more likely to be controlled by the occupant or a local temperature sensor monitoring the temperature of the body surface in contact with the VC. With this respect further energy saving can be expected based on the fact that the VC may be turned off automatically when the call-operator leaves the workstation for lunch or break. This can be studied in a more detailed simulation model.
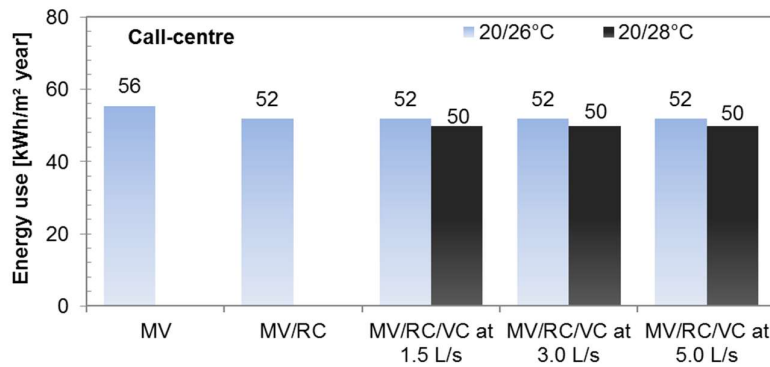
Figure 38: Yearly primary energy use for the four simulation cases with room temperature set-points of 20/26°C and 20/28°C.

4.7.3 Overall limitations of the performed energy simulations

The findings from the performed dynamic energy simulations have important implications for improving the delivery methods for conditioned air with regard to energy use in indoor

environments, where people spend considerable amount of time sitting or lying in bed. However, these findings need to be interpreted with caution as they are specifically valid for the current simulated models comprising a specific room type, room temperature set-points, cooling and heating methods, equipment, etc. In general, more realistic results might be obtained on the energy performance of the VC and VM by conducting human subject experiments during which individual control of the flow rate through the mattress or cushion is provided. As a result energy calculations can be performed based on a more realistic energy use pattern that would be identified from such experiments.

4.7.4 Conclusions

The results of the performed simulations show the following:

- The ventilated mattress in conjunction with background ventilation at 3 air changes per hour (ACH) will decrease the annual energy use by 24% to 52% for a double patient room located in a cold climate or hot and humid climate as compared to conventional mixing ventilation at 4-6 ACH. The highest percentage of energy savings in the patient room for both climatic regions was achieved when combining the use of the VM with reduced background mixing ventilation and radiant ceiling panels;

- Increasing the maximum allowed room operative temperature and maintaining occupants' thermal comfort due to the local cooling provided by the two local exhaust methods is an effective energy-saving strategy;

- Combining the ventilated cushion with background mixing ventilation (MV) and radiant ceiling panels for cooling (also known as chilled ceiling) in a call-centre located in Copenhagen reduced the energy use by 7% compared to a system with only mixing ventilation.

5   Conclusions of the study

This study presented the results of experimental investigations of the relationships between airflow characteristics in the breathing zone and exposure to airborne contaminants. The importance of the dynamic characteristics of instruments for tracer gas concentration measurement in exposure assessments is argued. The results of this study will contribute to a better understanding the relationship between the transport behaviour of tracer gas and particles in a ventilated room. New methods based on elimination of pollution at the source are proposed which may guide the design of efficient localized exhaust ventilation to improve each individual microenvironment and at the same time save energy use. The detailed conclusions from the experimental and numerical analyses are given in the corresponding chapters and publications. The main findings of the study can be summarized as follows:

- Exposure assessment based on tracer gas concentration measurement can be incorrect if the measuring instrument has long response time and the complex airflow interaction at the breathing zone is not correctly simulated;

- Exposure to body bio-effluents depends on the complex airflow interaction of the convective boundary layer, flow of exhalation and locally applied ventilation flow on the breathing zone;

- The interaction of the exhaled flow with the convective boundary layer increases the exposure to own body released pollution especially when the site is close to the breathing zone;

- Breathing does not influence exposure to gaseous pollutants emitted from the lower part of the body;

- The interaction of the exhaled flow with the convective boundary layer increases the exposure to own body released pollution especially when the site is close to the breathing zone;

- Particles in the fine size range (0.7 μm) are the least influenced by deposition mechanisms and thus should have the most similar behaviour to the tracer gas;

- The ventilation rate is important for comparing the behaviour of the ultrafine particles and tracer gas. Ultrafine particles (0.07 μm) and N_2O tracer gas did not behave in the same way at 3.5 ACH and 7 ACH in an empty room and in a furnished room without heat sources. Therefore tracer gas might not be suitable method to study behaviour of ultrafine particles. Conversely, the studied ventilation rates did not have an impact on the similar transport pattern of the 3.5 μm and the 0.7 μm particles and the tracer gas;

- Increasing the room surface area did not influence the similarity of the 0.7 μm, and 3.5 μm particle dispersal to that of the tracer gas;

- At the breathing zone of the seated heated manikin, N_2O gas emerged as a reliable predictor of the exposure to all tested different-sized particles. Furthermore, the results of this study suggest that tracer gas can be used to indicate the exposure of a person lying in bed to resuspended 0.7 μm particles close to his/her body;

- In patient rooms, the application of the new local exhaust ventilation method, namely the ventilated mattress, helps decrease the exposure and risk of cross-contamination to bio-effluents and aerosols emitted from a lying patient's body;

- The use of the ventilated mattress at background ventilation rates much lower than the recommended standard ventilation rates for hospital patient rooms is able to reduce the exposure to pollution and improve indoor air quality;

- The ventilated mattress can reduce completely body-emitted pollutants from a person lying in bed and covered by a quilt (or blanket);

- Using air cleaning material inside the VM is an effective method to clean the extracted polluted air and allows for recirculating it back into the room, thus providing flexibility of bed use;

- The ventilated mattress provides body cooling. The back side and the back are the body parts that will be cooled the most since most of their surface area is in contact with the mattress. The surfaces of the ventilated mattress in contact with these body segments can be heated under individual user control to provide comfort;

- In rooms with mixing ventilation the use of the ventilated cushion can reduce occupants' exposure to body generated bio-effluents. Exhausting 1.5 L/s of air through the ventilated cushion to reduce the bio-effluents' concentrations into the room and combining it with total volume ventilation at 1 ACH proved to be 30% more efficient in providing clean air into the occupied zone than total volume ventilation alone at 1.5 ACH;

- Exhausting air through the ventilated cushion provides local cooling to the body parts in contact with the cushion. The ventilated cushion has the potential to improve the thermal comfort in warm climates and during seasons when the outdoor temperature is high;

- Increasing the maximum allowed room operative temperature and maintaining occupants' thermal comfort via the local convective cooling provided by the studied local exhaust methods (ventilated mattress and ventilated cushion respectively) is an effective energy-saving strategy;

- The ventilated mattress in conjunction with background ventilation at 3 ACH will decrease the annual energy use by 24% to 52% for a double patient room located in a cold climate or hot and humid climate as compared to conventional mixing ventilation at 4-6 ACH;

- Combining the ventilated cushion with background mixing ventilation and radiant ceiling panels for cooling in a call-centre located in Copenhagen reduced the energy use by 7% compared to a system with only mixing ventilation.

References

ASHRAE. 2003. HVAC Design Manual for Hospitals and Clinics, first ed., American Society of Heating, Refrigerating, and Air-conditioning Engineers, Atlanta, GA,2003.

ASHRAE. 2013. ANSI/ASHRAE Standard 170-2013, Ventilation of Health Care Facilities, American Society of Heating, Refrigerating and Air-Conditioning Engineers, Inc, Atlanta, 2013.

ASHRAE. ASHRAE Handbook-HVAC Applications, Chapter 46, Control of Gaseous Indoor Air Contaminants, ASHRAE, Atlanta, 2011.

Beat-Arribas, B., McDonagh, A., Noakes, C.J., and Sleigh, P.A. (2015) Assessing the near-patient infection risk in isolation rooms. Proceedings of Healthy Buildings 2015, ISIAQ International Conference, Eindhoven, the Netherlands, May 18-20, paper #537. 26;

Beggs C., L. D. Knibbs, G. R. Johnson, L. Morawska. (2015) Environmental contamination and hospital-acquired infection: factors that are easily overlooked. Indoor Air 2015; 25: 462–474.

Bekö Gabriel., Fadeyi M., Clausen Geo, Weschler Charles. (2009) Sensory pollution from bag-type fiberglass ventilation filters: Conventional filter compared with filters containing various amounts of activated carbon. Building and Environment 44 (2009) 2114–2120;

Bellanti, J.A., Zeligs, B.J., Macdowell-Carneiro, A.L., Abaci, A.S. and Genuardi, J.A. (2000) Study of the effects of vacuuming on the concentration of dust mite antigen and endotoxin, Annals of Allergy Asthma & Immunology, 84, 249-254.

Bivolarova, M. P., Rezgals, L., Melikov, A. K., Bolashikov, Z. D. (2016a) Seat-integrated localized ventilation for exposure reduction to air pollutants in indoor environments. In Proceedings of 9th International Conference on Indoor Air Quality Ventilation & Energy Conservation In Buildings, Oct., 2016 Seoul, Korea;

Bivolarova, M. P., Rezgals, L., Melikov, A. K., & Bolashikov, Z. D. (2016b). Exposure Reduction to Human Bio-effluents Using Seat-integrated Localized Ventilation in Quiescent Indoor Environment. Proceedings of the 12th Rehva World Congress;

Bivolarova, M.P., Melikov, A.K., Mizutani, C., Kajiwara, K. and Bolashikov, Z.D. (2016c) Bed-integrated local exhaust ventilation system combined with local air cleaning for improved IAQ in hospital patient rooms, Building and Environment, 100, 10-18;

Bolashikov, Z.D., Barova, M., Melikov, A. (2015) Wearable personal exhaust ventilation: Improved indoor air quality and reduced exposure to air exhaled from a sick doctor, Science and Technology for the Built Environment, 21:8, 1117-1125, DOI;

Bolashikov, Z., Melikov, A. and M. Krenek. (2010) Control of the free convective flow around the human body for enhanced inhaled air quality: Application to a seat-incorporated personalised ventilation unit. Science and Technology for the Built Environment 16:2;

Bolashikov, Z.D., Melikov, A. (2011) Exposure to exhaled air from a sick occupant in a two-bed hospital room with mixing ventilation: effect of distance fromsick occupant and air change rate. *Proceeding of Indoor Air 2011*, *Austin*, *TX*;

Bolashikov, Z.D., Melikov, A.K., Kierat, W., PopioLek, Z., and M. Brand. (2012) Exposure of healthcare workers and occupants to coughed airborne pathogens in a double-bed hospital room with overhead mixing ventilation. HVAC&R Research 18:602–15;

Bolashikov, Z. D. and Melikov, A K. (2009) Methods for air cleaning and protection of building occupants from airborne pathogens, Building and Environment, 44, 1378-1385;

Bolashikov, Z., L. Nikolaev, A.K. Melikov, J. Kaczmarczyk, and P.O. Fanger. (2003) Personalised ventilation: air terminal devices with high efficiency. Proceedings of Healthy Buildings 2003, Singapore, 2:850–5;

Bjørn, E. and Nielsen, P.V. (2002) Dispersal of exhaled air and personal exposure in displacement ventilated room, Indoor Air, 12, 147–164;

Boor, B.E., Järnström, H., Novoselac, A. and Xu, Y. (2014) Infant exposure to emissions of volatile organic compounds from crib mattresses, Environ. Sci. Technol., 48, 3541–3549;

Boor, B.E., Spilak, M.P., Corsi, R.L. and Novoselac, A. (2015) Characterizing particle resuspension from mattresses: chamber study, Indoor Air, 25, 441-456.

Boyce JM, Potter-Bynoe G, Chenevert C, King T. Environmental Contamination Due to Methicillin-Resistant Staphylococcus aureus: Possible Infection Control Implications. Infection Control and Hospital Epidemiology Vol. 18, No. 9 (Sep., 1997), pp. 622-627;

Brohus, H. and Nielsen, P.V. (1995), Personal Exposure to Contaminant Sources in a Uniform Velocity Field, Proceedings of Healthy Buildings, 1555-1560;

Brohus, H. and Nielsen, P.V. (1996) Personal Exposure in Displacement Ventilated Rooms, Indoor Air, 6, 157–167;

Burge H. (2009) Bioaerosols: prevalence and health effects in the indoor environment. J. Allergy Clin. Immunol. 1990; 86, 687–701. 4. Bolashikov ZD, Melikov AK. Methods for air cleaning and protection of building occupants from airborne pathogens. *Build Environ*. 2009;44:1378-1385;

Cal M.P., M.J. Rood, S.M. Larson. (1997) Gas phase adsorption of volatile organic compounds and water vapor on activated carbon cloth, Energy Fuel 11 (2) (1997) 311-315;

Cao, G., Liu, S., Boor, B. E., Novoselac, A. (2015) Characterizing the Dynamic Interactions and Exposure Implications of a Particle- Laden Cough Jet with Different Room Airflow Regimes Produced by Low and High Momentum Jets. Aerosol and Air Quality Research, 15: 1955–1966;

Causer, S.M., Lewis, R.D., Batek, J.M. and Ong, K.H. (2004) Influence of wear, pile height, and cleaning method on removal of mite allergen from carpet, Journal of Occupational and Environmental Hygiene, 1, 237-242;

CDC. Centers for Disease Control and Prevention (CDC) https://www.cdc.gov/mrsa/index.html. Last accessed on 24. March, 2017;

Cermak R., Holshøe J., Meyer K.E., Melikov A. (2002). PIV Measurements at the Breathing Zone with Personalized Ventilation. Proceedings of ROOMVENT 2002, Copenhagen.

Cermak, R., Melikov, A.K., Forejt, L.and Kovar, O.. (2006) Performance of personalised ventilation in conjunction with mixing and displacement ventilation, International Journal of Heating, Ventilation and Refrigeration Research 12(2):295–311;

Cermak, R., and A.K. Melikov. (2007) Protection of occupants from exhaled infectious agents and floor material emissions in rooms with personalised and underfloor ventilation, HVAC&R Research 13(1) 23–38;

Chen, Q.Y. (2009) Ventilation performance prediction for buildings: A method overview and recent applications, Building and Environment, 44, 848-858;

Clark, R. P. & Cox, R. N. (1974) An application of aeronautical techniques to physiology. 2. Particle transport within the human micro-environment. Med. Biol. Eng. 12, 275– 279. (doi:10.1007/BF02477791);

Clark, R. P. Chapter 4. Human Skin Temperature and Convective Heat Loss. Studies in Environmental Science 1981;Vol. 10:57-76. doi:10.1016/S0166-1116(08)71081-1

Curseu, D., Popa, M., Sirbu, D. and Popa, M.S. (2009) Engineering Control of Airborne Disease Transmission in Health Care Facilities, 26, 1-4;

Davies, R.R. and Noble, W.C. (1962) Dispersal of bacteria on desquamated skin,Lancet, ii, 1295;

Dormont L, Bessiere JM, Cohuet A. (2013) Human Skin Volatiles: A Review. Journal of Chemical 17 Ecology. 2013 May;39(5):569-78;

Douwes, J., Thorne, P., Pearce, N., Heederik, D. (2003) Bioaerosol health effects and exposure assessment: 11 Progress and prospects. Annals of Occupational Hygiene. 2003 Apr;47(3):187-200;

Dygert, R. K., Dang, T. Q. (2012) Experimental validation of local exhaust strategies for improved IAQ in aircraft cabins. *Building and Environment.* 2012, 47, 76-88;

Fang L., D.P. Wyon, G. Clausen, P.O. Fanger, Impact of indoor air temperature and humidity in an office on perceived air quality, SBS symptoms and performance, Indoor Air 14 (Suppl. 7) (2004) 74-81;

Faulkner, D., W.J. Fisk, D.P. Sullivan, and D.P. Wyon. 1999. Ventilation efficiencies of desk mounted task/ambient conditioning systems. Indoor Air 9(4):273–281;

FprCEN/TR 16244, Ventilation for Hospitals 16244, 2011. Technical report 2011, FprCEN/TR;

Gao NP, Niu JL. (2005) Study of the Thermal Environment around a Human Body: A Review. Indoor Built Environ, 14 (1):5–16;

Guity, A., P. Gulick, and P. Marmion. 2009. Healthcare Ventilation Research Collaborative: Displacement ventilation research. Phase II summary report, December 2009, Health care without harm. http://www.noharm.org/us canada/reports/ 2009/dec/rep2009–12 01.php;

Gupta JK, Lin CH, Chen Q. (2010) Characterizing exhaled airflow from breathing and talking. Indoor Air 2010; 20: 31-39;

Haselton FR, Sperandio PGN. (1988) Convective exchange between the nose and the atmosphere, Journal of Applied Physiology 1988; 64 (6): 2575-2581;

Homma, H. and Yakiyama, M. (1988) Examination of free convection around occupant's body caused by its metabolic heat. ASHRAE Transactions, 94(1):104–24;

Hoyt T, Kwang HL, Zhang H, Arens E, Webster T. (2009) Energy Savings from Extended Air Temperature Setpoints and Reductions in Room Air Mixing. 2009;

Hyldgård CE. (1994) Humans as a source of heat and air pollution. In: Proceedings of the 4th International Conference on air distribution in rooms - Roomvent 1994, Cracow, Poland, vol. 1; 1994. p. 413-33;

IOM. (2000) Clearing the Air: Asthma and Indoor Air Exposures, Washington, DC, Institute of Medicine, National Academy of Sciences, National Academy Press;

ISO, 2004a. 8996, Ergonomics of the Thermal Environment—Determination of metabolic heat production;

ISO. 2004b. ISO 14505-2, Ergonomics of the Thermal Environment—Evaluation of Thermal Environment in Vehicles—Part 2: Determination of Equivalent Temperature. Geneva: International Organization for Standardization;

ISO, International Standard ISO/DIS/7730. (2005) Moderate Thermal Environments-Determination of PMV and PPD Indices and Specification of the Conditions for Thermal Comfort: International Standard;

ISO/IEC Guide 98-3:2008. (2008) Uncertainty of measurements -- Part 3: Guide to the expression Itakura T, Mitsuda M. Servey of characteristics of the odour in medical facilities. The 6th International Conference on Indoor Air Quality, Ventilation & Energy Conservation in Buildings IAQVEC 2007, Oct. 28e31, Sendai, Japan.of uncertainty in measurement (GUM: 1995);

Jarvis J, Seed MJ, Elton R, Sawyer L, Agius R (2005) Relationship between chemical structure and the occupational asthma hazard of low molecular weight organic compounds. Occup Environ Med 62:243–250;

Kaczmarczyk, J., Melikov, A., & Fanger, P. O. (2004). Human response to personalized ventilation and mixing ventilation. Indoor Air, 14(s8), 17-29;

Kaczmarczyk J., Q. Zeng, A.K. Melikov, and P.O. Fanger. 2002. Individual control and people's preferences in an experiment with a personalized ventilation system. *Proceedings of Roomvent 2002* pp. 57–60;

Kaczmarczyk, J., A. Melikov, Z. Bolashikov, L. Nikolaev, and P.O. Fanger. 2006. Human response to five designs of personalized ventilation. *HVAC& R* 12(2):367–84;

Kazanci, O. B., & Olesen, B. W. (2015). IEA EBC Annex 59 - Possibilities, limitations and capacities of indoor terminal units. Energy Procedia - 6th International Building Physics Conference, IBPC 2015, 78, 2427–2432;

Kazanci, O. B. (2016) Low Temperature Heating and High Temperature Cooling in Buildings. PhD thesis, Technical University of Denmark, Kgs. Lyngby 2800;

Kemmlein, S., Hahn, O., and Jann, O. (2003) Emissions of organophosphate and brominated flame retardants from selected consumer products and building materials, Atmos. Environ., 37, 548-554;

Kierat, W. and Popiolek Z. (2017) Dynamic properties of fast gas concentration meter with nondispersive infrared detector. Measurement, 95, 149–155;

Kogawa Y, Nobe T, Onga A. (2007) Practical investigation of cool chair in warm offices. *Proceedings of Clima '07, Helsinki, Finland*;

Koullapis, P.G., Kassinos, S.C., Bivolarova, M.P. and Melikov, A.K. (2016) Particle deposition in a realistic geometry of the human conducting airways: Effects of inlet velocity profile, inhalation flowrate and electrostatic charge, Journal of Biomechanics, 49, 2201-2212;

Lagarias, J.C., Reeds, J.A., Wright, M.H. and Wright, P.E. (1998) Convergence properties of the Nelder-Mead simplex method in low dimensions, Siam Journal on Optimization, 9, 112-147;

Laverge J., Spilak, M., Novoselac, A. (2014). Experimental assessment of the inhalation zone of standing, sitting and sleeping persons. Building and Environment 82 (2014) 258-266;

Lee P and Davidson J. (1999) Evaluation of activated carbon filters for removal of ozone at the PPB level. American Industrial Hygiene Association Journal, 60, (5), 589-600.

Li, Y., Nielsen, P.V. and Sandberg, M. (2011) Displacement ventilation in hospital environments, ASHRAE J., 53, 86–88;

Li, Y., Leung, G.M., Tang, J.W., Yang, X., Chao, C.Y.H., Lin, J.Z., Lu, J.W., Nielsen, P.V., Niu, J., Qian, H., Sleigh, A.C., Su, H.J.J., Sundell, J., Wong, T.W. and Yuen, P.L. (2007) Role of ventilation in airborne transmission of infectious agents in the built environment - a multidisciplinary systematic review, Indoor Air, 17, 2-18;

Li F., J. Liu, J. Pei, C.H. Lin, Q. (2014) Chen Experimental study of gaseous and particulate contaminants distribution in an aircraft cabin Atmos. Environ., 85 (2014), pp. 223–233;

Licina, D., Melikov, A.K., Sekhar, C., Tham, K.W. 2014a. Human convective boundary layer and its interaction with room ventilation flow, Indoor Air, doi:10.1111/ina.12120, 25(1): 21–35, 2014;

Licina, D., A. Melikov, J. Pantelic, C. Sekhar, and K.W. Tham. 2014b. Experimental investigation of the human convective boundary layer in a quiescent indoor environment. Building and Environment 75:79–91;

Licina, D., Melikov, A., Pantelic, J., Sekhar, C. and Tham, K.W. (2015a) Human convection flow in spaces with and without ventilation: personal exposure to floor-released particles and cough-released droplets, Indoor Air, 25, 672-682;

Licina, D., Melikov, A., Sekhar, C. and Tham, K.W. (2015b) Transport of gaseous pollutants by convective boundary layer around a human body, *Science and Technology for the Built Environment*, **21**, 1175-1186.

Licina, D., Melikov, A.K., Sekhar, C., Tham, K.W. (2015c). Air temperature investigation in microenvironment around a human body, Building and Environment, DOI: http://dx.doi.org/10.1016/j.buildenv.2015.04.014, 92: 39-47;

Licina, D. and C. Sekhar, (2012) Energy and water conservation from air handling unit condensate in hot and humid climates. Energy and Buildings 45, pp. 257-263;

Long, C.M., Suh, H.H., Catalano, P.J. and Koutrakis, P. (2001) Using time- and size-resolved particulate data to quantify indoor penetration and deposition behavior, Environmental Science & Technology, 35, 2089-2099.

Marr D., Khan T., Glauser M., Higuchi H. and Jianshun Z.D. (2005) On Particle Image Velocimetry (PIV) Measurements in the Breathing Zone of a Thermal Breathing Manikin, ASHRAE Transactions, Vol. 111 Issue 2, p299;

Melikov, A. (2011) Advanced air distribution, ASHRAE J., November, 73–78;

Melikov, A.K. (2016). Advanced air distribution: improving health and comfort while reducing energy use, Indoor Air, 26 (1): 112–124, doi:10.1111/ina.12206;

Melikov AK, Bolashikov ZD, and Georgiev E. (2011) Novel ventilation strategy for reducing the risk of airborne cross infection in hospital rooms. *Proceedings of Indoor Air 2011*, June 5–10,Austin, TX, Paper 1037;

Melikov, A.K. and Dzhartov, V. (2013) Advanced air distribution for minimizing airborne cross-infection in aircraft cabins, Hvac&R Research, 19, 926-933;

Melikov, A. (2004) Breathing thermal manikins for indoor environment assessment: important characteristics and requirements, European Journal of Applied Physiology, 92, 710-713.

Melikov, A.K. (2015) Human body micro-environment: The benefits of controlling airflow interaction, Building and Environment 91: 70-77.

Melikov, A.K., Ivanova, T., Stefanova, G. (2012) Seat Headrest-Incorporated Personalised Ventilation: Thermal comfort and Inhaled Air Quality, Building and Environment, 47, pp. 100-107;

Melikov, A.K., Cermak, R., Kovar, O., Forejt, L. (2003) Impact of airflow interaction on inhaled air quality and transport of contaminants in rooms with personalised and total volume ventilation. In: Proceedings of healthy buildings 2003, 2. Singapore: 7-1 National University of Singapore, Department of Building; 2003. p. 592-7;

Melikov AK, Kaczmarczyk J. (2007) Measurement and prediction of indoor air quality using a breathing thermal manikin. Indoor Air. 2007; 17:50-9;

Melikov, A.K. (2004) Personalized ventilation. Indoor Air 14(Suppl. 7), 157–167;

Melikov A., Zhu S. and Bolashikov Z. (2016) Patent for Hospital Ventilation Unit – "Device and Method for Reducing Spread of Microorganisms and Airborne Health Hazardous Matter and/or

for Protection from Microorganisms and Airborne Health Hazardous Matter" in US (granted: Apr. 12, 2016 US No: 9,310,0880B2), Japan (granted: Feb. 16, 2016 JP No: 5859960 B2) and Patent Application in Europa (filed on: July 17, 2009; European Patent Application No. 10799455.0).

Mizutani C, Yahata A, Tsuiki H, Morikawa H, Kajiwara K, Takahashi K, Shigeta T, Kurosawa H, Otsuka C, and Shirai H (2013) Application of Nursing Care Using Deodorant and Antibacterial Fiber. Sen'I Gakki, pp.141-145 (in Japanese).

Morawska, L. (2006) Droplet fate in indoor environments, or can we prevent the spread of infection?, Indoor Air, 16, 335-347;

Morawska, L., Afshari, A., Bae, G.N., Buonanno, G., Chao, C.Y.H., Hanninen, O., Hofmann, W., Isaxon, C., Jayaratne, E.R., Pasanen, P., Salthammer, T., Waring, M. and Wierzbicka, A. (2013) Indoor aerosols: from personal exposure to risk assessment, Indoor Air, 23, 462-487;

Mosley RB, Greenwell DJ, Sparks LE, Guo Z, Tucker WG, Fortmann R, Whitfield C. (2001) Penetration of ambient fine particles into the indoor environmemnt. Aerosol Sci Technol. 2001;34:127-136;

Müller, D. (Ed.), Kandzia, C., Kosonen, R., Melikov, A. K., & Nielsen, P. V. (2013) Mixing Ventilation - Guide on mixing air distribution design. Brussels: REHVA - Federation of European Heating, Ventilation and Air Conditioning Associations;

Mundt, E. (1995) Displacement ventilation systems - convection flows and temperature gradients, Building and Environment; 30(1):129-33;

Murakami, S. (2004) Analysis and design of micro-climate around the human body with respiration by CFD, Indoor Air, 14 (Suppl 7): 144–156;

Nazaroff, W.W. Indoor particle dynamics. Indoor Air. 2004; 14:175–183.

Nielsen, P.V. (2009) Control of airborne infectious diseases in ventilated spaces, J. R. Soc. Interface, 6, 747–755.

Nielsen PV, Olmedo I, Manuel RA,Piotr G, Rasmus LJ. (2012) Airborne cross-infection risk between two people standing in surroundings with a vertical temperature gradient. HVAC R Res 2012;18(4):1e10.

Nielsen, P.V., Buus, M., Winther, F.V., Thilageswaran, M. and Ashrae. (2008) Contaminant Flow in the Microenvironment Between People Under Different Ventilation Conditions, Ashrae Transactions 2008, Vol 114, Pt 2, 114, 632-638.

Nielsen, P. V., Jensen, R. L., Litewnicki, M., & Zajas, J. J. (2009). Experiments on the Microenvironment and Breathing of a Person in Isothermal and Stratified Surroundings. In

Healthy Buildings 2009, 9th International Conference & Exhibition, September 13-17, 2009, Syracuse, NY USA;

Nishida K., T. Kodama, M. Yamakawa, The changes in psychophysical coefficient by the composition of nightsoil, Kankyo Gijytsu 10 (1981) 462e473.

Niu J., Gao N., Phoebe M., Huigang Z. (2007) Experimental study on a chair-based personalised ventilation system, Building and Environment 42 (2007) 913–925;

Noakes, C.J., Fletcher, L.A., Sleigh, P.A., Booth, W.B., Beato-Arribas, B., and Tomlinson, N. (2009) Comparison of tracer techniques for evaluating the behaviour of bioaerosols in hospital isolation rooms. Proceedings of Healthy Buildings 2009, 9th international conference and exhibition, Syracuse, NY, USA. Paper #504;

Noble, W.C., Habbema, J.D.F., Furth van R et al. (1976) Quantitative studies on the dispersal of skin bacteria into the air. J. MED. MICROBI0L.-VOL. 9, 1976;

Olmedo, I., Nielsen, P.V., De Adana, M.R., Jensen, R.L. and Grzelecki, P. (2012) Distribution of exhaled contaminants and personal exposure in a room using three different air distribution strategies, Indoor Air, 22, 64-76;

Özcan O, Mayer KE, Melikov AK. (2005) A visual description of the convective flow field around the head of a human, Journal of Visualization 2005; 8, 1: 23-31.

Pantelic, J. and Tham, K.W. (2013) Adequacy of air change rate as the sole indicator of an air distribution system's effectiveness to mitigate airborne infectious disease transmission caused by a cough release in the room with overhead mixing ventilation: A case study, HVAC&R Research, 19, 947-961;

Panu M., Bolashikov, Z., Kostov K.,Melikov,A., Kosonen, R. (2016) Thermal environment in simulated offices with convective and radiant cooling systems under cooling (summer) mode of operation. Building and Environment 100 (2016) 82-91;

PopioLek, Z., Z. Bolashikov, K.Kostadinov,W.Kierat, andA.Melikov. 2012. Exposure of health care workers and occupants to coughed air in a hospital room with displacement air distribution: impact of ventilation rate and distance from coughing patient. Proceedings of Healthy Buildings 2012, June 8–12, Brisbane, Australia.

Qian, H., Y. Li, P.V. Nielsen, C.E. Hyldgaard, T.W. Wong, and A.T.Y. Chwang. (2006) Dispersion of exhaled droplet nuclei in a two-bed hospital ward with three different ventilation systems. Indoor Air 16:111–28.

Qian, J., Hospodsky, D., Yamamoto, N., Nazaroff, W.W. and Peccia, J. (2012) Size-resolved emission rates of airborne bacteria and fungi in an occupied classroom, Indoor Air, 22, 339–351;

Rai, A.C., Guo, B., Lin, C.H., Zhang, J.S., Pei, J.J., Chen, Q.Y. (2013) Ozone reaction with clothing and its initiated particle generation in an environmental chamber. Atmospheric Environment. 2013 Oct;77:885-92;

Rim D, Novoselac, A. (2009) Transport of particulate and gaseous pollutants in the vicinity of a human body. Build Environ. 2009;44:1840-1849;

Rim, D. and Novoselac, A. and Morrison, G. (2009) The influence of chemical interactions at the human surface on breathing zone levels of reactants and products, Indoor Air, 19, 324–334;

Salmanzadeh, M., Zahedi, Gh., Ahmadi, G., Marr, D.R. and Glauser, M. (2012) Computational modeling of effects of thermal plume adjacent to the body on the indoor airflow and particle transport, Journal of Aerosol Science, 53, 29–39

Schiavon, S., Melikov, A.K., Sekhar, C. (2010) Energy analysis of the personalized ventilation system in hot and humid climates., Ch. 42, 2010, Energy and buildings, pp. 699-707;

Schiavon, S. and. Melikov, A.K. (2009) Energy-saving strategies with personalized ventilation in cold climates". Energy and Buildings 41,5, pp. 543-550;

Seitz T, Mortimer V, Martinez K. (1998) A tracer gas evaluation at a garment manufacturing facility with extensive transmission of tuberculosis. Applied Occupational Environmental Hygiene 1998;13: 335–42;

Sidheswaran, H. Destaillats, D. Sullivan, S. Cohn, J. Larsen, W. (2012) Fisk, Energy efficient indoor VOC air cleaning with activated carbon fiber (ACF) filters, Build. Environ. 47 (2012) 357e367.

Simone A., B. Olesen, J. Stoops, A.W. Watkins. 2013. Thermal comfort in commercial kitchens (RP-1469): procedure and physical measurements (Part 1), HVAC&R Res. 19 (2013) 1001-1015;

Smolík, J., Lazaridis, M., Moravec, P., Schwarz, J., Zaripov, S. K. , Ždímal, V. (2005) Indoor aerosol particle deposition in an empty office, Water, Air and Soil Pollution 165, 301-312.

Spendlove, J. C., Fannin, K. F. (1983) Source, Significance, and Control of Indoor Microbial Aerosols – Human Health-Aspects. Public Health Reports, 98(3), 229-244;

Spilak, M.P., Boor, B.E., Novoselac, A. and Corsi, R.L. (2014) Impact of bedding arrangements, pillows, and blankets on particle resuspension in the sleep microenvironment, Building and Environment, 81, 60-68;

Sørensen, D.N., Nielsen, P.V. (2003) Quality control of computational fluid dynamics in indoor environments, Indoor Air, 13, 2-17.

Sun C, Lian Z, Lan L, Zhang H. (2013) Investigation on temperature range for thermal comfort in nonuniform environment. HVAC&R Research 2013;19:103-12.

Tang, J.W., Noakes, C.J., Nielsen, P.V., Eames, I., Nicolle, A., Li, Y. and Settles, G.S. (2011) Observing and quantifying airflows in the infection control of aerosol- and airborne-transmitted diseases: an overview of approaches, Journal of Hospital Infection, 77, 213-222.

Tang JW, Nicolle AD, Klettner CA, Pantelic J, Wang L. Airflow Dynamics of Human Jets: Sneezing and Breathing - Potential Sources of Infectious Aerosols. PLoS ONE 2013; 8(4): 59970. doi:10.1371/journal.pone.0059970.

Thatcher, T.L., Lai, A.C.K., Moreno-Jackson, R., Sextro, R.G. and Nazaroff, W.W. (2002) Effects of room furnishings and air speed on particle deposition rates indoors, Atmospheric Environment, 36, 1811-1819;

Tsushima S, Bekö G, Bossi R, Tanabe S, and Wargocki P. (2016) Measurements of Dermal and Oral Emissions from Humans. In: Proceedings of the14th International Conference on Indoor Air Quality and Climate –Indoor Air '16', Ghent, paper 288;

Verhulst N.O., W. Takken, M. Dicke, G. Schraa, R.C. Smallegange. (2010) Chemical ecology of interactions between human skin microbiota and mosquitoes, FEMS Microbiol. Ecol. 74 (2010) 1-9;

Wang, M., Lin, C.H. and Chen, Q.Y. (2012) Advanced turbulence models for predicting particle transport in enclosed environments, Building and Environment, 47, 40-49;

Wargocki, P., Wyon, D. P. and Fanger, P. O. (2004) The performance and subjective responses of call-center operators with new and used supply air filters at two outdoor air supply rates. *Indoor Air*, vol. 14 Suppl 8, pp. 7–16;

Watanabe S, Shimomura T, Miyazaki H. (2009) Thermal evaluation of a chair with fans as an individually controlled system. Building and Environment 2009;44:1392-8;

Wisthaler, A., Weschler, C.J. (2010) Reactions of ozone with human skin lipids: sources of carbonyls, dicarbonyls, and hydroxycarbonyls in indoor air. Proceedings of the National Academy of Sciences, 107, 6568–6575;

Wyon et al. (1989) Ventilated chair or similar device. D. P. Wyon, C. Tennstedt. Int. Cl.: A47C 7/72. Jun. 14, 1989.United States Patent. 4,946,220. Feb. 23, 1989;

Wysocki, C., and G. Preti. (2004) Facts, fallacies, fears, and frustrations with human pheromones. The anatomical record 281A:1201–1211;

Yan, W., Zhang, Y., Sun, Y., Li, D. (2009) Experimental and CFD study of unsteady airborne pollutant transport within an aircraft cabin mock-up. Building and Environment 44 (2009) 34–43;

Yang, J., Sekhar, C., Cheong, D.K.W. and Raphael, B. (2014) Performance evaluation of a novel personalized ventilation–personalized exhaust system for airborne infection control. Indoor Air, DOI: 10.1111/ina.12127;

Yau, Y.H., Chew, B.T. (2009) Thermal comfort study of hospital workers in Malaysia, Indoor Air 19 (2009) 500e510, http://dx.doi.org/10.1111/j.1600- 0668.2009.00617.x.

Yeh, H.C., Cuddihy, R.G., Phalen, R.F. and Chang, I.Y. (1996) Comparisons of calculated respiratory tract deposition of particles based on the proposed NCRP model and the new ICRP66 model, Aerosol. Sci. Technol., 25, 134–140;

Zhang, H., C. Huizenga, E. Arens, and D. Wang, (2004) Thermal sensation and comfort in transient non-uniform thermal environments. European Journal of Applied Physiology, Vol. 92, pp. 728—733;

Zhang, Z., Chen, X., Mazumdar, S., Zhang, T.F. and Chen, Q.Y. (2009) Experimental and numerical investigation of airflow and contaminant transport in an airliner cabin mockup, Building and Environment, 44, 85-94;

Zhang, X.J., Wargocki, P. and Lian, Z.W. (2016a) Effects of exposure to carbon dioxide and bioeffluents on perceived air quality, self-assessed acute health symptoms, and cognitive performance, Indoor Air, doi: 10.1111/ina.12284.13;

Zhang, X.J., Wargocki, P. and Lian, Z.W. (2016b) Physiological responses during exposure to carbon dioxide and bioeffluents at levels typically occurring indoors, Indoor Air, doi: 10.1111/ina.12286;

Zhao B, Zhang Y, Li XT, Yang XD, Huang DT. (2004) Comparison of indoor aerosol particle concentration and deposition in different ventilated rooms by numerical method. *Build Environ*. 2004;39:1-8.

Zhu, S., Kato, S., Murakami, S. and Hayashi, T. (2005) Study on inhalation region by means of CFD analysis and experiment, Building and Environment, 40, 1329-1336;

Zukowska D., Melikov A. and Popiolek Z. 2012. Impact of personal factors and furniture arrangement on the thermal plume above a sitting occupant. Building and Environment, 49, pp. 104 - 116.

Appendix A – List of publications that are part of the PhD study but not included in the thesis

Bivolarova, M.P., Kierat, W., Zavrl, E., Popiolek, Z., Melikov, A. K., (paper accepted) Exposure to human body bio-effluents: impact of airflow interaction at the breathing zone. *Submitted in Healthy Buildings 2017, ISIAQ International Conference, July 2-5, 2017, Lublin, Poland, paper ID 0231.*

Kierat W., **Bivolarova M.P.**, Zavrl E., Popiolek Z., Melikov A., (paper accepted). Measurement of exposure to gaseous contaminants. *Submitted in Healthy Buildings 2017, ISIAQ International Conference, July 2-5, 2017, Lublin, Poland, paper ID 0233.*

Bivolarova, M. P., Melikov, A. K., and Kehayova, N. Energy Saving by Novel Bed-Integrated Local Exhaust Ventilation. *In Proceedings of the 5th International Conference on Human-Environment System ICHES 2016 Nagoya, October 29 - November 2, 2016.*

Bivolarova, M. P., Ondràček, J., Ždímal, V., Melikov, A.K., and Bolashikov, Z. D., 2016, Exposure to aerosol and gaseous pollutants in a room ventilated with mixing air distribution. *In Proceedings of 14th International Conference on Indoor Air Quality and Climate*, Ghent, Belgium, July 3-8, 2016.

Bivolarova, M. P., Rezgals, L., Melikov, A. K., Bolashikov, Z. D., 2016, Exposure Reduction to Human Bio-effluents Using Seat-integrated Localized Ventilation in Quiescent Indoor Environment. *In Proceedings of 12th REHVA World Congress CLIMA 2016, Aalborg, Denmark in May 2016, Paper 668*.

Bivolarova, M. P., Mizutani, C., Melikov, A.K., and Bolashikov, Z. D., 2015, Advanced Air Distribution Method for Exposure Reduction to Bioeffluents Contaminants in Hospitals. *In Proceedings of Healthy Buildings 2015, ISIAQ International Conference, Eindhoven, the Netherlands, May 18-20, paper ID 632.*

Bivolarova, **M.P.**, Melikov, A.K., Kokora, M., Mizutani, C. and Bolashikov, Z. D., 2014, Novel bed integrated ventilation method for hospital patient rooms. *In Proceedings of ROOMVENT 2014, 13th International Conference on Air Distribution In Rooms, Sao Paolo, Brazil, October 20-22, 2014, p. 49-56.*

Bivolarova, M. P., Melikov, A. K., Kokora, M., & Bolashikov, Z. D., 2014, Local Cooling of The Human Body Using Ventilated Mattress in Hospitals. *In Proceedings of ROOMVENT 2014, 13th SCANVAC International Conference on Air Distribution in Rooms, October 19-22, 2014, Sao Paolo, Brazil, p. 279-286.*

Mizutani, C., **Bivolarova, M. P**., Melikov, A.K., Bolashikov, Z. B., Sakoi, T. and Kajiwara, K., 2014, Air Cleaning Efficiency of Deodorant Materials Under Dynamic Conditions: Effect Of Air Flow Rate. *In Proceedings of Indoor Air 2014, 13th International Conference on Indoor Air Quality and Climate, Hong Kong, July 7-12, 2014, p. 745-749.*

Appendix B – Publications, accepted and submitted papers that are included in the thesis

PAPER I

Bivolarova M., Kierat W., Zavrl E., Popiolek Z., Melikov A., (submitted). Effect of airflow interaction in the breathing zone on exposure to body released bio-effluents. Submitted to Building and Environment, March 2017.

Effect of airflow interaction in the breathing zone on exposure to body released bio-effluents

Mariya Bivolarova[1*], Wojciech Kierat[2], Eva Zavrl[1], Zbigniew Popiolek[2], Arsen Melikov[1]

[1]International Centre for Indoor Environment and Energy, Department of Civil Engineering, Technical University of Denmark, Niels Koppels Allé, building 402, DK-2800 Lyngby, Denmark

[2]Silesian University of Technology, Department of Heating, Ventilation and Dust Removal Technology, Konarskiego 20, 44-100 Gliwice, Poland

Abstract

The influence of the complex interaction of breathing flow, convective flow around human body and ventilation flow directed against the face on the exposure to body released effluents was examined together with the effects of source location and control. A breathing thermal manikin was used to simulate a sitting person in a full-scale climate chamber. Bio-effluents released at the armpits and groins were simulated with two tracer gases. It was found that the flow of exhalation substantially affects the exposure to body-emitted bio-effluents released close to the breathing flow, e.g. armpits. The exposure in the case of exhalation nose is higher compared to exhalation mouth. Breathing does not influence the exposure to gaseous pollutants emitted from the lower part of the body, e.g. groins. Local pollution source control by exhaust ventilation integrated into the seat reduced the exposure. Airflow imposed against the face can reduce substantially the exposure regardless of the pollution source location. However, when the flow is combined with local source control the exposure may increase depending on the airflow interaction at the breathing zone and the source location.

Keywords: human body micro-environment, breathing, airflow interaction, bio-effluents, exposure, fast concentration measurements

1. Introduction

The human body emits particles (bio-aerosols) and gasses (bio-effluents). Human respiration activities (exhalation, coughing, sneezing) generate bio-aerosols that may carry viruses and bacteria [1] which may cause airborne transmission of infection in spaces [2]. Human body movement and friction between the clothing and the skin generate skin flakes that contain a wide variety of contagious pathogens [3]. The flakes can be transported by air, inhaled and infect indoor occupants. The bio-effluents are volatile and non-volatile organic compounds that may be detected by human olfactory system as odours. Oral cavity, armpits, groins, head and feet are the sites where bio-effluents are mostly generated [4]. Sweating is important for human body thermal regulation. The sweat is accumulated by the skin microbial and further metabolized into volatile and non-volatile odours compounds [5]. The odour from human groins area is coming from the skin and from human wastes (e.g. urine). The compounds found in human wastes are acids, ammonia, sulphur, nitrogen compounds and other volatile metabolites [4]. Flatus also contributes to the body odour and smells

mainly because it contains combination of volatile sulphur compounds [6] (). Ozone reactions contributed to squalene (found in skin oil) occur on occupants' skin, clothing and hair [7-9] (,). The reactions produce sub-micron particles and volatile products which may cause headaches, eye and respiratory irritation and increased susceptibility to respiratory illness [10]. Studies report that body-emitted pollution have higher odour intensity compared to pollutants from exhaled air and may have negative impact on occupants' health, well-being and productivity [11, 12].

The micro-environment around human body has a major role for the heat and mass exchange between the body and the surrounding environment and exposure of people to indoor pollution [13]. A building occupant can be exposed to his/her own contaminants as well as contaminants emitted from others. The importance of the separate and combined impact of the free convection flow and the flow of respiration on the exposure of bio-effluents released by occupant's own body is in the focus of the present study.

The convective boundary layer (CBL) develops due to a temperature difference between the air surrounding the body and the surface of the body [14, 15]. The CBL develops in a thermal plume above person [16]. Gaseous and particulate pollutants generated from the body and in the surrounding are entrained into the CBL of a sitting person and are transported to the breathing zone [15, 17-19]. The concentration of seated body released pollution in the breathing zone is highest when it is released at the chest and lowest when it is emitted at the upper back or behind the chair and increases when the room air temperature decrease and the body is inclined backward [20]. The exposure is also influenced by the position of a desk in front of the body and the chair design. However, the referred above studies did not take into account the respiratory flow and the impact of its interaction with the CBL on the personal exposure.

The breathing is transient and most often consists of inhalation, exhalation and pause. The dynamics of the inhalation flow very close to the nose and to the mouth are similar [21]. Large variations in the spread of exhaled flows exist between people [22]. The exhalation generates jets with relatively high velocity, 1– 2 m/s [21, 23, 24], which depending on the head position can penetrate the CBL resulting in a small amount of the exhaled air re-inhaled [25]. The velocity in the exhaled jets decreases rapidly with the distance from the face. However the flow of exhalation through the nose and mouth is different [25, 26]. Two independent jets apart of each other and deflected downward from the horizontal axes are exhaled from the nostrils [22, 23, 27]. In a calm environment and at upright position of the head the jet exhaled almost horizontally from the mouth with temperature of approximately 34°C and a relative humidity close to 100% (according to [28]) moves upward at some distance from the face [24, 29]. Person at low activity level inhales air mostly from the front areas of the CBL, and little from the back and sides of the body [30].

Depending on several factors (head position, breathing rate, strength of the CBL, etc.) the flow of exhalation may or may not penetrate the CBL [14, 24, 25, 29, 31-33]. The interaction of the exhalation flow from the nose and the CBL increases the turbulence in the breathing zone [29, 34, 35]. Rim and Novoselac [17] reported that simulating breathing activity of a seated thermal manikin (inhalation/exhalation through the nose) has noticeable impact on the airflow distribution in the

breathing zone and may increase or decrease the particle concentrations measured at the mouth and above the head, depending on the source location in the room.

The interaction of the CBL with the surrounding airflow and the spread of exhaled polluted air depend on several factors including strength and direction of the airflow, location and size of the body exposed to the flow, etc. [27, 30, 36, 37]. Laverge et al. [38] reported that in a room with low velocity floor standing diffuser (i.e. supplied airflow distributed over the floor) the CBL remained dominant flow at the inhalation zone. However the CBL and the ventilation flow in spaces may interact differently depending on whether they are assisting, opposing or transfer to each other [37, 39, 40]. Advanced air distribution, such as personalized ventilation (PV), that supplies clean air directly to the breathing zone can penetrate the CBL and have great impact on the exposure [41, 42].

The interaction of flows around human body has been studied mainly with focus on spread of pollution between people. The reported research on airflow interaction at the breathing zone and its effect on exposure of persons to their own bio-effluents are limited and incomplete. Local source control has been almost not studied. Bivolarova et al. [43, 44] showed that it is possible to apply efficiently source control and remove human body generated pollution by local suction before it is mixed with the surrounding air.

Tracer gas has been used to simulate body released pollution. The tracer gas concentration used to assess exposure has been measured with instruments with slow response time. The measurements have been performed for relatively long time periods including inhalation and exhalation phases. This may have impact on accuracy of the assessment because in reality the exposure depends on the inhaled air contamination only but not on the exhaled air.

The importance of the breathing mode (inhalation nose/exhalation mouth/pause, inhalation mouth/exhalation nose/pause), the strength of the invading ventilation flow against the face, the location of the pollution source and the source control on the exposure of person to his/her body generated pollution was in the focus of the present study.

2. **Methods**

   2.1. Experimental setup and facilities

Full-scale experiments were carried out in a climate chamber with dimensions of 4.7 m x 6.0 m x 2.5 m (W x L x H). The chamber was ventilated by an upward piston air flow supplied from the entire floor area with air velocity of less than 0.05 m/s. The air was exhausted through a square opening (0.38 x 0.38 m^2) in the ceiling (Fig. 1). The chamber has been constructed to ensure a mean radiant temperature equal to the room air temperature and negligible radiant temperature asymmetry.

A breathing thermal manikin with realistic female body shape (size 38, 1.68 m height) was used to simulate the dry heat loss of a seated occupant [45]. The manikin had 23 body segments with individually controlled heat output. The surface temperature of the manikin's body was controlled to be similar to the skin temperature of an average human under thermal comfort state when

exposed to the same room conditions. The manikin was seated behind a desk on a computer chair (Fig. 2). The distance between the manikin's abdomen and the edge of desk was 0.1 m. The manikin and the desk were positioned in the centre of the chamber on a wooden plate (2 m x 1.21 m) in order to prevent disturbance of the CBL. The seated manikin had slightly inclined backward body posture (10° from the vertical axis) and its height in this position was 1.2 m. The manikin was dressed in tight clothing comprising of a t-shirt, tight-fitting trousers, underwear, socks and shoes (total thermal insulation together with the chair 0.55 clo). There was a short hair wig on manikin's head.

Breathing was simulated by artificial lung placed outside the chamber and connected with two plastic tubes (Ø 8 mm) and connectors (placed on the lower back of the manikin) to its mouth and nose. It was possible to adjust the breathing frequency, the pulmonary ventilation rate as well as the temperature of the exhaled air. The nostrils are shaped so that they resemble those of an average person – round opening with area of 38.5 mm^2 each. The mouth of the manikin is slightly open and with ellipsoid shape with area of 158 mm^2. Jets emerging from the nostrils are deflected 40° downwards from the horizontal axes [25].
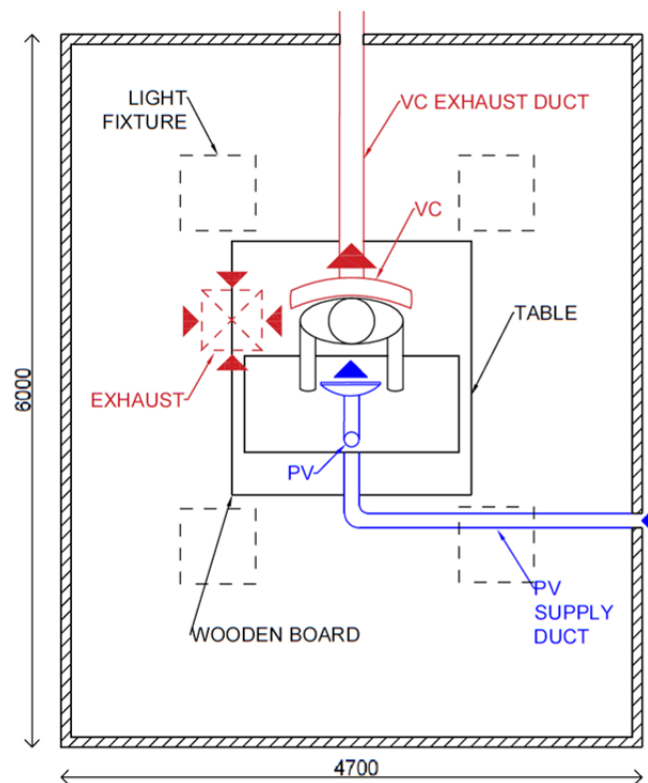
Fig. 1. The climate chamber arrangement.
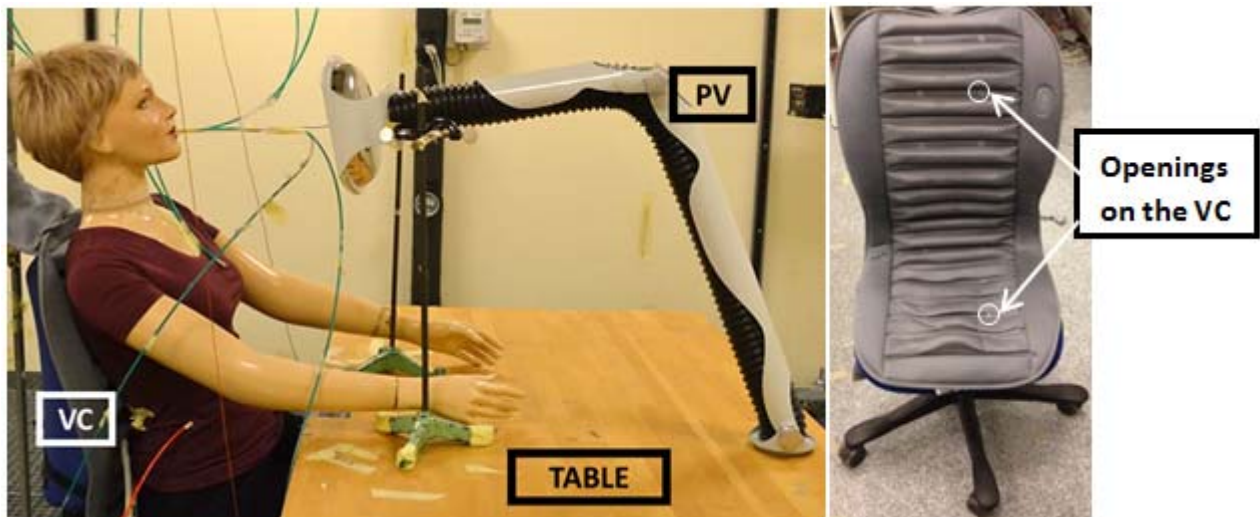
Fig. 2. Left: The thermal manikin seated on the chair with incorporated ventilated cushion in front of the table; right: the chair with the ventilated cushion.

In some experiments a seat-integrated local exhaust named "Ventilated cushion" (VC) was used to exhaust the contaminants emitted from the manikin's body. The VC was placed on top of the chair. The surface of the VC in contact with the manikin's body had openings each with diameter of 6 mm used to suck air through the cushion (Fig. 2 left). The openings were placed in eight horizontal channels to avoid their blocking by manikin's body. There were two openings per row and the distance between them was 0.135 m. The VC was connected to a local exhaust system which moved the exhausted air out of the chamber. A plastic mesh inside the ventilated cushion was built-in to provided body support and allowed the exhaust air to move inside the cushion. The flow rate of air sucked through the VC was measured in the exhaust system with sensors Micatrone MFS C-80 (accuracy ±3 % of measured flow rate) connected to a differential pressure micro-manometer FCO510 (accuracy of 0.01 Pa [0.15 × 10−5 psi] ±0.25% of reading). The flow rate was controlled by adjusting the speed of a fan integrated in the exhaust duct.

Personalized ventilation (PV) supplying clean air to the breathing zone of the thermal manikin via a round movable panel (RMP) was used in this study to generated external ventilation flow. The RMP had a circular outlet with diameter of 0.185 m which is a highly efficient air terminal device [46]. The RMP was installed on the desk in front of the manikin and positioned so that the distance between the outlet and the face of the manikin was 0.3 m.

2.2. Measuring procedure and instrumentation

Two tracer gases nitrous oxide (N_2O) and carbon dioxide (CO_2) were used to simulate bio-effluents contaminants emitted below the clothing at the armpits and groins of the manikin. The tracer gases were constantly released through cylindrical porous air stones (2.5 cm height and Ø1.2 cm). Thus even tracer gas release with negligible initial momentum was ensured. The air stones were

connected with tubes to gas cylinders located outside the chamber. The supply flow rates of the N_2O and CO_2 were controlled by gas Rotameters and kept constant at 0.5 L/min and 1.2 L/min respectively. The dosed CO_2 was split equally (measured with Rotameters) to both armpits of the manikin.

N_2O and CO_2 concentrations were measured continuously at the manikin's chest (3 cm away from the centre of the chest and 23 cm bellow the mouth), at the mouth (between the centres of the lips, at 0.5 cm distance) and at the nose (at the opening of the left nostril). Specially developed instruments (fast meters) with sampling rate of 4 Hz and time constant of 0.8 s were used to measure tracer gas concentration. The fast meters are based on non-dispersive infrared absorption (NDIR) method and are described in detail by Kierat and Popiolek [47, 48]. At each measurement location a separate N_2O and CO_2 fast meter was sampling the gas through a plastic tube (Ø 3 mm and length 1 m). In order to avoid too many tubes being attached to the manikin's face, the N_2O and CO_2 tubes at each sampling point were joint into one tube via Y-connecting piece. The resolution of the instruments was 1 ppm and the expanded uncertainty ±20 ppm (95% confidence level). Fourier transformation was applied for frequency correction of the signals from the instruments. Compensation of the data for the time needed for the N_2O and CO_2 samples to travel in the sampling tube from the measuring point to the fast meters was performed [48]. Two separate Innova 1312 photoacoustic gas analysers (accuracy 5% of the reading), each coupled with an Innova 1303 gas sampler, were used as well to measure the N_2O and CO_2 concentrations at 0.5 m above the manikin's head, at the supply and total exhaust air [49]. The Innova gas analysers and the fast meters were cross-calibrated before and the end of each experimental session.

Instantaneous air speed and temperature were measured at the mouth of the manikin. The air speed was measured with omni-directional low velocity thermal anemometer with sampling rate of 8 Hz and accuracy of the readings of ±0.02 m/s ±1%. The air temperature was measured with a micro bead VECO thermistor (time constant 0.12 s) with sampling rate of 16 Hz and measuring error of less than ±0.1°C. The velocity and temperature sensors were placed 1 cm apart and 1 cm away from the mouth.

The average air speed of the personalised flow, referred in the following as velocity of the personalised flow, was determined based on velocity profiles measured across the flow at distance of 30 cm from the RMP without presence of the manikin. At this distance the velocity was uniformly distributed (deviation less than 10%) in an area with diameter of 20 cm around jet axis. The turbulence intensity was in the range 4 – 20 %. The described above omni-directional low velocity thermal anemometer was used.

2.3. Experimental conditions

All measurements were conducted under steady state conditions. 100% clean outdoor air was supplied in the chamber. The air temperature in the chamber was controlled to be 23°C±0.2°C. The relative humidity was not controlled. It was measured during all experiments and was in the range

of 30-40% (±5% relative error). The only heat sources in the chamber were the thermal manikin and four fluorescent light fixtures (6 W each) located on the ceiling away from the thermal manikin (Fig. 1).

The simulated breathing process of the manikin corresponded to a person at light sedentary activity: breathing frequency was 10 times per min with a cycle of 2.5 s inhalation, 2.5 s exhalation and 1 s pause and pulmonary ventilation equal to 6 l/min. At these conditions the initial velocity of the jet exhaled from the mouth was 1.5 m/s and from the nostril 3.1 m/s. The temperature of the exhaled air was set to 34°C. Experiments at two breathing modes, namely inhalation nose/exhalation mouth/pause and inhalation mouth/exhalation nose/pause, were studied. Experiments without breathing were performed for comparison.

The personalized flow was applied at two velocities, 0.2 and 0.4 m/s and the ventilated cushion operated at exhaust airflow rate of 1.5, 3 and 5 L/s. The personalized air was supplied to the breathing zone at 23°C (isothermal condition). The studied experimental cases are listed in Table 1.

Table 1. Studied cases – combinations between breathing mode, use of VC and PV.

BR mode	NO BREATHING			INHALATION NOSE/ EXHALATION MOUTH				INHALATION MOUTH/ EXHALATION NOSE	
VC [L/s]	OFF	1.5	5.0	OFF	1.5	3.0	5.0	OFF	1.5
PV [m/s]	OFF 0.2 0.4	OFF 0.2	OFF 0.2	OFF 0.2 0.4	OFF 0.2	OFF	OFF 0.2	OFF	OFF

2.4. Exposure assessment and data analyses

The personal exposure was assessed by taking into account only the measured tracer gas concentrations during the inhalation period. At first signals measured at the mouth and nose, were synchronized in time to each other using cross-correlation function. Next, the exhalation periods were identified on the measured signal as cyclically repeating fragments with very low concentration (approx. 0 ppm). In this way a binary signal of the whole breathing process was obtained giving the possibility to extract the inhalation periods. The concentrations measured at the nose (during "inhalation nose") and at the mouth (during "inhalation mouth") during 40 min steady state conditions were used in the analyses. Over 8192 of N_2O and CO_2 samples were obtained for all 2.5 s inhalation periods during one experimental condition. The obtained data were used to calculate the mean, standard deviation (SD) and 95th percentile of the concentration. The uncertainty of the tracer gas measurements was 20 ppm. During the experiments with no breathing function the mean, SD and 95th percentiles of the concentrations measured at the nose and mouth were averaged in order to compare the results with the results obtained with different breathing modes.

The mean, SD and 95th percentile of the concentrations measured for some of the studied conditions were normalised with the mean concentration of respective measurements performed without

breathing, VC and PV. Normalized concentration lower than "1" indicates that inhaled pollutant is reduced, i.e. reduced exposure. The excess concentration of CO_2 over the background level was used as criteria for exposure assessment to armpit-emitted pollutants.

3. Results

Exposure due to interaction of CBL and flow of exhalation

Fig. 3 compares the mean, SD and the 95th percentile of the N_2O concentration (generated at the groins) measured during inhalation mouth/exhalation nose/pause (InM/ExN), inhalation nose/exhalation mouth/pause (InN/ExM) and without breathing (No breathing). The results of a separate experiment performed to study the importance of the source control (VC at 1.5 L/s) are also shown in the figure. The breathing mode has little impact on the measured tracer gas concentration (Fig. 3a). The mean and 95th percentile values for the two breathing modes differed only by 10%. The concentration of N_2O measured without breathing is similar to the concentration measured with breathing. The slightly higher concentration obtained in the case of exhalation through the mouth can be explained by the flow interaction at the breathing zone. The pollution generated at the groins is transported upward by the CBL in front of the body. The exhaled jet entrains air from the surrounding, including from the CBL and thus "pulls" more pollution to the breathing zone. The interaction of the jet exhaled almost horizontally from the mouth with the CBL causes mixing which however calms down during the break, the CBL re-establishes but with slightly higher concentration of N_2O. In the case of exhalation from the nose the two jets discharged from the nostrils are diverted with 30°-50° downward towards the left and right side of the chest. The jets are opposing to the CBL at the chest and interact more with its sides. The clean exhaled air mixes with the CBL and generates mixing. It generates mixing also with the surrounding clean air. This results in dilution of the CBL and decrease of the pollution. During the break the CBL recovers and moves up to the breathing zone with slightly lower tracer gas concentration resulting in decreased exposure. This airflow interaction is demonstrated in Fig. 4. The standard deviation of the concentration fluctuations in the three cases is almost the same, suggesting the same level of mixing. The use of the VC as local source control is very efficient and drastically reduces the N_2O concentration (Fig. 3b). The mean, SD and 95th percentile are reduced by almost 40-45% compared to the case without cushion (Fig. 3a). The results reveal that the airflow interaction and its impact on the exposure in the case of inhalation through the nose (i.e. InN/ExM)), inhalation through the mouth (i.e. InM/ExN) and No breathing remained the same as in the case without source control. A slight tendency of the effect of the breathing can be seen in the results shown in Fig. 3b even in case with VC in use.
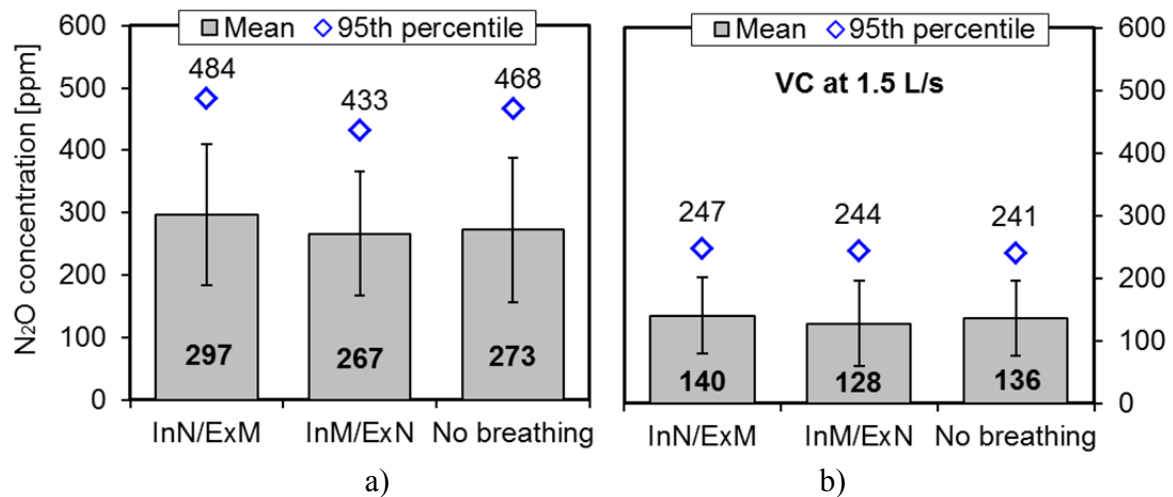
Fig. 3. Impact of breathing mode on the exposure to pollution generated at the groins (a) and effect of breathing combined with the pollution source control i.e.VC performing at 1.5 L/s (b). The SD is shown as error bars.
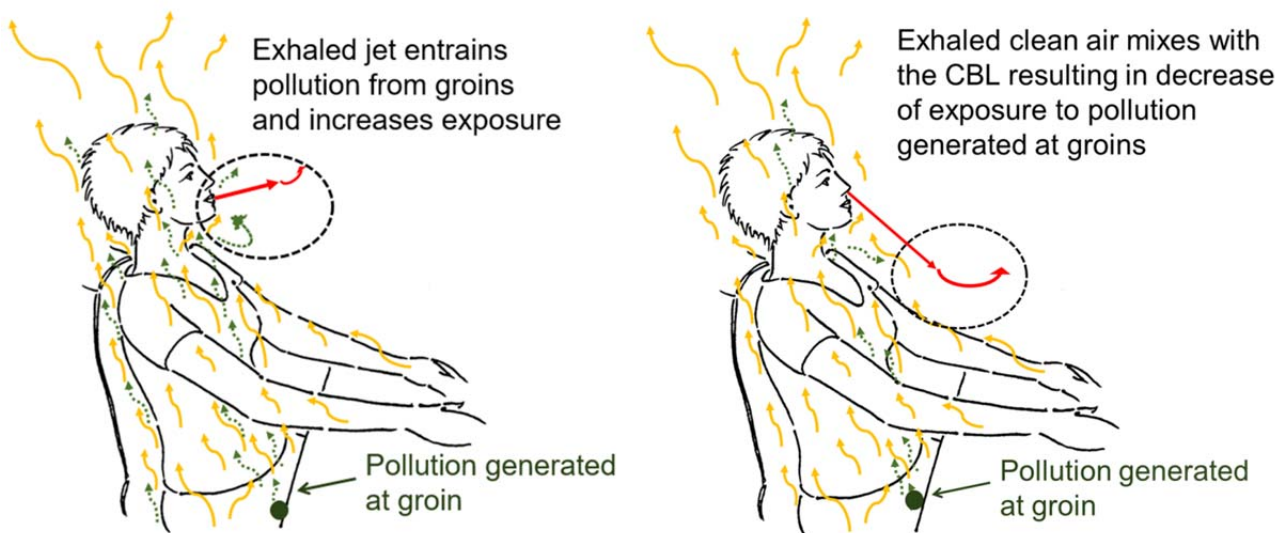
Fig. 4. Possible interaction of flow exhaled from nose or mouth and its impact on transport of pollution generated at the groins to the inhalation zone.

In contrast, when the pollution is generated at the armpits the mean and 95th percentile of CO_2 concentrations measured during the two studied breathing modes are substantially different (Fig. 5a). The mean CO_2 concentration is 46% lower when the manikin is inhaling air through the nose/exhaling from mouth compared to the case when it is inhaling from the mouth/exhaling from the nose. The difference is about 52% for the 95th percentile values. Compared to the "No breathing" case the jet exhaled from the mouth increases slightly the exposure mainly because it entrains the pollution generated at the armpits in direction to the face, where it is mixed with the CBL and is inhaled after the break. The jets exhaled from the nose have two effects: first, they mix and dilute to some extend the pollution carried by the CBL and second, they cause mixing in the

CBL flow and increase of the CO_2 in the inhaled air. Therefore as it can be seen in Figure 5a the mean, SD and 95th percentile of CO_2 concentration are higher when air is inhaled through the mouth compare to the other two cases. The effect of the exhaled jet is important for the performance of the local source control. When the VC works at 1.5 L/s it pools air and some pollution but this does not have effect on the inhaled CO_2 concentration because the entrainment effect of the exhaled jet from the mouth is stronger (Fig.5b); when the exhalation is from the nose the increased mixing overcomes the effect of VC on the removal of the CO_2 and this results in CO_2 increase in the inhaled air (Fig. 4b). When breathing is not present the performance of the VC at 1.5 l/s is not disturbed, some of the CO_2 is removed by the VC, some of it is move above the shoulder and the head and some is entrained by the CBL and moved upward to the face where it is inhaled. Therefore as it can be seen in Fig. 5b the mean, SD and 95th percentile of the CO_2 concentration are higher when air is inhaled through the mouth compare to the other two cases. At flow rate of 1.5 L/s air sucked through the cushion was not sufficiently strong to entrain and remove the pollution released at the armpits. The cushion was not in a good contact with manikin's body at the area of the armpits and thus the relatively strong CBL flow prevailed in transporting the released CO_2. In contrary at the location of the groins the cushion was in better contact with manikin's body and could efficiently evacuated the generated pollution (N_2O). The discussed above flow interaction and its impact on transport of pollution and the exposure is illustrated in Fig. 6.
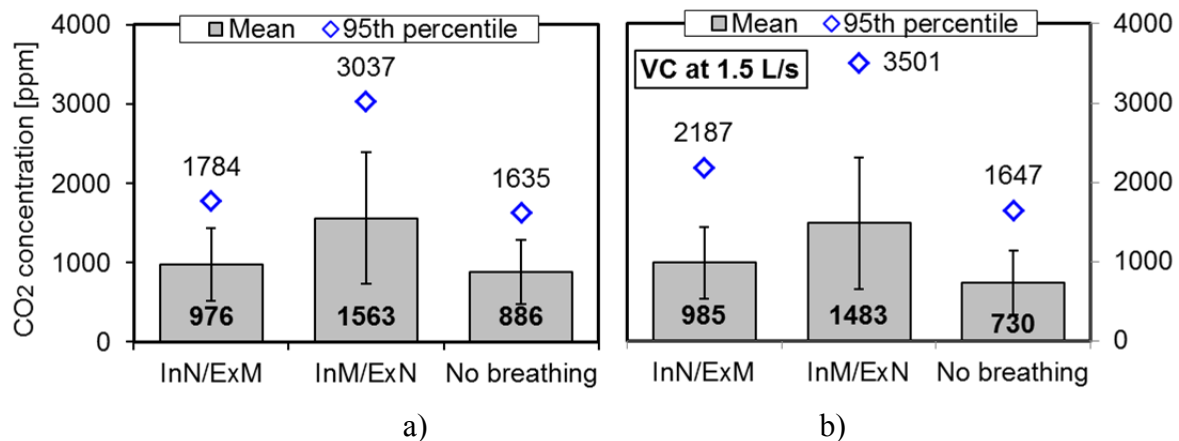
Fig. 5. Impact of breathing mode on the exposure to pollution generated at the armpits (a) and effect of breathing combined with the pollution source control i.e.VC performing at 1.5 L/s (b). The error bars show the SD.
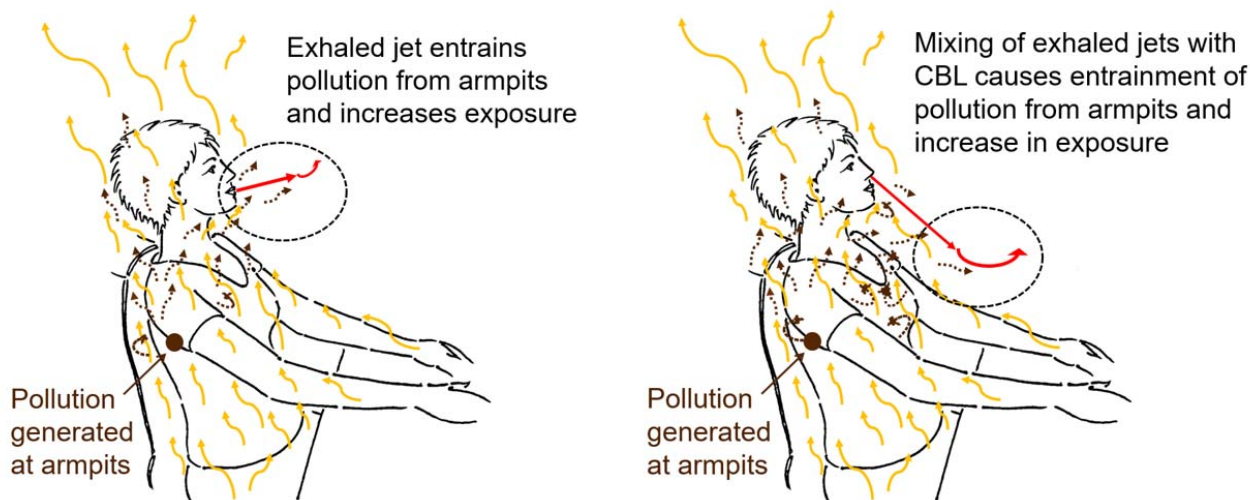
Fig. 6. Possible interaction of flow exhaled from nose or mouth and its impact on transport of pollution generated at the armpits to the inhalation zone.

Impact of source control on exposure

The importance of the source control was studied at 0, 1.5, 3 and 5 L/s exhausted through the VC. The experiments were performed only for the case of inhalation nose/exhalation mouth/pause. It can be seen in Fig. 7 that the normalized mean and 95th percentile values for N_2O and CO_2 decreased substantially when the airflow rate exhausted through the cushion increased. This means that the ventilated cushion was able to capture the emitted pollutants both at the groins and the armpits when the flow rate of the exhaust air was sufficiently high.

a)   b)
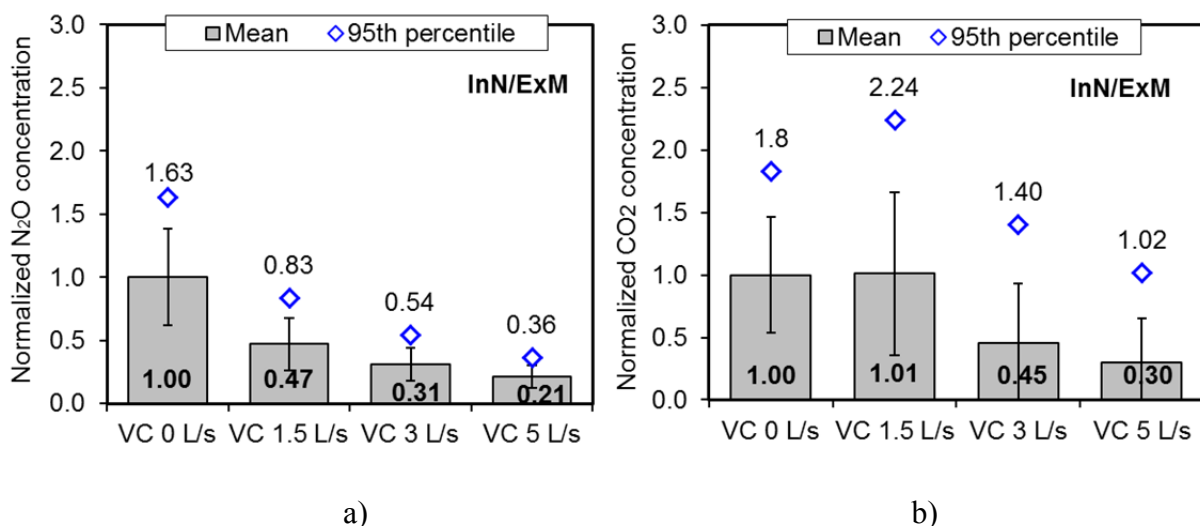
Fig. 7. a) Normalized mean and 95th percentile of N_2O concentration (pollution from the groins) and b) Normalized mean and 95th percentile of excess CO_2 concentration (pollution from the armpits). The error bars show the normalized standard deviation.

Exposure due to interaction of CBL, flow of exhalation and facially applied ventilation flow

The results of the measurements of N_2O concentration under more complex flow interaction including CBL, inhalation nose/exhalation mouth/pause and personalised flow against the face are shown in Fig. 8. Results obtained at several cases are compared. Fig. 9 shows results measured without breathing. The comparison of the results in Figures 8 and 9 shows that in case with and without breathing the use of PV at 0.2 m/s reduces the exposure to N_2O. This is because the supplied clean personalised air is mixed with the polluted air of the CBL and dilution takes place (bars 1 and 2 in Fig. 8 and 9). However as shown with the visualisation in Fig. 10 the personalised flow at 0.2 m/s is not able to penetrate the CBL which pushes it upward. The use of VC at 1.5 and 5 L/s reduces the N_2O in inhaled air because the source control is efficient due to its location near the source (bars 3 and 5 in the figures). The combined use of VC at 1.5 l/s and PV at 0.2 m/s reduces further the inhaled N_2O concentration (bars 4 in the figures) though the reduction is not as high as the sum of the separate effect of the VC and the PV.

The increase of PV flow rate (increase of its target velocity from 0.2 m/s to 0.4 m/s) brings more air to the breathing zone, i.e. more dilution, pills the CBL off and the clean personalised air reaches the nose (bar 7 in Fig. 8 and bar 6 in Fig. 9; see also visualisation in Fig. 10). From the obtained results it is not clear why when VC at 5 L/s is combined with PV at 0.2 m/s the exposure does not improve more compared to the case VC at 5 L/s alone (Fig. 8, bars 5 and 6). A possible reason may be that the improvement by the PV at 0.2 m/s is much smaller than the effect of VC. However this needs to be studied. The results obtained with breathing and without breathing follow one and the same tendency.

Fig. 8. Normalized N_2O concentration with breathing ON. Mean and 95th percentile are normalized by the mean concentration measured during VC 0 L/s, PV 0 m/s.

Fig. 9. Normalized N_2O concentration with breathing OFF. Mean and 95th percentile are normalized by the mean concentration measured during VC 0 L/s, PV 0 m/s.
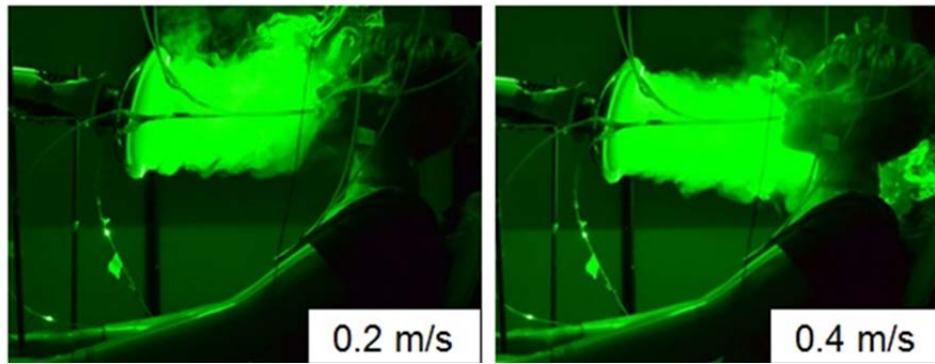
Fig. 10. Personalised flow supplied from front at 0.2 m/s and 0.4 m/s.

The results of the CO_2 concentration measurements under the more complex flow interaction including CBL, breathing and PV are shown in Fig. 11 for two target velocities of the personalized flow, namely 0.2 and 0.4 m/s. The PV applied at 0.2 m/s does not work efficiently in providing clean air for breathing because it is weak to penetrate completely the CBL. The supplied clean personalised air dilutes the polluted CBL and improves the exposure but substantial part of the exhaled air moves upward by the CBL (Fig. 10b). The results in Fig. 11 show that the mean CO_2 concentrations are the same in the cases with PV regardless if there is breathing or not. However, the 95th percentiles and SDs are higher in the cases with breathing and PV compared to the corresponding cases without breathing.
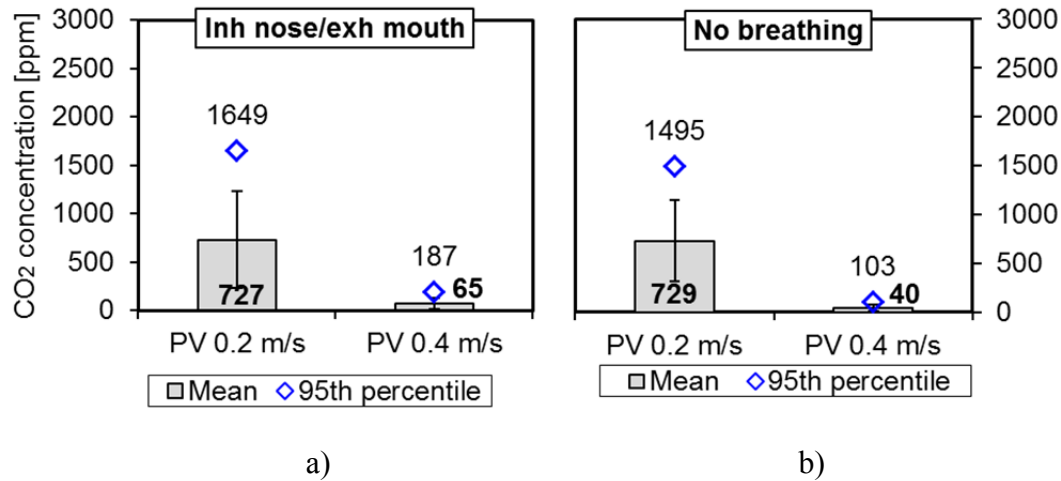
Fig. 11. Mean and 95th percentile of excess CO_2 concentration (i.e. pollution from the armpits). a) Results obtained during inhalation nose/exhalation, b) Results obtained during "no breathing". The error bars show the standard deviation.

The normalised concentration of CO_2 (generated at the armpits) in the inhaled air under different conditions is compared in Figures 12 and 13 respectively obtained with and without breathing. The CBL flow entrains CO_2 generated at the armpits and transports it upward to the breathing zone. Thus part of the CO_2 released at the armpits is mixed with the CBL and inhaled. The use of the VC at 1.5 L/s does not work efficiently, i.e. only little of the CO_2 released at the armpits is removed without any impact on the entrainment effect of the CBL and thus the exposure. As in the case without VC the CBL moves part of the CO_2 upward to the face where it is inhaled. Therefore no difference in the concentration of CO_2 in the inhaled air exists without and with VC in operation (Fig. 12 – bars 1 and 3). When the breathing is not present the inhaled CO_2 concentration decreases because the entrainment effect of the exhaled jet is not present and more CO_2 is transported above the shoulders and the head by the CBL and less to the face (bar 1 in Fig. 12 and bar 1 in Fig. 13; bar 3 in Fig. 12 and bar 3 in Fig. 13). The minimal effect of the VC at 1.5 L/s is observed also when it is combined with the PV at 0.2 m/s. In this case as discussed before the reduction of exposure is mainly due to the dominant effect of the dilution on the CBL by the clean personalised air (Fig. 12 bar 4 and Fig. 13 bar 4). The exposure is reduced due the efficient local removal of CO_2 when the flow rate through the VC is increased (bars 3 and 5 in Figures 12 and 13). The results in figures show that increase of the PV velocity to 0.4 m/s makes it possible to remove the CBL at the face and provide clean air to breathing (Fig. 12 bar 7 and Fig. 13 bar 6). In the case of combined use of the VC at 5 L/s and the PV at 0.2 m/s the interaction of the PV flow with the CBL generates mixing resulting of increase of CO_2 in the inhaled air (entrainment of CO_2 by the exhaled jet may also help exposure to CO_2). This can be seen in Fig. 12 bars 5 and 6. The results in Figures 12 and 13 show that in case of breathing the concentration of CO_2 in the inhaled air is higher compare to without breathing because the exhaled jet entrains CO_2, more CO_2 is mixed with the CBL and is transported to the nose (Fig. 12 bar 3 and Fig. 13 bar 3). Without breathing more of the generated CO_2 is moved upward above the shoulder and the head by the CBL on the side of the body. The importance of the entrainment of CO_2 by the exhaled jet and thus on the increase of exposure is present when the VC

works even at 5 L/s (Fig. 12 bar 6). This is because the VC removes the CO_2 from the back side of the armpits while the exhaled jet entrains the CO_2 present at the front of the armpits.
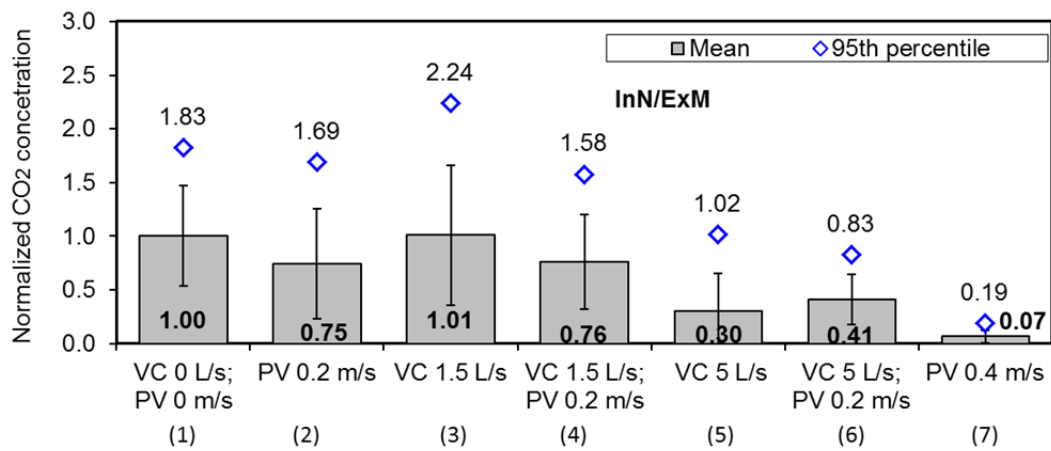
Fig. 12. Normalized CO_2 concentration with breathing ON. Mean and 95th percentile are normalized by the mean concentration measured during VC 0 L/s, PV 0 m/s.
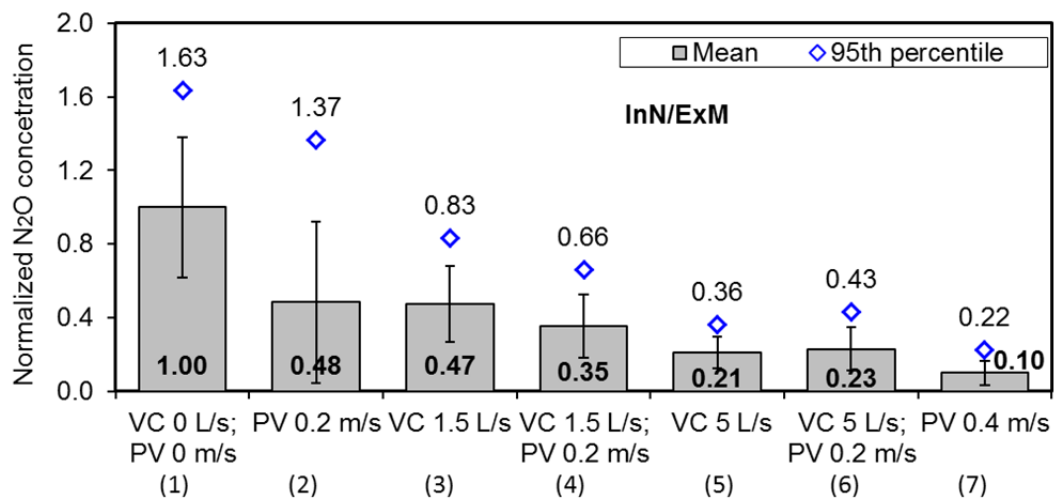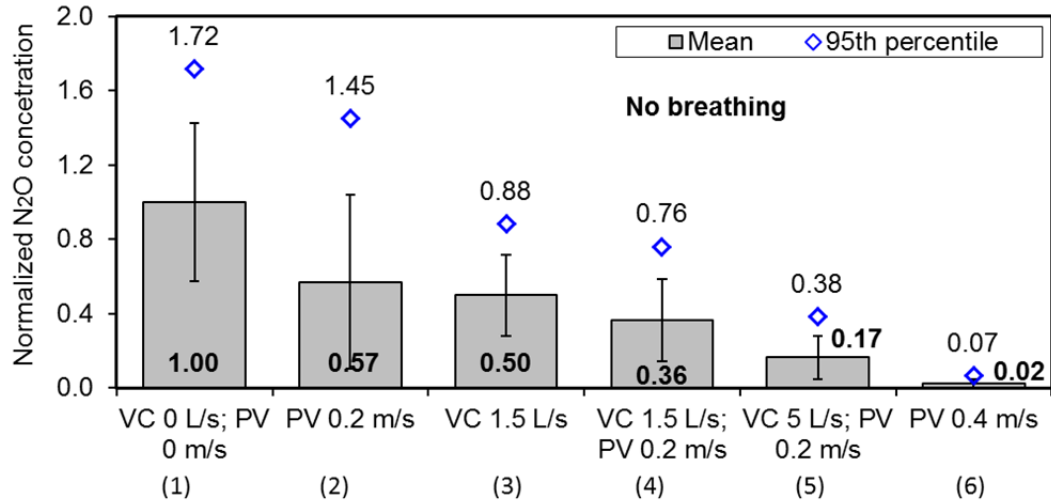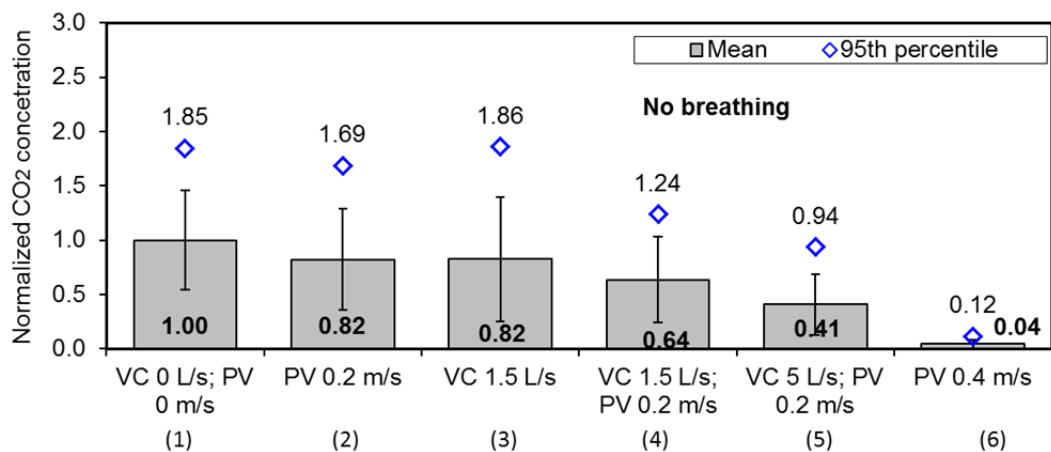

Fig. 13. Normalized CO_2 concentration with breathing OFF. Mean and 95th percentile are normalized by the mean concentration measured during VC 0 L/s, PV 0 m/s.

4. Discussion

This study focuses on exposure of a sitting person to own body released pollution. The obtained results reveal that flow of exhalation increases the exposure to gaseous pollution released from body sites close to the breathing zone, such as the armpits. The exposure was higher for the breathing mode inhalation mouth/exhalation nose/pause compared to inhalation nose/exhalation mouth/pause. As discussed in the results section the reason may be the interaction of the exhaled jets with the CBL. The interaction of the jet exhaled from the nose with the CBL generates mixing near the armpits, i.e. near the pollution source and help its transportation to the inhalation zone. This is an important observation since assessment of exposure to own body released bio-effluents without breathing simulation may lead to incorrect exposure assessment depending on the location of the

128

pollution source. We found that breathing was not important for the exposure to pollution generated far from the zone influenced by the exhaled flows, e.g. groins. This result is in agreement with previous studies reporting that the breathing mode has no significant effect on the personal exposure to room polluted air [25, 50]. Melikov and Kaczmarczyk [25] also showed that the temperature, the relative humidity and the concentration of the polluted room air measured in the air inhaled by a breathing thermal manikin were almost the same as those measured close to the upper lip of a non-breathing thermal manikin. Rim and Novoselac [17] also reported that breathing increases the exposure. They found that in case of stratified flow after activation of the breathing the concentrations of fine and course particles released at floor level, i.e. far from the breathing zone of a seated breathing thermal manikin, increase at the mouth. When tracer gas was released with activated breathing (exhalation nose/inhalation nose/pause) its concentration at the mouth showed tendency to be higher than at the feet located close to the source. In our study the concentration of tracer gas released at the groins was measured higher at the chest compared to the face which may be expected. The reason for the discrepancies needs to be studied.

The CBL can produce a vertical air velocity up to 0.25 m/s [15] which is comparable or higher than the maximum indoor velocity recommended in standards. Thus in rooms with little mixing (e.g. displacement ventilation) but also in rooms with mixing ventilation (e.g. diffuse ceiling) the CBL will be stronger than the ventilation flow and will increase the exposure to own body bio-effluents. Removal of pollution at the location where it is generated is the first step to be applied for reduction of exposure. With this respect pollution source control by the ventilated cushion we used was efficient. However our results show that its design needs improvement in order to be able to evacuate efficiently pollution generated at the armpits. The body posture and movement will play important role in case of seated occupants.

The results of this study concur with previous findings that the interaction of the clean personalized flow directed against the face with the CBL is of major importance for reduction of exposure to body released pollution. The highest exposure reduction to the armpit- and groin- generated pollutants was achieved when applying to the face of the manikin the PV flow with mean target velocity of 0.4 m/s. Yet, it should be taken into account that in reality the users of the PV will have control over the supplied flow rate and might prefer lower airflow rate to avoid draft discomfort. This will increase the exposure to body bio-effluents.

Different methods for control of airflow interaction at the face by weakening of the CBL and thus making possible its penetration by personalized flow at low velocity have been reported. A radiant cooling panel has been used as a front desk partition to decrease the clothing surface temperature at the chest and thus to weakened the CBL [51], a retractable board pressing against the stomach of a sitting occupant to "obstruct" the CBL at the lower chest has been shown to be efficient [52], supply of clean air beneath the CBL from nozzles installed at seat head rest [53, 54] have been able to provide clean air for breathing. Even though such methods can be applied to increase the efficiency of the PV at lower flow rates, it should be noted that local source control still remains a better solution since the contaminants will be removed before they are spread in the room. However it has to be applied after careful consideration of the airflow interaction at the vicinity of the body and at

the breathing zone. Our results show that the combined use of the ventilated cushion and the personalised ventilation may increase the exposure under some conditions. The source control may be designed to remove pollution and at the same time part of the CBL air and thus to reduce its strength and make possible its penetration at the breathing zone by low velocity flow of clean air.

Important finding of this study is that the 95th percentile of the concentration fluctuations was measured much higher than the mean concentration. The question which of these two parameters is more important for exposure assessment remains to be answered.

In this study for the first time the exposure to body released bio-effluents as a result of complex interaction of flows and local source control is investigated by proper tracer gas concentration measurements only during the inhalation period. The results were obtained at limited number of experimental conditions. Different body size and posture, head positioning, clothing design, breathing mode, cycle, respiration rate and other individual difference between people, as well as table positioning, chair design, room air and radiant temperature, direction and characteristics of the ventilation flow at the vicinity of the body, etc. will affect the airflow interaction at the breathing zone and thus the exposure. Therefore further studies are recommended.

5. Conclusions

Exposure to body bio-effluents depends on the complex airflow interaction of the CBL, flow of exhalation (breathing mode) and locally applied ventilation flow on the breathing zone.

The interaction of the exhaled flow with the CBL increases the exposure to own body released pollution especially when the site is close to the breathing zone.

Breathing does not influence exposure to gaseous pollutants emitted from the lower part of the body.

The use of mean tracer gas concentration in inhaled air is quite different than its 95th percentile. These two parameters will lead to different exposure assessment.

Well-designed source control can substantially reduce the exposure to body released pollution regardless of the flow interaction at the breathing zone.

The combined use of source control and personalised ventilation may not reduce but even may increase the exposure to body bio-effluents. Careful design of the combined systems is recommended when such systems are to be implemented in practice.

References

1. Douwes J, Thorne P, Pearce N, Heederik D. Bioaerosol health effects and exposure assessment: Progress and prospects. Annals of Occupational Hygiene. 2003 Apr;47(3):187-200.
2. Nielsen PV. Control of airborne infectious diseases in ventilated spaces. Journal of the Royal Society Interface. 2009 Dec;6:S747-S55.
3. Spendlove JC, Fannin KF. Source, significance, and control of indoor microbial aerosols: human health aspects. Public Health Reports. 1983;98:229-44.
4. Dormont L, Bessiere JM, Cohuet A. Human Skin Volatiles: A Review. Journal of Chemical Ecology. 2013 May;39(5):569-78.
5. Peterson RA, Gueniche A, de Beaumais SA, Breton L, Dalko-Csiba M, Packer NH. Sweating the small stuff: Glycoproteins in human sweat and their unexplored potential for microbial adhesion. Glycobiology. 2016 Mar;26(3):218-29.
6. Suarez FL, Springfield J, Levitt MD. Identification of gases responsible for the odour of human flatus and evaluation of a device purported to reduce this odour. Gut. 1998 Jul;43(1):100-4.
7. Wisthaler A, Weschler CJ. Reactions of ozone with human skin lipids: Sources of carbonyls, dicarbonyls, and hydroxycarbonyls in indoor air. Proceedings of the National Academy of Sciences of the United States of America. 2010 Apr;107(15):6568-75.
8. Coleman BK, Destaillats H, Hodgson AT, Nazaroff WW. Ozone consumption and volatile byproduct formation from surface reactions with aircraft cabin materials and clothing fabrics. Atmospheric Environment. 2008 Feb;42(4):642-54.
9. Pandrangi LS, Morrison GC. Ozone interactions with human hair: Ozone uptake rates and product formation. Atmospheric Environment. 2008 Jun;42(20):5079-89.
10. Rai AC, Guo B, Lin CH, Zhang JS, Pei JJ, Chen QY. Ozone reaction with clothing and its initiated particle generation in an environmental chamber. Atmospheric Environment. 2013 Oct;77:885-92.
11. Tsushima S, Bekö G, Bossi R, Tanabe S, Wargocki P. Measurements of Dermal and Oral Emissions from Humans. 14th international conference of Indoor Air Quality and Climate; 2016; Ghent, Belgium; 2016.
12. Zhang X, Wargocki P, Lian Z, Thyregod C. Effects of exposure to carbon dioxide and bioeffluents on perceived air quality, self-assessed acute health symptoms, and cognitive performance. Indoor Air. 2017 Jan;27(1):47-64.
13. Melikov AK. Human body micro-environment: The benefits of controlling airflow interaction. Building and Environment. 2015 Sep;91:70-7.
14. Homma H, Yakiyama M. Examination of free convection around occupant's body caused by its metabolic heat. ASHRAE Transactions; 1988; Dallas, USA; 1988. p. 104-24.
15. Licina D, Melikov A, Sekhar C, Tham KW. Air temperature investigation in microenvironment around a human body. Building and Environment. 2015 Oct;92:39-47.
16. Zukowska D, Melikov A, Popiolek Z. Impact of personal factors and furniture arrangement on the thermal plume above a sitting occupant. Building and Environment. 2012 Mar;49:104-16.
17. Rim D, Novoselac A. Transport of particulate and gaseous pollutants in the vicinity of a human body. Building and Environment. 2009 Sep;44(9):1840-9.
18. Rim D, Novoselac A, Morrison G. The influence of chemical interactions at the human surface on breathing zone levels of reactants and products. Indoor Air. 2009 Aug;19(4):324-34.
19. Gao NP, Niu JL. CFD study of the thermal environment around a human body: A review. Indoor and Built Environment. 2005 Feb;14(1):5-16.
20. Licina D, Melikov A, Sekhar C, Tham KW. Transport of gaseous pollutants by convective boundary layer around a human body. Science and Technology for the Built Environment. 2015 Nov;21(8):1175-86.

21.   Haselton FR, Sperandio PGN. Convective exchange between the nose and the atmosphere. Journal of Applied Physiology. 1988 Jun;64(6):2575-81.

22.   Gupta JK, Lin CH, Chen QY. Characterizing exhaled airflow from breathing and talking. Indoor Air. 2010 Feb;20(1):31-9.

23.   Tang JLW, Nicolle AD, Klettner CA, Pantelic J, Wang LD, Bin Suhaimi A, et al. Airflow Dynamics of Human Jets: Sneezing and Breathing - Potential Sources of Infectious Aerosols. Plos One. 2013 Apr;8(4).

24.   Xu C, Nielsen PV, Gong G, Liu L, Jensen RL. Measuring the exhaled breath of a manikin and human subjects. Indoor Air. 2015 Apr;25(2):188-97.

25.   Melikov A, Kaczmarczyk J. Measurement and prediction of indoor air quality using a breathing thermal manikin. Indoor Air. 2007 Feb;17(1):50-9.

26.   Villafruela JM, Olmedo I, Jose JFS. Influence of human breathing modes on airborne cross infection risk. Building and Environment. 2016 Sep;106:340-51.

27.   Hyldgaard CE. Humans as a source of heat and air pollution. 4th International Conference on air distribution in rooms, Roomvent 1994; 1994; Cracow, Poland; 1994. p. 413-33.

28.   Hoppe P. Temperatures of expired air under varying climatic conditons. International Journal of Biometeorology. 1981;25(2):127-32.

29.   Ozcan O, Meyer KE, Melikov AK. A visual description of the convective flow field around the head of a human. Journal of Visualization. 2005;8(1):23-31.

30.   Zhu SW, Kato S, Murakami S, Hayashi T. Study on inhalation region by means of CFD analysis and experiment. Building and Environment. 2005 Oct;40(10):1329-36.

31.   Johnson AE, Fletcher B, Sanders CJ. Air movement around a worker in a low-speed flow field. Annals of Occupational Hygiene. 1996;40:57-64.

32.   Bjorn E, Nielsen PV. Dispersal of exhaled air and personal exposure in displacement ventilated rooms. Indoor Air. 2002 Sep;12(3):147-64.

33.   Zhang TF, Yin S, Wang SG. Quantify impacted scope of human expired air under different head postures and varying exhalation rates. Building and Environment. 2011 Oct;46(10):1928-36.

34.   Marr D, Khan T, Glauser M, Higuchi H, Jianshun ZD. On Particle Image Velocimetry (PIV) Measurements in the Breathing Zone of a Thermal Breathing Manikin. ASHRAE Transactions; 2005; Denver, USA; 2005. p. 299-305.

35.   Feng LY, Yao SY, Sun HJ, Jiang N, Liu JJ. TR-PIV measurement of exhaled flow using a breathing thermal manikin. Building and Environment. 2015 Dec;94:683-93.

36.   Ge QJ, Li XD, Inthavong K, Tu JY. Numerical study of the effects of human body heat on particle transport and inhalation in indoor environment. Building and Environment. 2013 Jan;59:1-9.

37.   Licina D, Melikov A, Sekhar C, Tham KW. Human convective boundary layer and its interaction with room ventilation flow. Indoor Air. 2015 Feb;25(1):21-35.

38.   Laverge J, Spilak M, Novoselac A. Experimental assessment of the inhalation zone of standing, sitting and sleeping persons. Building and Environment. 2014 Dec;82:258-66.

39.   Melikov AK, Cermak R, Kovar O, Forejt L. Impact of airflow interaction on inhaled air quality and transport of contaminants in rooms with personalized and total volume ventilation. 7th International Conference on Healthy Buildings 2003; 2003; Singapore; 2003. p. 592-7.

40.   Cermak R, Melikov AK, Forejt L, Kovar O. Performance of personalized ventilation in conjunction with mixing and displacement ventilation. Hvac&R Research. 2006 Apr;12(2):295-311.

41.   Melikov AK. Personalized ventilation. Indoor Air. 2004 Aug;14:157-67.

42.   Niu JL, Gao NP, Ma PB, Zuo HG. Experimental study on a chair-based personalized ventilation system. Building and Environment. 2007 Feb;42(2):913-25.

43.   Bivolarova MP, Rezgals L, Melikov AK, Bolashikov ZD. Exposure Reduction to Human Bio-effluents Using Seat-integrated Localized Ventilation in Quiescent Indoor Environment. Proceedings of the 12th Rehva World Congress; 2016; Aalborg Denmark; 2016.

44.   Bivolarova MP, Rezgals L, Melikov AK, Bolashikov ZD. Seat-integrated localized ventilation for exposure reduction to air pollutants in indoor environments. Proceedings of 9th International Conference on Indoor Air Quality Ventilation & Energy Conservation In Buildings. Seoul, Korea; 2016.

45.   PT Teknik. Thermal Manikins for Scientific and Industrial Use.   [cited; Available from: http://pt-teknik.dk/

46.   Bolashikov ZD, Nikolaev L, Melikov AK, Kaczmarczyk J, Fanger PO. Personalized ventilation: air terminal devices with high efficiency. 7th International Conference on Healthy Buildings 2003; 2003; Singapore; 2003.

47.   Kierat W, Popiolek Z. Methods of the gas concentration sinusoidal and step changes generation for dynamic properties of gas concentration meters testing. Measurement. 2016 Jun;88:131-6.

48.   Kierat W, Popiolek Z. Dynamic properties of fast gas concentration meter with nondispersive infrared detector. Measurement. 2017 Jan;95:149-55.

49.   LumaSense technologies.   [cited; Available from: http://innova.lumasenseinc.com

50.   Brohus H, Nielsen PV. Personal exposure in displacement ventilated rooms. Indoor Air-International Journal of Indoor Air Quality and Climate. 1996 Sep;6(3):157-67.

51.   Melikov AK, Dzhartov V. Control of the free convection flow around human body by radiant cooling. 9th International Healthy Building Conference and Exhibition 2009; 2009; Syracuse, USA; 2009.

52.   Bolashikov ZD, Melikov AK, Kranek M. Improved Performance of Personalized Ventilation by Control of the Convection Flow around an Occupant's Body. ASHRAE Transactions. 2009;115, part 2.

53.   Bolashikov ZD, Melikov AK, Krenek M. Control of the Free Convective Flow around the Human Body for Enhanced Inhaled Air Quality: Application to a Seat-Incorporated Personalized Ventilation Unit. Hvac&R Research. 2010 Mar;16(2):161-88.

54.   Melikov A, Ivanova T, Stefanova G. Seat headrest-incorporated personalized ventilation: Thermal comfort and inhaled air quality. Building and Environment. 2012 Jan;47:100-8.

PAPER II

A comparison between tracer gas and aerosol particles distribution indoors: the impact of ventilation rate, interaction of airflows, and presence of objects

Abstract

The study investigated the separate and combined effects of ventilation rate, free convection flow produced by a thermal manikin, and the presence of objects on the distribution of tracer gas and particles in indoor air. The concentration of aerosol particles and tracer gas was measured in a test room with mixing ventilation. Three layouts were arranged: an empty room, an office room with an occupant sitting in front of a table, and a single-bed hospital room. The room occupant was simulated by a thermal manikin. Monodisperse particles of three sizes (0.07, 0.7, and 3.5 μm) and nitrous oxide tracer gas were generated simultaneously at the same location in the room. The particles and gas concentrations were measured in the bulk room air, in the breathing zone of the manikin, and in the exhaust air. Within the breathing zone of the sitting occupant, the tracer gas emerged as reliable predictor for the exposure to all different-sized test particles. A change in the ventilation rate did not affect the difference in concentration distribution between tracer gas and larger particle sizes. Increasing the room surface area did not influence the similarity in the dispersion of the aerosol particles and the tracer gas.

Key words: Tracer gas; Particles; Room air distribution; Transport behaviour; Exposure; Thermal Manikin;

Practical Implications

The results of this study will contribute to a better understanding of the relationship between the transport behaviour of gas and particles. Such knowledge is important for the realistic prediction of aerosol particles distribution in ventilated rooms when using tracer gas techniques. The data can be used to validate CFD models for the evaluation of the distribution of pollutant concentrations and airflow patterns in rooms with overhead mixing ventilation.

Introduction

In indoor spaces people are constantly exposed to different pollutants present in the air. Airborne particles (also known as aerosol particles) are a major exposure concern due to their effects on human health. They can penetrate into the respiratory system and cause inflammatory effects.[1,2] Particles with biological origins, such as bacteria and fungi, can activate allergic alveolitis and allergic asthma symptoms among occupants. [3] Additionally, particles expelled (i.e. droplets) by people can carry pathogens and cause the transmission of infectious diseases to other occupants.[4-5] Therefore, it is vital to have a good understanding of the spread of indoor aerosol particles, especially when they are released in occupied spaces. The most important reason that indoor environments are ventilated is to provide occupants with clean air for breathing. Many studies have shown that the effect of airflow distribution on personal exposure to indoor air pollutants varies with regards to the air distribution method used.[5, 7-13] Full-scale experiments and computational fluid dynamics (CFD) predictions are among the most popular methods used today to help understand the air pollution distribution in ventilated rooms.[14,15]

CFD modelling has become a powerful tool for studying indoor particle dispersion and spatial distribution [13,16] Although CFD provides highly time- and space-resolved simulations, there are uncertainties and errors associated with the CFD boundary conditions and numerical schemes.[17,18] Therefore, it is essential that the numerical simulations are validated with data obtained from experimental measurements. Full-scale experiments are valuable because they include actual thermo-fluid conditions, which allow studies to be performed at close to real conditions. A number of experimental studies relied only on tracer gas measurements to simulate the behaviour of both gaseous and particle indoor-emitted pollutants. For instance, tracer gases such as N_2O and CO_2 have been used to mimic the movement of infectious aerosol droplets emitted by air exhaled from a

breathing thermal manikin in simulated hospital wards.[7,8,19] However, particles are larger and heavier than gas molecules, and thus behave differently.

There are several differences between the behaviour of tracer gas and aerosol particles. The key difference is observed when they approach a surface; the tracer gas molecule reflects from the surface, whereas the aerosol particle attaches to the surface via an adhesive force. Moreover, the probability of particle deposition on a surface depends strongly on particle size. Ultrafine particles, up to diameters of a couple hundred nanometers, exhibit Brownian motion and deposit on all surfaces by diffusion; the smaller the particle the more intense the diffusional deposition is observed. Particles larger than several hundred nanometers in diameter exhibit non-negligible mass and inertia. They can be deposited either by gravitational settling at longer residence times on upward-facing surfaces or by inertial impaction at higher Stokes numbers on surfaces facing their original direction of motion. The larger the particles, the higher are the observed deposition rates. Particles in the middle size range, say between 200 nm to 1μm, are only weakly influenced by the above-mentioned mechanisms and their deposition rates minimal.

Tang et al.[15] reported in their review article that airborne particles (particularly exhaled droplet nuclei) smaller than 5 - 10 μm can be simulated with tracer gas, since they often stay suspended in the air for long time. The study suggested that the particles will follow the air stream. However, only a few studies have conducted direct comparisons of tracer gas and particle behaviour in ventilated rooms. Zhang et al.[16] made a direct comparison of the distribution of SF_6 tracer gas and 0.7 μm particles in an air-conditioned full-scale airliner cabin mock-up. They found that the distribution of the two simulated pollutants within the cabin was similar. However, they also concluded that the dispersion characteristics of micron-sized particles can still be different from that of a gas despite their general similarity. A study by Noakes et al.[20], simulating a hospital isolation

room with mixing air distribution (10 air changes per hour (ACH)), showed good agreement between the behaviour of N_2O tracer gas and $3 - 5$ μm particles, both of which were released from a heated cylinder (resembling a patient in bed). Another related study by Beato-Arribas et al.[21] concluded that CO_2 tracer gas and aerosolised *Bacilus Subtilus* bacteria are comparable in their distribution in a single isolation hospital mock-up ventilated at 12 ACH. However, measurements of the pollutant concentrations at the breathing zone of a simulated person with realistic body geometry and skin temperature distribution were not performed in these studies. The complex human body shape and the buoyancy flows generated from the body are important for transport of pollution at the vicinity of the body, exposure, and air distribution in spaces.[22,23]

It is well-documented that the free convection flow (FCF) around the human body adds to the complexity of a room's airflows interactions and occupants' exposure to pollutants.[12,24-26] Licina et al.[24,25] studied the importance of FCF around a sitting person and its impact on the transport of gaseous and particle pollutants towards the breathing zone. However, the exposure to particles and tracer gas was studied in different set-ups and thus cannot be directly compared. Rim and Novoselac[12] investigated the concentration distribution of particulate and gaseous pollutants in the vicinity of a human body at the same time. They considered the effects of the source position and the overall airflow patterns on the inhalation exposure to the airborne pollutants. These studies provide valuable information on the relationship between air distribution patterns in rooms and the transport of gaseous and particle pollutants. However, they did not provide information on how separate parameters, such as air change rate and increase of surface area by objects in rooms (furniture, etc.), may affect the deposition of particles and, therefore, the relationship between the distribution of gas and aerosol particles in the room. Such information is especially important when studies aim to evaluate the personal exposure to airborne particles in ventilated spaces using only tracer gas.

Conducting experiments with particles is generally much more challenging than experiments with tracer gases. Due to the particles' complex nature and highly variable sizes, it is not easy to find and select available measuring techniques. [27] The advantages of using only tracer gas in exposure measurements are the easy and inexpensive setup, possibility of sampling at many locations, and the relatively simple processing of the measured data. On the other hand, the gas cannot be used as a complex substitute for particles of all sizes due to the different physical forces acting on them. Moreover, particles have various morphologies and shapes, making the simplification of utilizing tracer gas as surrogate even more difficult.

The main objective of this study was to verify the use of tracer gas as a relatively accurate means of identifying exposure to different well-defined indoor aerosol particle sizes. It was examined the relationship between gas and particles dispersion in a room with overhead mixing air distribution. An important aim of this study was to identify the influence of factors, such as air change rate, the surface area inside the room, and the FCF around a sitting person (heated thermal manikin), on the distribution of monodispersed aerosol particles and tracer gas. This paper also investigated the effects of the interaction between the FCF generated by a lying person in bed and local exhaust airflow on the dispersion of particles and tracer gas released close to a body.

Methods

Experimental set-up and design

The experiments were performed in a test room of 2.6 m (height) x 4.7 m (length) x 1.66 m (width). The walls of the room were made of particleboard and were insulated with 0.06 m thick styrofoam plates. One of the walls was made from thick single-layer glazing. The room was carefully sealed prior to the experiments in order to avoid undefined infiltration. The room was air conditioned via mixing total volume air distribution. Outdoor air was supplied to the room through a two-way square ceiling diffuser with solid faceplate (the directions in which the two air jets were discharged

by the supply diffuser are shown in Figure 1). The air supply diffuser was mounted in the centre of the ceiling. Just before entering the test room the supplied outdoor air was filtered by a high-efficiency particulate (HEPA) filter, class H14, to assure particle-free air. The air was exhausted through a ceiling mounted circular diffuser (Ø 200 mm). The ventilation rate during the experiments was either 3.5 ACH or 7 ACH. Air supply diffusers with different sizes were used to achieve similar air jet pattern at 3.5 ACH and 7 ACH. The effective surface area of the diffusers was 0.0065 m^2 at 3.5 ACH and 0.015 m^2 at 7 ACH. Detailed descriptions of the supply and exhaust diffusers are presented in Supporting Information section (Figures S1, S2; Tables S1, S2). The supply and exhaust airflow rates were kept constant using an electronic fan speed control and calibrated Iris orifice damper (Ø250). The room was under positive pressure during each experiment. Accuracy of the iris orifice damper was ±5% of the actual pressure difference across the orifice damper.

The air temperature inside the room was controlled and kept at 23.2°C ± 0.2°C during all experiments. The temperature around the room was kept at 23.2°C ± 0.2ºC as well. The relative humidity inside the room was recorded with a HOBO data logger (Model ONSET U12-013) and was in the range of 30% - 38% ±2% throughout all experiments.

In this study five experimental scenarios were investigated in order to evaluate the effect of different parameters on the distribution of tracer gas and particles:

Empty room (Scenarios 1 and 2): scenarios 1 and 2 were performed in an empty room ventilated at 3.5 ACH and 7 ACH, respectively. The purpose was to determine the effect of different ventilation rates on the particle and gas concentration distributions. No heat sources were presented during these experiments, i.e. isothermal conditions.

Furnished room with unheated manikin (Scenario 3): in this scenario a real-size unheated dressed thermal manikin was seated (on a computer chair) behind a table in the room. The distance between the abdomen of the manikin and the table was 0.1 m. The ventilation rate in the room was 7 ACH. The purpose of this scenario was to quantify the particles and gas distribution in the presence of obstructions, such as furniture and a manikin. Obstructions increase the surface area that the air carrying the particles and gas was in contact with. There were no heat sources in the room, so isothermal conditions were studied.

Furnished room with heated manikin (Scenario 4): in this scenario the thermal manikin was switched on to represent realistic thermal conditions in an occupied indoor environment. The manikin was the only heat source in the room. The ventilation rate in the room was 7 ACH. The supply air temperature was set to 21.6 °C±0.2 °C to keep the room 23 °C.

In scenarios 3 and 4 the manikin was dressed with a tight long-sleeve shirt, trousers, underwear, socks, and shoes (the total clothing insulation was 0.48 clo). The thermal manikin had a realistic female body size and shape and consisted of 23 body segments. In scenario 4, each segment was individually controlled to maintain surface temperature equal to the skin temperature of an average person in a state of thermal comfort. The average total heat released from the manikin was 74.9 W ±0.24 W (in scenario 4), which simulated the dry heat loss from a human body in a thermally comfortable state. The heat output from the manikin was measured using the MANIKIN software which controls the transfer of necessary power to each body part of the manikin.[28] The height of the manikin in a sitting position was 1.3 m. The layout of the room with the manikin is shown in Figure 1.

Single-bed hospital room (Scenario 5): In this scenario a patient hospital room was simulated. The test room was furnished with a bed with the thermal manikin lying on top (Figure 2). The mattress

of the bed was covered with a cotton sheet. A localized exhaust system, ventilated mattress (VM), was placed on top of the regular mattress. The VM had an exhaust opening that was positioned below the gluteal region of the manikin. A full description of the VM can be found in Bivolarova et al.[29] The manikin was dressed in short-sleeve hospital pyjamas (thermal insulation of 0.60 Clo). The head of the manikin was supported by a pillow. The measured average total heat released from the manikin was 73.2 W ±0.13 W. The ACH in the room was 3.5 and the supply air temperature was 21.7 °C. The exhaust airflow rate of the ventilated mattress was adjusted to be 1.5 L/s. The exhausted air of the VM was taken out of the room through a separate exhaust system.

Tracer gas and particle generation and measurement

During the experiments for scenarios 1-4, particles of one of the three well-defined sizes (0.07, 0.7, and 3.5 μm) and nitrous oxide (N_2O) tracer gas were generated simultaneously at a constant rate from one location in the room, Figure 1. The three particle sizes were selected to represent particles from the ultrafine, fine, and coarse size ranges, each of which were influenced by different deposition mechanisms. Previous studies[30,31] have shown that fine and coarse particles deposited on the surface of a mattress can be re-suspended by a person's movement in bed. In scenario 5 fine particles with 0.7 μm size were released to compare their behavior with that of the tracer gas and at the same time to study the efficiency of the local exhaust ventilation when capturing particles. The pollution source for scenarios 1-4 was located 0.8 m behind the manikin with a height of 1 m (Figure 1). The pollution source for scenario 5 was located close to the gluteal region of the manikin (Figure 2b). The flows of the tracer gas and the particles were mixed in a T-piece connected to a plastic ball (Ø 0.38 m) with a number of small openings equally distributed across its surface. This provided low initial velocity of the tracer gas and particles released into the room.

An AGK 2000 (Palas) aerosol generator connected to an electrostatic classifier (LACP made) was used to generate monodisperse ultrafine particles consisting of dry ammonium sulphate with mobility diameters (dp) of 0.07 μm. A MAG 3000 (Palas) aerosol generator was used to produce fine particles with aerodynamic diameters (da) of 0.7 μm and coarse particles with da=3.5 μm. The fine and coarse particles consisted of a crystalline NaCl core covered with condensed DEHS (bis-2(ethylhexyl)sebacate). The operating conditions of both aerosol generators were set to generate required sizes of aerosol particles according to aerosol spectrometers (with their measurement uncertainty <3% in particle diameter). Both aerosol generators have in their specifications the geometric standard deviation, σ_g, and these definitions agree well with measured size distributions from these generators. In the case of AGK 2000, during the experiments when producing the ultrafine particles with 0.07 μm size in diameter, σ_g was 1.5. In the case of MAG 3000, when we were producing 0.7 μm and 3.5 μm particles, σ_g was below 1.2. To suppress Brownian coagulation, experiments with ultrafine, fine, and coarse particles were conducted separately, the size distribution was kept as close as possible to the monodisperse fraction, and the tracer gas was always released with the particles. The N_2O tracer gas was released from a compressed gas cylinder equipped with a gas rotameter (with accuracy of ±5 of full scale reading) to control the N_2O flow rate. The N_2O flow rate was kept at 0.15 L/min across all experiments.

The tracer gas and particle concentrations were measured at three points in the room (during all scenarios 1-5) - at the exhaust air, at the centre of the room (1.7 m height), and either at the mouth of the manikin or, in the case of empty room, at a height of 1.12 m at the exact position of the manikin's mouth when it was installed. The particle number size distributions and total number concentration were measured with several types of aerosol spectrometers: Scanning Mobility Particle Sizer – SMPS 3936L (consisting of an Electrostatic Classifier EC 3080, Differential Mobility Analyzer DMA 3081, and Condensation Particle Counter CPC 3775), Optical Particle

Sizer OPS 3330, Aerodynamic Particle Sizer APS 3321, and Condensation Particle Counter CPC 3022 (all TSI Inc., USA). The SMPS measured the ultrafine particle size distribution, whereas the APS and the three OPSs measured the size range of fine and coarse particles. The SMPS and APS were used as control measures to monitor the number size distribution of the ultrafine, fine, and coarse particles during the measurements and to verify the modal size of aerosol particles injected into the room. The SMPS was also used to monitor the total number concentration of ultrafine particles in the breathing zone of the manikin, while the CPC measured the total number concentration in the other two locations (centre of the room and exhaust), Figure 1b. In order to measure the ultrafine particle concentrations in the two locations an electrically actuated 2-way valve was used to automatically switch the sampling between the exhaust and the centre of the room (ambient air). The switching period of the valve was 5 min. The sampling at the mouth of the manikin or at 1.12 m height (breathing zone) was performed without switching (i.e. the sampling at this position was continuous). The time resolution of the SMPS was 5 min (3 min scan, 1 min retrace of the voltage, 1 min waiting). The time resolution of the CPC was 1 sec. In the case of fine and coarse particles, APS was sampled together with one of the OPSs in the breathing zone of the manikin, while the other two OPSs were placed at the same spots as the sampling tubing for ultrafine particles (exhaust and centre of the room). The OPSs sampling time was 10 seconds, while the APS was sampled with a time resolution of 1 minute. The tracer gas concentration was measured simultaneously at all locations using an Innova 1303 multi-channel sampler and a photoacoustic Innova 1312 multi-gas monitor. The sampling time of the Innova gas monitor was 40 sec/channel. All instruments were placed outside the room except for the three OPSs. The sampling of the particles with the SMPS, CPC, and APS was performed through individual copper tubes of the same length (in order to avoid different losses in sampling tubings) connected to the instrument inlet. Co-location measurements using the three OPSs were performed and the linear correlation

coefficients between the measurements were in the range of 0.9997-0.9999. The SMPS and CPC measure in practice the same concentrations (within maximum uncertainty of 10%) at particle sizes around 0.07μm using the same dimensions of the sampling lines. The Innova gas monitor was also placed outside the room. The N_2O gas was sampled through four plastic tubes with silicon lining (Ø 4 mm) connected to the channels of the gas monitor. The sampling points were the same as for the particles. It should be noted that the sampling tubes at the mouth of the thermal manikin were placed at the upper lip at a distance of <0.01 m from the face. This way of sampling provides a representative measurement of the inhaled air concentration with a thermal manikin without breathing simulation.[32]

Measurements of particles and tracer gas concentrations were carried continuously from the start of the particle injection and the tracer gas until a steady-state was observed and a sufficient number of repeated measurements were obtained in order the variation in the tracer gas concentration to become <10% (see Data analysis section). After a measurement was completed the concentration decay of aerosol particles and tracer gas were measured in most cases.
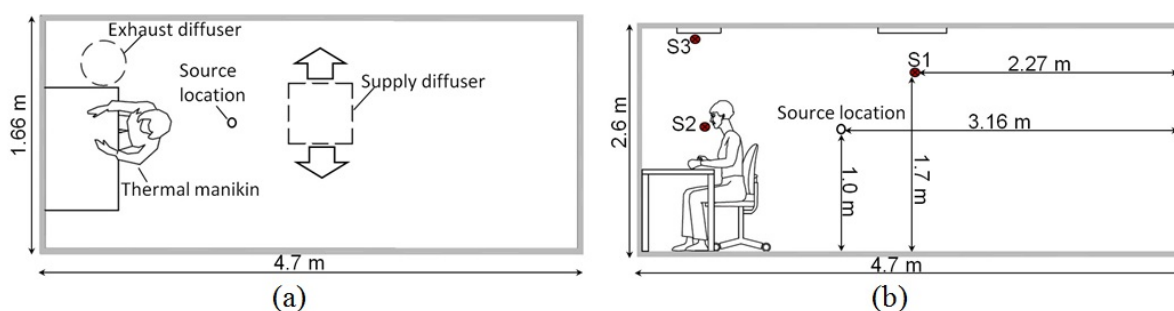
Figure 1. Top view (a) and side view (b) sketches of the room layout for scenarios 3 and 4. Tracer gas and particle air sampling points are designated with S1, S2, and S3.
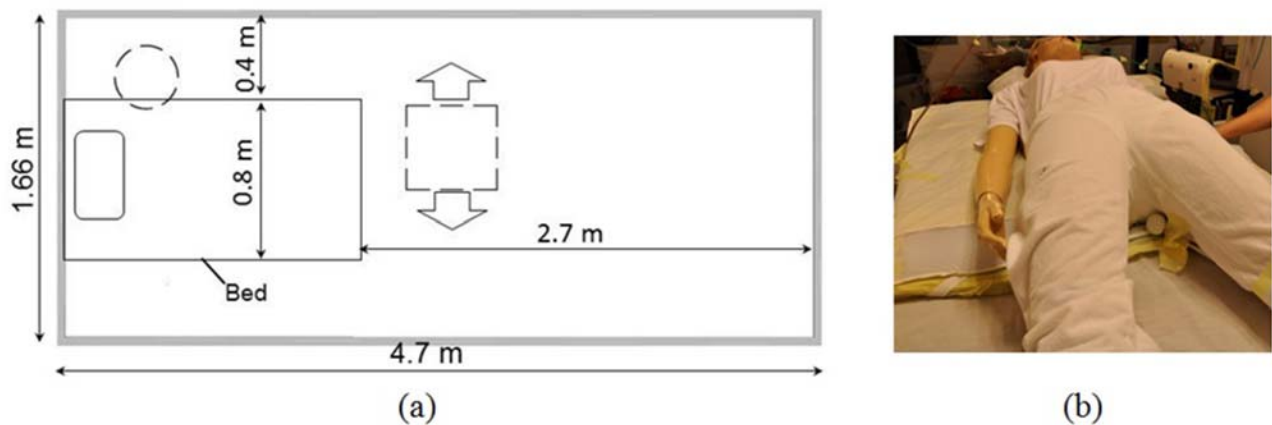
Figure 2. Experimental setup for scenario 5: (a) top view sketch of the room layout (b) pollution source close to the thermal manikin's gluteal region.

Data analysis

The data were analysed by estimating the average concentration of particles ($\#/cm^3$) and tracer gas (parts per million (ppm)) during the steady-state time period. The results were then normalized by the average concentration at the exhaust air. This type of normalization allowed comparison between all data sets across all the particles sizes. When the normalized concentration was less than "1" it meant that the concentration obtained at the measured location (breathing zone or centre of the room) was lower than the concentration at the exhaust (i.e. lower contaminant exposure). The variability (coefficient of variation (CV)) of the measurements of the particles and tracer gas is given in the results as error bars on the column chart. The CV, calculated as the ratio of standard deviation to mean concentration obtained for each location, was less than 10% in most measurements and in the range of 11% - 19% for only a few measurements. The standard deviation and the mean were calculated based on 50 samplings for the tracer gas, about 100 for the coarse and fine particles, and about 1400 for the ultrafine particles (sampled with the CPC using the 2-way valve). 20 samplings for the ultrafine particles were taken with the SMPS. All sample numbers were held for one steady-state only.

Furthermore, the data were analysed in accordance with the ISO/IEC Guide[33] for the expression of uncertainty. The absolute expanded uncertainty was estimated based on the bias and resolution of the instruments used to measure the aerosol particles and tracer gas concentrations as well as the reproducibility (standard deviation) of the measured concentrations. All uncertainties estimated based on the measured particle concentrations were 10% of the mean value for all particle instruments. All uncertainties of the tracer gas concentration measurements were calculated to be 5% of the mean. The absolute expanded uncertainties are reported at a 95% confidence interval with a coverage factor of 2. The measured concentrations ($C_{i,tn}$) during scenario five were also normalized to the tracer gas and particle concentrations measured at time $t_0 = 0$ s at the manikin's mouth and centre of the room ($C_{i,t0}$). The normalized concentrations ($C_{i,tn} / C_{i,t0}$) for each sampling location were calculated by the following equation:

$$C_{norm} = C_{i,tn} / C_{i,t0} \qquad (1)$$

where $C_{i,tn}$ is the measured tracer gas or particle concentration at time t_n and $C_{i,t0}$ is the measured gas or particle concentration at time t_0.

Further analyses were performed on the concentration decay measurements in scenarios 1-4 in order to estimate the overall loss rates of aerosol particles of different sizes. Overall particle loss rate (λ^*) includes the deposition rate of aerosol particles (β) and air change rate (λ):

$$\lambda^* = \lambda + \beta . \qquad (2)$$

The overall particle loss rate can be derived from a simple mass balance equation[34] describing the change in concentration of aerosol particles in an indoor environment:

$$V \cdot \frac{dC_i}{dt} = V \cdot \lambda \cdot (P \cdot C_o - C_i) + Q - S , \qquad (3)$$

where V is the volume of the room , C_i and C_o are the concentrations of aerosol particles indoors and outdoors, t is time, λ is the air change rate, P is the penetration factor, Q represents possible

particles sources. Parameter S represents total sink strength of aerosol particles, including deposition, measured in number of particles removed from the volume V per unit time. If we neglect coagulation of particles and their transformation due to condensation/evaporation and chemical reaction, the sink strength S can be simplified to $S=C_i V \beta$, where β is the deposition rate in the room comprising all deposition mechanisms and all surfaces.

Equation (3) can be simplified assuming that: 1) there is no source of aerosol particles in the room; 2) there is no resuspension of deposited aerosol particles; 3) particle coagulation can be neglected, 4) the initial aerosol particles concentration C_i is equal to the initial condition $C_i(0) = C_0$ in order to obtain (after solving the differential equation) the equation describing the loss of aerosol particles:

$$C_i(t) = C_\infty + (C_0 - C_\infty) \cdot e^{-\lambda^* \cdot t}, \qquad (4)$$

where $C_i(t)$ represents concentration of aerosol particles of a given size indoors at time t, C_0 is the concentration of aerosol particles when the particle generation was stopped, C_∞ is the concentration of aerosol particles in a steady-state (i.e. background aerosol particles concentration) and λ^* is the overall particle loss rate.

The above mentioned assumptions were fulfilled during the measurements: 1) after the particle generation was finished there was no other source of aerosol particles; 2) the room air velocities were too low to be able to cause any measurable resuspension of deposited particles; 3) generated particles of all sizes were close to monodisperse distribution (with a geometric standard deviation below 1.2), and concentrations were relatively low, so Brownian coagulation could be neglected; 4) the particle concentration after the generation stopped was taken as the initial concentration at time 0.

The experimental curves measured at the three locations for the three particle sizes and the scenarios 1-4 were fitted with the model using a MATLAB code utilizing the constrained Nelder-Mead Simplex method[35] in the code procedure. The method is used to find such parameters of the model equation that minimize the sum of squares of residuals between theoretical prediction and experimental data.

Results

Overall particle loss rate for scenarios 1-4

Figure 3 shows particle overall loss rates obtained using the fitting of the simplified solution of mass balance model to experimental data by the procedure described above. It has to be noted that the mass balance model assumes ideal mixing in the space (homogeneous concentration). As will be shown later, this assumption was not fulfilled in all studied scenarios. Nevertheless, in the case of point measurements this method can be used assuming sufficient local mixing in the vicinity of the sampling point. Also, the overall particle loss rates are presented here instead of deposition rates. The deposition rates can be calculated by subtracting the air change rate from the overall particle loss rate assuming constant air change rate. The local air change rate in the sampling points was not measured and therefore it was not used for the calculation of the deposition rates. Moreover, the SMPS total concentration (breathing zone position) is burdened with higher uncertainty than CPC (centre of the room and exhaust position). These deviations may come from the higher charge on the generated aerosol particles (from the nebulizer) following incomplete particle charge neutralization (not reaching Boltzmann charge equilibria), which can result in under- or over-estimation of particle concentrations in measured size bins (depending on the prevailing charge polarity). Nevertheless, keeping these limitations in mind, the SMPS data still represent valid information about aerosol particle concentration and its time evolution in the given point.

Generally, it can be stated that in the scenarios 1-4 the fine particles (0.7 μm) reached the lowest values of overall particle loss rate, meaning that these particles should have had the most similar behaviour to the tracer gas. In other words, these particles were the least influenced by main deposition mechanisms (Brownian motion or gravitational settling). Figures 3A and 3B show that the particle loss was enhanced when the air change rate in the room was increased from 3.5 to 7 ACH. The other general feature observed from the overall particle loss rate curves was that the lowest particle loss rates were obtained at centre of the room and were the highest in the breathing zone of the manikin (except for the fine and coarse particles with the heated manikin). This can be explained by non-ideal mixing in the room, which decreased the overall particle loss rates in the centre of the room and increased it in the breathing zone. The overall breathing zone particle loss rates were also increased by the presence of the manikin. The effect of increased deposition surface area (manikin, table, and chair) was more pronounced for ultrafine particles (0.07 μm) than for coarse particles (3.5 μm). These results can be explained by the fact that ultrafine particles are able to deposit on all the available surfaces due to Brownian diffusion. By contrast, coarse particles deposit by gravitational settling and settle mostly on upward facing surfaces – represented only by the table and manikin's cross-sections. On the other hand, the heating of the manikin decreased the values of overall particle loss rate substantially for fine and coarse particles at the breathing zone of the manikin. This effect could have been caused by the FCF around the manikin body, which narrows the boundary layer around the manikin. In addition, the non-ideal surface of manikin's clothing causes turbulence. The combined effect of these two factors can be enhancing deposition onto the manikin's surface. Therefore it can lower the initial concentration at the sampling point at the breathing zone.
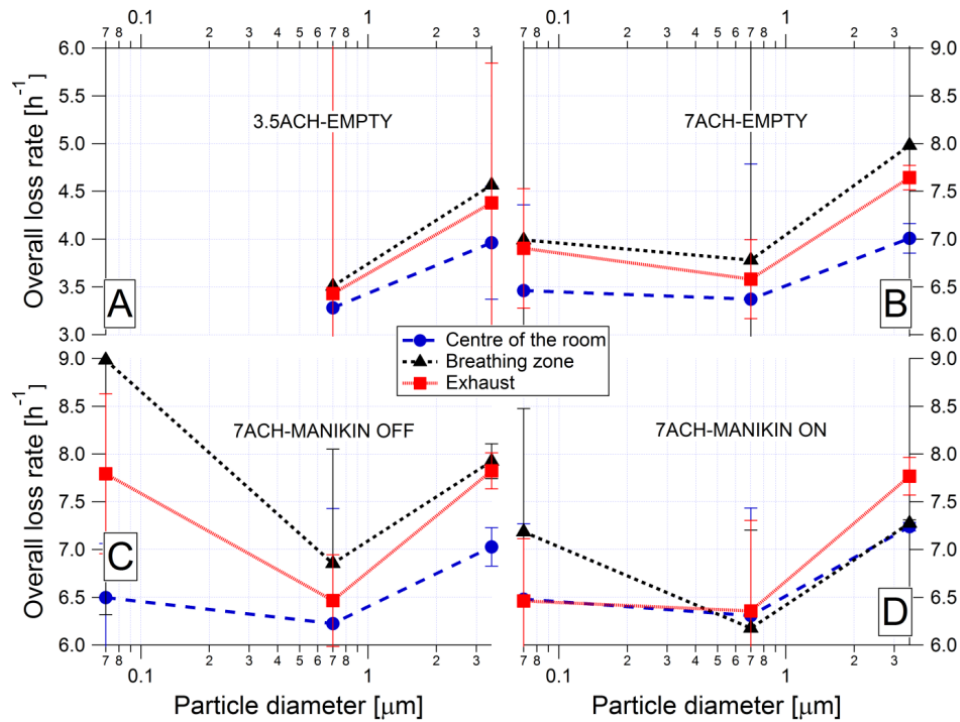
Figure 3. Aerosol particle overall loss rates calculated for different positions and particle sizes for different scenarios: A) 3.5 ACH in an empty room, B) 7 ACH in an empty room, C) 7 ACH, manikin heating OFF, D) 7 ACH, manikin heating ON. Points represent values determined by fitting the model equation. The error bars represent the values of root mean square error (RMSE), which corresponds to differences between model and the measured data. The connecting lines do not have any physical meaning and were added just to lead the readers' eye in order to easier recognize points which belong to the same scenario..

Distribution of tracer gas and particles under steady-state conditions (scenarios 1-4)

Figure 4 presents the normalized concentrations of the tracer gas and particles measured at the breathing zone and at the centre of the room during the first four experimental scenarios under steady-state conditions. The results in the figure indicate that there was a non-uniform concentration pattern in the room during each scenario. It can be seen that both tracer gas and particles' transport behaviour resulted in lower normalized concentrations at the centre of the room than at the breathing zone. Results for the ultrafine particles measured at the breathing zone are missing in

Figure 4A due to instrument failure during these measurements. In Figure 4A the results show that the N_2O tracer gas, fine (0.7 μm) particles, and coarse (3.5 μm) particles followed identical patterns at both measuring points with only 2 - 9 % difference between the normalized concentrations. On the other hand, it is apparent that the concentration distribution of ultrafine (0.07 μm) particles was quite different at the centre of the room than the N_2O gas and the other particle sizes. This difference may be because more of the 0.07 μm particles already deposited before being exhausted from the room due to diffusion compared to the tracer gas and the other particle sizes. As a result, the measured particle number concentration of the ultrafine particles was lower at the exhaust than at the centre of the room and therefore the normalized concentration of these particles was the highest in Figure 4A.

In order to find the impact of the ventilation rate on the gas and particle concentration distribution, the ACH in the empty room was increased from 3.5 ACH to 7 ACH. The results are presented in Figure 4B. In contrast to the experiment at 3.5 ACH, it can be seen that at 7 ACH the ultrafine particle concentration pattern at the centre of the room was similar to the behaviour of the gas. The results in Figure 4B also show that in both measuring points there were no large differences between the 3.5 μm and 0.7 μm particle concentration distributions and the concentration pattern of the gas. These results suggest that the ventilation rate is important for comparing the behaviour of the ultrafine particles with tracer gas, whereas for coarse and fine particles it does not have big effect in the studied range. It should be noted that the concentration of the 0.07 μm particles at the breathing zone in the empty room was slightly higher than the gas distribution and the other particle sizes.

In mechanically ventilated spaces airborne particles tend to deposit on indoor surfaces without being exhausted from the space. A table and an unheated dressed manikin sitting on a computer

chair were added to the room in order to determine if the particle concentration distribution would be affected. The results from this experiment are shown in Figure 4C. Overall, the normalized concentration distribution of all particles, as well as the tracer gas, was not changed by the additional surfaces in the room. By comparing the results shown in Figure 4B and 4C, it is observed a tendency that the particles' normalized values obtained at the breathing zone decrease when the furniture and the manikin were added to the room. Since mixing air distribution does not always assure totally mixed flow, it should always be expected a change in the normalized values when the flow pattern in the room is changed by other air speed or geometry, etc. The gas and particle concentration at the centre of the room remained the same (Figure 4C), as was the case of the empty room at 7 ACH (Figure 4B).

The results obtained from the experiment with the heated manikin are shown in Figure 4D. In Figure 4D the concentration distributions of the N_2O gas and the particles show similar behaviour as can be observed in Figures 4B and 4C. In contrast to the results in Figure 4B and 4C, the difference between the normalized concentration of the gas and the 0.07 μm particles in the breathing zone of the heated manikin was the smallest. When comparing Figures 4C and 4D it is clear that the normalized concentration of 0.07 μm particles at the breathing zone decreased by about 18% when there was FCF around the manikin. The FCF around the manikin did not prevent the smallest particles to move around the manikin. In fact, the FCF made the boundary layer thinner and, in combination with the non-ideal surface of the manikin's clothing caused some turbulence. As a result the ultrafine particles deposited more on the manikin's surface due to diffusional deposition (both Brownian and turbulent). Figure 4D also shows that the normalized values of the gas and the three sizes of particles at the centre of the room were closer to '1' than the other two experimental scenarios at 7 ACH. The results suggest that the presence of the free convection flow

that transformed to a thermal plume above the manikin's head enhanced the mixing of the air in the room.

Strong linear correlation was found between the mean concentration values of all different size particles and N_2O tracer gas. The linear relationship (r^2) between the tracer gas and the particle sizes 3.5 µm and 0.7 µm was above 0.9. The r^2 coefficients of determination between the ultrafine particles and the gas for the different scenarios (1-4) were in the range of 0.7-0.85.
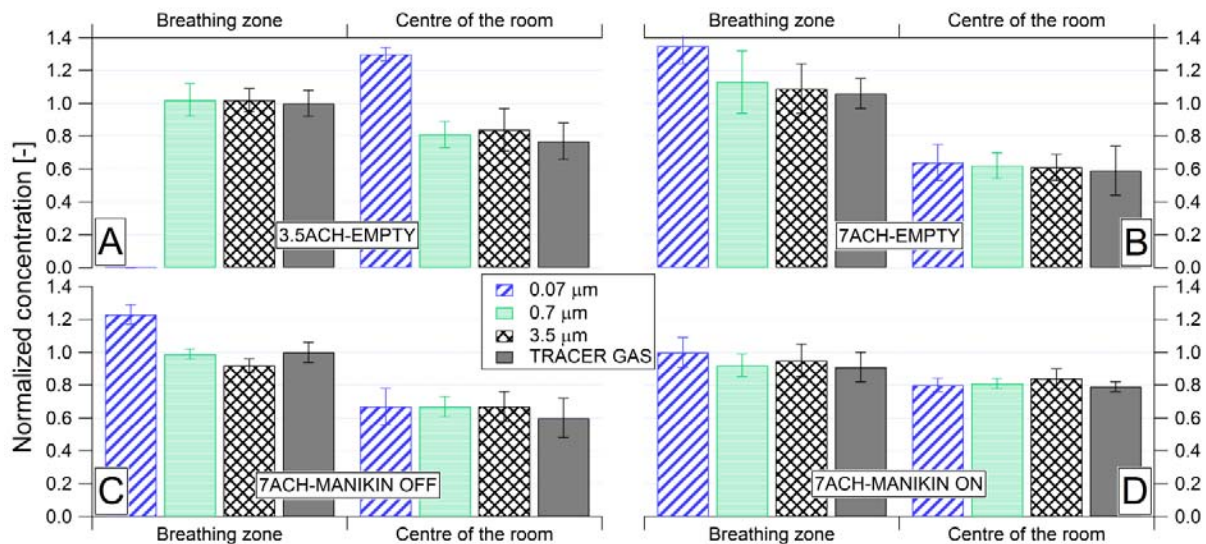
Figure 4. Comparison of normalized concentrations across N_2O tracer gas and different-sized particles for the first four scenarios: A) 3.5 ACH in empty room, B) 7 ACH in empty room, C) 7 ACH, manikin heating OFF, and D) 7 ACH, manikin heating ON.

Scenario 5: single-bed hospital room

Figure 5 illustrates the variation of the normalized concentrations of the tracer gas and 0.7 µm particles measured at the mouth, centre of the room, and the exhaust as a function of time. The ventilated mattress (VM) worked from the start of the gas and particles generation i.e. at time 0 s. The generation of the pollutants was constant during the whole measuring period shown in Figure 5. It can be seen that the concentration curves for the gas and particles are identical. The normalized

steady-state data showed that there was only 5 % difference between the gas and the fine particles normalized (by the average concentration at the exhaust) average values at the breathing zone and 2% difference at the centre of the room. From the data in Figure 5, it can also be seen that the VM had high capturing efficiency, reducing the contaminant concentrations by about 90% after reaching steady-state N_2O gas and particle concentrations.
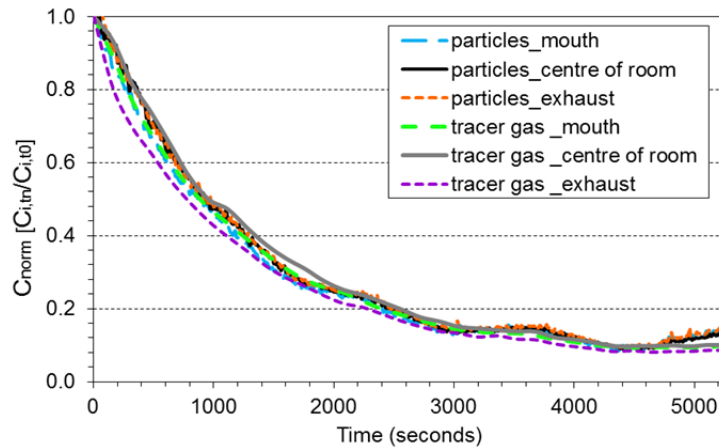
Figure 5. Comparison of the normalized 0.7 μm particle concentration with tracer gas normalized concentration based on release close to the manikin's body, and effect of local exhaust ventilation.

Discussion

Overall particle loss rate

The overall loss of the particles due to deposition was affected by the different controlled parameters. Our results show that the increased surface (presence of manikin, table, and chair) mainly influenced ultrafine particles (0.07 μm) deposited on all surfaces as opposed to coarse particles deposited dominantly on upward facing surfaces. This agreed with the finding reported by Thatcher et al.[36] that large particles are not strongly influenced by increases in vertical and downward facing surface area. On the contrary, submicron particles are more strongly affected, since they deposit effectively to surfaces of all orientations. In the current study it was also found that at the higher airflow rate the loss rate of the particles of all sizes increased. These results are

consistent with other research which found the same effect of increasing the room airflow rate on the particles deposition.[36,37] In general, aerosol particle deposition indoors is important because it decreases the air particle concentration and thus the occupants' exposure. It is interesting to note that in this study the convective flow created a "protective" boundary layer around the heated manikin surface and decreased the overall particle loss rate in the breathing zone. Thus the interaction of the background flow and the free convection flow are important for the transport of and exposure to aerosol particles.

Impact of ventilation rate

The airflow pattern within a room can have a considerable effect on the transport of airborne normalized pollutants. This study shows that there was a concentration gradient in the room (when steady-state was reached) for the gas and particles at both 3.5 ACH and 7 ACH. Yet, the normalized concentration of the N_2O tracer gas, the fine particles, and the coarse particles followed similar distributions at the measured points in the room during scenarios 1-4. This indicates that airborne particles behave like tracer gas for air change rates exceeding 3.5 ACH However, it was also found that the transport behavior of ultrafine particles is influenced by the ventilation rate more than fine and coarse particles. It is known that Brownian diffusion is an important deposition mechanism for ultrafine particles.[38] In the present study at the lower ventilation rate the Brownian diffusion seems to be dominant over the airflow pattern in the room when compared to the higher ventilation rate. The Brownian motion is moving the particles in all directions with the same probability unless there is another driving force directing the particles. Whenever the particle gets close to the surface it has to overcome the boundary layer. The deposition is thus also influenced by the thickness of the boundary layer. In the case of the Brownian diffusion, the wall acts as a particle sink causing concentration gradient across the boundary layer and therefore results in diffusional flux of particles towards the wall. However, the magnitude of this effect needs to be verified by direct measurements

156

of particle deposition on surfaces and visualizating flow patterns or modelling of the flow field by CFD tools. Nevertheless, it is possible to hypothesize that ultrafine particles will not act as tracer gas in a room where the air change rate (ACR) is low (in our case 3.5 ACH or lower). In contrast, at 7 ACH and with an empty room the distribution of 0.07 μm particles was similar to that of the other particles and gas, suggesting that the particles followed the airflow pattern in the room better than 3.5 ACH. It is worthwhile to note that the air change rate has a huge influence on the absolute concentrations (double flow rate, half concentration). In the current study the used normalization of the data is to be able to compare gas concentrations with particle concentrations.

Comparison with other studies

The findings in this study are in agreement with the findings of previous studies that showed tracer gas can be used to evaluate the distribution of aerosol particles in ventilated rooms.[12,16,20] The concentration patterns of tracer gas measured at the mouth of the heated manikin and the centre of the room appeared to be comparable to that of all the studied particle sizes. These results are in agreement with Rim and Novoselac's findings[12], which showed that highly mixed airflow (4.5 ACH) in a room creates relatively uniform and comparable gas and particles concentration patterns in the vicinity of a thermal manikin. The study by Rim and Novoselac[12] was carried out with monodispersed particles with aerodynamic diameters of 0.03, 0.77, and 3.2 μm and the pollution source was located either 1 m above the floor (similar to the pollution source in this study) or near the occupant's feet. The measurements in this study were carried out using SMPS and APS instruments. These instruments have high size resolution that allowed us to monitor the number size distribution of the ultrafine, fine, and coarse particles and to justify with high accuracy the modal size of the injected aerosol particles.

Impact of interaction of airflows and objects

An important finding was that the increase in the contact surface area of room objects with room air by the addition of a table and seated unheated manikin did not change the similarity of the distribution pattern of the 0.07 μm, 0.7 μm, and 3.5 μm particles to that of the tracer gas, Figure 4C. Despite these results, it should be noted that the additional surfaces were relatively small in comparison to the surface of the empty room. That is why no significant change was observed in the normalized concentration distribution.

The interaction between the FCF generated around the body of the heated manikin with the background room changed the air distribution in the room and resulted in a more homogeneous environment, Figure 4D. Nonetheless, it did not influence the similar transport pattern of the particles and the gas. On the contrary, it seems that when there is FCF around the manikin the difference in the normalized concentration distributions between the 0.07 μm particles and the tracer gas at the breathing zone decreases. This finding suggests that tracer gas can be used as a measure of occupants' exposure even to ultrafine particles.

The above results confirm that the convective boundary layer is important for personal exposure as well as the level of mixing between the supply air and room air.[12,24-26] Depending on the source location and background pollution distribution the free convection boundary layer may increase exposure or reduce it. It also may not affect the exposure (i.e. complete mixing). Since the room air distribution is difficult to control, an advanced air distribution supplying clean air to the breathing zone is recommendable.[39] Localized exhaust methods can also be used to remove particles from active indoor heat sources such as the human body and exhaled air.[8,29,40]

Single-bed hospital room

The results from this scenario clarified to what extent measurement of tracer gas distribution can be used to predict 0.7 μm particle transport when released or re-suspended from a person's body or

from a mattress while a person is resting in bed. The results show that the particles behave exactly the same as the tracer gas when a person is in a supine position and his/her FCF is disturbed by local exhaust airflow. To develop a full picture of the tracer gas and particle behaviour when they are released from a lying person, additional studies will be needed that include measurements of other particle sizes and do not include a local exhaust in the bed.

Implication of results

The current results suggest that tracer gas can be used to assess the removal of particles (range: 0.07-3.5 μm) to validate the performance of mixing air distribution in certain room layouts. Comparison of tracer gas and particle normalized concentrations measured at the mouth of the heated manikin also suggest that tracer gas can be used to predict potential personal exposure to 0.07 μm, 0.7 μm, and 3.5 μm particles. There are many disease-causing microorganisms that have similar particle sizes to the ones used in this study. For instance, most contagious bacteria have sizes within the fine range of 0.2 – 1 μm. Furthermore, airborne droplet nuclei (evaporated droplets generated by human respiratory activities) range from 1-5 μm.[41] Curseu et al.[41] also reported that spores of *Aspergillus fumigatus* have diameters of 2-3.5 μm and can exhibit similar behaviour in the air as droplet nuclei. Understanding the dynamic behavior of ultrafine particles is also of interest since there are health concerns associated with the inhalation exposure to abiotic ultrafine particles. It should be noted that the tracer gas concentration cannot be directly used to determine the health risk of such infectious pathogens, but it can give an indication for personal exposure to air contaminated with such pathogens.

Previous studies have demonstrated that a significant fraction of human-induced resuspension of particles from mattresses and bedding can be inhaled by sleeping occupant.[30,31] The airflow interaction in the microenvironment of a person has a fundamental effect on their exposure to

pollutants generated in the vicinity of the body.[26] Hence, in order to improve a person's inhaled air quality, it is suggested that the microenvironment close to the human body is locally controlled. The present study shows that there is the possibility of testing local exhaust ventilation systems for their ability to remove fine aerosol particle contaminants using tracer gas.

Study limitations

These results raise the possibility of using tracer gas techniques to predict the distribution of aerosol particles in ventilated rooms with some limitations in regards to particle size. The findings in the study cannot be extrapolated to all particle sizes, especially for particles in the coarse-mode range larger than 3.5 μm. It is expected that the use of gaseous tracers to mimic the behavior of aerosol particles would progressively decrease as size increases in this range. The study did not take into account also other air distribution patterns, such as displacement air distribution or other positions of the supply and exhaust diffusers. The study is also restricted to processes taking place only in rooms without recirculation. The location and type of the source and occupants' activity may also have different effects on particle and gas dispersion. The current source location may produce better particle and gas comparisons in contrast, for example, if the source was located close to a surface such as the floor, for which particles deposition losses before mixing occurs would be more important. The lack of proper simulations of the occupant's breathing flow in this study might lead to some incorrect predictions, especially for coarse particles (as shown by Rim and Novoselac[12]). This needs to be further studied.

The tracer gas and particles concentrations were measured at only three points in the room due to not enough available particle counters. It is hard to draw a general conclusion about the use of tracer gas to simulate the aerosol particles behavior in all possible situations in practice. All conclusions are based on the variation in the measured values at the three sampling points in the room. Future

studies on the current topic are therefore recommended and should include more measuring points as well as analysis of the decay rate of tracer gas and different particle sizes compared to local air change rate. Such analysis can provide better understanding if it is the particle deposition or just mixing patterns that lead to differences or similarities between observed gas and particle behavior.

Another restriction of the current study is that the effect of ACR was examined only in the case of an empty room. Future studies should also examine the impact of different ACRs on the gas and aerosol particles dispersion in a furnished room and the presence of heat sources.

Conclusions

This study focused on the comparison of the concentration dispersion of tracer gas and particles with different sizes in a full-scale test room. The effects of different parameters on the gas and the particles distribution were studied, including air change rate, change in the room surface area, and FCF around an occupant body. The results show that:

- Particles in the fine size range (0.7 μm) are the least influenced by deposition mechanisms and thus should have the most similar behaviour to the tracer gas;

- The ventilation rate was important for comparing the behaviour of the ultrafine particles and tracer gas; for the 3.5 μm and the 0.7 μm particles the studied ventilation rates did not have a large effect;

- Increasing the room surface area did not influence the similarity of the 0.07 μm, 0.7 μm, and 3.5 μm particle dispersal to that of the tracer gas;

- At the breathing zone of the seated heated manikin N_2O gas emerged as a reliable predictor of the exposure to all tested different-sized particles. Furthermore, the results of this study suggest that tracer gas can be used to indicate the exposure of a person lying in bed to 0.7 μm aerosol particles.

More research is needed to provide data on rooms with different furniture layout, source location, thermal plumes generated by various heated objects, and occupant movement.

Supporting Information

Additional Supporting Information may be found in the online version of this article:

Figure S1. a) Picture of the supply air diffuser, b) common dimensions of the two supply diffusers.
Figure S2. a) Picture of the exhaust air diffuser, b) dimensions of the exhaust diffuser.
Table S1. Specific dimensions of the supply air diffusers.
Table S2. Specific dimensions of the exhaust air diffuser.

Reference

1. Koullapis PG, Kassinos SC, Bivolarova MP, Melikov AK. Particle deposition in a realistic geometry of the human conducting airways: Effects of inlet velocity profile, inhalation flowrate and electrostatic charge. *J Biomech*. 2016;49:2201-2212.

2. Long CM, Suh HH, Catalano PJ, Koutrakis P. Using time- and size-resolved particulate data to quantify indoor penetration and deposition behavior. *Environ Sci Technol*. 2001;35:2089-2099.

3. Burge H. Bioaerosols: prevalence and health effects in the indoor environment. J. Allergy Clin. Immunol. 1990; 86, 687–701. 4. Bolashikov ZD, Melikov AK. Methods for air cleaning and protection of building occupants from airborne pathogens. *Build Environ*. 2009;44:1378-1385.

5. Li Y, Leung GM, Tang JW, et al. Role of ventilation in airborne transmission of infectious agents in the built environment - a multidisciplinary systematic review. *Indoor Air*. 2007;17:2-18.

6. Morawska L. Droplet fate in indoor environments, or can we prevent the spread of infection? *Indoor Air*. 2006;16:335-347.

7. Bjørn E and Nielsen PV. Dispersal of exhaled air and personal exposure in displacement ventilated room. *Indoor Air*. 2002;12:147–164.

8. Bolashikov ZD, Melikov AK, Kierat W, Popiolek Z, Brand M. Exposure of health care workers and occupants to coughed airborne pathogens in a double-bed hospital patient room with overhead mixing ventilation. *Hvac&R Research*. 2012;18:602-615.

9. Cermak R, Melikov AK. Air quality and thermal comfort in an office with underfloor, mixing and displacement ventilation, *International Journal of Ventilation. 2006;*5, 323–332.

10. Nielsen PV, Buus M, Winther FV, Thilageswaran M, Ashrae. Contaminant Flow in the Microenvironment Between People Under Different Ventilation Conditions. *Ashrae Transactions*. 2008;114:632-638.

11. Olmedo I, Nielsen PV, de Adana MR, Jensen RL, Grzelecki P. Distribution of exhaled contaminants and personal exposure in a room using three different air distribution strategies. *Indoor Air*. 2012;22:64-76.

12. Rim D, Novoselac A. Transport of particulate and gaseous pollutants in the vicinity of a human body. *Build Environ*. 2009;44:1840-1849.

13. Zhao B, Zhang Y, Li XT, Yang XD, Huang DT. Comparison of indoor aerosol particle concentration and deposition in different ventilated rooms by numerical method. *Build Environ*. 2004;39:1-8.

14. Chen QY. Ventilation performance prediction for buildings: A method overview and recent applications. *Build Environ*. 2009;44:848-858.

15. Tang JW, Noakes CJ, Nielsen PV, et al. Observing and quantifying airflows in the infection control of aerosol- and airborne-transmitted diseases: an overview of approaches. *J Hosp Infect*. 2011;77:213-222.

16. Zhang Z, Chen X, Mazumdar S, Zhang TF, Chen QY. Experimental and numerical investigation of airflow and contaminant transport in an airliner cabin mockup. *Build Environ*. 2009;44:85-94.

17. Sørensen DN, Nielsen PV. Quality control of computational fluid dynamics in indoor environments. *Indoor Air*. 2003;13:2-17.

18. Wang M, Lin CH, Chen QY. Advanced turbulence models for predicting particle transport in enclosed environments. *Build Environ*. 2012;47:40-49.

19. Qian H, Li Y, Nielsen PV, Hyldgaard CE, Wong TW, Chwang ATY. Dispersion of exhaled droplet nuclei in a two-bed hospital ward with three different ventilation systems. *Indoor Air*. 2006;16:111-128.

20. Noakes CJ, Fletcher LA, Sleigh PA, Booth WB, Beato-Arribas B, Tomlinson N. Comparison of tracer techniques for evaluating the behaviour of bioaerosols in hospital isolation rooms. *Proceedings of Healthy Buildings*. 2009; 9th international conference and exhibition, Syracuse, NY, USA. Paper #504.

21. Beat-Arribas B, McDonagh A, Noakes CJ, Sleigh PA. Assessing the near-patient infection risk in isolation rooms. *Proceedings of Healthy Buildings 2015*, ISIAQ International Conference, Eindhoven, the Netherlands, May 18-20, paper #537.

22. Melikov A. Breathing thermal manikins for indoor environment assessment: important characteristics and requirements. *Eur J Appl Physiol*. 2004;92:710-7[13].

23. Zukowska D, Melikov A, Popiolek Z. Impact of geometry of a sedentary occupant simulator on the generated thermal plume: Experimental investigation. *Hvac&R Research*. 2012;18:795-811.

24. Licina D, Melikov A, Pantelic J, Sekhar C, Tham KW. Human convection flow in spaces with and without ventilation: personal exposure to floor-released particles and cough-released droplets. *Indoor Air*. 2015;25:672-682.

25. Licina D, Melikov A, Sekhar C, Tham KW. Transport of gaseous pollutants by convective boundary layer around a human body. *Sci Technol Built Environ*. 2015;2:1175-1186.

26. Melikov AK. Human body micro-environment: The benefits of controlling airflow interaction. *Build Environ*. 2015;91:70-77.

27. Morawska L, Afshari A, Bae GN, et al. Indoor aerosols: from personal exposure to risk assessment. *Indoor Air*. 2013;23:462-487.

28. Manikin software for controlling a Thermal Manikin, www.manikin.com

29. Bivolarova MP, Melikov AK, Mizutani C, Kajiwara K, Bolashikov ZD. Bed-integrated local exhaust ventilation system combined with local air cleaning for improved IAQ in hospital patient rooms. *Build Environ*. 2016;100:10-18.

30. Boor BE, Spilak MP, Corsi RL, Novoselac A. Characterizing particle resuspension from mattresses: chamber study. *Indoor Air*. 2015;25(4):441-456.

31. Spilak MP, Boor BE, Novoselac A, Corsi RL. Impact of bedding arrangements, pillows, and blankets on particle resuspension in the sleep microenvironment. *Build Environ*. 2014;81:60-68.

32. Melikov AK, Kaczmarczyk J. Measurement and prediction of indoor air quality using a breathing thermal manikin. *Indoor Air*. 2007; 17: 50–9.

33. ISO/IEC Guide 98-3:2008. Uncertainty of measurements -- Part 3: Guide to the expression of uncertainty in measurement (GUM: 1995); 2008.

34. Smolík, J., Lazaridis, M., Moravec, P., Schwarz, J., Zaripov, S. K. , Ždímal, V. Indoor aerosol particle deposition in an empty office. *Water, Air and Soil Pollution*. 2005; 165:301-312

35. Lagarias JC, Reeds JA, Wright MH, Wright PE. Convergence properties of the Nelder-Mead simplex method in low dimensions. *Siam J Optimiz*. 1998;9:112-147.

36. Thatcher TL, Lai ACK, Moreno-Jackson R, Sextro RG, Nazaroff WW. Effects of room furnishings and air speed on particle deposition rates indoors. *Atmos Environ*. 2002;36:1811-1819.

37. Mosley RB, Greenwell DJ, Sparks LE, Guo Z, Tucker WG, Fortmann R, Whitfield C. Penetration of ambient fine particles into the indoor environmemnt. *Aerosol Sci Technol*. 2001;34:127-136.

38. Nazaroff WW. Indoor particle dynamics. *Indoor Air*. 2004; 14:175–183.

39. Melikov AK. Advanced air distribution: improving health and comfort while reducing energy use. *Indoor Air*. 2016;26:112-124.

40. Melikov AK, Dzhartov V. Advanced air distribution for minimizing airborne cross-infection in aircraft cabins. *Hvac&R Research*. 2013;19:926-933.

41. Curseu D, Popa M, Sirbu D, Popa MS. Engineering Control of Airborne Disease Transmission in Health Care Facilities. *IFMBE Proceedings.2009; 26:1-4*.

PAPER III

Bivolarova, M., Melikov, A. K., Kokora, M., & Bolashikov, Z. D., 2015. Performance Assessments of a Ventilated Mattress for Pollution Control of The Bed Microenvironment in Health Care Facilities. In Proceedings of Healthy Buildings 2015, ISIAQ International Conference, Eindhoven, the Netherlands, May 18-20, paper ID 633.

PERFORMANCE ASSESSMENT OF A VENTILATED MATTRESS FOR POLLUTION CONTROL OF THE BED MICROENVIRONMENT IN HEALTHCARE FACILITIES

Mariya P Bivolarova[1,*], Arsen K Melikov[1], Monika Kokora[1], and Zhecho D Bolashikov[1]

[1]International Centre for Indoor Environment and Energy, Department of Civil Engineering, Technical University of Denmark, Kgs. Lyngby, Denmark.

*Corresponding email: mbiv@byg.dtu.dk

Keywords: Advanced local ventilation, Pollution control, Bed microenvironment, Decreased ventilation, Energy saving

SUMMARY

A new method for minimizing the spread of bioeffluents emitted from hospitalized patients lying in beds was developed and studied. The method consists of a ventilated bed mattress that is able to exhaust the human bioeffluents at the area of the body where generated before spreading around in room. Full-scale experiments were conducted in a climate chamber furnished as a two-bed hospital patient room. A thermal manikin and two heated dummies were used to simulate two lying patients and a standing doctor. The bed with the thermal manikin had the ventilated mattress (VM). The tracer gases CO_2 and N_2O were used to mimic human bioeffluents released from the feet and armpits of the manikin, respectively. The concentration of the tracer gases was measured in six points including the breathing zone of the simulated occupants. The results show that the VM combined with mixing ventilation at 1.5 air changes per hour (ACH) proved to be more effective in reducing exposure to body contaminants compared to mixing ventilation alone at 3 ACH and 6 ACH. The findings also show that the lying position and the size of the local exhaust of the VM affect the efficiency of the mattress to exhaust bioeffluents.

INTRODUCTION

People create a microenvironment when lying or sleeping in bed. The mattress, pillows, bedding, the people including their breathing and the convective flow established around the body all together form the bed microenvironment. The generated bed microenvironment can be a source of pollution. A variety of volatile compounds can be emitted from several areas of the human body that are prone to odour production, e.g., scalp, armpits, feet, groin, and oral cavity (Pandey and Kim, 2011). In hospitals and other healthcare functional facilities there are patients that spend considerable amount of time confined to the bed unable to frequently refreshing themselves. Thus the left on the body sweat can produce a strong unpleasant odour.

In recent years, there has been an increasing amount of studies on new air distribution methods for providing better indoor air quality. A novel method for hospital bed ventilation based on the "push and pull" air distribution principle has been developed (Melikov et al., 2011; Melikov 2011). This method comprises two devices, the hospital bed integrated ventilation and cleansing units (HBIVCUs), which are attached on both sides of the patient's bed near the head. These devices have proven to act as an efficient means to reduce the risk of airborne cross-infection in hospitals (Bolashikov 2010). However, the method might not be efficient for capturing polluted air released from the body bioeffluents while the person is lying in bed.

A new air distribution strategy for controlling the air pollution spread in the bed microenvironment has been introduced by Bivolarova et al. (2014a). The method named "Ventilated mattress" is based on source control with localized exhaust implemented within the mattress to locally extract the air pollutants before being spread in the surrounding air via the background air distribution.

The purpose of the present study is to present results on the performance of the ventilated mattress (VM) for exposure reduction to gaseous contaminants/body odours (bioeffluents). The performance of the VM was studied in a simulated two-bed hospital patient room. The VM pollutant extraction efficiency was also examined with regards to different parameters including occupant's lying position and size of the exhaust opening of the VM, which was design to be in contact with the body of the lying person.

METHODOLOGIES

Full-scale experiments were performed in a climate chamber with dimensions: 4.7 m x 5.3 m x 2.6 m (W x L x H), built in a laboratory hall, 0.7 m above the floor. The laboratory hall has a separate ventilation system and temperature control. In order to reduce the heat exchange the ambient temperature in the hall was kept the same as that in the test room. Overhead mixing air distribution (MV) was used to supply 100% outdoor air to the chamber. The outdoor air was supplied through a square diffuser mounted in the middle of the room ceiling. No recirculation was used during the experiments. The air was exhausted through two perforated square diffusers located symmetrically on the ceiling above each bed right above the head of every patient (Figure 1).

The climate chamber was furnished to simulate a two-bed hospital patient room. The distance between the beds was adjusted to be 1.06 m. On each bed with dimensions 0.9 m x 2.0 m x 0.8 m (W x L x H) there was a mattress with thickness of 0.06 m and a pillow. A thermal manikin and a heated dummy with a simplified body shape ("head", "torso" and "legs") were used to simulate lying patients in the two beds. The thermal manikin has the physics of an adult Scandinavian female with a height of 1.68 m of size 38 based on EU clothing size (10 in UK and 8 in USA). The manikin consists of 23 body parts. Each body part was individually controlled to maintain surface temperature equal to the skin temperature of an average person in a state of thermal comfort. The heated dummy lying on the second bed was adjusted to generate heat with power of 80 W. A second heated dummy (230 W) was used to simulate a doctor standing next to the manikin's bed at a 0.83 m distance from the

manikin's mouth. During the experiments the two "patients" were covered with summer duvets. The duvet was covering the whole body of each "patient" up to the neck. The thermal manikin was dressed in a short-sleeve hospital pyjama and its total clothing isolation was 0.60 Clo. The layout of the test chamber is shown in Figure 1.

The manikin was referred to as a "source patient" since it was used as a source of body emitted bioeffluents. The bioeffluents were mimicked by using a constant emission of three different tracer gases. Carbon dioxide (CO_2) and nitrous oxide (N_2O) were used to simulate emissions of bioeffluents from manikin's feet and armpits, respectively.

The ventilated mattress (VM) was placed on top of the regular mattress in the source patient's bed. The VM was used in some of the experiments to exhaust locally the contaminants emitted from the patient's body. Part of the surface of the VM is designed as an exhaust opening, from which contaminants generated from the human body (e.g. bioeffluents) were exhausted. The exhaust opening of the VM was located below the pelvis of the "source patient". The exhaust airflow rate of the VM was adjusted to be 1.5 ± 0.2 L/s during the experiments. More detailed description of the ventilated mattress and how the exhaust airflow was controlled can be found in Bivolarova et al. (2014a).

In order to optimize the performance of the ventilated mattress, two sizes of the local exhaust opening of the mattress were tested: 1) 0.8 m length x 0.16 m width equal to exhaust surface area (ESA) of 0.13 m^2 and 2) 0.4 m length x 0.16 m width equal to surface area of 0.06 m^2.

During the experiments three lying positions of the thermal manikin ("source patient") were studied. The manikin was positioned on its back in the centre of the bed and the arms placed on the side of the torso under the duvet. In the second position, the manikin was lying on its right side facing the "doctor". In the third lying position, the manikin was placed on its stomach with arms on the side of the torso. In this position the head was facing the "doctor".

Series of experiments were conducted at three background ventilation rates, namely 27, 55 and 109 L/s corresponding to 1.5, 3 and 6 air changes per hour, ACH. The room air temperature was kept at 23 °C during the experiments. The relative humidity in the chamber was not controlled; it was measured to be within the range of 25 – 40% RH. The air mixed with the tracer gases was sampled and its gas concentration was analysed under steady-state conditions using an Innova 1303 multi-channel sampler and a photo-acoustic multi-gas monitor Innova 1312. The concentration of the three gases was measured simultaneously at 1) the mouth of the "doctor", 2) the mouth of the source patient 3) the mouth of the exposed patients, 4) the air supply diffuser, 5) the duct of the total exhaust room air, and 6) in the center of the room between the two beds and close to the source patient's feet at 1.7 m height from floor, referred to as "1.7 m center". The experiments at 1.5 ACH were performed with either the VM operating or VM not. Experiments at 3 and 6 ACH were conducted without using the VM. All experimental cases are listed in Table 1.
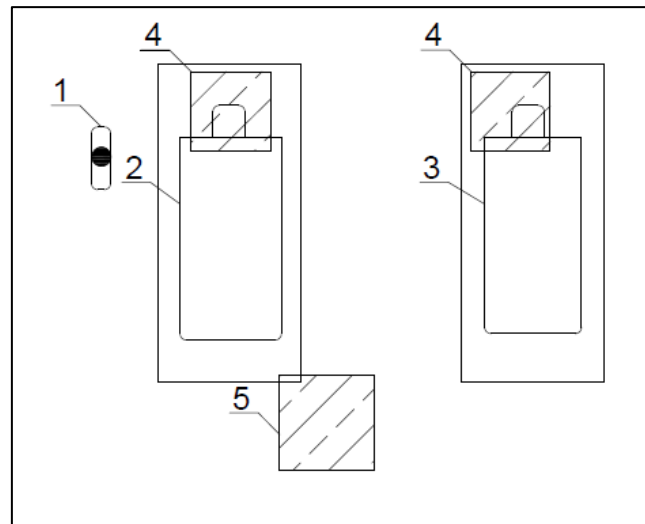
Figure 1. Top view sketch of the chamber layout: 1 – "doctor", 2 – "source patient", 3 – "exposed patient", 4 – room air exhaust diffusers, 5 - air supply diffuser.

Table 1. Experimental cases.

№	Lying position of the thermal manikin	Exhaust surface area (ESA) of the VM	Background ventilation rate
1	Lying on back	*N/A	1.5 ACH
2	Lying on back	N/A	3 ACH
3	Lying on back	N/A	6 ACH
4	Lying on stomach	0.13 m^2	1.5 ACH
5	Lying on one side	0.13 m^2	1.5 ACH
6	Lying on back	0.13 m^2	1.5 ACH
7	Lying on back	0.06 m^2	1.5 ACH
8	Lying on back	1.4 m^2	1.5 ACH

*N/A – not applicable

The data were analysed by collecting 20 repeated measurements of the tracer gas concentration at all 6 measuring points after reaching a steady state concentration in the room. The median values of the concentrations were normalized according to the following equation:

Normalized concentration = $C_i/C_{i,Ref}$ (1)

where C_i is the concentration acquired at a certain measuring point, $C_{i,Ref}$ is the concentration acquired at the same measuring point during the reference condition of 1.5 ACH without using the VM. The normalization index is also referred in the text as 'pollutant extraction efficiency'.

When the normalized concentration is less than "1" it means that the concentration obtained at the measured location (C_i) was less than the concentration at the reference point ($C_{i,Ref}$) and vice versa when the normalized concentration is higher than "1".

RESULTS AND DISCUSSION

As shown in Figure 2, the obtained dimensionless pollution concentration released from the feet reached almost zero values when the VM was used at 1.5 ACH. Even supplying 109 L/s (6 ACH) of clean air in the room was not enough to dilute completely the simulated body released bioeffluents in the room. The highest level of bioeffluents was obtained at the mouth of the "source patient" for both conditions at 3 and 6 ACH. These results can be explained with the proximity between the point of the pollution release and the mouth of the "source patient". Also the duvet did not allow the feet bioeffluents to move directly into the room. So most of the feet bioeffluents had to move upwards towards the head (manikin was covered up to neck).
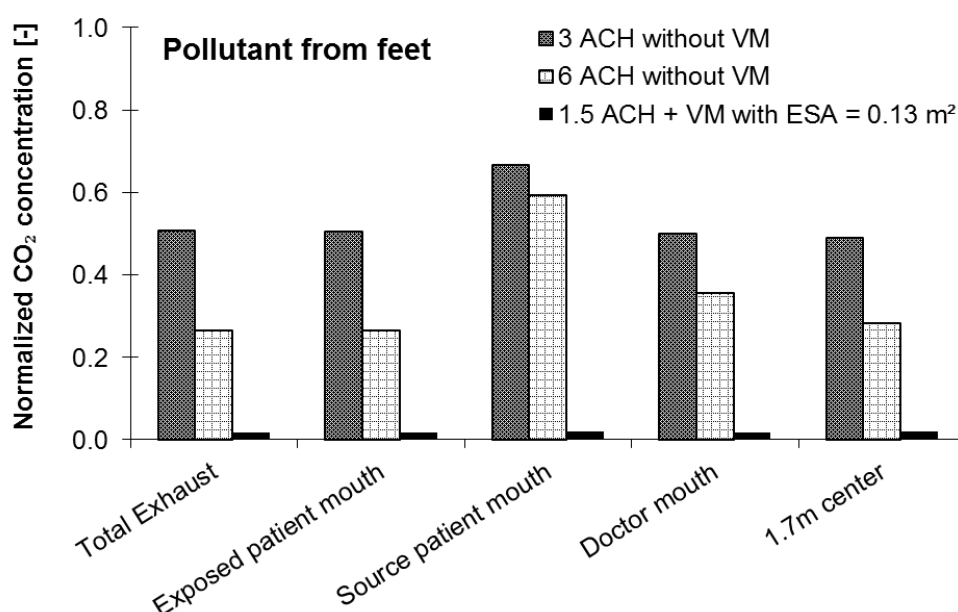
Figure 2. Comparison of the normalized concentration in the six measuring point at 1.5 ACH with the VM operating at 1.5 L/s, 3 ACH and 6 ACH without using the VM. The "source patient" was lying on its back.

The performance of the method in terms of the effectiveness to evacuate the bioeffluents from the body was examined at two sizes of the local exhaust opening. Figure 3 shows the concentration of the N_2O tracer gas released from the armpits of the thermal manikin with the two tested local exhausts. We can see that the N_2O concentration (armpits bioeffluents) was closest to zero under all tested conditions shown in Figures 3, confirming once again the high capturing efficiency of the VM. Since the manikin's arms were under the duvet, most of the N_2O tracer gas was sucked through the mattress before the gas to spread across the room. The concentration of the tracer gas in all measuring points using the VM with ESA=0.13 m^2 was the lowest compared with the other local exhaust. This result indicates that the size of the VM exhaust opening make a difference in the suction ability of the VM.

Figure 3. Comparison of the normalized concentration in the six measuring locations at the three different local exhausts of the VM and for the pollution source patient's armpits. The air change rate was 1.5 ACH and the "source patient" was lying on its back.

The impact of the manikin's lying position on the spread of the body bioeffluents when the VM was sucking air through its exhaust opening below the pelvis was assessed. The results for the lying positions on 'back', 'stomach' and 'one side' are shown in Figure 4. When the pollution source was manikin's feet, the lying positions on 'stomach' and 'one side' had a mild effect on the spread of the gas concentration, Figure 4a. In the lying on the back position both concentrations of the tracer gases (CO_2 and N_2O) were 99.9% discharged from the room (Figures 4a and 4b). The lying position had much stronger impact on the pollution distribution from the armpits, Figure 4b. We can see that when the manikin was positioned to lie on stomach the N_2O concentration in the room increased. In Figure 4b it can be noted that the normalized concentration (0.23) at the mouth of the "source patient" was less than at the other measuring locations (0.40 ± 0.02).
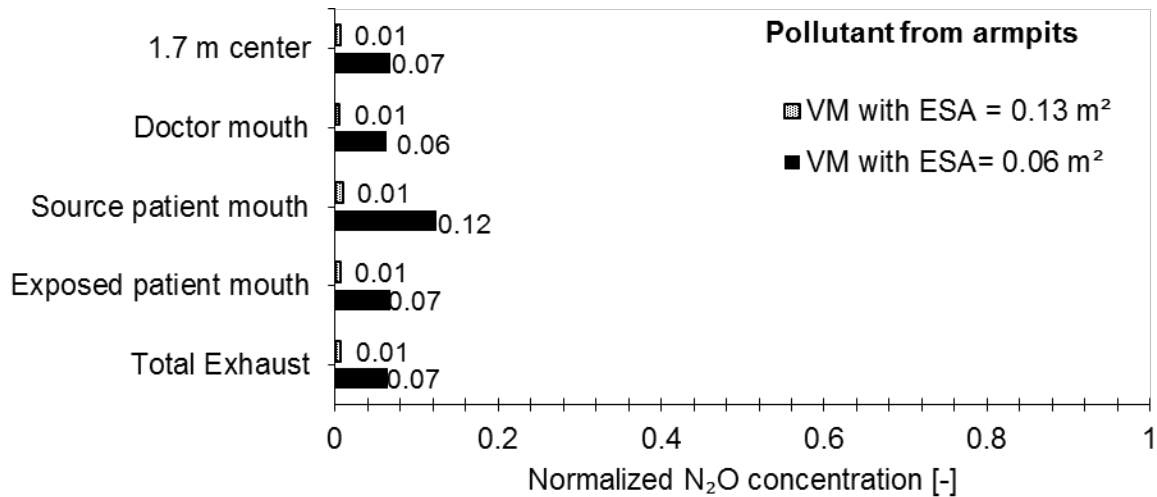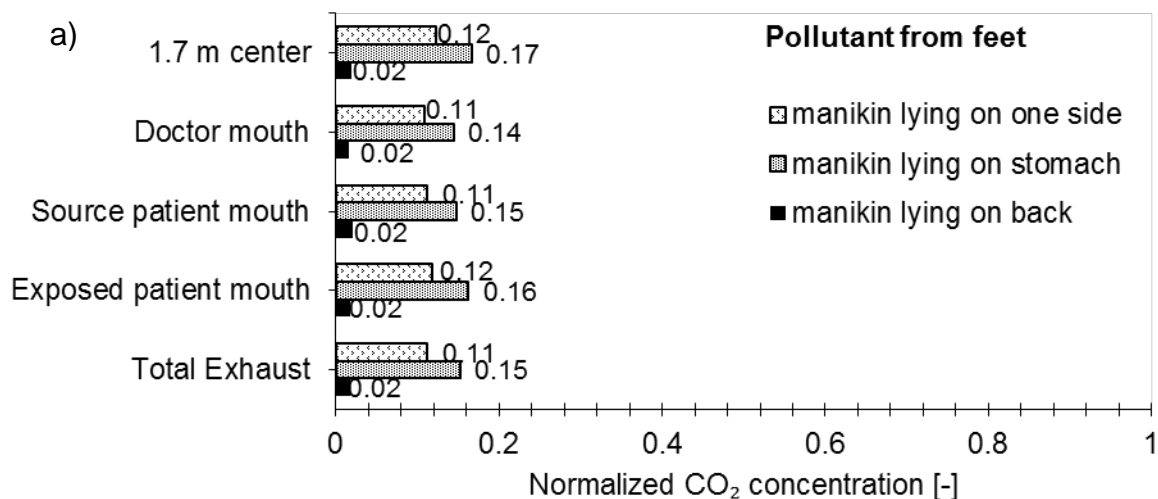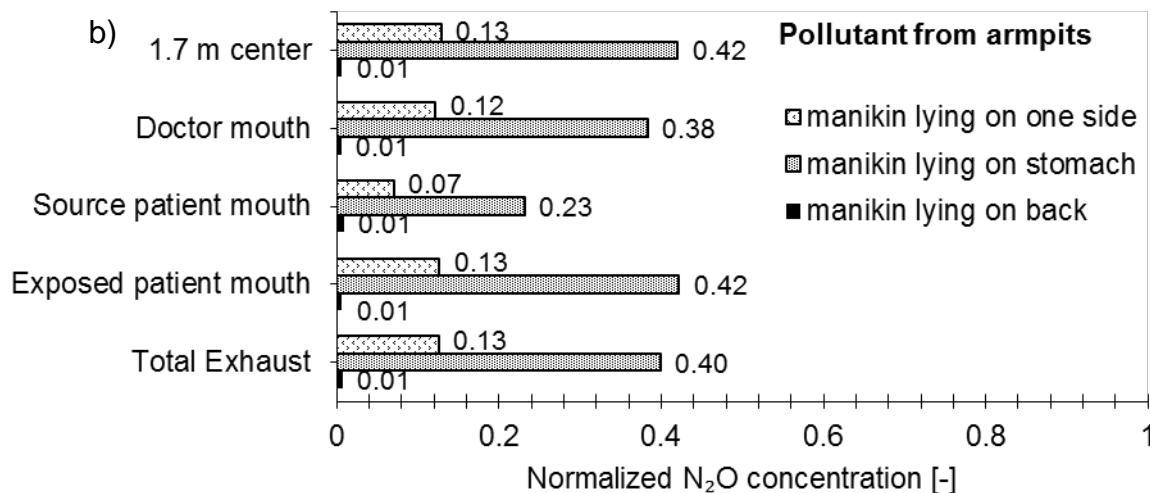
Figure 4. Comparison of the normalized concentration in the six measuring locations for the three different lying positions of the manikin and for the pollution sources: a) patient's feet and b) patient's armpits. The results were obtained at 1.5 ACH using the VM with ESA = 0.13 m^2.

The results of the present study show the ability of the ventilated mattress to successfully reduce exposure to gaseous contaminants when released from the body of a lying person. As shown in Figure 2, mixing ventilation alone is not able to completely dilute the bioeffluents emission from feet even when the ventilation rate in the room is 6 ACH. Similar result reported by Bivolarova et al. (2014) was obtained when the pollution source was the armpits of the patient.

In hospitals about 74% of all the building energy is utilized by the HVAC system (ASHRAE HVAC Design Manual for Hospitals and Clinics, 2013). For a general patient room ASHRAE Standard 170-2008 recommends overhead mixing type ventilation with up to 6 ACH. The findings in the current study show that the implication of the VM in hospitals can be an effective solution in minimizing the exposure to patients' bioeffluents at 4 times lower room ventilation rate. In Figure 2 the pollution concentration in the room was almost zero when the air change rate was only 1.5 ACH (27 L/s) and the ventilated mattress was operating at 1.5 L/s compared to the pollution concentration when the room was ventilated at 6 ACH (109 L/s) without the VM operated. It is therefore likely that such localized ventilation exhaust strategy as the VM will lead to substantial energy savings due to less air (only 1.5 L/s) used by the mattress to exhaust the air pollutants. Further studies, which take the energy use into account, will need to be undertaken.

The tested local exhausts of the mattress were both quite efficient in evacuating the generated bioeffluents before spreading into the room air. According to the results the most efficient local exhaust was the one under the pelvis with bigger surface area of 0.13 m^2 (Figure 3). There exist textile materials that are suitable to clean different gaseous contaminants including unpleasant odours generated from people (Bivolarova et al., 2014b, Mizutani et al., 2014). Thus the local exhaust of the VM can be made of such material and also provide cleaning of the polluted air. In this way the sucked polluted air by the VM will be cleaned locally and will be discharged back into the room allowing flexibility and further energy utilization.

The position of the source patient had effect on the spread of body emitted pollutants from armpits and feet. When the tracer gas was released from the armpits the concentration in all six measuring locations was the highest for when lying on stomach (Figure 4b). It is possible that when the manikin was position to lie on its stomach, bigger area of the exhaust opening of the mattress was blocked because of the different body curvature. This can be solved by designing a larger exhaust opening along the mattress.

CONCLUSIONS

The present study was designed to determine the effect of using the ventilated mattress to reduce the exposure indoors to body emitted bioeffluents. This study has shown that the VM is highly efficient advanced ventilation method for local pollution control. The VM combined with mixing ventilation at 1.5 ACH has proved to be more effective in reducing exposure to body contaminants compared to mixing ventilation alone at either 3 or 6 ACH. Thus, it seems that the use of VM in health care settings has a potential to reduce the energy consumption for such buildings.

The size of the exhaust opening of the VM and the lying position of the person on the mattress affect the Pollutant Extraction Efficiency of the mattress. It is recommended to use large local exhaust openings in the mattress.

ACKNOWLEDGEMENT

REFERENCES

ASHRAE (2008) Ventilation of healthcare facilities, Technical Report BSR/ASHRAE/ASHE Standard 170-2008, American Society of Heating, Refrigerating, and Air-Conditioning Engineers, Inc.

ASHRAE (2013) HVAC Design Manual for Hospitals and Clinics. 2nd Edition.

Bivolarova MP, Melikov AK, Kokora M et al. (2014a) Novel bed integrated ventilation method for hospital patient rooms. In Proceedings of ROOMVENT 2014, 13th SCANVAC International Conference on Air Distribution in Rooms. pp. 49-56.

Bivolarova MP, Mizutani C, Melikov AK et al (2014b) Efficiency of deodorant materials for ammonia reduction in indoor air. In Proceedings of Indoor Air 2014. International Society of Indoor Air Quality and Climate. pp. 573-580.

Bolashikov ZD (2010) Advanced Methods for Air Distribution in Occupied Spaces for Reduced Risk from Air-Borne Diseases and Improved Air Quality, Ph.D. thesis, R-239,BYG, DTU, Denmark

Melikov AK, Bolashikov ZD, and Georgiev E (2011) Novel ventilation strategy for reducing the risk of airborne cross infection in hospital rooms. *Proceedings of Indoor Air 2011*, June 5–10,Austin, TX, Paper 1037.

Mizutani C, Bivolarova MP, Melikov AK et al 2014 Air cleaning efficiency of deodorant materials under dynamic conditions: effect of air flow rate. In Proceedings of Indoor Air 2014. International Society of Indoor Air Quality and Climate. pp. 745-749.

PAPER IV
Bivolarova, M., Melikov, A. K., Kokora, M., & Bolashikov, Z. D., 2014. Local Cooling of The Human Body Using Ventilated Mattress in Hospitals. In Proceedings of ROOMVENT 2014, 13th SCANVAC International Conference on Air Distribution in Rooms, October 19-22, 2014, Sao Paolo, Brazil, p. 279-286.

LOCAL COOLING OF THE HUMAN BODY USING VENTILATED MATRESS IN HOSPITALS

Mariya Bivolarova[1], Arsen Melikov[1], Monika Kokora[1,2] and Zhecho Bolashikov[1]

[1]International Centre for Indoor Environment and Energy, Department of Civil Engineering, Technical University of Denmark, Kgs. Lyngby, Denmark.

[2]Department of Environmental Engineering, Warsaw University of Technology, Warsaw, Poland.

Abstract

A series of experiments were conducted in order to examine the cooling of the human body in bed equipped with a ventilated mattress (VM). The experiments were performed in a climate chamber (4.65 m width x 5.3 m length x 2.6 m height) which was air-conditioned by mixing ventilation system. A thermal manikin lying in the bed with the VM was used to simulate a person. The surface temperature and heat loss of the thermal manikin were controlled to correspond to those of an average person in a state of thermal comfort. The local cooling effect of the VM was studied at room air temperatures of 23, 26 and 30 $^{\circ}$C. The performance of the VM was tested when VM was operating at different air flow rates (1.5, 3, 4.5 and 6 L/s). The impact of body covering on the cooling effect from the VM was also studied. The performance of the cooling method was evaluated based on comparison of the segmental and whole body equivalent temperature (t_{eq}) with those determined at the reference temperature of 23 $^{\circ}$C or when at the same room temperature with VM not in operation. The obtained results reveal that the body segments in contact with the VM were cooled, especially the back side and the back. The cooling effect increased with the increase of the airflow rate through the VM. These results suggest that in warm environment the VM may improve thermal comfort of people lying in bed. The use of the VM may lead to energy saving by operating the background ventilation system at elevated set point for the room temperature or by use of natural ventilation. However the non-uniform body cooling may cause local thermal discomfort. This needs to be further studied in human subject experiments.

Keywords: Local cooling, Ventilated mattress, Bed thermal comfort, Hospital environment

1   Introduction

On average people sleep eight hours every day. The quality of sleep affects peoples' work performance and well-being. In some premises such as hospitals, elderly homes, etc., some occupants spend most of their time lying in bed. The indoor environment, including their thermal comfort affects their health conditions. High room temperatures can result in reduced quality of sleep.

Large amount of energy is used in buildings. Substantial part of this energy is used for generating healthy and comfortable environment indoors. Energy saving policies has been introduced in many countries. In warm climates and seasons when outdoor temperature is high air conditioning is used to keep the room temperature within the comfortable range specified in the standards (EN 15251 2007, ASHRAE 55 2013). This however is not energy efficient because the air in the entire room volume, most of which is not occupied, is conditioned. One energy saving strategy suggested in the standards (EN 15251 2007, ASHRAE 55 2013) is to keep operative temperature indoors high and to provide occupants with thermal comfort by air movement at elevated velocity. However as reported by Melikov et al. (2012) in warm environments elevated velocity is not efficient method to provide people lying in bed with thermal comfort. Generating comfortable bed micro-environment may save energy.

Melikov et al. (2012) reported on improved bed micro-environment by water cooled mattress and bed ventilation simulated by a flexible pipe providing air bellow the quilt from the side of feet. In this paper cooling provided by a ventilated mattress with air flow through the mattress was studied.

2   Method

2.1   Experimental set-up

Full-scale experiments were performed in a climate chamber with dimensions: 4.65 m (width), 5.3 m (length), and 2.6 m (height). Overhead mixing air distribution (MV) was used to supply 100% outdoor air to the chamber through a three –way square diffuser mounted in the middle of the ceiling. No recirculation was used during the experiments. The air was exhausted through two perforated square diffusers located symmetrically on the ceiling.

A thermal manikin was used to simulate lying patients in a bed. The bed had dimensions 0.9 m x 2.0 m x 0.8 m (W x L x H) and had a mattress with thickness of 0.06 m. The mattress was covered with a thin cotton sheet. The thermal manikin has the physics of an average Scandinavian female with a height of 1.68 m and size 38. The manikin consists of 23 body parts. Each body segment was individually controlled to maintain surface temperature equal to the skin temperature of an average person in a state of thermal comfort. The manikin was lying in the bed on its back. The manikin was dressed in a short-sleeve hospital pyjama (clothing isolation was 0.60 Clo). The layout of the test chamber is shown in Figures 1 and 2.

A ventilated mattress (VM) was placed on top of the regular mattress (Figure 1). Air was drawn through the ventilated mattress from an exhaust opening at the feet area of the manikin. The dimensions of the exhaust opening were 0.8 x 0.16 m^2. The exhaust opening was covered with textile mesh with free area ratio of approximately 90%. There was a mesh inside the ventilated mattress which provided support and allowed the exhaust air to move through the whole mattress. For the purpose of the experiments the VM was connected to a separate exhaust system having an axial fan outside of the chamber via a flexible duct (Ø 80 mm). The exhaust flow rate of the VM was regulated by changing the frequency of the fan and by adjusting the damper installed in the duct connected to the VM. In order to adjust the desired airflow rate exhausted from the VM two air flow sensors were installed in the duct.

2.2   Experimental conditions

The ability of the ventilated mattress to cool the thermal manikin lying in the bed was examined at numerous combinations of the flow rate through the mattress (1.5, 3, 6 and 10 L/s), room air temperature (23, 26 and 29 ℃) and different body covering (body covered with sheet (0.32 clo), with light quilt (3.2 clo) and without body covering). During the experiments the background room ventilation was set at 1.5 air changes per hour. The relative humidity in the chamber was not controlled; it was measured to be in the range of 25 – 40%.

2.3   Data analyses and presentation

Heat loss from the segments and whole body of the thermal manikin as well as their surface temperature was measured. The collected data were used to calculate the equivalent temperature, t_{eq}, for the segments and the whole body. The equivalent temperature is defined as "The uniform temperature of the imaginary enclosure with air velocity equal to zero in which a person will exchange the same dry heat by radiation and convection as in the actual non-uniform environment" (SAE 1993, ISO 2004). The segmental and whole body cooling effect of the ventilated mattress was assessed by the change in the equivalent temperature determined for the studied condition compared to the equivalent temperature, $t_{eqi,ref}$, determined at a given reference condition. The calculations were made in two ways as presented in equations 1 and 2:

$$\Delta_{teq1} = t_{eq,i} - t_{eqi,ref1} \tag{1}$$

$$\Delta t_{eq2} = t_{eq,i} - t_{eq,ref23} \qquad\qquad (2)$$

Where $t_{eq,i}$ and $t_{eqi,ref1}$ (ºC) is the segmental or whole body equivalent temperature determined for the same room air temperature respectively with and without ventilated mattress in operation; $t_{eqi,ref23}$ (ºC) is the segmental or whole body equivalent temperature determined without ventilated mattress at 23 ºC. Δt_{teq1} is a measure for the cooling performance of the ventilated mattress while Δt_{eq2} may be used to assess the thermal comfort provided with the ventilated mattress at elevated temperature compared to comfortable temperature of 23 ºC without additional cooling of the body. Negative values of Δt_{teq1} mean that the mattress increases the heat loss from the body, i.e. provides cooling. Negative values of Δt_{teq23} mean that people will report cooler thermal sensation compared to that at 23 ºC without mattress and positive values will mean warmer thermal sensation.
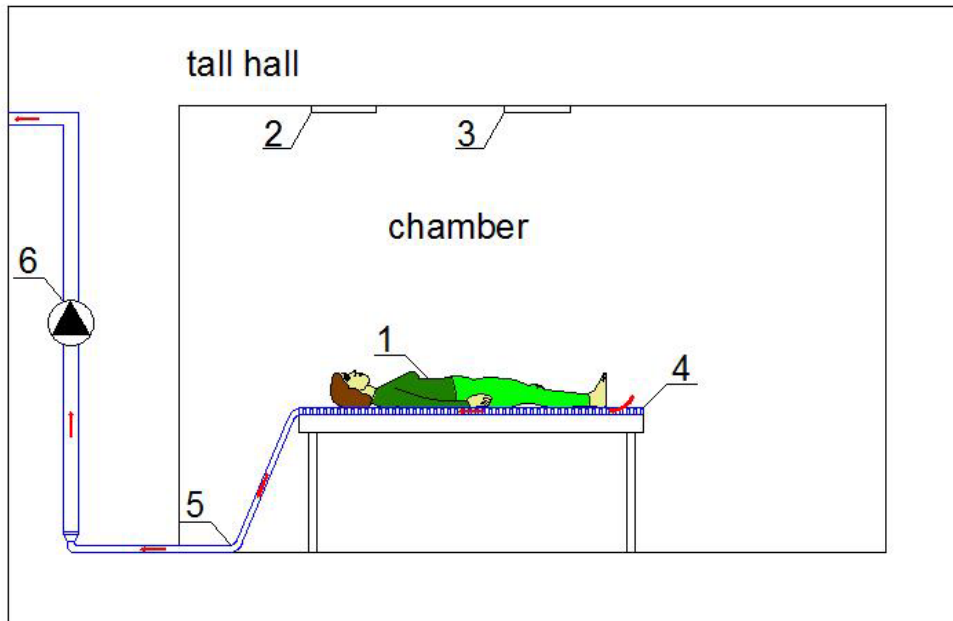

Figure 1. Side view sketch of the experimental set-up in the chamber: 1 –lying patient, 2 – exhaust diffusers, 3 – supply diffuser, 4 – the ventilated mattress, 5 – exhaust duct from the ventilated mattress, 6 – axial fan.

3 Results and Discussion

Figure 2 shows the change of the equivalent temperature, Δt_{teq1}, as a result of the use of the mattress. The results obtained at 23, 26 and 29 ºC and flow rate of 1.5, 3 and 6 L/s (also 10 L/s at 29 ºC) through the mattress when the manikin was covered with a sheet are shown. As expected the results reveal that the body segments in contact with the ventilated mattress were cooled. The head region (crown, left and right face and the back of neck) were almost not affected by the cooling provided with the VM. The results show that the cooling from the mattress decreased with the increase of the room temperature. Increase of the ventilation flow through the mattress increased the heat loss from most of the body segments. Back side (lower back) and the back were the most cooled body segments.

The importance of manikin's body covering on the cooling provided by the VM was studied as well. Results obtained with the VM at different flow rate and room air temperature was compared when the manikin's body was not covered, when it was covered with sheet and when it was covered with light quilt. The use of body covering increased the cooling from the VM at 23, 26 and 29 ºC. The increase of the cooling effect was observed for the whole body and all body segments except the head

region that was not covered. The body cooling increased when the thermal insulation of the covering increased (Figure 3, sheet and light quilt). Figure 4 compares the results obtained at 23 °C.

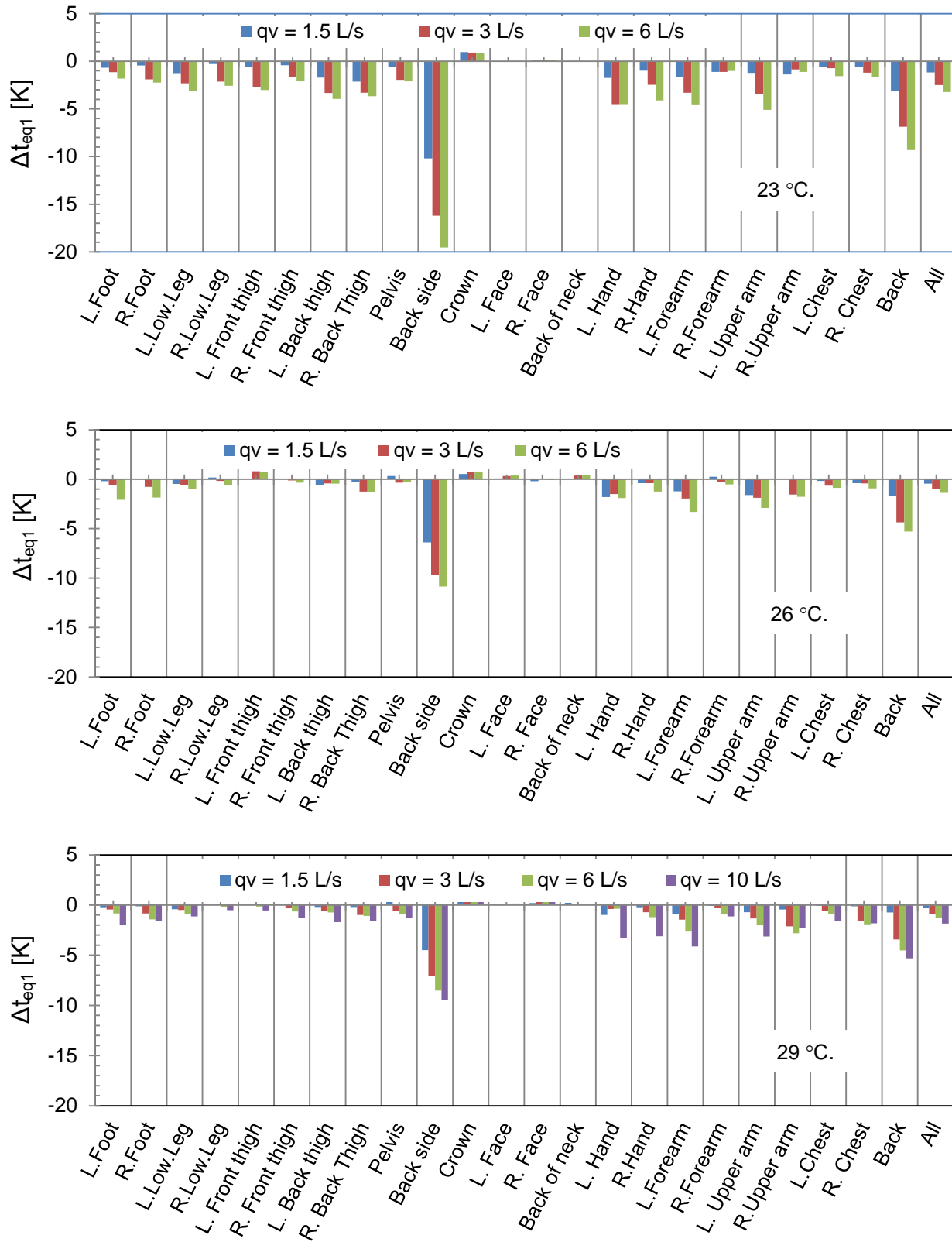*Figure 2. Change in the equivalent temperature, Δ_{teq1}, for manikin's segments and whole body at different flow rates and room air temperature with VM in operation. Manikin covered with sheet.*
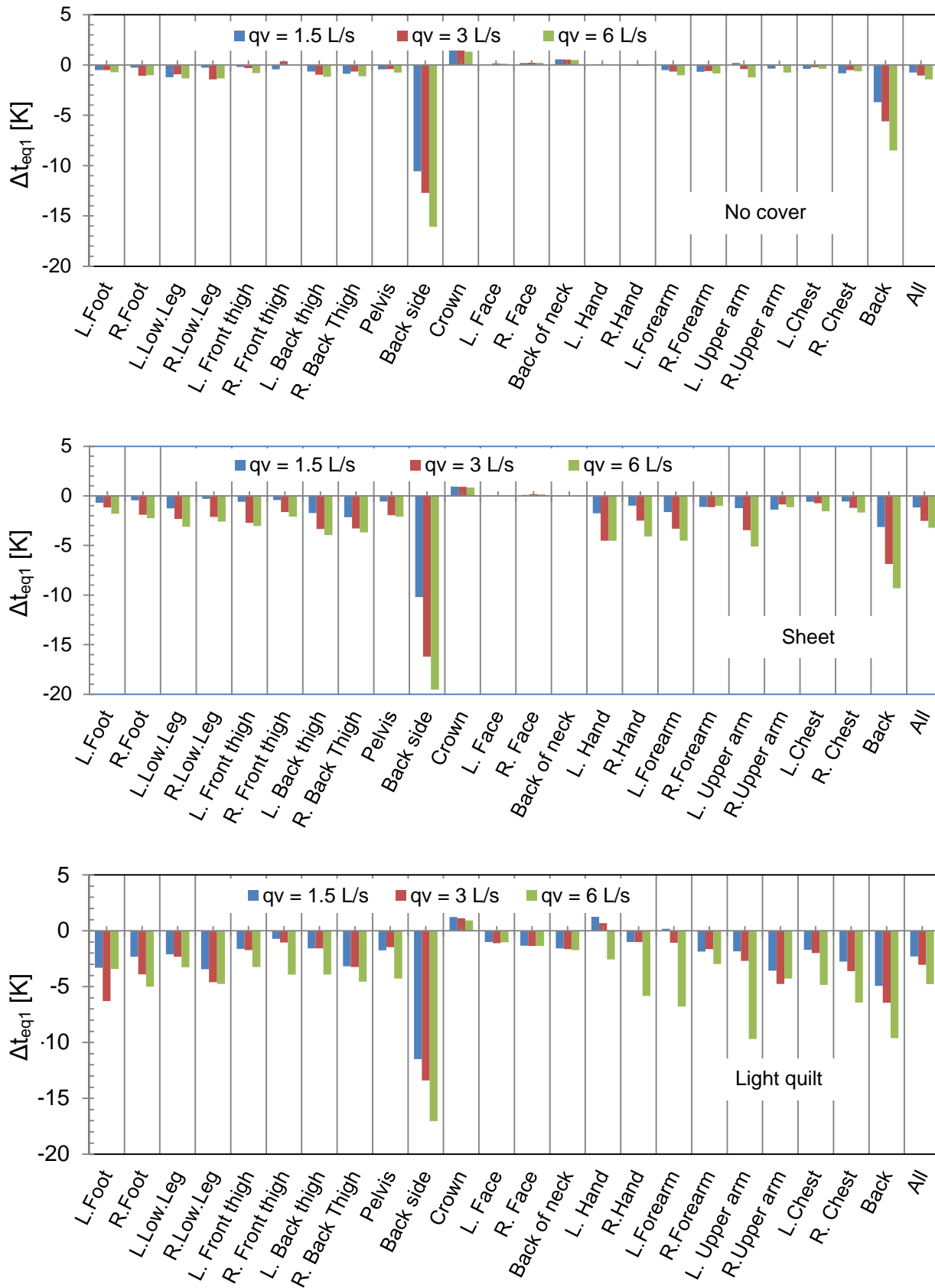
Figure 3. Change in the equivalent temperature, Δ_{teq1}, for manikin's segments and whole body at different flow rates and body covering with VM in operation. Room air temperature at 23 °C.

The ability of the VM to improve a person´s thermal comfort at elevated room temperature to the thermal comfort level at comfortable temperature of 23 °C was assessed with the change in the equivalent temperature Δt_{eq2}. Some of the obtained results are shown in Figure 4. The results in the figures show that the increase of the room temperature will make the person lying in bed with the VM in operation to feel warmer than at 23 °C. This thermal sensation will be felt for the body as a whole and for all body segments except the back side and the back. The results suggest that at these two body parts, especially at the back side, a person in a bed with VM will feel locally cooler than at 23 °C. The analyses of the results reveal that at 26 °C and 29 °C a person lying in a bed with VM will feel cooler when his/her body is covered with sheet compared to when the body is not covered.

Figure 4. Change in the equivalent temperature, Δt_{eq2}, at room air temperature of 26 °C *compared to at room air temperature of* 23 °C. *VM in operation. Results when the body is covered with sheet and not covered are shown.*

4   Discussion

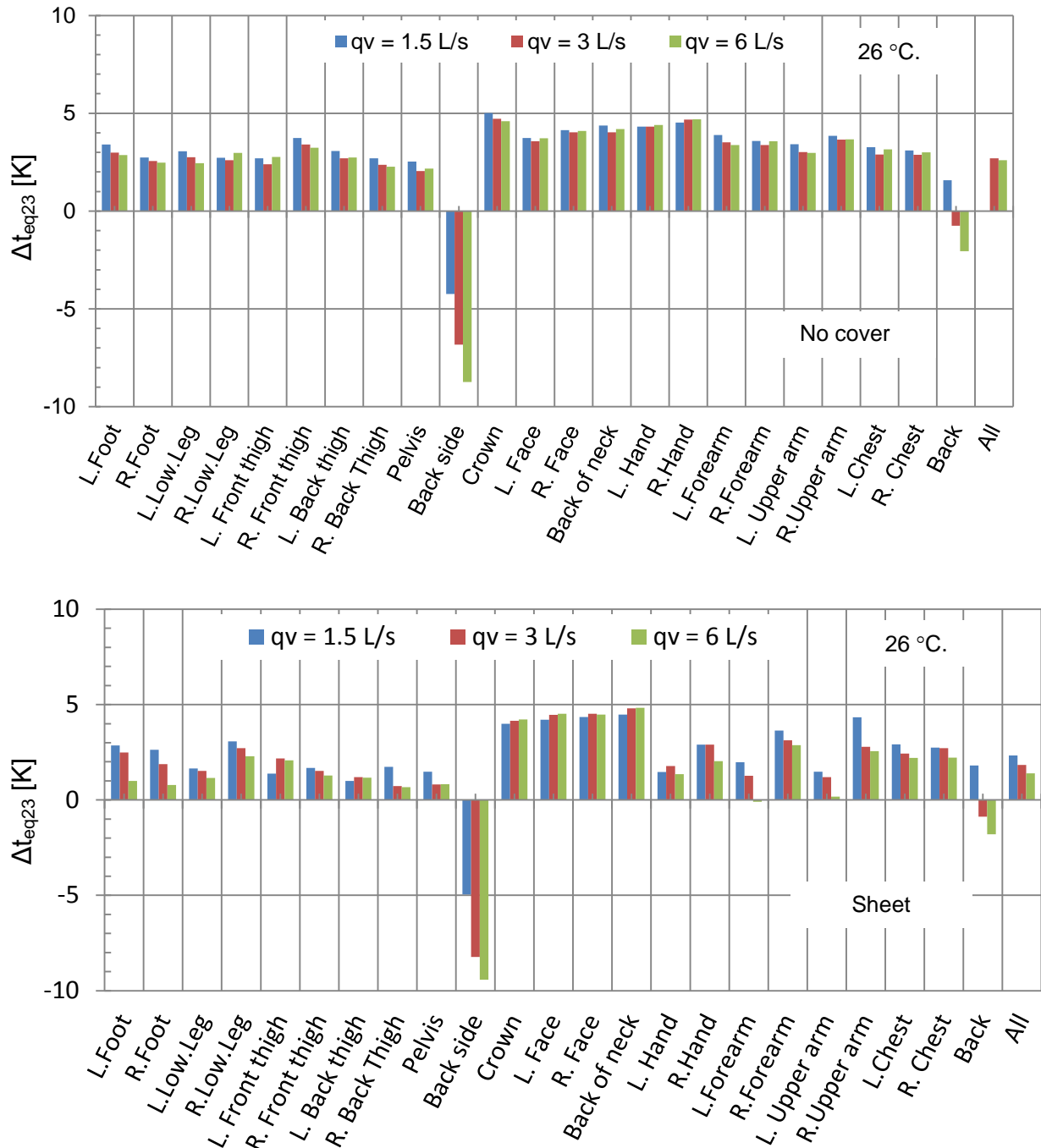The results of the present study reveal that the ventilated mattress provides body cooling. Only the head region isolated from the mattress with pillow was not cooled. The cooling increased with the increase of the airflow rate through the mattress and decreased with increase of the room temperature. All body segments in contact with the mattress were cooled. Covering the manikin's body with sheet or light quilt increased the cooling of the manikin's body segments when the VM was in operation. The back side and the back of the thermal manikin were cooled intensively since most of their surface area was in contact with the mattress. For the remaining cooled body segments only relatively small part of their surface area was in contact with the VM and cooling was measured mainly when manikin's body was covered, e.g. with sheet. The cooling was equal to that obtained by decrease of the room air temperature by several degrees, between 4 and 20 K for the lower back, 2-10 K for the back and up to 4 K for the remaining body segments (for most of them less than 1K). The cooling for the whole body of the manikin was equal to that achieved by decrease of the room temperature by up to 3 K.

The results suggest that the use of the VM at elevated room temperature will decrease the local thermal sensation at the back side and the back (not measured at 29 °C) compared to the thermal sensation at 23 °C. For the remaining body parts and for the whole body the thermal sensation will be warmer than at 23 °C. The increase of the airflow rate through the VM and covering of the body with sheet will improve the thermal sensation when the mattress is in operation and will move it toward the thermal sensation reported at 23 °C. However the large differences in local thermal sensation as a result of the non-uniform body cooling may cause discomfort. This needs to be studied in human subject experiments.

The use of the VM has potential for energy saving in warm climates and during seasons when outdoor temperature is high and cooling with mechanical ventilation is used for improving the thermal environment in rooms. In this case room temperature can be kept relatively high, i.e. the room will be less cooled, and local body cooling will be provided with the ventilated mattress in order to obtain comfortable bed micro-environment. However as already suggested this strategy needs to be verified in human subject experiments because of the non-uniform body cooling which may cause discomfort.

Hospitals, hotels, elderly homes, bedrooms, etc. are some of the premises where the VM can be used. The VM can be used for to exhaust/clean the air polluted with body bioeffluents and squama as reported by Bivolarova et al. (2014). This will lead to decrease of the needed room ventilation leading to energy saving. Thus use of the VM may improve thermal comfort of people lying in bed, increase room air quality and save energy.

5   Conclusions

The ventilated mattress provided cooling to the thermal manikin's body segments it was in contact with. The cooling increased with the increase of the airflow rate through the mattress, decreased with increase of the room temperature and increased when manikin's body was covered with sheet or light quilt. The back side and the back of the thermal manikin were cooled intensively since most of their surface area was in contact with the mattress. The remaining body segments in contact with the VM were cooled when the manikin's body was covered. The cooling effect for the whole body of the manikin was smaller than that for the segments.

Large differences in the local thermal sensation may be expected when the VM is used. Human subject experiments are needed to identify the impact of the non-uniformity in the local body cooling on the overall thermal sensation of people lying in bed and acceptability of the generated bed micro-environment.

The use of the mattress has potential for energy saving. This needs to be studied.

6   Acknowledgement

7   Reference

1. EN 15251 (2007) Indoor environmental input parameters for design and assessment of energy performance of buildings addressing indoor air quality, thermal environment, lighting and acoustics, European Committee for Standardization, Brussels.
2. ASHRAE. Standard 55: Thermal environmental conditions for human occupancy. Atlanta. GA: 2013.
3. Melikov, A.K., Li, Y., Georgiev, E., Wu, J., 2012, Bed Micro-environment in Hospital Patient Rooms with Natural or Mechanical Ventilation, Proceedings of Healthy Buildings 2012, 8-12 July 2012, Brisbane, session 10G, paper 10G.6.
4. ISO. 2004. ISO 14505-2, Ergonomics of the Thermal Environment—Evaluation of Thermal Environment in Vehicles—Part 2: Determination of Equivalent Temperature. Geneva: International Organization for Standardization.
5. Bivolarova, M.P., Melikov, A.K., Kokora1, M., Mizutani, C. and Bolashikov, Z.D., Novel bed integrated ventilation method for hospital patient rooms. Proceedings of Roomvent 2014, Sao Paulo, Brasil, Oct. 20-22 2014, paper 169.

PAPER V
Bivolarova, M., Mizutani, C., Melikov, A.K., Bolashikov, Z. D., Sakoi, T. and Kajiwara, K., 2014. Efficiency of Deodorant Materials for Ammonia Reduction in Indoor Air. In Proceedings of Indoor Air 2014, 13th International Conference on Indoor Air Quality and Climate, Hong Kong, July 7-12, 2014 , p. 573-580 p.8.

EFFICIENCY OF DEODORANT MATERIALS FOR AMMONIA REDUCTION IN INDOOR AIR

Mariya P BIVOLAROVA[1,*], Chiyomi MIZUTANI[2], Arsen K MELIKOV[1], Zhecho D BOLASHIKOV[1], Tomonori SAKOI[3] and Kanji KAJIWARA[3]

[1]International Centre for Indoor Environment and Energy, Department of Civil Engineering, Technical University of Denmark, Kgs. Lyngby, Denmark
[2]Department of Clothing and Textiles, Otsuma University, Tokyo, Japan
[3]Faculty of Textile Science and Technology, Shinshu University, Ueda, Japan.

[*]*Corresponding email: mbiv@byg.dtu.dk*

Keywords: Deodorant materials, Ammonia, Deodorant property, Indoor air purification

SUMMARY

A comparative study about the removability of ammonia gas in the air by activated carbon fiber (ACF) felt chemically treated with acid and a cotton fabric processed with iron phthalocyanine with copper (Cu) was performed in small-scale experiments. The test rig consisted of a heated plate and its purpose was to simulate surface body temperature of 34 ^{o}C. The textiles were tested at two levels of relative humidity of 25% and 80% and two air temperatures of 20 ^{o}C and 28 ^{o}C. During the experiments, the airflow supplied to the test rig was controlled at a low constant flow rate of 0.46 L/s. Results proved activated carbon fiber felt with acid to be highly efficient in removing ammonia gas. Air temperature did not have profound effect on ACF performance. However, efficiency of the carbon fiber felt decreased when relative humidity was raised from 20 to 80%.

INTRODUCTION

Human's perception of indoor air is a key factor in evaluating the quality of indoor environment as acceptable. In hospitals and healthcare facilities, it is of high priority to provide comfortable environment with good air quality for better care of patients and fast recovery. Consequently, the spread of unpleasant smells into the air coming from patients' body odor and waste can cause increased nuisance and deteriorate the perceived air quality of occupants, visitors and staff. One of the compounds that contribute greatly to the offensive odor of human waste (feces and urine) is considered ammonia (Nishida et al., 1981). Ammonia (NH_3) is irritating and smelly substance found also in human sweat (Hart, 1980).

Typical removal methods for airborne molecular contaminants including malodors act on the principle of adsorption phenomenon and chemical reaction. A commonly used adsorbent is activated carbon. Through the available materials, activated carbon fibers (ACFs) have proven to exhibit higher adsorption capacity and to have faster adsorption kinetics compared with granular or powder activated carbon (Ruy, 1990;

186

Brasquet and Le Cloirec, 1997). Moreover, by impregnating ACF with various chemicals which might react with gaseous pollutants, the adsorption capacity can be increased. ACFs are easy to handle, their high strength and stiffness, combined with their light weight, makes these fibers appropriate for high-volume applications ranging from commercial air filters to clothing goods. Nowadays, textile industry has a great potential for commercialization of air cleaning products. Recently, a novel cotton fabric processed with iron phthalocyanine with copper has been developed for air purification purposes. It has been shown that the textile is very effective in reducing gaseous pollutants among which, was also ammonia (Mizutani et al., 2013).

There are numerous studies on the performance of activated carbon to control gaseous pollutants when incorporated in air filters for HVAC systems or used in portable air cleaners (Lee and Davidson, 1999). However, the knowledge of its application as localized filter for air cleaning purposes in the vicinity of the human body is limited.

This study aims to evaluate the pollutant removal potential of two materials serving as deodorants for the odor of ammonia when applied in form of clothing or bed lining. The examined textile materials were activated carbon fiber (ACF) felt treated with acid and a cotton fabric processed with iron phthalocyanine with copper (Cu). The effect of air temperature and relative humidity on the air cleaning efficiency of three different types of textiles was investigated.

METHODOLOGIES

Samples

The textile materials used in the present study are commercially available and were provided by a Japanese company. The tested activated carbon fiber (ACF) felt was nonwoven fabric chemically treated with acid. The nonwoven textile was produced from activated pitch-based carbon fiber. The other tested materials were made of cotton fabric as one of them was treated with iron phthalocyanine with copper (Cu) (referred as ¨treated cotton fabric¨). The untreated cotton fabric was used in this study as a reference case.

Experimental set-up and procedure

Samples of ACF, cotton with iron phthalocyanine with Cu and untreated cotton fabric were cut in square pieces with area of 0.04 m^2 and comparatively evaluated for their ammonia gas removal capacity, using a test rig specially developed for this study (Figure1b). The test rig consisted of a small box attached to a heated plate maintaining surface temperature of 34 ^{o}C (average skin temperature of human body). The heated plate was made of aluminium (Al) block (0.2 width x 0.2 length x 0.05 height m) and heated by a silicon wire from inside. The heated plate was isolated from the bottom and the sides with polystyrene to allow the heat to transfer only upwards along the textile sample placed over the top. PID controller was used to keep constant temperature over the Al plate. The box attached to the Al plate was

made of plexiglas and consisted of three parts: a square chamber area having two symmetrical cone-shaped parts on each side. The dimensions of the plexiglas box are designated in Figure 1a.

The test rig was placed in a climate chamber which is equipped with a ventilation system. The temperature and relative humidity of the air in the chamber were controlled during all experiments. Air was supplied from the climate chamber to the test rig using a DC fan (0-24 V). At the start of each experiment, the flow rate inside the test rig was measured by tracer gas constant dosing method using nitrous oxide (N_2O) as a tracer gas. The supply flow rate was controlled by adjusting the fan voltage and regulating the two ball valves installed after the fan. During the experiments, the airflow supplied to the box was controlled at a low constant flow rate of 0.46 L/s, corresponding to a velocity of 0.04 m/s at the cross-sectional area of the box, where the sample was placed horizontally on the top of the heated plate (Figure 1b).
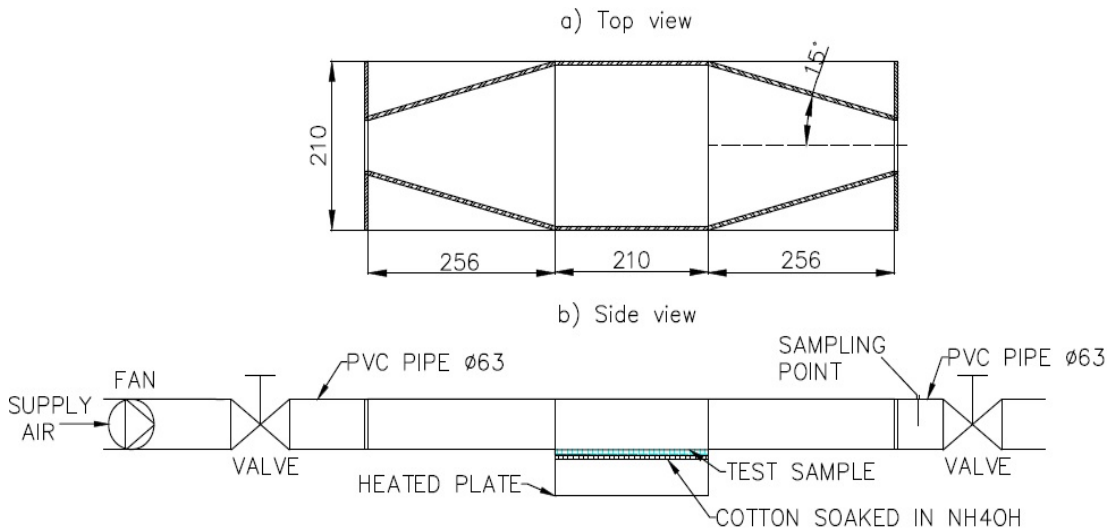

Figure 1. a) Top view of plexiglas box, the given dimensions are in millimetres; b) A schematic drawing of the experimental set-up.

To generate ammonia gas, cotton soaked in ammonium hydroxide (NH_4OH) solution was put on top of the heated plate, covering the whole surface area of the plate. Distilled water mixed with ammonium hydroxide was used to prepare 200 mL of 0.03% NH_4OH solution to achieve approximately 20 ppm initial concentration of NH_3 in the air. Prior to each experiment a fixed amount (11 g) of unused cotton was soaked in a newly prepared NH_4OH solution. The concentrations of ammonia gas were measured downstream of the tested sample. A sample fixed on a stainless steel mesh was placed over the soaked cotton. The purpose of the mesh was not to allow the tested material to be in a direct contact with the liquid NH_4OH solution. Ammonia concentration was sampled and analyzed using Innova 1303 multi-channel sampler and a photoacoustic multi-gas monitor Innova 1312.

Experiments and Test Conditions

Each sample of ACF felt with acid, treated and untreated cotton fabric was exposed to ammonia gas for 1 hour. Series of experiments were conducted under four different conditions combining low and high levels of relative humidity (25% and 80%) and air temperatures (20 and 28°C). A HOBO data-logger was used to measure and record the temperature and relative humidity during all experiments. The temperature in the chamber was regulated with an accuracy of ±0.5^{o}C and the humidity (RH) with ±5%.

Since ammonia concentration naturally decays with time during the evaporation process, control experiments without sample, i.e. only cotton soaked in aqueous NH$_4$OH were carried out under the same 4 conditions as described above.

Data Analyses

For each experiment freshly made ammonium hydroxide solution was used. The maximum concentrations of ammonia in the air varied in the range of 17 ppm - 22 ppm for the control case measurements with no sample. The same variation range of 5 ppm was noticed also in the experiments including sample. Therefore, in order to eliminate this error the obtained data were normalized to the maximum value of ammonia concentration in each condition for each different sample. The normalized data were compared in order to identify the cleaning performance of the deodorant materials. The normalized concentrations (C_i/C_{max}) for each material were calculated by the following equation:

Normalized concentration = C_i/C_{max} (1)

where C_i is the measured values of ammonia concentration and C_{max} is the maximum of the measured concentrations for each experiment.

RESULTS AND DISCUSSION

Figure 2 shows the variation of NH$_3$ concentration as a function of time for all tested materials under low air temperature and relative humidity of 20 ^{o}C and 25%, respectively. It can be seen that the highest NH$_3$ concentration decrease was achieved when using activated carbon fiber (ACF) with acid. The ACF managed to reduce the ammonia gas to almost zero concentration at the end of the experiment. When comparing the other textiles with the control case without sample, it was observed no cleaning effect. Moreover, no clear difference in the NH$_3$ concentration was found between the cotton fabric treated with iron phthalocyanine with copper and the untreated cotton fabric.
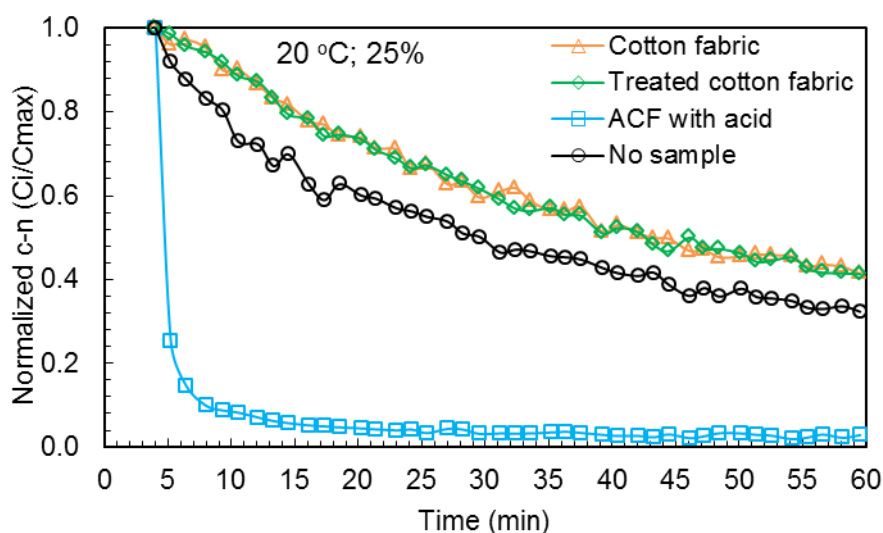
Figure 2. Normalized ammonia gas concentrations with all tested textiles and without any sample obtained at 20 $^{\circ}$C temperature and 25% relative humidity. ACF stands for activated carbon fiber. Treated cotton fabric stands for cotton fabric treated with iron phthalocyanine with copper.

Figure 3 compares the ammonia concentration for all textile samples at high air temperature of 28 $^{\circ}$C and 25% of relative humidity. The obtained results are similar to the results gained at low air temperature (Fig. 2), suggesting no impact of temperature on the performance of the tested textiles. The results demonstrate again better effectiveness of ACF in reducing the NH_3 concentration compared to the other tested deodorant materials. No effect was found in ammonia removal with treated cotton fabric when comparing with the condition with untreated cotton fabric or no sample at high air temperature.
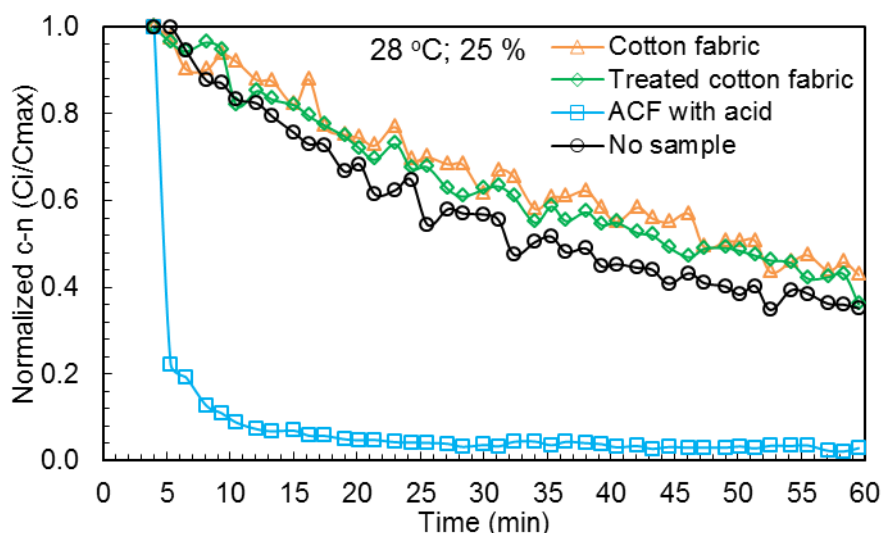
Figure 3. Normalized ammonia gas concentrations with all tested textiles and without any sample obtained at 28 ^{o}C temperature and 25% relative humidity. ACF stands for activated carbon fiber. Treated cotton fabric stands for cotton fabric treated with iron phthalocyanine with copper.

The impact of relative humidity is shown in Figures 4 and 5. The results reveal that in the case of high relative humidity (80%) the adsorption capacity of activated carbon fiber has been reduced compared to the conditions at low relative humidity, where the decay of NH_3 immediately drop to less than 0.2 after the fifth minute (Figures 2 and 3). Similar tendency in the decay curves for the other textiles is observed under the conditions with 80 % relative humidity in comparison with conditions at 25%.

Figure 4. Normalized ammonia gas concentrations with all tested textiles and without any sample obtained at 20 ^{o}C temperature and 80% relative humidity. ACF stands for activated carbon fiber. Treated cotton fabric stands for cotton fabric treated with iron phthalocyanine with copper.
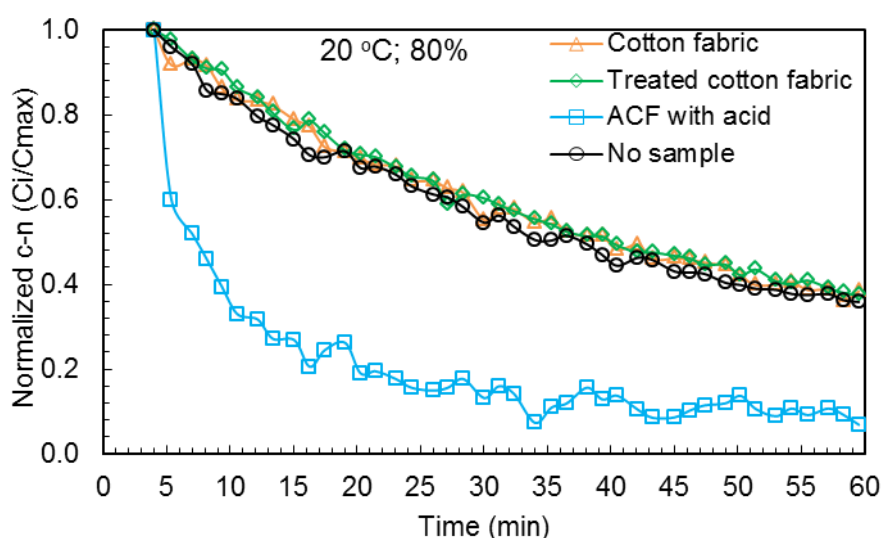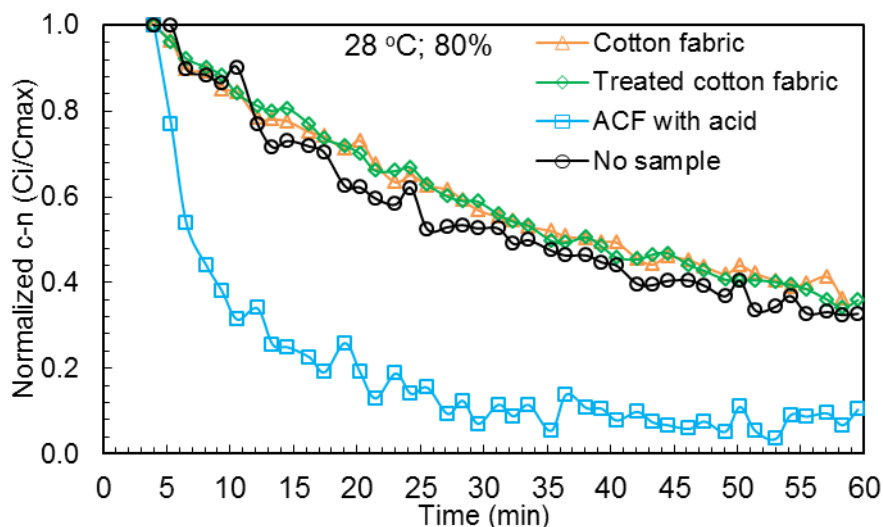
191

Figure 5. Normalized ammonia gas concentrations with all tested textiles and without any sample obtained at 28 °C temperature and 80% relative humidity. ACF stands for activated carbon fiber. Treated cotton fabric stands for cotton fabric treated with iron phthalocyanine with copper.

The conducted comparative evaluation for the removal of ammonia by different types of textile materials revealed that using activated carbon fiber felt can efficiently adsorbed the NH_3. Furthermore, it seems that temperature does not influence its performance. In contrast the results of the present study show that high humidity can lower the performance of ACF. This result is in agreement with results reported by Lee and Davidson (1999) that adsorption efficiency of activated carbon fiber decreased when increasing the relative humidity from 20 to 50%. The reason for this effect of the humidity might be due to micropores in the activated carbon being blocked by water molecules. Thus, the ammonia molecules had to compete with water vapor molecules.

As already mentioned the ACF used in this study was treated with acid. Due to the fact that ammonia reacts with different acids the deodorant effect of ACF was enhanced.

In the case of the treated cotton with iron phthalocyanine with Cu the test results show poor performance compared to the performance of ACF. However, in a recent study this material showed promising results in being able to reduce ammonia concentrations from 100 ppm to less than 20 ppm (Mizutani et al., 2013). The reported cleaning performance was obtained in a static test in which the material was brought in equilibrium with the ammonia gas without applying any air movement as in the present study. The present work indicates that even though the supply air flow in the test rig was very low, 0.46 L/s, the time for which the ammonia molecules pass through the material was not enough for a reaction to occur.

CONCLUSION

Removal of ammonia in air by commercial deodorant textiles intended for control of odors was studied using a test rig developed for the purpose of the experiments. Airflow with low ammonia concentration was used to simulate odor produced from the human body and to evaluate the deodorant efficiency of the textiles.

Activated carbon fiber felt treated with acid was efficient for the elimination of the ammonia gas. Changes in air temperature did not decrease its cleaning efficiency. However increase in relative humidity from 25% to 80% slightly decreased the efficiency of ACF. The acid blended with the fibers of the activated carbon material results in strengthening its performance.

This study showed the potential application of ACF as clothing or adapted in some other form for deodorization of air in the vicinity of human body.

REFERENCES

Brasquet C and Le Cloirec P (1997) Adsorption onto activated carbon fibers: application to water and air treatments. Carbon, 35, 1307-1313.

Hart R (1980) Human body odor. Nexus 1.

Lee P and Davidson J (1999) Evaluation of activated carbon filters for removal of ozone at the PPB level. American Industrial Hygiene Association Journal, 60, (5), 589-600.

Mizutani C, Yahata A, Tsuiki H, Morikawa H, Kajiwara K, Takahashi K, Shigeta T, Kurosawa H, Otsuka C, and Shirai H (2013) Application of Nursing Care Using Deodorant and Antibacterial Fiber. Sen'I Gakki, pp.141-145 (in Japanese).

Nishida K, Kodama T and Yamakawa M (1981) The changes in psychophysical coefficient by the composition of nightsoil. Kankyo Gijytsu, 10, 462– 473.

Ruy S K (1990) Porosity of activated carbon fibre. High Temp. – High Press., 22, 345-354.

Sato H, Hirose T, Kimura T et al (2001) Analysis of Malodorous Volatile Substances of Human Waste: Feces and Urine. Health Sci. 47 - 483.

PAPER VI

Bivolarova, M., Melikov, A.K., Mizutani, C., Kajiwara, K., and Bolashikov, Z. D., 2016. Bed-integrated local exhaust ventilation system combined with local air cleaning for improved IAQ in hospital patient rooms. Build& Environ. 2016; 100:10-18.

Bed-integrated local exhaust ventilation system combined with local air cleaning for improved IAQ in hospital patient rooms

Mariya P. Bivolarova [a, *], Arsen K. Melikov [a], Chiyomi Mizutani [b], Kanji Kajiwara [c], Zhecho D. Bolashikov [a]

[a] International Centre for Indoor Environment and Energy, Department of Civil Engineering, Technical University of Denmark, Niels Koppels Allé, Building 402, DK-2800, Lyngby, Denmark
[b] Department of Clothing and Textiles, Otsuma University, 12 Sanban-cho, 102-8357, Tokyo, Japan
[c] Faculty of Engineering and Design, Kyoto Institute of Technology, Matsugasaki, Sakyo-ku, 606-8585, Kyoto, Japan

ARTICLE INFO

ABSTRACT

The performance of a ventilated mattress (VM) used as a bed-integrated local exhaust ventilation system combined with air cleaning fabric (acid-treated activated carbon fibre (ACF) fabric) was developed and studied. The separate and combined effect of the VM and the local air cleaning for reducing the exposure to body generated bio-effluents in a hospital room was determined. Full-scale experiments were conducted in a climate chamber furnished as a single-bed patient room. Two heated dummies were used to simulate a patient and a doctor in the room. The patient was lying on a bed equipped with the VM. The patient's body was covered with either a cotton sheet or with the ACF material used as a blanket. Ammonia gas released from the patient's groins simulated the body generated bio-effluents. At the location of the groins the surface area of the VM was perforated through which the contaminated air of the bed micro-environment was exhausted. Two modes of operation were studied: 1) the exhausted polluted air was discharged out of the room and 2) the polluted air was cleaned by the ACF material installed inside the mattress and recirculated back into the room. Both modes of operation efficiently reduced the generated bio-effluents in the room with about 70%. Reduction in the exposure to body-emitted ammonia was up to 96% when the VM was operated at only 1.5 L/s and the ACF was used as a blanket.

© 2016 Elsevier Ltd. All rights reserved.

1. Introduction

Patient rooms in health care facilities, such as hospitals, require ventilation to provide a healthy and comfortable environment for patients' recovery and efficient performance of medical staff [1]. Indoor air quality (IAQ) is more critical in these facilities than in most other building environments, because of the hazardous microbial and chemical agents present (many of which airborne) as well as the increased susceptibility of the patients [1]. Studies have shown that hospital employees reported more indoor air problems and indoor air related symptoms, such as sick building syndrome symptoms, than staff employed in office buildings [2,3]. Thus, it is important to provide proper air conditioning of health care facilities in order to meet the needs of all occupants, i.e. patients, staff and visitors.

Most often, mechanical ventilation is used to condition and ventilate the various hospital units. Natural ventilation can also be applied, but there is still need to develop a detailed design and operation guide for hospital engineers and architects [4].

Efficient air distribution within a patient room will depend on many factors including: ventilation rate, choice of air distribution principle, location of the supply and exhaust air terminal devices (ATDs), heat load distribution, occupants' activities, etc. [5]. The conventional mechanical ventilation principles (mixing, displacement or unidirectional airflow distribution) are well-documented to ventilate the entire room volume. With these principles, usually high amount of air should be supplied to the space to maintain proper IAQ and to reduce the risk of airborne cross-infection. ASHRAE standard for ventilation of health care facilities [6] recommends ventilation rates for general patient rooms to be from 4

* Corresponding author.
    E-mail addresses: mbiv@byg.dtu.dk (M.P. Bivolarova), akm@byg.dtu.dk (A.K. Melikov), mizutani@otsuma.ac.jp (C. Mizutani), kajiwara@shinshu-u.ac.jp (K. Kajiwara), zdb@byg.dtu.dk (Z.D. Bolashikov).

to 6 air changes per hour (ACH) and 12 ACH for infectious wards. However, the high ventilation rates will not only increase the associated energy costs. Air velocity in the occupied zone will increase and can cause draught discomfort for occupants. Moreover, experimental studies have documented an interesting phenomenon showing that increased ventilation rate from 6 to 12 ACH in rooms increases the occupants' exposure to cough-released air [7,8]. Bolashikov et al. [7] suggested that the increased exposure to the coughed air was due to several factors: the air flow interaction in the space, the distance between the exposed person and the source (sick person), posture of the two persons, etc.

People are a source of various airborne odorous contaminants (bio-effluents) that decrease the IAQ. Some hospitalized patients spend most of their time confined to the bed, unable to frequently perform personal hygiene routines. Hence, some of the pollutants found in the air are generated from bacterial decomposition of metabolic byproducts (urine, feces and sweat). For instance, by sweating the human body regulates its temperature, but if not removed from the body, sweat can produce a strong odour contributing greatly to the scent known as body odour [9]. As mentioned, the skin microbiota plays an important role for the production of human odours, especially in the conversion of odourless sweat into sweat with its characteristic odour [10]. Some of the main components of the human sweat are ammonia and lactic acid [11,12]. Ammonia is also one of the compounds that contributes greatly to the offensive odour of human waste (feces and urine) [13]. Ammonia (NH_3) has an unpleasant odour therefore it can reduce indoor air quality and affect negatively occupants' health and perceived air quality. A questionnaire survey study shows that there is a problem with unpleasant odours in hospitals [14]. The study found that 88.5% of the nurses sensed odours in hospitals, of whom 81.0% considered it a problem and 67.2% recognized a need for improvement. Odours from excrement and urine were answered the most. In bedridden patients, patients with urinary incontinence, patients who use diapers, etc. the odours from excrements were considered the biggest problem.

In the recent years, bed-integrated advanced air distribution methods have been developed and studied for their potential application in hospitals [15–17]. One limitation of these methods is that they mainly focused on controlling and preventing the airborne transmission of infectious diseases due to human expiratory activities, i.e. breathing and coughing. The current study examines the performance of a novel bed-integrated local ventilation unit, known as "ventilated mattress", aiming for reducing the exposure to airborne contaminants (bio-effluents) generated from the lying patients' body [18,19]. Part of the surface of the ventilated mattress is designed as an exhaust opening for removing the body emitted pollutants. The idea behind the ventilated mattress (VM) is to capture and to locally exhaust the bio-effluents before they spread into the room (Fig. 1). There is a mesh inside the ventilated mattress which provides body support and allows the exhausted air to move inside the mattress.

Different filtration and air cleaning methods can be used to

Fig. 1. Ventilated mattress (VM) with two exhaust openings: below the gluteals and below the feet [18].

reduce the exposure to indoor pollutants and thus to improve the IAQ. Typical removal methods for gaseous contaminants work on the principles of physical adsorption and chemical reaction. Activated carbon is one of the most widely used adsorbents. There have been a number of studies on the performance of activated carbon for controlling gaseous pollutants, when it is incorporated in air filters for HVAC systems or used in portable air cleaners [20–23]. However little is known about its application as a localized filter for removing gaseous contaminants within the vicinity of the human body. Recent studies show that textile materials made of acid-treated activated carbon fibres (ACF) can be applied as deodorants for the unpleasant odour of ammonia [24,25]. Bivolarova et al. [24] reported that when the acid-treated ACF material was placed close to the emission source, it reduced the NH_3 gas concentration almost to zero. The ACF material is capable of adsorbing alkaline substances, such as ammonia gas, because of its acid treatment [25]. However, the material is not able to adsorb acidic substances.

The application of the VM alone or combined with local air cleaning (in this case acid-treated ACF was used) for improving the IAQ in patient rooms in health care facilities was examined. An objective of this study was to determine if the exposure to airborne contaminants generated from the body will be reduced. An important aim was to investigate if it is efficient to clean the sucked polluted air inside the mattress using the local cleaning and then discharge it back into the surrounding room air. In this way, cleaning of locally polluted air and recirculating it will improve the IAQ and reduce the needed background ventilation rate. The cleaning effect of the ACF used as a patient's body cover (blanket) was studied only to show potential applications of air cleaning materials. It was not an objective of this study to examine the properties of the ACF material.

2. Methods

2.1. Experimental set-up

The experimental measurements were carried out in a stainless steel climate chamber furnished with a single-bed to simulate a hospital patient room. The dimensions of the chamber were as follows: length − 3.6 m, width − 2.5 m and height − 2.5 m. The climate chamber was air conditioned using underfloor air distribution supplying 100% outdoor air at 10 L/s (equal to1.6 ACH), corresponding to the minimum requirement of supply air flow rate per person or bed for patient rooms, as proposed in the FprCEN/TR 16244 technical report for hospital ventilation [26]. During the measurements, three fans were constantly operating to generate complete mixing in the chamber. The room air was exhausted through a circular opening located on the ceiling (Fig. 2).

Two heated dummies were used to simulate a lying patient and a standing doctor next to the patient's bed. The standing dummy was positioned 0.2 m from the side of the bed near the head of the lying dummy, Fig. 2. Each dummy consisted of 3 parts − "legs", "torso" and "head". The head and legs were made from circular ducts with diameters of 0.2 m and 0.12 m, respectively. The torso was made from a duct of rectangular cross section with dimensions 0.6 m × 0.35 m × 0.2 m (H × L × W). The total height of dummies was 1.65 m. Inside each dummy, six light bulbs were operating during the experiments. One bulb was installed in the head, one in the torso and 2 bulbs per each leg. A fan was also positioned in the torso for better mixing of the heated air and thus creating a uniform temperature distribution over the whole surface area of the dummy. The total generated heat power was 62 W for the "patient" and 130 W for the "doctor" corresponding to the metabolic heat load of a lying person in rest and standing person in rest,
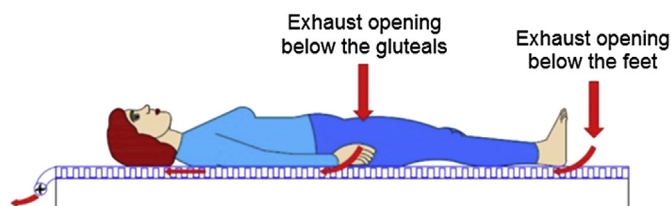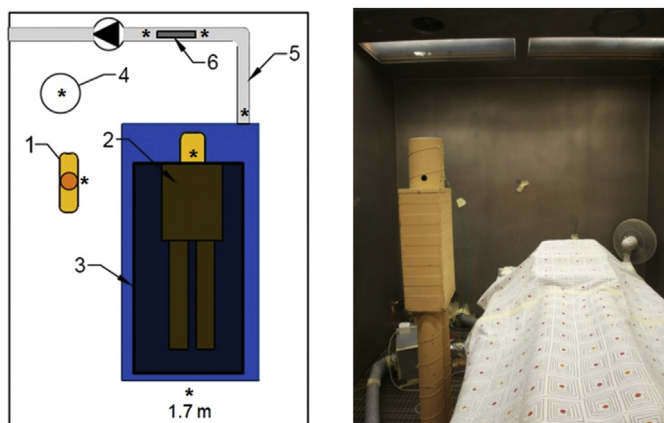
Fig. 2. Experimental setup: (left) Floor plan of the chamber showing the position of the sampling gas tubes (*), where 1 − "doctor", 2 − "patient", 3 − a double bed sheet or ACF material used as a blanket, 4 − total exhaust opening, 5 − exhaust duct of the VM connected to a fan, 6 − 'duct ACF' position; (right) Interior of the chamber with the standing dummy next to the bed with the ventilated mattress and the lying dummy covered with a sheet.

respectively. During the experiments, the legs and the torso of the lying dummy were fully covered with a double bed sheet or in some cases with a piece of the ACF material used as a blanket. In reality, the human body shape is more complex than the simplified figure of the dummy. Therefore, additional small wooden blocks were placed on top of the torso of the lying dummy to create small gaps between the chest and the sheet covering the lying person.

The studied ventilated mattress (VM) was placed on top of the regular mattress of the bed. The exhaust opening of the VM was located under the area where the legs of the dummy were connected to the torso (i.e. corresponding to the gluteal region of a human body). The dimensions of the local exhaust opening were: 0.8 m × 0.16 m (L × W). The exhaust opening of the VM was covered with a polyester mesh with free area ratio of about 90%. The surface of the VM was made of synthetic fibre (polyester), which is permeable for air. Thus, the mattress was sealed in nylon from everywhere but the exhaust opening, in order to assure that the exhausted air passed only through the exhaust opening.

The VM was connected to a separate exhaust system. A small axial fan, placed inside the chamber, was connected with a straight duct (ø 0.08 m) to the VM. Through this separate system the ammonia gas was exhausted from the mattress and discharged out of the chamber. In one experiment (Table 2, case number 5, recirculation case), the exhausted air mixed with ammonia gas was discharged back into the chamber after it was locally cleaned by the ACF material installed within the mattress. The local airflow rate through the VM was measured with the help of an air flow sensor (MFS-C-080) installed in the straight connection between the fan and the VM. The MFS sensor was installed by following the recommendations of the manufacturer to ensure correct readings. The maximum error in the measurement with this sensor is ±3% of the actual flow. The pressure difference at the MFS sensor was measured with a differential pressure micro-manometer FCO510 (accuracy of 0.01 Pa [0.15 × 10−5 psi] ±0.25% of reading). The required flow rate was then adjusted by a manually operated damper, based on the pressure difference readings from the micro-manometer. During the experiments when the ventilated mattress was in operation its exhaust air flow rate was kept constant and equal to 1.5 L/s.

The used activated carbon fibre (ACF) material was nonwoven fabric that had been chemically treated with acid. The nonwoven textile was produced from activated pitch-based carbon fibre. The

properties of the studied ACF material are given in Table 1. In this study, the ACF material was: 1) installed as two single rectangular sheets inside the mattress below and above its mesh like a "sandwich" (Fig. 3); 2) a rectangular piece of the ACF fabric was attached to a cylindrical frame which was installed in the exhaust duct of the mattress (Fig. 4) or 3) the ACF fabric was used as a patient's cover/blanket. The size of each sheet of the "sandwich" ACF was 0.8 × 0.87 m^2 (L × W), and the size of the ACF material attached to the cylindrical frame was 0.37 × 0.13 m^2 (L × W). The cylindrical frame had a diameter of 0.037 m and it was placed in the straight section of the exhaust duct of the ventilated mattress before the fan allowing the airflow along the duct to "wash" the ACF material along its two surfaces. The size of the ACF material that was studied as a blanket was 1.54 m (width) × 1.95 m (length). In order to hold the ACF cover on top of the dummy, a regular double sheet was placed on top of the ACF cover. For every case with the ACF material, a new sample was used at the start of the experiment.

To simulate body generated bio-effluents, ammonia gas was released from the lying dummy's "groin" area. A specially designed gas-generator system was used to release the ammonia gas. The gas generator consisted of two gas washing bottles each having an inlet and an outlet nozzle. The inlets were connected to a diaphragm pump, which was supplying fresh air to the washing bottles. The configuration is shown in Fig. 5. The air flow rate of the pump was kept constant (0.2 L/min) and controlled by a gas Rotameter. To generate ammonia gas, each washing bottle contained 300 mL distilled water mixed with 35.3 mL of 28% ammonium hydroxide (NH_4OH) solution. The two outlets of the washing bottles were connected through tubes to a perforated plastic ball in order to provide a uniform spatial dispersion of the generated ammonia gas. An Innova 1412 Photoacoustic Gas Monitor was used to monitor the NH_3 concentration released from the plastic ball in order to ensure that the NH_3 concentration was in the desired range. The Gas Monitor was calibrated prior to the experiments and was able to measure ammonia gas up to 6000 parts per million (ppm). The measured NH_3 gas concentration at the point of release was approximately 5400 ppm (with a relative error of 2%) throughout the whole experiment. In this study, considering the detection limit (0.1 ppm) of the gas Monitor, the tracer gas was dosed at 5400 ppm in order to achieve high enough background concentration of the NH_3 gas in the chamber and be able to identify the effect of the VM and the local cleaning. In practice, the bio-effluent concentrations may be much lower and measured in ppb [27].

The air in the chamber, which was mixed with the ammonia gas, was sampled by two Innova 1303 Multipoint Samplers and its ammonia gas concentration was analysed using a second Photoacoustic Gas Monitor Innova 1312 connected to the two Innova 1303 Samplers. Each of the Innova 1303 samplers had 6 channels. The sampling time of the Innova 1312 was 40 s/channel and 12 channels were measured in sequence, giving a period of 8 min between measurements in the same location. The Innova gas analyser was calibrated prior to the experiment and its lower detection limit for NH_3 gas was 0.1 ppm. The measuring error of the instrument was 5% of the actual value. The NH_3 concentration in the chamber was measured at the breathing zone (BZ) of both the "doctor" and the "patient", at the total exhaust opening, and at 1.7 m height 0.2 m from the patient's legs. The ammonia gas was sampled in the exhaust duct of the VM, downstream of the "sandwich" ACF, and downstream and upstream of the duct ACF material (Fig. 2). The rest of the channels were placed in several positions outside the chamber as a control measure during the experiment to check if there were leakages from the chamber. No leakages were measured. No NH_3 was measured in the supply air as well.

Table 1
Properties of the acid-treated activated carbon fibre material.

Specific surface area (m^2/g)	Pore volume (mL/g)	Pore diameter (nm)	Thickness (μm)	pH level of the acid
1350	0.6	1.9	17	3

Table 2
Experimental conditions.

N°	Conditions at low RH = 25%
1	'1.6 ACH' (reference case)
2	'1.6 ACH + VM'
3	'1.6 ACH + VM + duct ACF'
4	'1.6 ACH + VM + "sandwich" ACF'
5	'1.6 ACH + VM + "sandwich" ACF + recirculation'
6	'1.6 ACH + ACF cover'
7	'1.6 ACH + VM + ACF cover'
	Conditions at high RH = 70%
8	'1.6 ACH'
9	'1.6 ACH + VM + "sandwich" ACF'
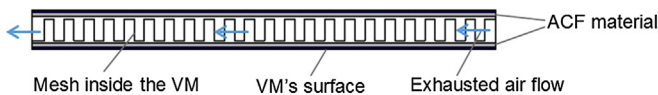
Fig. 3. Diagrammatic representation of the "sandwich" ACF material installed inside the VM.
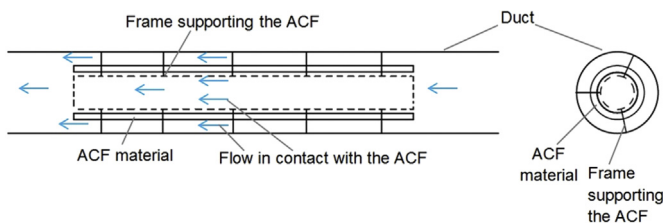
Fig. 4. Diagrammatic representation of the duct ACF material installed inside the exhaust duct connected to the VM.
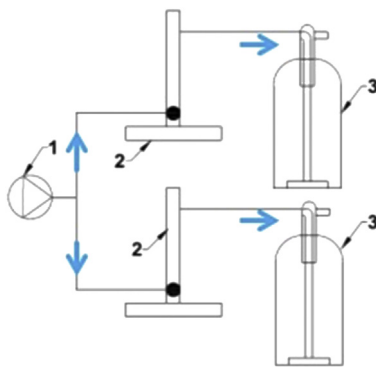
Fig. 5. Diagrammatic representation of the NH_3 gas generation setup, where 1 – pump, 2 – gas Rotameter and 3 – washing bottle with NH_4OH solution.

2.2. Experimental conditions

The chamber was ventilated with 1.6 ACH during all the measurements. The temperature inside the chamber was 29 ± 1 °C. This temperature was in the range recommended in standards and guidelines for patient rooms (20–32 °C). For instance, conditions of 32 °C air temperature and 35% relative humidity has been found beneficial in treating certain types of arthritis [5]. An air temperature of 32 °C is sometimes kept for burn patients and 30 °C in paediatric surgery [5]. Furthermore, a study on the performance of the method under high room air temperatures is important when considering perceived air quality which, decreases with increase of air temperature and humidity [28]. The ASHRAE standard 170-2013-Ventilation of health care facilities recommends a maximum of 60% RH in patient rooms [6]. However, in countries with hot and humid climate (e.g. Singapore, Malaysia, Japan, etc.) this recommendation might be difficult to fulfil. Yau and Chu [29] reported that the air temperature in two Malaysian hospitals varied in the range of 20–32.2 °C and the measured RH varied in the range of 44%–79%. Thus, considering the possible practical applications of the studied method, the relative humidity in the chamber was controlled and kept in some experiments at 25% (with ±5% relative error) and in some at 70% (with ±6% relative error). A HOBO datalogger was used to measure and record the relative humidity in the chamber with an uncertainty of 2.5%. The air temperature in the chamber was measured by an air temperature sensor with an uncertainty of 0.3 °C as described by Simone et al. [30]. The output from the sensor was logged by a portable data logger.

The experimental conditions comprised (Table 2): 1 – background ventilation alone at 1.6 ACH, without the VM was working ('1.6 ACH'); 2 – the ventilated mattress was operating without using the ACF material ('1.6 ACH + VM'); 3 – the VM working and the ACF material installed on the cylindrical frame placed inside the exhaust duct of the VM ('1.6 ACH + VM + duct ACF'); 4 – the VM working and having the ACF material installed as a "sandwich" ('1.6 ACH + VM + "sandwich" ACF'); 5 – the VM working having the ACF material installed as a "sandwich" with recirculation of the air exhausted by the VM back into the chamber ('1.6 ACH + VM + "sandwich" ACF + recirculation'); 6 – using only the ACF material as a cover, i.e. the VM was not working, ('1.6 ACH + ACF cover'); 7 – the VM working in conjunction with the ACF used as a cover ('1.6 ACH + VM + ACF cover'). The effect of relative humidity of the room air on the cleaning efficiency of the ACF material was studied at 25% and 70% RH (experimental conditions 8 and 9, Table 2).

2.3. Experimental procedure and exposure assessment

The total volume ventilation system and the two dummies were switched on all the time to keep the air temperature in the chamber stable. Prior to the experiments with the ventilated mattress in operation, the air flow rate through the mattress was adjusted to 1.5 L/s. The experiments were started after reaching steady state level of the desired relative humidity. When used, the ACF was set to the desired position prior to the experiment. Afterwards ammonia gas dosing was started. For each condition a newly prepared NH_4OH solution was used.

One experimental condition lasted approximately 7 h and 20 min (counted from the time when the ammonia gas dosing was started). When steady state, i.e. constant gas concentration at the sampling points was reached, 20 values of the NH_3 concentration for each measuring point were acquired. The data were then analysed by averaging all 20 values collected during one experimental condition.

2.4. Uncertainty of measurement

The measured data of ammonia gas concentration were analyzed in accordance with ISO/IEC Guide for the expression of uncertainty [31]. The absolute expanded uncertainty with 95% confidence interval and coverage factor of 2 was estimated based on the bias and resolution of the Innova instrument as well as the reproducibility (standard deviation) of the measured concentrations. The uncertainties are given in the results as error bars on the column charts or listed in Table 3 for some of the measurement results.

The repeatability error of the measuring procedure, due to uncertainty in boundary conditions, position of the dummies, etc. was estimated by repeated experiments. Several of the experimental conditions (conditions number 1, 2 & 6 in Table 2) were repeated two to five times to quantify if the results were affected by the experimental procedure and the boundary conditions such as the volume air flow rate in the room, the air temperature, the RH and the dosing rate of NH_3 gas. The maximum difference between the repeated measurements was ±0.3 ppm.

3. Results

Fig. 6 shows the ammonia gas concentration measured in the room as a function of time from the start of dosing the gas. The results in the figure were obtained during the reference case '1.6 ACH'. Small fluctuations of the gas concentration are observed in all sampling points except in the breathing zone of the patient after reaching steady state gas concentration (after 277 min). The ammonia concentration in the breathing zone of the patient is higher and fluctuates more compared to the rest of the measured points. This may be due to the complex interaction of weak convective flow above the heated "head", a weak flow with high ammonia concentration escaping through the gaps between the sheet and the body at the head region, and the background airflow in the room. This needs to be studied.

3.1. Exposure reduction

The exposure reduction in the room due to the effectiveness of the VM and the ACF material was quantified as follows:

$$Exposure\ reduction = \frac{C_{i,Ref} - C_i}{C_{i,Ref}} \times 100\% \qquad (1)$$

where C_i is the concentration (ppm) of the contaminant acquired at a measuring point when the VM or ACF or both were used in the experiment and $C_{i,Ref}$ is the concentration (ppm) acquired at the same measuring point during the reference condition '1.6 ACH' background ventilation only.

Fig. 7 compares the exposure reduction due to the use of the VM alone and when it was combined with the "sandwich" ACF (cases 2 and 5, Table 2). The results indicate that up to 71% of the body-emitted pollutants were discharged through the ventilated mattress out of the room before they were mixed with the inhaled air (the condition '1.6 ACH + VM' in Fig. 7). The same percentage of
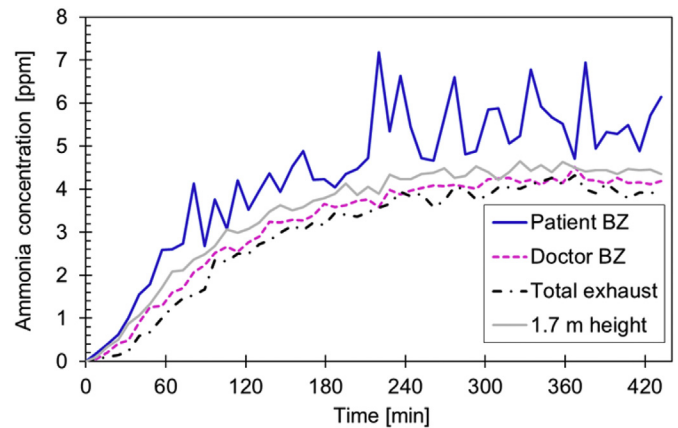

Fig. 6. Ammonia concentration in the sampling points throughout the chamber for the exposure period (7 h 20 min) during the condition of '1.6 ACH' (reference case).
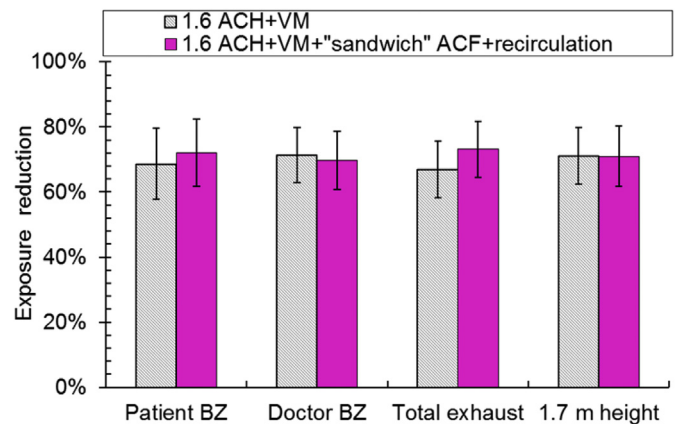

Fig. 7. Exposure reduction using the VM only and VM combined with "sandwich" ACF material relative to the background mixing ventilation alone.

exposure reduction (up to73%) was achieved when the sucked polluted air was locally cleaned inside the VM by the ACF material and recirculated back to the room. In every experiment equal amount of NH_3 gas was released from the patient's groins and also the VM exhaust flow rate was kept unchanged, therefore the amount of sucked contaminants in the mattress was the same during the two experiments. Thus, the results in Fig. 7 imply that the sucked polluted air was fully cleaned by the ACF material. Hence, about 30% of the polluted air was not captured by the local suction and it was therefore mixed with the background room air.

Fig. 8 shows the exposure reduction when the ACF material was used as a cover/blanket for the patient and when the VM and the ACF cover were used together. When only the ACF cover was used, the exposure reduction in all points, except the patient's BZ, was more than 80%. The most significant result in Fig. 8 is that the exposure to ammonia gas was almost entirely reduced (up to 96% exposure reduction) when employing both the ventilated mattress

Table 3
Air cleaning efficiency of the "sandwich" ACF and duct ACF.

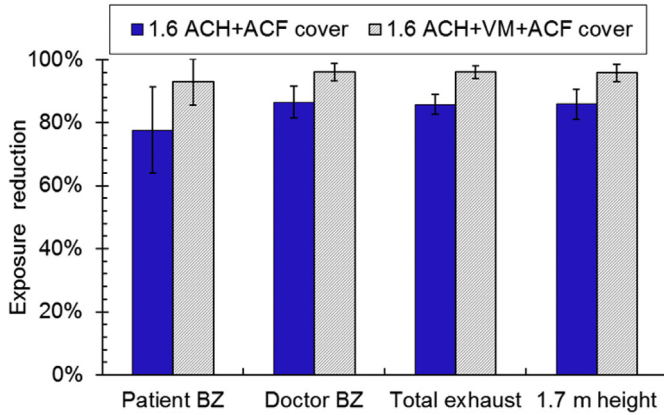| №	Application	Relative humidity	Air cleaning efficiency	Expanded uncertainty in ppm
1	Duct ACF	25%	23%	2.4
2	"Sandwich" ACF	25%	99%	0.02
3	"Sandwich" ACF	70%	98%	0.09

Fig. 8. Exposure reduction using the ACF as a blanket and when using the VM combined with ACF as a cover compared to the case of background mixing ventilation alone.

Fig. 9. Ammonia gas concentration measured in the exhaust duct of the VM when there was no ACF material installed.

and the ACF cover. It should be noted that during this case the ventilated mattress was extracting the pollutants out of the room through the separate exhaust system. Thus, the rest of the pollutants, which were not captured by the VM, were cleaned by the activated carbon fibre cover.

3.2. Cleaning efficiency of the ACF material and effect of RH

To investigate the potential use of the acid-treated ACF as a filter for the air exhausted by the VM, two applications were compared. The ACF material was installed either in the VM's exhaust duct (duct ACF) or inside the mattress ("sandwich" ACF), cases 3 and 4 in Table 2. The air cleaning efficiency of the two applications was assessed according to the following equation:

$$Air\ cleaning\ efficiency = \frac{C_j - C_{ACF}}{C_j} \times 100\% \qquad (2)$$

where in the case of "sandwich" ACF: C_{ACF} is the average NH_3 gas concentration (ppm) measured in the exhaust duct of the operating ventilated mattress downstream of the ACF material, C_j is the average ammonia concentration (ppm) measured at the same point when there was no material installed; in the case of the duct ACF: C_j was measured upstream 3 cm from the material and C_{ACF} was measured downstream 3 cm from the duct ACF.

The results are listed in Table 3. The air cleaning efficiency of the duct filter was not high (only 23%). On the contrary, the air cleaning efficiency was high (99%) when the ACF was placed inside the mattress as a "sandwich". The difference in the cleaning efficiency of the two ACF applications is clearly high; hence, it is important the way the material is used. This may be due to the different residence time of the ammonia molecules within the boundaries of the ACF (in the duct and inside the mattress) and also the different total area of the two ACF samples. The objectives of the current study were not to examine the properties of the ACF material. This needs to be studied separately.

For practical applications, it was studied the influence of relative humidity on the air cleaning efficiency of the ACF fabric. The cleaning efficiency of the "sandwich" ACF was studied at 25% and 70% room relative humidity. The results listed in Table 3 (cases 2 and 3) show that the increased level of RH did not affect the air cleaning efficiency of the ACF. The air cleaning efficiency at 25% RH and 70% RH differed only by 1%.

The concentration of the sucked by the VM ammonia gas as a function of time is shown in Fig. 9. The measurements were
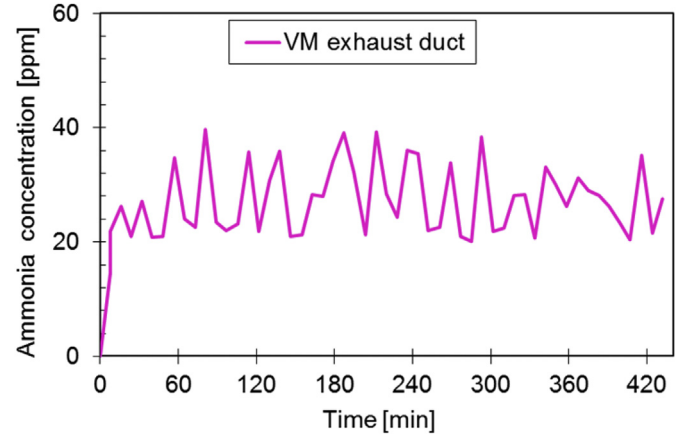
performed in the exhaust duct connected to the VM when there was no ACF material installed. Steady-state in time ammonia concentration with large fluctuations was measured. The NH_3 concentration measured downstream of the "sandwich" ACF filter when the material was exposed to 25% and 70% relative humidity is shown in Fig. 10. It is apparent from these two figures (Figs. 9 and 10) that the ACF material has high cleaning effectiveness. In Fig. 10, however, there is a trend for the ammonia concentration to increase at the end of the exposure. When the relative humidity in the chamber was 70%, the cleaning efficiency of the ACF material was started to decrease after approximately 6 h of ammonia exposure. These results suggest that after exposure for longer than 7 h, the efficiency of the tested ACF may decrease significantly at 70% RH.

4. Discussion

Melikov [32] has reported that airflow interaction in the micro-environment of a person has a major effect on exposure to pollution generated at the vicinity of the body. Thus, in order to improve inhaled air quality, it is needed the air flow interaction around the human body to be locally controlled. The results of the present study show that the VM and the ACF material, used as a pollution control strategy, substantially reduce the exposure to ammonia gas
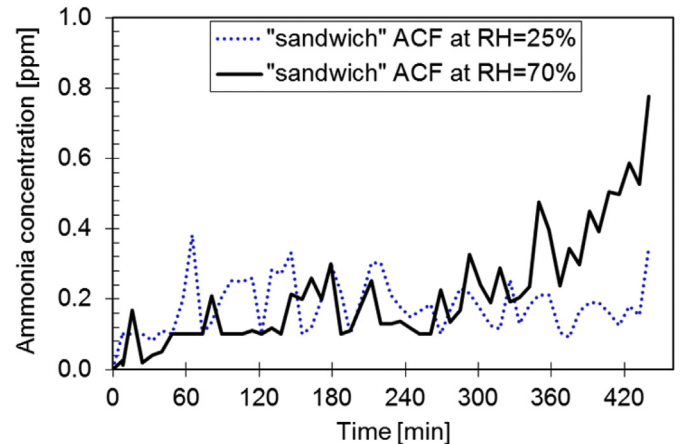

Fig. 10. Ammonia gas concentration measured in the exhaust duct of the VM downstream of the "sandwich" ACF material in the cases the relative humidity was 25% and 70% in the room.

under low room background ventilation rate of 1.6 ACH (10 L/s).

An important finding is that the ventilated mattress can be used to improve the IAQ even when it is not connected to a separate exhaust system. The method of incorporating the ACF material inside the mattress to clean the sucked polluted air and then recirculated it back to the room proved to be an effective measure for exposure reduction to groin-generated NH_3 gas (Fig. 7). Other body parts which are sources of human bio-effluents are the underarms and feet [33]. The ability of the ventilated mattress to remove different tracer gases dosed from the armpits and feet of a lying thermal manikin has been previously studied and shown to be highly efficient ventilation method [18,19]. It can therefore be expected that in the future the VM equipped with new materials that clean wide spectrum of bio-effluents will be more efficient. Moreover, the recirculation mode of operation of the VM will avoid using additional ducting and making changes in already existing background room system for ventilation. This will increase the flexibility of the patient's bed location as well, allowing the bed to be moved around.

Interestingly, when using only the ACF as a patient's cover it was observed that the exposure to ammonia decreased more compared to using only the ventilated mattress. Such method of local air cleaning will be much more efficient in practice than the widely used room air cleaners. However, there are limits of applying cleaning textiles as a cover. In reality, the patient will move and thus the body odours may escape before reacting with the material. Hospital clothing for the patients and bed linens made from different air cleaning textiles could be a solution.

In all measurements the exhaust air flow rate of the VM was adjusted to 1.5 L/s which managed to capture about 70% of the ammonia gas. The efficiency of the VM was studied in separate experiments at different exhaust airflow rates, blanket/cover arrangements and background air distribution. The results will be presented in a separate paper.

The combined together localized ventilation and air cleaning methods, namely the VM and ACF cover, can achieve more than 90% high exposure reduction, as the results in Fig. 8 show. This result support the idea that when applying local control strategies close to the source it can be much more effective approach to reduce the exposure of occupants to airborne contaminants generated indoors than using background air distribution to dilute within the entire space. The high exposure reduction efficiency of the ACF fabric applied as a cover/blanket for the patient is a good illustration of the potential use of existing, new and forthcoming textile materials in conjunction with the VM. Recently, a new non-woven fabric coated with nanoparticles that has antibacterial effect has been introduced on the market [34]. The new material can inactivate different bacteria including methicillin-resistant *Staphylococcus aureus* (MRSA), *Klebsiella pneumonia*, *Bacillus coli*, etc. MRSA is a bacterium known to be resistant to many antibiotics and is still a major patient threat in hospital environments [35]. It has been shown that desquamated skin flakes from the body can be carriers of the pathogenic bacteria [36]. Another study reported that some of the frequently contaminated objects in a hospital included also the bed linens and the patient's gown [37]. It has been shown that it is likely particles deposited on mattresses and blankets to resuspend and reach the breathing zone of the lying person [38]. One viable solution for purifying the inhaled air in hospital patient rooms can be the use of textile materials with antibacterial and deodorizing properties in form of covers, bed linens, gowns, etc.

Bivolarova et al. [24] reported that the acid-treated ACF material's removal efficiency was not affected by changes of the air temperature, from 20 °C to 28 °C, and only slightly was reduced in the case of an increase of the relative humidity from 25% to 80%. The current study found that the ventilated mattress can efficiently work when it was equipped with the "sandwich" ACF at room air temperature of 29 °C. It was found that when the ACF material was used to cover the inside mesh of the mattress the measured ammonia concentration downstream of the material was almost entirely reduced under room conditions of 29 °C and 25% RH. The same result was obtained when the room relative humidity was increased from 25% to 70% (Table 3). These results show that the VM combined with the ACF material can be used also in countries with hot and humid climate.

Only a slight decrease in the cleaning efficiency of the "sandwich" ACF was observed at the end of the exposure when the relative humidity in the chamber was 70% (Fig.10). A study by Lee and Davidson [20] showed that the adsorption efficiency of different type of activated carbon fibre decreased when the relative humidity was increased from 20% to 50%. The mechanism for this effect of humidity was believed to be that micro-pores in the activated carbon were blocked by water molecules, leaving a reduced number of sites for the adsorption of gas molecules. In the present study, an effect of increase in RH level on the performance of the acid-treated ACF material was not observed. This could be explain with the fact that ammonia reacts with a number of acids, thus the air cleaning effect of the ACF occurs due to chemical adsorption (chemisorption). Normally, water vapour facilitates chemisorption, whereas it usually hinders physical adsorption [39]. This, however, means that lower than 25% RH level might decrease the ACF performance. In general, there are existing analytical and empirical models for estimating the gas-phase filter breakthrough time and adsorption capacity at different gas concentrations and RH levels [40,41].

The findings in the present study may be somewhat limited by factors such as body posture of the person lying on the mattress, different bedding arrangements and effect of human respiratory rate on the inhaled pollutants. In the study by Bivolarova et al. [19], it was found that when a person is lying on his/her stomach this may decrease to some extent the ability of the ventilated mattress to capture pollutants emitted from his/her armpits. Further studies, which take these variables into account, will need to be undertaken.

Another issue related to the ventilated mattress is whether the air movement through the mattress will provide local body cooling which may cause thermal discomfort. In fact, this has been already tested in a recent study involving a thermal manikin lying on the VM [42]. The results of the study indicated that the ventilated mattress provided cooling to the body parts in contact with the surface of the mattress at 23, 26 and 29 °C room air temperature. The cooling was increased with the increase of the airflow rate through the mattress from 1.5 L/s to 3, 6 and 10 L/s. It was suggested in the study that the use of the VM at elevated room temperature will decrease the local warm thermal sensation especially at the back side and the back. This effect of the mattress will be beneficial for bedridden people who are exposed to elevated air temperatures. However, the large differences in local thermal sensation as a result of the non-uniform body cooling may cause thermal discomfort. At the comfortable range of room air temperature (i.e. 21–25 °C), the surfaces of the VM in contact with the body can be heated under individual control of user to provide comfort. Noise can be also an issue to be considered when the VM is used in practice. The performance of the VM should be studied with human subjects.

The present hospital HVAC systems are usually designed to ventilate the entire room volume in order to dilute the concentration of the airborne pollutants and to provide comfortable environment. This method in order to be effective needs careful considerations of the type and location of the room supply and exhaust diffusers in relation to the room geometry, temperature

difference between supply air and room air, etc. [5]. Energy and money can be saved by conditioning and ventilating only the occupied zone of spaces or part of it, which will require less air. The studied method goes beyond this and provides the possibility for effective control strategy for reduction of indoor exposure to body-emitted contaminants at decreased ventilation rate. Energy will be saved.

The application of the VM has a potential to increase flexibility in the use of hospital rooms. The HVAC system in all patients' rooms can be designed to maintain 3 ACH. In the rooms where higher ACH rate is required, the additional improvement of the IAQ can be achieved with the use of the local exhaust ventilation (VM) and an air cleaning material. The VM can be also combined with the personalized hospital bed ventilation suggested by Melikov et al. [16] for preventing airborne spread of infectious respiratory diseases. An optimal control of the air pollutants generated from both the body and the respiratory activities of patients can be provided using these two local ventilation methods.

5. Conclusions

In this study, measurements in a full-scale mock-up of a hospital patient room were carried out to assess the performance of bed-integrated local exhaust. Ammonia gas was used to simulate a constant emission of airborne pollution from the groins of a lying in bed patient. Acid-treated ACF material, which is able to clean air from ammonia, was used for local cleaning method.

The results show that the ACF fabric applied as a patient's cover/blanket is an effective way of reducing exposure to ammonia gas by more than 80%. The combined use of the VM and ACF cover was the most efficient exposure reduction strategy, since more than 90% of the ammonia gas in the room air was removed.

70% exposure reduction was achieved, when the air exhausted through the VM was removed from the room. Exposure reduction of about 70% was achieved also when the captured polluted with ammonia air was cleaned with the ACF material inside the VM and afterwards was discharged it back to the room.

An increase in relative humidity from 25% to 70% did not decrease the ACF's removal efficiency. This result is promising for applications in spaces in which humidity may vary over a wide range. The studied principle of local air exhaust combined with local cleaning can have broader application not only in health care facilities but also in elderly homes, hotels, and transportation.

Further research might explore the effect of body posture, bedding arrangement and human respiratory rate on the exposure reduction efficiency of the VM. It is important also to study human response to the VM.

Acknowledgement

References

[1] ISIAQ, ISIAQ Review on Indoor Air Quality in Hospitals and Other Health Care Facilities, International Society of Indoor Air Quality and Climate, 2003.
[2] U.-M. Hellgren, K. Reijula, Indoor-air-related complaints and symptoms among hospital workers, Scand. J. Work Environ. Health 32 (Suppl. 2) (2006) 47–49.
[3] K. Nordstrom, D. Norback, R. Akselsson, Influence of indoor air quality and personal factors on the sick building syndrome (SBS) in Swedish geriatric hospitals, Occup. Environ. Med. 52 (3) (1995) 170–176.
[4] Y. Li, IAQ applications: natural ventilation use, ASHRAE J. 55 (5) (2013) 78–82.
[5] ASHRAE, HVAC Design Manual for Hospitals and Clinics, first ed., American Society of Heating, Refrigerating, and Air-conditioning Engineers, Atlanta, GA, 2003.
[6] ASHRAE, ANSI/ASHRAE Standard 170-2013, Ventilation of Health Care Facilities, American Society of Heating, Refrigerating and Air-Conditioning Engineers, Inc, Atlanta, 2013.
[7] Z.D. Bolashikov, A.K. Melikov, W. Kierat, Z. Popiołek, M. Brand, Exposure of health care workers and occupants to coughed airborne pathogens in a double bed hospital patient room with overhead mixing ventilation, HVAC&R Res. 18 (04) (2012) 602–615 issue.
[8] J. Pantelic, K.W. Tham, Adequacy of air change rate as the sole indicator of an air distribution system's effectiveness to mitigate airborne infectious disease transmission caused by a cough release in the room with overhead mixing ventilation: a case study, Sci. Technol. Built Environ. 19 (2013) 947–961.
[9] S. Yamazaki, K. Hoshino, M. Kusuhara, Odor associated with aging, Anti – Aging Med. 7 (2010) 60–65.
[10] N.O. Verhulst, W. Takken, M. Dicke, G. Schraa, R.C. Smallegange, Chemical ecology of interactions between human skin microbiota and mosquitoes, FEMS Microbiol. Ecol. 74 (2010) 1–9.
[11] W.C. Noble, D.A. Somerville, Microbiology of human skin, W.B. Saunders Company Ltd, London, 1974.
[12] S. Robinson, A.H. Robinson, Chemical composition of sweat, Physiol. Rev. 34 (1954) 202–220.
[13] K. Nishida, T. Kodama, M. Yamakawa, The changes in psychophysical coefficient by the composition of nightsoil, Kankyo Gijyutsu 10 (1981) 462–473.
[14] Itakura T, Mitsuda M. Servey of characteristics of the odor in medical facilities. The 6th International Conference on Indoor Air Quality, Ventilation & Energy Conservation in Buildings IAQVEC 2007, Oct. 28–31, Sendai, Japan.
[15] A.K. Melikov, Advanced air distribution, ASHRAE J. 53 (11) (2011) 73–77.
[16] A.K. Melikov, Z.D. Bolashikov, E. Georgiev, Novel ventilation strategy for reducing the risk of cross infection in hospital rooms, Proc. Indoor Air (2011). Paper 1037, Available at: http://www.aivc.org/resource/survey-characterisitics-odor-medical-facilities.
[17] Nielsen P, Jiang H, Polak M. Bed with integrated personalized ventilation for minimizing of cross infection. In Proceedings of Roomvent 2007; the 10th International Conference on Air Distribution in Rooms.
[18] Bivolarova MP, Melikov AK, Kokora M, Mizutani C, Bolashikov ZD. Novel bed integrated ventilation method for hospital patient rooms. Proceedings of Roomvent 2014; 13th SCANVAC International Conference on Air Distribution in Rooms. pp. 49–56.
[19] Bivolarova MP, Melikov AK, Kokora M, Bolashikov ZD. Performance Assessment of a Ventilated Mattress for Pollution Control of The Bed Microenvironment in Health Care Facilities, Healthy Buildings 2015, ISIAQ International Conference, Eindhoven, the Netherlands, May 18–20, paper ID 633.
[20] P. Lee, J. Davidson, Evaluation of activated carbon filters for removal of ozone at the PPB level, Am. Ind. Hyg. Assoc. J. 60 (5) (1999) 589–600.
[21] M. Sidheswaran, H. Destaillats, D. Sullivan, S. Cohn, J. Larsen, W. Fisk, Energy efficient indoor VOC air cleaning with activated carbon fiber (ACF) filters, Build. Environ. 47 (2012) 357–367.
[22] M.P. Cal, M.J. Rood, S.M. Larson, Gas phase adsorption of volatile organic compounds and water vapor on activated carbon cloth, Energy Fuel 11 (2) (1997) 311–315.
[23] A. Khazraei Vizhemehr, F. Haghighat, C.S. Lee, H. Kholafaei, Evaluation of gas-phase filter performance for a mixture gas, CSAWAC 43 (4) (2015) 463–620.
[24] Bivolarova MP, Mizutani C, Melikov AK, Bolashikov ZD, Sakoi T, Kajiwara K. Efficiency of deodorant materials for ammonia reduction in indoor air. In Proceedings of Indoor Air 2014. International Society of Indoor Air Quality and Climate. pp. 573–580.
[25] Mizutani C, Bivolarova MP, Melikov AK, Bolashikov ZD, Sakoi T, Kajiwara K. Air cleaning efficiency of deodorant materials under dynamic conditions: effect of air flow rate. In Proceedings of Indoor Air 2014. International Society of Indoor Air Quality and Climate; pp. 745–749.
[26] FprCEN/TR 16244, Ventilation for Hospitals 16244, 2011. Technical report 2011, FprCEN/TR.
[27] T.C. Wang, A study of bio-effluents in a college classroom, ASHRAE Trans. 82 (1975) (Part I).
[28] L. Fang, D.P. Wyon, G. Clausen, P.O. Fanger, Impact of indoor air temperature and humidity in an office on perceived air quality, SBS symptoms and performance, Indoor Air 14 (Suppl. 7) (2004) 74–81.
[29] Y.H. Yau, B.T. Chew, Thermal comfort study of hospital workers in Malaysia, Indoor Air 19 (2009) 500–510, http://dx.doi.org/10.1111/j.1600-0668.2009.00617.x.
[30] A. Simone, B. Olesen, J. Stoops, A.W. Watkins, Thermal comfort in commercial kitchens (RP-1469): procedure and physical measurements (Part 1), HVAC&R Res. 19 (2013) 1001–1015.
[31] ISO/IEC Guide, Evaluation of Measurement Data – Guide to the Expression of Uncertainty in Measurement, 2008. ISO/IEC Guide 98–3.
[32] A.K. Melikov, Human body micro-environment: the benefits of controlling airflow interaction, Build. Environ. 91 (2015) 70–77, http://dx.doi.org/10.1016/j.buildenv.2015.04.010.
[33] L. Dormont, J. Bessiere, A. Cohuet, Human skin volatiles, J. Chem. Ecol. 39 (2013) 569–578, http://dx.doi.org/10.1007/s10886-013-0286-z. Available from:.
[34] NBC Meshtec Inc., http://www.nbc-jp.com/eng/product/cufitec/Last accessed on 23. January, 2016.
[35] Centers for Disease Control and Prevention (CDC) http://www.cdc.gov/mrsa/

index.html Last accessed on 23. January, 2016.

[36] R.R. Davies, W.C. Noble, Dispersal of bacteria on desquamated skin, Lancet 2 (1962), 1295±7.

[37] J.M. Boyce, G. Potter-Bynoe, C. Chenevert, T. King, Environmental contamination due to Methicillin-resistant Staphylococcus aureus: possible infection control implications, Infect. Control Hosp. Epidemiol. 18 (No. 9) (Sep., 1997) 622—627.

[38] M.P. Spilak, B.E. Boor, A. Novoselac, R.L. Corsi, Impact of bedding arrangements, pillows, and blankets on particle resuspension in the sleep microenvironment, Build. Environ. 81 (2014) 60—68, http://dx.doi.org/10.1016/j.buildenv.2014.06.010.

[39] ASHRAE, ASHRAE Handbook—HVAC Applications, Chapter 46, Control of Gaseous Indoor Air Contaminants, ASHRAE, Atlanta, 2011.

[40] A. Khazraei Vizhemehr, F. Haghighat, C.S. Lee, Predicting gas-phase air-cleaning system efficiency at low concentration using high concentration results: development of a framework, Build. Environ. 68 (2013) 12—21.

[41] A. Khazraei Vizhemehr, F. Haghighat, Gas-phase filters breakthrough models at low concentration − effect of relative humidity, Build. Environ. 75 (2014) 1—10.

[42] M.P. Bivolarova, A.K. Melikov, M. Kokora, Z.D. Bolashikov, Local cooling of the human body using ventilated mattress in hospitals, in: Proceedings of Roomvent 2014, 13th SCANVAC International Conference on Air Distribution in Rooms, October 19-22, Sao Paolo, Brazil, 2014, pp. 279—286.

PAPER VII

Bivolarova, M., Rezgals, L., Melikov, A. K., Bolashikov, Z. D.,2016. Seat-integrated localized ventilation for exposure reduction to air pollutants in indoor environments. In Proceedings of 9th International Conference on Indoor Air Quality Ventilation & Energy Conservation In Buildings, Oct., 2016 Seoul, Korea. Paper ID 1258.

Seat-integrated localized ventilation for exposure reduction to air pollutants in indoor environments

Mariya P. Bivolarova[1,*], Lauris Rezgals[1], Arsen Melikov[1] and Zhecho Bolashikov[1]

[1]International Centre for Indoor Environment and Energy, Department of Civil Engineering, Technical University of Denmark, Kgs. Lyngby, Denmark

[*]*Corresponding email: mbiv@byg.dtu.dk*

ABSTRACT

A novel ventilation method for minimizing the spread of bioeffluent contaminants generated from sedentary people indoors was developed and studied. The concept of the method consists of a ventilated cushion which is able to suck the human bioeffluents at the area of the body where they are mainly generated before they disperse around a room. The polluted near the body air is exhausted into the cushion and it is removed from the room by a separate exhaust system. The performance of the method was studied in series of experiments. Full-scale room and a dressed thermal manikin sitting in front of a desk were used to simulate one person office. The chair on which the thermal manikin was sitting had the ventilated cushion (VC). Tracer gases, carbon dioxide (CO_2) and nitrous oxide (N_2O), were used to simulate bioeffluents emitted by the manikin's armpits and groin region respectively. The experiments were conducted at 26°C room air temperature. The performance of the VC in conjunction with mixing total-volume background ventilation at 1 air change per hour (ACH) was compared with that of mixing background ventilation alone operating at 1, 1.5, 3 and 6 ACH. Experiments at exhaust airflow rate from the cushion at 1.5, 3 and 5 L/s were performed. The pollution removal efficiency was assessed by measuring the pollution concentration in the breathing zone of the manikin and at several other locations in the room bulk air. Exhausting air through the VC decreased the concentration of the tracer gases at the breathing zone and in the room. The higher the exhaust flowrate, the more the concentration was decreased.

KEYWORDS
Indoor air quality, human bioeffluents, exposure, localized exhaust ventilation

INTRODUCTION
People spend most of the time in indoor environments such as office buildings, at home, vehicle compartments, etc. Occupants' health, well-being and productivity in these environments are affected by the indoor air quality (IAQ) (Wargocki et al. 1999, Zhang et al. 2016). Primary pollution sources in indoor premises can be the occupants themselves (Zhang et al. 2016). Human metabolism not only produces carbon dioxide (CO_2) but also generates odorous gaseous compounds (bioeffluents), which are volatile organic compounds (Wang et al. 2014). Volatile organic compounds (VOCs) are one of the bioeffluents that are emitted from the skin. Production of VOCs by the human skin is governed mainly by the secretion of apocrine and sebaceous glands (Noël et al. 2012). Apocrine glands are located in the axillae, genital area and areolas. Secretions from these glands provide favourable environment for numerous populations of bacteria which are considered main contributors to the formation of human body odor (Dormont et al. 2013).

It has been reported that heating ventilation and air-conditioning (HVAC) equipment accounts for nearly 40 percent of total global building energy consumption (Navigant Consulting 2016). The most commonly used method to reduce the indoor contaminants in the air is by

means of mechanical (forced) ventilation. The current total volume air distribution principles (i.e. mixing and displacement) should supply large volume of filtered outdoor air to the entire space to dilute or remove the contaminants from the occupied zone. This method is highly inefficient (Melikov 2016) and uses significant amount of energy to exchange the air in a room.

To obtain high quality indoor environments at reduced background ventilation rate, different advanced local ventilation systems have been developed and studied (Melikov 2016). Recently, experimental studies (Bivolarova et al. 2016, Bivolarova et al. 2014) examined the effectiveness of using local exhaust ventilation to remove body generated bioeffluents while a person is in bed and thus to reduce the indoor exposure to those pollutants. A ventilated mattress with suction openings below the feet and the groin area of a thermal manikin was used. The results showed that the use of the ventilated mattress at 1.5 L/s together with background ventilation rate of 1.5 air changes per hour (ACH) improved the air quality in the room and the breathing zone compared to when the background ventilation was used alone at 6 ACH (Bivolarova et al. 2014).

The present study aimed to implement local exhaust ventilation into a cushion for a seat and to identify its efficiency for capturing body-emitted bioeffluents in a single office environment.

METHODS

The experiment was performed in a test room furnished to simulate a single office room. The dimensions of the room were 5.9 m x 6 m x 3.2 m (W x L x H). A typical office working environment was simulated by a thermal manikin seated on a computer chair in front of a desk with a laptop on it (Figure 1). The room had 12 ceiling mounted light fixtures (32 W each) spread over the entire ceiling.

Mixing air distribution was used to supply 100% outdoor air to the room through a square diffuser mounted in the middle of the ceiling. No recirculation was used during the experiments. During the measurements, summertime conditions were maintained in the office room. The air temperature in the room was kept 25.5 °C ±0.5 °C. Series of experiments were conducted at four background ventilation rates -1, 1.5, 3 and 6 ACH. Two different four way supply diffusers were used: Ø160 (sizes 295 mm x 295 mm) for 1 and 1.5 ACH ventilation rates and Ø250 (sizes 495 mm x 495 mm) for 3 and 6 ACH. In both cases the diffuser was supplying the outdoor air in three directions (position 7 in Figure 1). One of the air supply slots of the diffuser was blocked in order to avoid possible short circuit with the exhaust. To exhaust the air from the room, a rectangular exhaust grill (sizes 970 mm x 170 mm) mounted on the wall close to the ceiling was used (position 8 in Figure 1).

The office room was assumed to be located in a low-polluting building. According to the European Standard EN 15251 (2007) the ventilation rate required for diluting emissions (pollutants) from the building components (building and furnishing, and HVAC system) is 0.7 L/s per m^2 floor area for IAQ category II and 1 L/s per m^2 floor area for IAQ category I. The required ventilation rate for diluting emissions (bio-effluents) from people is 7 L/s per person for IAQ category II and 10 L/s per person for IAQ category I. The total required ventilation rate for each category is the sum of these two calculated ventilation rates. The required total ventilation rate for the simulated single office in this study (35.4 m^2 floor area and 1 occupant in the room) was calculated to be 31.8 L/s (1 ACH) for category II and 45.4 L/s (1.5 ACH) for category I. The new localized ventilation system was operated only with the background

ventilation of category II. Additionally, two more cases at high background ventilation rates were performed - 94.4 L/s (3 ACH) and 188.8 L/s (6 ACH).

A dressed thermal manikin with realistic human body size, shape, and surface temperature distribution was used as a sitting occupant. The manikin was dressed in panties, short sleeve shirt, normal trousers, normal socks and thin soled shoes with the overall thermal insulation of 0.47 clo (DS EN ISO 7730 2005). The thermal manikin maintained the same sensible heat as that released by a healthy average person in a state of thermal comfort.

The manikin was sitting on a ventilated cushion which was placed on a computer chair (Figure 2). The ventilated cushion (VC) was used in some of the experiments to exhaust locally simulated contaminants emitted from the manikin's body. Along the surface of the VC there were eight rows of small openings each with diameter of 6 mm. There were two openings per row and the distance between them was 0.135 m. The VC was connected to a local exhaust which was able to suck air through the openings and exhaust it out of the room (Figure 1). There was a mesh inside the ventilated cushion which provided support and allowed the exhaust air to move through the cushion. During the measurements, the exhaust airflow rate of the VC was provided by an axial fan connected to the VC with flexible and straight ducts (Ø 0.08 m). The airflow rate through the VC was measured with an air flow sensor (MFS-C-0080) installed in the straight connection between the fan and the VC. The maximum error in the measurement with this sensor is ±3 % of the actual flow. The pressure difference at the MFS sensor was measured with a differential pressure micro-manometer FCO510 (accuracy of 0.01 Pa [0.15×10^{-5} psi] ±0.25% of reading). Based on the pressure difference readings from the micro-manometer, the desired flow rate was adjusted by a manually operated damper. The performance of the VC was tested at three exhaust flow rates - 1.5 L/s, 3 L/s and 5 L/s.

Tracer gases, namely carbon dioxide (CO_2) and nitrous oxide (N_2O), were used to simulate bioeffluents emitted by the manikin's armpits and groin region respectively. The tracer gases were dosed at constant emission rates directly from compressed gas cylinders. The gas was transported from the cylinders to the manikin through separate pipes and released through porous sponges that were fixed to the end of the pipes and attached to the polluting body parts. The emission rate of CO_2 and N_2O were adjusted to be 0.4 L/min and 0.1 L/min respectively. The air mixed with the tracer gases was sampled and its gas concentration was analysed under steady-state conditions using two Innova 1303 multi-channel samplers and two photoacoustic multi-gas monitors Innova 1312. The instruments were calibrated prior to the experiments and the gas detection limits after calibration were defined 5 ÷ 3500 ppm and 0.5 ÷ 350 ppm for CO_2 and N_2O respectively. The instruments were placed outside the test room. The gases were sampled through nylon tubes in diameter 4 mm. The concentration of each tracer gas was measured at six measuring points: at the breathing zone of the manikin, 0.5 m above the head, at the supply, total exhaust air, and in the centre of the room at 1.7 m height. At each sampling point, 40 values of the tracer gas concentration were collected after reaching steady state.
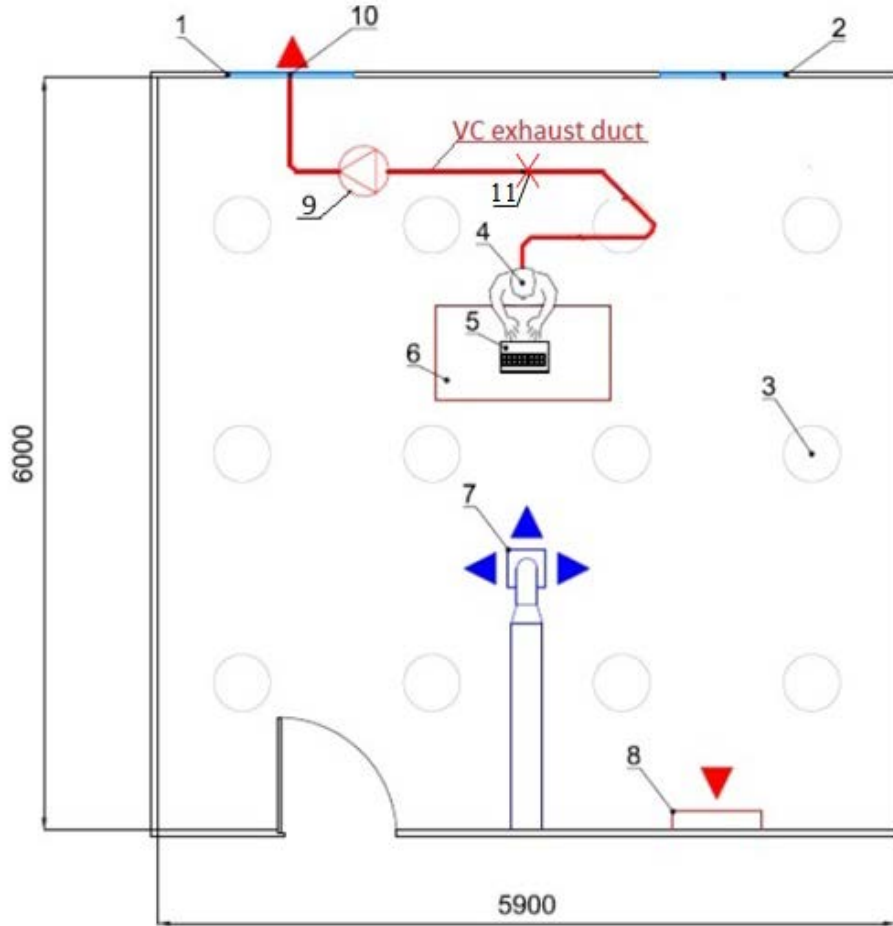
Figure 1. Room layout: 1; 2 – windows, 3 – lights (12 in total), 4 – occupant, 5 – laptop PC, 6 – table, 7 – supply, 8 – total exhaust, 9 – fan, 10 – air exhaust, 11 – air flow sensor MFS-C-0080.

Figure 2. The ventilated cushion (VC) positioned on the computer chair and connected to the exhaust duct.

In order to assess the efficiency of the VC in removing body bioeffluents, the measured concentrations were normalized as follows:

Normalized concentration $= C_{i,avg}/C_{i,avg,Ref}$ (1)

where $C_{i,avg}$ is the average concentration measured at the sampling location during each of the studied conditions; $C_{i,avg,Ref}$ is the average concentration measured at the same sampling location during the reference condition when the VC was not operating at 1 ACH background ventilation rate. The value of the normalized concentration lower than "1" shows that the concentration of the contaminants at the measuring point is lower compared to the reference case (i.e. improvement of air quality) and vice versa when the value is higher than "1". For the reference case the normalized concentration is equal to 1.
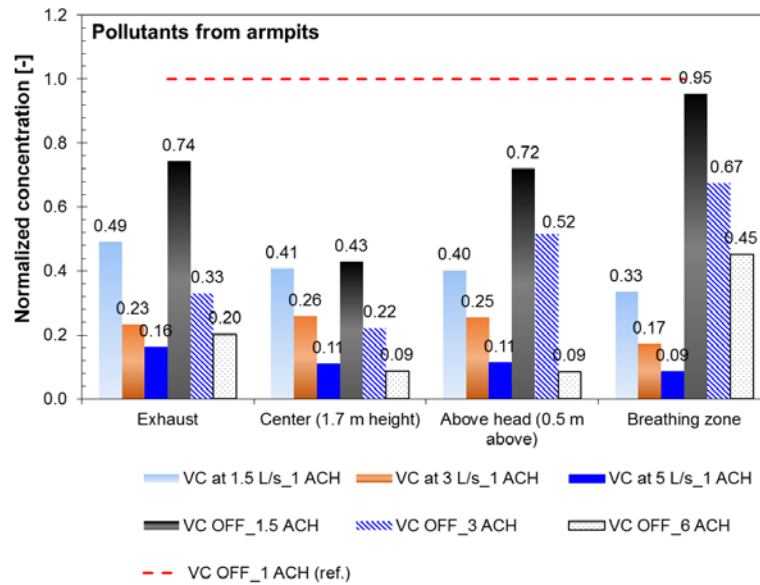
RESULTS

The results of the normalized concentrations at all measured locations for both pollution sources (armpits and groins) are shown in Figure 3a and 3b respectively. Results obtained at background ventilation of 1.5, 3 and 6 ACH with VC turned OFF and when the VC operated at 1.5, 3 and 5 L/s at background ventilation of 1 ACH are shown. The results in Figures 3a and 3b show that the normalized values are the highest at the mouth of the thermal manikin. In both figures there is a clear trend of the pollution concentration decreasing as the exhaust flowrate through the VC increased. Similarly, the concentrations decreased as the mixing background ventilation rate increased and the VC was not working. The results show that when the VC was exhausting air at 1.5 L/s the concentration of the pollutants generated from the groin region was reduced by 69% in the mouth compared to the reference case. By increasing the exhaust flow rate to 3 L/s, the reduction of concentration reached 87%. The concentration of the pollutants was reduced by 94% when the VC was operating with 5 L/s exhaust flowrate. The same concentration reduction, with respect to the reference case, was observed in the other measured locations for both pollution sources (armpits and groins), differing from each other by about ±9 %.

What is interesting in this data (Figure 3a and 3b) is that supplying 188 L/s (or 6 times) more clean air into the room was less efficient to reduce the concentration of the pollutants in the breathing zone than exhausting 1.5 L/s air from the VC and supplying 32 L/s into the room.
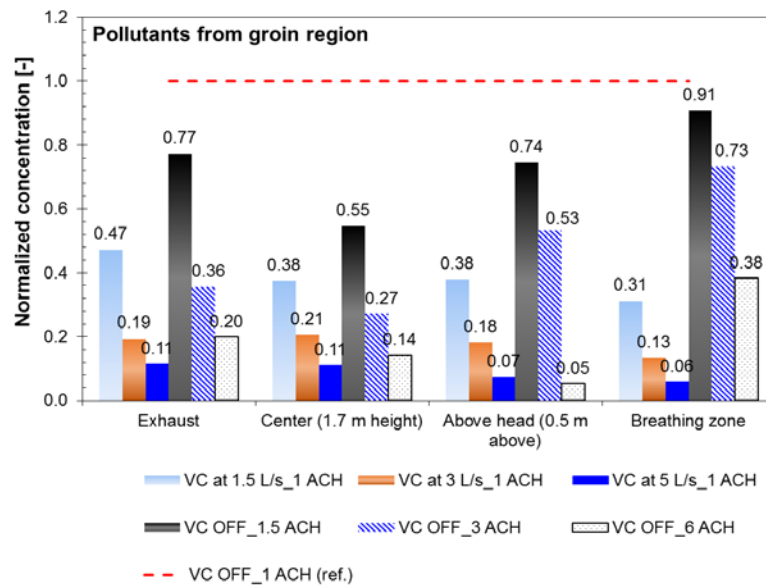
a)

b)

Figure 3. Average concentration at all measuring points a) dosing from the groin region and b) dosing from the armpits.

DISCUSSIONS

Overall, the results from the current study show that when the ventilated cushion (VC) is in operation, the concentration of the pollutants released from the groins and the armpits of the thermal manikin decreased at the measured locations. This is because the body of the thermal manikin was in contact with the cushion. Higher exhaust flow rate through the VC increase the suction of the air that allows more pollutants to be captured and removed before they are spread in the room.

The results show that in comparison with the condition without VC and the background ventilation at 1.5 ACH (45.4 L/s), the concentration of the pollutants emitted from the thermal manikin (groins and armpits) decreased in the breathing zone by about 65% when the VC was working at exhaust flowrate of 1.5 L/s and background ventilation at 31.8 L/s. In the total exhaust air of the room the decrease was by more than 30% when using the VC at 1.5 L/s compared to the concentrations at 1.5 ACH VC OFF. It means that when the VC was in use, better IAQ was achieved by transporting about 12 L/s less air (1.5 L/s instead of 13.6 L/s). According to the European Standard EN 15251 (2007) background ventilation rate of 45.4 L/s (1.5 ACH) corresponds to IAQ of category I for a single office in a low polluting building. It can therefore be assumed that the implementation of the VC would provide better air quality at lower ventilation rate per person. This may lead to energy savings. Further studies, which take the energy use into account, will need to be undertaken.

The results for both simulated air pollutants, namely groins and armpits, showed that the concentrations at the mouth are higher than the concentrations measured above the head and in the exhaust of the room. This is because the breathing zone is closer to the body-emitted pollutants. It has been reported that the natural convective flow around a seated person has the ability to transport gaseous pollutants released from the body upward to the breathing zone and above the head (Licina et al. 2014). Therefore, the self-exposure of these pollutants is rather high. The concentrations of the pollutants at the mouth are important as they directly influence the inhaled air quality. Therefore, it is expected that the VC will improve the quality

of inhaled air in terms of body-emitted gaseous pollutants since it will reduce their transport by direct local exhaustion.

It should be noted that the practical application of the VC may be changed under different room conditions and occupant behavior. The current study does not consider different body postures, human respiration, different outfits and physical movements when a person is sitting. Several issues, related to control and optimization of the VC as well as human response remain to be studied. It should be noted that a filter can be easily incorporated inside the VC, where the polluted air will be cleaned locally and discharged it back into the room. This method was shown by Bivolarova et al. (2016). The "plug and play" method can be applied, which will prevent the use of additional ducting. This will increase the flexibility of the chair and it will be possible the chair equipped with the VC to be moved without difficulty.

CONCLUSIONS

This study investigates the performance of the ventilated cushion with regard to indoor air quality. The experimental results reveal the following:

- Exhausting air through the VC decreased the concentration of pollutants, released from the groin and armpits region of the simulated person, at the breathing zone and in the room. The higher the exhaust flowrate, the more the concentration was decreased.
- Exhausting 1.5 L/s of air through the VC at 1 ACH in the room to reduce the bioeffluents' concentration at the breathing zone was about 65% more efficient than proving the recommended 1.5 ACH for category I IAQ in low polluting building.
- The use of the VC not only can improve the air quality by reducing the unpleasant body odors, but also may lead to energy savings due to deduced background ventilation rate.

REFERENCES

Bivolarova M.P., Melikov A.K., Mizutani C., Kajiwara K. and Bolashikov, Z.D. (2016) Bed-integrated local exhaust ventilation system combined with local air cleaning for improved IAQ in hospital patient rooms. Building and Environment 2016: 100 10-18.

Bivolarova MP, Melikov AK, Kokora M, Mizutani C, Bolashikov ZD. Novel bed-integrated ventilation method for hospital patient rooms. Proceedings of Roomvent 2014; 13th SCANVAC International Conference on Air Distribution in Rooms. pp. 49-56.

Dormont L., Bessiere J., Cohuet A.. Human Skin Volatiles. J Chem Ecol, vol.39. 2013, pp.569-578. Available from: doi: 10.1007/s10886-013-0286-z.

DS EN 15251, 2007. Indoor environmental input parameters for design and assessment of energy performance of buildings addressing indoor air quality, thermal environment, lighting and acoustics. 1st ed. Brussels, Belgium: European Committee for standardization. ICS 91.140.01.

DS EN ISO 7730. 2005. Ergonomics of the thermal environment – Analytical determination and interpretation of the PMV and PPD indices and local thermal comfort criteria. 2005, 3rd ed. Brussels, Belgium: European Committee for Standardization.

Licina D., Melikov A, Sekhar C, Tham K.W. 2015. Transport of gaseous pollutants by convective boundary layer around a human body, Science and Technology for the Built Environment 2015, 21:8, 1175-1186.

Melikov A. K. 2016. Advanced air distribution: improving health and comfort while reducing energy use. Indoor Air 2016; 26: 112–124.

Navigant Consulting, Inc. 2016. Energy-Efficient HVAC Systems for Commercial Buildings: Report on Unitary Systems, Heat Pumps, Furnaces, Boilers, VRF Systems, Chillers, and Geothermal Heat Pumps for Energy-Efficient Buildings.

Noël F., Pierard-Franchimont C., Pierard G. E., Quatresooz P.. Sweaty skin, background and assessments. Int. J. Dermatol. 2012 (516), pp.647-655.

Wargocki, P., Wyon, D. P., Baik, Y. K., Clausen, G. et al. Perceived Air Quality, Sick Building Syndrome (SBS) Symptoms and Productivity in an Office with Two Different Pollution Loads. In: Indoor Air 1999.1999, (9), 165-179. ISSN 0905-6947.

Wang J., Long E., Zhang X., Characteristics of human bioeffluents "common core" quantity varying with occupant density in indoor respiratory region. *HVAC&R Research 2014:* 20, 188–193.

Zhang, X.J., Wargocki, P. and Lian, Z.W. (2016) Effects of exposure to carbon dioxide and bioeffluents on perceived air quality, self-assessed acute health symptoms, and cognitive performance, Indoor Air, doi: 10.1111/ina.12284.13

The author examined the influence of the interaction of the breathing flow and the convective flow around the human body on the exposure to pollutants. The study shows that tracer gas can be used as a predictor for indoor exposure to aerosols. The research also contributes to the development of bed- and chair- integrated exhaust methods for removing pollutants emitted from occupants. The author shows that the studied methods provide the possibility to reduce the personal exposure to such contaminants and also to decrease the energy used for ventilating offices and hospital environments.